frontiers | Research Topics

Tropical fungal diseases

Edited by
Carlos Pelleschi Taborda, Julian Esteban Muñoz and Angel Gonzalez

Published in
Frontiers in Cellular and Infection Microbiology
Frontiers in Microbiology

ISSN 1664-8714
ISBN 978-2-83251-313-2
DOI 10.3389/978-2-83251-313-2

About Frontiers

Frontiers is more than just an open access publisher of scholarly articles: it is a pioneering approach to the world of academia, radically improving the way scholarly research is managed. The grand vision of Frontiers is a world where all people have an equal opportunity to seek, share and generate knowledge. Frontiers provides immediate and permanent online open access to all its publications, but this alone is not enough to realize our grand goals.

Frontiers journal series

The Frontiers journal series is a multi-tier and interdisciplinary set of open-access, online journals, promising a paradigm shift from the current review, selection and dissemination processes in academic publishing. All Frontiers journals are driven by researchers for researchers; therefore, they constitute a service to the scholarly community. At the same time, the *Frontiers journal series* operates on a revolutionary invention, the tiered publishing system, initially addressing specific communities of scholars, and gradually climbing up to broader public understanding, thus serving the interests of the lay society, too.

Dedication to quality

Each Frontiers article is a landmark of the highest quality, thanks to genuinely collaborative interactions between authors and review editors, who include some of the world's best academicians. Research must be certified by peers before entering a stream of knowledge that may eventually reach the public - and shape society; therefore, Frontiers only applies the most rigorous and unbiased reviews. Frontiers revolutionizes research publishing by freely delivering the most outstanding research, evaluated with no bias from both the academic and social point of view. By applying the most advanced information technologies, Frontiers is catapulting scholarly publishing into a new generation.

What are Frontiers Research Topics?

Frontiers Research Topics are very popular trademarks of the *Frontiers journals series*: they are collections of at least ten articles, all centered on a particular subject. With their unique mix of varied contributions from Original Research to Review Articles, Frontiers Research Topics unify the most influential researchers, the latest key findings and historical advances in a hot research area.

Find out more on how to host your own Frontiers Research Topic or contribute to one as an author by contacting the Frontiers editorial office: frontiersin.org/about/contact

Tropical fungal diseases

Topic editors

Carlos Pelleschi Taborda — University of São Paulo, Brazil
Julian Esteban Muñoz — Rosario University, Colombia
Angel Gonzalez — University of Antioquia, Colombia

Citation

Taborda, C. P., Muñoz, J. E., Gonzalez, A., eds. (2023). *Tropical fungal diseases*. Lausanne: Frontiers Media SA. doi: 10.3389/978-2-83251-313-2

Table of contents

frontiers | Frontiers in Cellular and Infection Microbiology

TYPE Editorial
PUBLISHED 29 December 2022
DOI 10.3389/fcimb.2022.1104519

OPEN ACCESS

EDITED AND REVIEWED BY
Anuradha Chowdhary,
University of Delhi, India

*CORRESPONDENCE
Carlos P. Taborda
Taborda@usp.br

SPECIALTY SECTION
This article was submitted to Fungal Pathogenesis, a section of the journal Frontiers in Cellular and Infection Microbiology

RECEIVED 21 November 2022
ACCEPTED 29 November 2022
PUBLISHED 29 December 2022

CITATION
Taborda CP, Muñoz JE and Gonzalez A (2022) Editorial: Tropical fungal diseases. *Front. Cell. Infect. Microbiol.* 12:1104519. doi: 10.3389/fcimb.2022.1104519

Editorial: Tropical fungal diseases

Carlos P. Taborda[1]*, Julián Esteban Muñoz[2] and Angel Gonzalez[3]

[1]Universidade de São Paulo, Instituto de Ciências Biomédicas, Departamento de Microbiologia, São Paulo, Brazil and Instituto de Medicina Tropical, Laboratório de Micologia Médica, LIM53/HCFMUSP, São Paulo, Brazil, [2]Studies in Translational Microbiology and Emerging Diseases (MICROS) Research Group, Translational Medicine Institute, School of Medicine and Health Science, Universidad del Rosario, Escuela de Medicina y Ciencias de la Salud, Bogota, Colombia, [3]Universidad de Antioquia, Escuela de Microbiología, Medellín, Colombia

KEYWORDS

tropical diseases, laboratory diagnostic, antifungal treatment, molecular biology, proteomics

Editorial on the Research Topic
Tropical fungal diseases

The tropical region of Earth occurs between the latitude lines of the Tropic of Cancer and the Tropic of Capricorn. The tropics include parts of North America, South America, Africa, Asia, and Australia (Figure 1). The climate in the tropics is characterized by a more direct sunlight than the rest of Earth, meaning that the tropics are generally hotter and wetter and less affected by the solar seasons.

According to the literature, there are many fungal infections that occur more frequently in tropical zones or are restricted to certain regions within the tropics. The interference in ecosystems mainly by deforestation of tropical areas and re-adaptation of wild animals into the cities has modified the spectrum of the mycoses. Many of these fungal infections, although with important impacts on public health, are still considered neglected and low visibility diseases. The number of reports of immunosuppressed patients with opportunistic fungal diseases has increased significantly across the world. In this special issue, we will explore some of the main or even rare fungal infections that affect tropical areas of the planet. Included among these diseases are cutaneous (dermatophytes or non-dermatophytes), subcutaneous (chromoblastomycosis and sporotrichosis), systemic (cryptococcosis), and endemic (histoplasmosis) mycoses.

Cutaneous mycoses are a group of fungal infections affecting the skin, hair, and nails; however, in patients with autosomal recessive CARF9 deficiency or immunodeficiencies, dermatophytes can cause systemic mycosis (de Oliveira Pereira et al., 2021). The use of tools such as multilocus phylogenetic analysis has distinguished seven main clades: the genera *Arthroderma*, *Lophophyton*, *Microsporum*, *Paraphyton*, *Nannizzia*, *Epidermophyton*, and *Trichophyton* (reviewed by de Oliveira Pereira et al., 2021). Treatment of dermatophytosis is very complex and depends on several factors arising from both the host and the fungus. Drug resistance is a major problem, especially in the treatment of dermatophytosis. Terbinafine is a

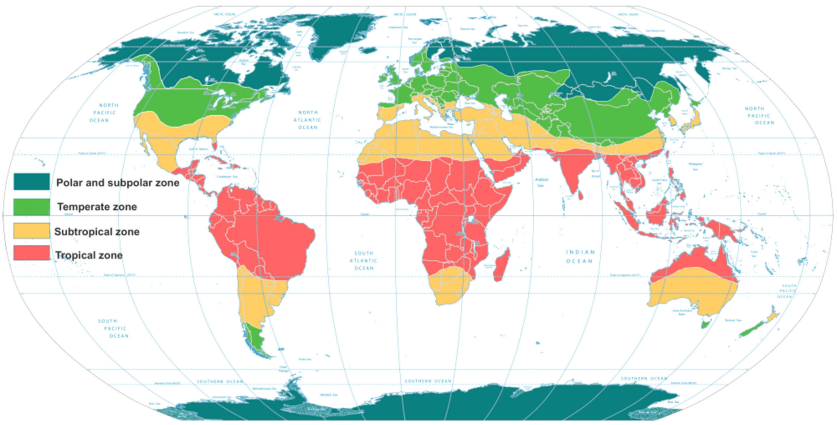

FIGURE 1
World map with the intertropical zone highlighted in red. (https://content.meteoblue.com/pt/research-education/educational-resources/meteoscool/zonas-climaticas-em-geral).

highly recommended drug to treat dermatophytosis. The determination of the antifungal susceptibility and punctual mutations in isolates of dermatophytes resistant to terbinafine is essential to assist physicians in the management of patients (Pashootan et al.).

Dematiaceous or melanized fungi include a large and heterogeneous group of fungi that cause several diseases including chromoblastomycosis, phaeohyphomycosis, and eumycetoma (reviewed by Arcobello and Revankar, 2020). Phaeohyphomycosis refers to a group of mycoses caused by pigmented fungi characterized by yeast-like cells, hyphae, or a combination of both morphotypes in tissues and should be distinguished from primary implantation mycoses. In the last two decades, the frequency of reports and the diversity of the etiological agents involved in this type of mycosis have increased, especially in immunosuppressed individuals (He et al.). Chromoblastomycosis is one of the most prevalent implantations or subcutaneous fungal infections characterized by traumatic inoculation from an environmental source with clinically polymorphic lesions (Queiroz-Telles et al., 2017). The main agents of Chromoblastomycosis include *Fonsecaea* spp., *Phialophora verrucosa*, *Cladophialophora carrionii*, *Exophiala dermatitidis*, and *Rinocladiella aquaspersa* (Queiroz-Telles et al., 2017). Uncommon agents such as *Chrysosporium keratinophilum*, a saprophytic filamentous fungus commonly found in soil, dung, and animal fur, and rarely involved in infections in humans, was reported in a patient with severe chromoblastomycosis-like lesions (Mijiti et al.).

Genomic studies involving *Fonsecaea* and *Cladophialophora* genera from adverse microhabitats and mammal tissue are extremely important to understand virulence factors. The results of a study suggested a higher level of extremotolerance of environmental species (Vicente et al.). Another study focused on the degree with which *Fonsecaea* agents are involved in pathogenicity. The authors aimed to evaluate a model of trans-kingdom infection. The plant infection models employed suggested that all *Fonsecaea* were saprobic. The authors observed, for the first time, structures similar to muriform cells, in a larvae model, that were produced during infection of human tissue, confirming the role of muriform cells as a pathogenic adaptation in animal tissues (Fornari et al.).

Sporotrichosis, caused by *Sporothrix brasiliensis*, a cat-transmitted fungal infection, is an endemic and neglected mycosis found mainly in Brazil (Gremião et al., 2021). The geographic expansion of this zoonosis has been reported in different regions of Brazil, and more recently, cases were reported in other countries in South America (Gremião et al, 2021). Environmental and epidemiological studies are essential to control the spread of this mycosis. A study conducted in Rio de Janeiro (Brazil), an area highly endemic for feline and human diseases, showed that *S. brasiliensis* can maintain itself persistently in its environment for years. In addition, antifungal susceptibility tests indicated that minimal inhibitory concentration of itraconazole from the environmental isolates was lower with cat isolates; however, with amphotericin B and terbinafine it was similar (Rabello et al.).

In general, invasive fungal diseases are rare in immunocompetent individuals; however, an increasing population of immunocompromised patients and ongoing climate change could significantly increase the prevalence of fungal diseases (Casadevall, 2022). *Histoplasma* spp., the causal agent of histoplasmosis, is an environmental dimorphic fungus with a worldwide distribution. In immunocompetent patients, histoplasmosis usually occurs in a less aggressive form, whereas immunocompromised patients present with a more aggressive clinical form. Hemophagocytic lymphohistiocytosis (HLH) is a rare disorder and is characterized by persistent

immune activation of natural killer (NK) and cytotoxic T cells. In this special issue, Chen et al. reviewed cases of HLH secondary to disseminated histoplasmosis in HIV seronegative patients and highlighted that this condition has become increasingly common in emerging endemic areas, carrying a high mortality rate. However, timely diagnosis and early use of antifungals can lead to a favorable prognosis.

Similarly, cryptococcosis is a fungal infection found in immunosuppressed patients, well described in HIV-infected patients, and more rarely occurring in immunocompetent individuals. Goupil de Bouillé et al. described the clinical, mycological, immunological, and genetic characteristics of six HIV-negative patients from French Guiana presenting with invasive cryptococcosis. Despite the available antifungal drugs for cryptococcosis treatment, morbidity and mortality rates remain high. A vaccine would be an important strategy against cryptococcosis infection. Normile and Del Poeta showed in previous studies that a live, attenuated, *Cryptococcus neoformans* Δsgl1 mutant accumulating steryl glucosides was found to be avirulent and protected mice from an otherwise lethal infection. In this study, the validation of three different models of successful vaccination strategies against cryptococcosis are shown, which used heat-killed *C. neoformans* Δsgl1 in a CD4+ T cell deficiency setting.

The contributions described above in this research topic illustrate the changes in behavior and the increase of fungal infections in the tropics, such as the increase in the spread of feline sporotrichosis, the increase in the resistance to antifungals of dermatophytes, and the invasive infection of immunocompetent hosts by "opportunistic" fungi such as *Cryptococcus*, as well as successful advances in experimental vaccines against cryptococcosis. Nonetheless, fungal diseases in tropical and subtropical areas continue to be a public health problem. Most of these fungal diseases are neglected and have low visibility, thereby affecting immunocompromised patients (such as persons living with HIV), people in low-income countries, and particularly agricultural workers in rural areas.

Author contributions

AG, CT, and JM edited the topic and wrote the manuscript. All authors contributed to the article and approved the submitted version.

Conflict of interest

The authors declare that the research was conducted in the absence of any commercial or financial relationships that could be construed as a potential conflict of interest.

Publisher's note

References

Arcobello, J. T., and Revankar, S. G. (2020). Phaeohyphomycosis. *Semin. Respir. Crit. Care Med.* 41 (1), 131–140. doi: 10.1055/s-0039-3400957

Casadevall, A. (2022). Immunity to invasive fungal dieseases. *Annu. Rev. Immunol.* 40, 121–141. doi: 10.1146/annurev-immunol-101220-034306

de Oliveira Pereira, F., Gomes, S. M., Lima da Silva, S., Paula de Castro Teixeira, A., and Lima, I. O. (2021). The prevalence of dermatophytoses in Brazil: A systematic review. *J. Med. Microbiol.* 70 (3). doi: 10.1099/jmm.0.001321

Gremião, I. D. F., Martins, da S., da Rocha, E., Montenegro, H., Carneiro, A. J. B., Xavier, M. O., et al. (2021). Guideline for the management of feline sporotrichosis caused by sporothrix brasiliensis and literature revision. *Braz. J. Microbiol.* 52 (1), 107–124. doi: 10.1007/s42770-020-00365-3

Queiroz-Telles, F., de Hoog, S., Santos, D. W., Salgado, C. G., Vicente, V. A., Bonifaz, A., et al. (2017). Chromoblastomycosis. *Clin. Microbiol. Rev.* 30 (1), 233–276. doi: 10.1128/CMR.00032-16

frontiers in Microbiology

CASE REPORT
published: 25 January 2017
doi: 10.3389/fmicb.2017.00083

Severe Chromoblastomycosis-Like Cutaneous Infection Caused by *Chrysosporium keratinophilum*

Juhaer Mijiti[1†], Bo Pan[2,3†], Sybren de Hoog[4], Yoshikazu Horie[5], Tetsuhiro Matsuzawa[6], Yilixiati Yilifan[1], Yong Liu[1], Parida Abliz[7], Weihua Pan[2,3], Danqi Deng[8], Yun Guo[8], Peiliang Zhang[8], Wanqing Liao[2,3] and Shuwen Deng[2,3,7]**

[1] Department of Dermatology, People's Hospital of Xinjiang Uygur Autonomous Region, Urumqi, China, [2] Department of Dermatology, Shanghai Changzheng Hospital, Second Military Medical University, Shanghai, China, [3] Key Laboratory of Molecular Medical Mycology, Shanghai Changzheng Hospital, Second Military Medical University, Shanghai, China, [4] CBS-KNAW Fungal Biodiversity Centre, Royal Netherlands Academy of Arts and Sciences, Utrecht, Netherlands, [5] Medical Mycology Research Center, Chiba University, Chiba, Japan, [6] Department of Nutrition Science, University of Nagasaki, Nagasaki, Japan, [7] Department of Dermatology, First Hospital of Xinjiang Medical University, Urumqi, China, [8] Department of Dermatology, The Second Affiliated Hospital of Kunming Medical University, Kunming, China

OPEN ACCESS

Edited by:
Leonard Peruski, US Centers for Disease Control and Prevention, USA

Reviewed by:
Nasib Singh, Eternal University, India
Ji Wang, Harvard Medical School, USA

***Correspondence:**
Shuwen Deng
shuwen.deng@gmail.com
Wanqing Liao
liaowanqing@sohu.com

[†] These authors have contributed equally to this work.

Specialty section:
This article was submitted to Infectious Diseases, a section of the journal Frontiers in Microbiology

Received: *18 November 2016*
Accepted: *12 January 2017*
Published: *25 January 2017*

Citation:
Mijiti J, Pan B, de Hoog S, Horie Y, Matsuzawa T, Yilifan Y, Liu Y, Abliz P, Pan W, Deng D, Guo Y, Zhang P, Liao W and Deng S (2017) Severe Chromoblastomycosis-Like Cutaneous Infection Caused by Chrysosporium keratinophilum. Front. Microbiol. 8:83. doi: 10.3389/fmicb.2017.00083

Chrysosporium species are saprophytic filamentous fungi commonly found in the soil, dung, and animal fur. Subcutaneous infection caused by this organism is rare in humans. We report a case of subcutaneous fungal infection caused by *Chrysosporium keratinophilum* in a 38-year-old woman. The patient presented with severe chromoblastomycosis-like lesions on the left side of the jaw and neck for 6 years. She also got tinea corporis on her trunk since she was 10 years old. *Chrysosporium keratinophilum* was isolated from the tissue on the neck and scales on the trunk, respectively. The patient showed satisfactory response to itraconazole therapy, although she discontinued the follow-up.

Keywords: *Chrysosporium keratinophilum*, cutaneous infection, fungal infection, diagnosis, treatment

INTRODUCTION

Chrysosporium species are saprophytic filamentous fungi occurring in soil, dung, animal fur, and bird feathers (Hocquette et al., 2005). *Chrysosporium keratinophilum* may cause mild infections in humans and is sometimes responsible for onychomycosis (Hocquette et al., 2005). However, subcutaneous infection resulting from *C. keratinophilum* has never been reported. Here, we present a case of severe chromoblastomycosis-like subcutaneous infection caused by *C. keratinophilum* from China.

CASE REPORT

A 38-year-old woman presented with a 4-year history of multiple verrucous nodules with a cauliflower-like appearance on her neck and face. The lesions were pruritic and progressively spread. Physical examination showed numerous verrucous nodules with superficial ulceration on the left side of her jaw and neck (**Figure 1A**). An isolated erythematous plaque with scale was also noted on her back (**Figure 1B**). The patient did not suffer from any known underlying disease or immunodeficiency. She noticed a first small nodule on her left ear without any trauma in 2010. The lesion gradually expanded to the left side of her neck. She did not pay attention to it until her pregnancy in 2012 when the lesions spread aggressively to the entire left side of the neck. Then

she was admitted to our hospital. She had a history of tinea corporis when she was 10 years old; at that time, other family members had the similar problem. Because of the patient's poor compliance with antifungal treatment (oral griseofulvin), the lesions on her trunk did not totally disappear but remained for years, although her family members were cured completely with the same therapy. Potassium hydroxide (KOH) direct examination of exudates from the plaque lesion in the neck

FIGURE 1 | (A) Initial presentation: plaques and multiple verrucous nodules as a cauliflower-like appearance, superficial ulceration filled with pus on her left side of jaw and neck. **(B)** Scaling lesions spontaneously appeared on her trunk. **(C,D)** Direct examination of 10% Potassium hydroxide (KOH) wet mounts of exudates from surface plaque of neck and scales from the trunk revealed hyphae fractions (×400).

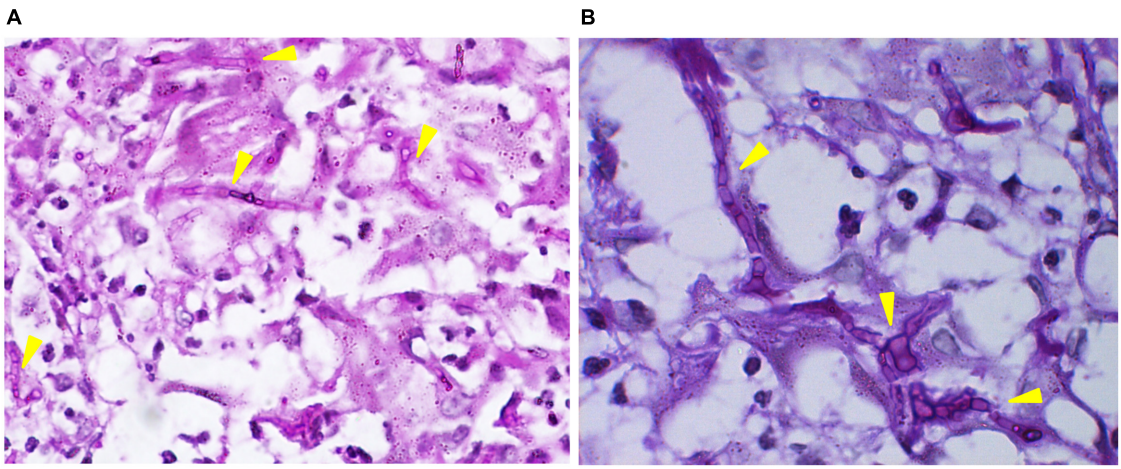

FIGURE 2 | (A,B) Septate hyphae were present in the dermis. (PAS stain, ×100 and ×400).

FIGURE 3 | (A) Aggravated lesion re-appeared on her neck. **(B)** Scaling lesions were also noticed on her trunk (arrows). **(C)** Lesions gradually disappeared after treatment.

and scales lesion from trunk revealed septate hyphal elements. Microscopic features of organisms from the two sites (her neck and trunk) were similar (**Figures 1C,D**). A biopsy taken from the lesion on the neck showed suppurative granulomata formation, and septate hyphal elements were found in the dermis and pus upon PAS (Periodic Acid-Schiff) staining (**Figures 2A,B**). Acid-fast staining was negative. Routine laboratory tests were unremarkable. Based on the histopathological and microscopic examination, a provisional diagnosis of a fungal infection was made, but no treatment was given during her pregnancy until her delivery when she received oral itraconazole (200 mg twice daily, BID) for 3 months. The rash dramatically reduced, and scaling lesions on her truck disappeared. However, the patient discontinued medication and was lost for follow-up. After 2 years (in 2014), the patient readmitted to our hospital with aggravated lesions on her neck again (**Figure 3A**). Scaling lesions were noticed on her trunk as well (**Figure 3B**). Therapy was given with itraconazole (200 mg, BID) for another 4 months. Plaques

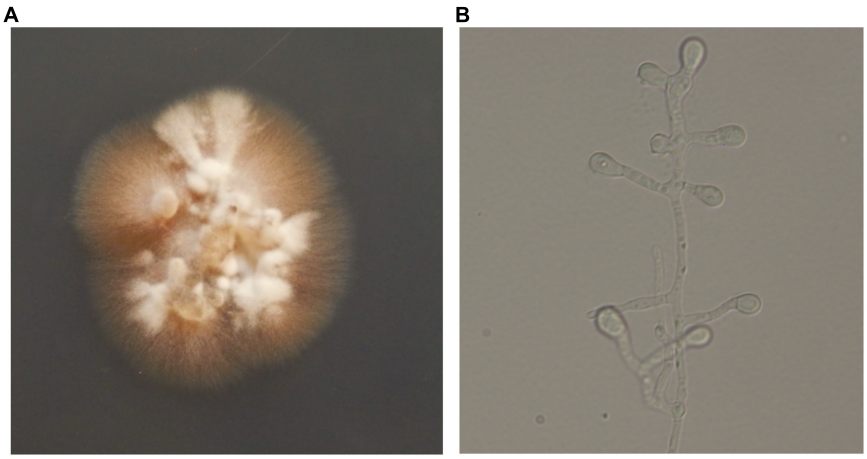

FIGURE 4 | (A) After incubating at 25°C for 2 weeks, colonies appeared yellowish white, fluffy, and dense, powdery at the center on potato dextrose agar (PDA). **(B)** Hyaline hyphae bearing conidia which were terminal or lateral, sessile or on short, cylindrical protrusions, thick-walled, obovoid to clavate with conspicuous basal scars (lactophenol solution, ×400).

and nodules gradually became flat with scarring left (**Figure 3C**). The scaling lesions on her trunk had disappeared completely. Unfortunately, the patient was lost for follow-up again.

MYCOLOGY

Direct microscopy of exudates from the lesion on the neck and scales on the trunk revealed septate hyphal elements (**Figures 1C,D**). Both clinical specimens were cultured on potato dextrose agar (PDA) at 25°C for up to 2 weeks. Colonies grew slowly, appeared yellowish white, fluffy, with a dense, powdery center (**Figure 4A**). Microscopy of hyphal colonies revealed the same morphology, hyaline hyphae bearing conidia which were terminal or lateral, sessile or on short, cylindrical protrusions, thick-walled, obovoid to clavate with conspicuous basal scars (**Figure 4B**), which were phenotypically identified as a *Chrysosporium* species. The identification was further confirmed by sequencing of ITS region of rDNA using the Blast program in GenBank which yielded a 99% identity match with the strain IFM 55159 of *C. keratinophilum* (accession no. AB361655). The isolate from neck was deposited in the collection of the Centraalbureau voor Schimmelcultures Fungal Biodiversity Centre (CBS) under strain number 142081 and the IFM collection (Medical Mycology Research Center of Chiba University, Japan) under strain number IFM 63626, ITS sequence was deposited in GenBank under accession number KT808269. The molecular investigation confirmed the mycological diagnosis and histopathological data led to the final diagnosis of chronic cutaneous granulomatous infection due to *Chrysosporium keratinophilum*.

DISCUSSION

The genus *Chrysosporium* contains morphologically simple fungi with one-celled, thallic conidia. With this definition, numerous unrelated species have been affiliated to the genus. Confusion has particularly been caused by reporting species of *Emmonsia* in the Onygenalean family *Ajellomycetaceae* comprising pulmonary colonizers of wild rodents, under the name *Chrysosporium* (Hubalek et al., 1998). In contrast, *Chrysosporium* species according to the current definition either reside as saprobes in habitats enriched with keratin such as bird feathers and animal hair when related to *Onygenaceae* (De Hoog et al., 2000; Hubalek, 2000), or cause skin infections in reptiles when affiliated to *Nannizziopsiacea* (Stchigel et al., 2013). In many reports in the literature, the etiologic agent had been identified only at genus level, which obviously is non-informative (Levy et al., 1991).

Chrysosporium keratinophilum is the anamorph of *Aphanoascus keratinophilus*, which is a member of *Onygenaceae* (Vidal et al., 2000). Species in this family are environmental saprobes on keratinous debris (Vidal et al., 2000). Asymptomatic carriage by animals and sometimes humans has been described (Woodgyer, 1977). Some species may be involved in human superficial infection and onychomycosis at low levels of virulence (Hocquette et al., 2005). Deep infections are extremely rare in immunocompromised patients (Warwick et al., 1991). In a retrospective study of onychomycosis in humans with diabetes mellitus, *C. keratinophilum* was isolated in 2.9% of the cases (Manzano-Gayosso et al., 2008). This suggests an advantage for the fungus with metabolic or immune disorders of the host. Our case concerned an exceptionally severe infection in an apparently immunocompetent female. Recent studies of primary immunodeficiencies (PIDs), a group of hereditary immune disorders with increased susceptibility to infection, have led to significant breakthroughs in our understanding of cellular and molecular mechanisms that predispose to both invasive and mucocutaneous fungal infections. Given the severity of the case, the recurrence of the fungus over decades, and the occurrence of similar infections in family members, a rare inherited immune disorder such as homozygous mutations in the CARD9 gene involved in the C-type lectin pathway may be surmised

(Alves de Medeiros et al., 2016; Wang and van de Veerdonk, 2016). Unfortunately, our patient was lost for follow-up before this was realized.

Etiology of *C. keratinophilum* in our case was proven by histological examination and mycological examination with presence of identical hyphal elements in both clinical specimens from neck and trunk. And two times of tissue biopsy culture revealed the same agent. These data provided strong evidence in favor of its pathogenicity in this exceptional, subcutaneous granulomatous infection. ITS sequencing further confirmed that the same species, which is not part of the commensal fungal flora of human skin, was involved in all lesions. The scaling lesions spontaneously appearing on the patient's trunk for over several decades caused by *C. keratinophilum* were prior to the neck lesions, which suggests fungal infection on the neck might have been acquired by scratching. The nodular lesions remind one of chromoblastomycosis because of significant dermal acanthosis, but differs by presence of exudates and septate hyphal elements rather than muriform cells in tissue. *In vivo* studies have shown the ability of *C. keratinophilum* to induce granulomatous lesions in white mice (Otcenasek and Dvorak, 1964; Hubalek and Hornich, 1977). However, to our knowledge, the species has never been reported from a cutaneous granulomatous infection in humans. Remarkably, the neck lesions took a different clinical aspect during pregnancy, strongly suggesting a hormonal contribution in addition to the surmised immune disorder. Similar aggravation of the infection during pregnancy was reported, e.g., *Veronaea botryosa* (Bonifaz et al., 2013) and *Exophiala spinifera* (Bonifaz et al., 2013; Wang et al., 2013). However, it remains unexplained why the trunk lesions remained as mildly hyperkeratotic patches during the same period of pregnancy. At present, no standard antifungal therapy can be recommended for *Chrysosporium* infections. In this case, the patient showed satisfactory response to the treatment with itraconazole, although she discontinued the follow-up. Considering the chronic course of the infection and the risk of sudden expansion and aggravation under hormonal influence, adequate monitoring to timely adjust the therapeutic regimen is recommended.

ETHICS STATEMENT

The study was carried out in accordance with the Declaration of Helsinki and was approved by the Committee on Ethics of Biomedical Research, Second Military Medical University (Shanghai, China). The written informed consent was obtained from the study patient.

AUTHOR CONTRIBUTIONS

JM, BP, SH, YH, TM, YY, YL, PA, WP, DD, YG, PZ, WL, and SD contributed to the conception of the work, the acquisition, analysis and interpretation of the clinical features and fungal characteristics. SH, JM, BP, WL, and SD substantially contributed to drafting and critically revising the work. All authors read and approved the final manuscript.

FUNDING

This study was supported by the Xinjiang Nature Science Fund No. 2012211A063 of China.

REFERENCES

Alves de Medeiros, A. K., Lodewick, E., Bogaert, D. J., Haerynck, F., Van Daele, S., Lambrecht, B., et al. (2016). Chronic and invasive fungal infections in a family with CARD9 deficiency. *J. Clin. Immunol.* 36, 204–209. doi: 10.1007/s10875-016-0255-8

Bonifaz, A., Davoudi, M. M., de Hoog, G. S., Padilla-Desgarennes, C., Vazquez-Gonzalez, D., Navarrete, G., et al. (2013). Severe disseminated phaeohyphomycosis in an immunocompetent patient caused by *Veronaea botryosa*. *Mycopathologia* 175, 497–503. doi: 10.1007/s11046-013-9632-5

De Hoog, G. S., Guarro, J., Figueras, M. J., Gené, J., and Hubalek, Z. (2000). *Atlas of Clinical Fungi*, 2nd Edn. Spain: Reus.

Hocquette, A., Grondin, M., Bertout, S., and Mallié, M. (2005). *Acremonium*, *Beauveria*, *Chrysosporium*, *Fusarium*, Onychocola, *Paecilomyces*, *Penicillium*, *Scedosporium* and *Scopulariopsis* fungi responsible for hyalohyphomycosis. *J. Mycol. Méd.* 15, 136–149.

Hubalek, Z. (2000). Keratinophilic fungi associated with free-living mammals and birds: revista iberoamericana de micologia. *Rev. Iberoam. Micol.* 17, 93–103.

Hubalek, Z., and Hornich, M. (1977). Experimental infection of white mouse with *Chrysosporium* and *Paecilomyces*. *Mycopathologia* 62, 173–178. doi: 10.1007/BF00444111

Hubalek, Z., Nesvadbova, J., and Halouzka, J. (1998). Emmonsiosis of rodents in an agroecosystem. *Med. Mycol.* 36, 387–390. doi: 10.1111/j.1365-280X.1998.00177.x

Levy, F. E., Larson, J. T., George, E., and Maisel, R. H. (1991). Invasive *Chrysosporium* infection of the nose and paranasal sinuses in an immunocompromised host. *Otolaryngol. Head Neck Surg.* 104, 384–388. doi: 10.1177/019459989110400317

Manzano-Gayosso, P., Hernandez-Hernandez, F., Mendez-Tovar, L. J., Palacios-Morales, Y., Cordova-Martinez, E., Bazan-Mora, E., et al. (2008). Onychomycosis incidence in type 2 diabetes mellitus patients. *Mycopathologia* 166, 41–45. doi: 10.1007/s11046-008-9112-5

Otcenasek, M., and Dvorak, J. (1964). The isolation of *Chrysosporium keratinophilum* (Frey) carmichael 1962 and similar fungi from czechoslovakian soil. *Mycopathol. Mycol. Appl.* 23, 121–124. doi: 10.1007/BF02049267

Stchigel, A. M., Sutton, D. A., Cano-Lira, J. F., Cabanes, F. J., Abarca, L., Tintelnot, K., et al. (2013). Phylogeny of chrysosporia infecting reptiles: proposal of the new family *Nannizziopsiaceae* and five new species. *Persoonia* 31, 86–100. doi: 10.3767/003158513X669698

Vidal, P., Vinuesa, M. A., Sanchez-Puelles, J. A., and Guarro, J. (2000). "Phylogeny of the anamorphic genus *Chrysosporium* and related taxa based on rDNA internal transcribed spacer sequences," in *Biology of Dermatophytes and other Keratinophilic fungi*, eds R. K. S. Kushwaha and J. Guarro (Spain: Bilbao), 22–28.

Wang, L., She, X., Lv, G., Shen, Y., Cai, Q., Zeng, R., et al. (2013). Cutaneous and mucosal phaeohyphomycosis caused by *Exophiala spinifera* in a pregnant patient: case report and literature review. *Mycopathologia* 175, 331–338. doi: 10.1007/s11046-012-9611-2

Wang, X., and van de Veerdonk, F. L. (2016). When the fight against fungi goes wrong. *PLoS Pathog.* 12:e1005400. doi: 10.1371/journal.ppat.1005400

Warwick, A., Ferrieri, P., Burke, B., and Blazar, B. R. (1991). Presumptive invasive Chrysosporium infection in a bone marrow transplant recipient. *Bone Marrow Transplant.* 8, 319–322.

Woodgyer, A. J. (1977). Asymptomatic carriage of dermatophytes by cats. *N. Z. Vet. J.* 25, 67–69. doi: 10.1080/00480169.1977.34360

Conflict of Interest Statement: The authors alone are responsible for the content and writing of the paper. The authors declare that the research was conducted in the absence of any commercial or financial relationships that could be construed as a potential conflict of interest.

frontiers in Microbiology

ORIGINAL RESEARCH
published: 09 October 2017
doi: 10.3389/fmicb.2017.01924

Comparative Genomics of Sibling Species of *Fonsecaea* Associated with Human Chromoblastomycosis

Vania A. Vicente[1,2†], Vinícius A. Weiss[3,4†], Amanda Bombassaro[1], Leandro F. Moreno[1,5,6], Flávia F. Costa[2], Roberto T. Raittz[3], Aniele C. Leão[2,3,4], Renata R. Gomes[1], Anamelia L. Bocca[7], Gheniffer Fornari[1], Raffael J. A. de Castro[7], Jiufeng Sun[8], Helisson Faoro[4], Michelle Z. Tadra-Sfeir[4], Valter Baura[4], Eduardo Balsanelli[4], Sandro R. Almeida[9], Suelen S. Dos Santos[9], Marcus de Melo Teixeira[7,10], Maria S. Soares Felipe[11], Mariana Machado Fidelis do Nascimento[1], Fabio O. Pedrosa[4], Maria B. Steffens[3,4], Derlene Attili-Angelis[12], Mohammad J. Najafzadeh[13], Flávio Queiroz-Telles[1,14], Emanuel M. Souza[3,4] and Sybren De Hoog[1,5,6*]*

[1] Microbiology, Parasitology and Pathology Post-Graduation Program, Department of Basic Pathology, Federal University of Paraná, Curitiba, Brazil, [2] Bioprocess Engineering and Biotechnology, Federal University of Paraná, Curitiba, Brazil, [3] Laboratory of Bioinformatics, Sector of Technological and Professional Education, Federal University of Paraná, Curitiba, Brazil, [4] Department of Biochemistry, Federal University of Paraná, Curitiba, Brazil, [5] CBS-KNAW Fungal Biodiversity Centre, Utrecht, Netherlands, [6] Institute for Biodiversity and Ecosystem Dynamics, University of Amsterdam, Amsterdam, Netherlands, [7] Department of Cell Biology, University of Brasília, Brasilia, Brazil, [8] Guangdong Provincial Institute of Public Health, Guangdong Provincial Center for Disease Control and Prevention, Guangzhou, China, [9] Department of Clinical and Toxicological Analysis, Faculty of Pharmaceutical Sciences, University of São Paulo, Sao Paulo, Brazil, [10] Pathogen and Microbiome Institute, Northern Arizona University, Flagstaff, AZ, United States, [11] Department of Genomic Sciences and Biotechnology, Catholic University of Brasília, Brasilia, Brazil, [12] Division of Microbial Resources (DRM/CPQBA), University of Campinas, Campinas, Brazil, [13] Department of Parasitology and Mycology, School of Medicine, Mashhad University of Medical Sciences, Mashhad, Iran, [14] Clinical Hospital of the Federal University of Paraná, Curitiba, Brazil

Fonsecaea and *Cladophialophora* are genera of black yeast-like fungi harboring agents of a mutilating implantation disease in humans, along with strictly environmental species. The current hypothesis suggests that those species reside in somewhat adverse microhabitats, and pathogenic siblings share virulence factors enabling survival in mammal tissue after coincidental inoculation driven by pathogenic adaptation. A comparative genomic analysis of environmental and pathogenic siblings of *Fonsecaea* and *Cladophialophora* was undertaken, including *de novo* assembly of *F. erecta* from plant material. The genome size of *Fonsecaea* species varied between 33.39 and 35.23 Mb, and the core genomes of those species comprises almost 70% of the genes. Expansions of protein domains such as glyoxalases and peptidases suggested ability for pathogenicity in clinical agents, while the use of nitrogen and degradation of phenolic compounds was enriched in environmental species. The similarity of carbohydrate-active vs. protein-degrading enzymes associated with the occurrence of virulence factors suggested a general tolerance to extreme conditions, which might explain the opportunistic tendency of *Fonsecaea* sibling species. Virulence was tested in the *Galleria mellonella* model and immunological assays were performed in order to support this hypothesis. Larvae infected by environmental *F. erecta* had a lower survival.

OPEN ACCESS

Edited by:
Hector Mora Montes, Universidad de Guanajuato, Mexico

Reviewed by:
Sonia Rozental, Federal University of Rio de Janeiro, Brazil
Luis Antonio Pérez-García, Universidad Autónoma de San Luis Potosí, Mexico

***Correspondence:**
Emanuel M. Souza
souzaem@ufpr.br
Sybren De Hoog
s.hoog@westerdijkinstitute.nl

† These authors have contributed equally to this work.

Specialty section:
This article was submitted to Fungi and Their Interactions, a section of the journal Frontiers in Microbiology

Received: *02 August 2017*
Accepted: *21 September 2017*
Published: *09 October 2017*

Citation:
Vicente VA, Weiss VA, Bombassaro A, Moreno LF, Costa FF, Raittz RT, Leão AC, Gomes RR, Bocca AL, Fornari G, de Castro RJA, Sun J, Faoro H, Tadra-Sfeir MZ, Baura V, Balsanelli E, Almeida SR, Dos Santos SS, Teixeira MdM, Soares Felipe MS, do Nascimento MMF, Pedrosa FO, Steffens MB, Attili-Angelis D, Najafzadeh MJ, Queiroz-Telles F, Souza EM and De Hoog S (2017) Comparative Genomics of Sibling Species of Fonsecaea Associated with Human Chromoblastomycosis. Front. Microbiol. 8:1924. doi: 10.3389/fmicb.2017.01924

Fungal macrophage murine co-culture showed that *F. erecta* induced high levels of TNF-α contributing to macrophage activation that could increase the ability to control intracellular fungal growth although hyphal death were not observed, suggesting a higher level of extremotolerance of environmental species.

Keywords: *Fonsecaea* species, black yeast, genomics, chromoblastomycosis, comparative genomics, *Fonsecaea erecta*

INTRODUCTION

Melanized fungi belonging to the order Chaetothyriales are clinically relevant as agents of a gamut of diseases in humans and animals, varying in severity from superficial to systemic and fatal infections (De Hoog et al., 2004; Badali et al., 2008; Seyedmousavi et al., 2011). A large number of species have complex life cycles, indicating dynamic niches or vectored transmission (Sudhadham et al., 2008). In the environment, they occupy adverse micro-habitats, which is probably stimulated by their low competitive ability toward co-occurring microorganisms, judged from the fact that their isolation is enhanced significantly by the use of selective methods (Vicente et al., 2014). Many species of Chaetothyriales cause implantation diseases from an environmental source. One of the common disorders is chromoblastomycosis, a mutilating and recalcitrant skin disease eventually leading to emerging eruptions. Fungal cells in host tissue provoke as an inflammatory granulomatous disease (De Hoog et al., 2007; de Azevedo et al., 2015a; Queiroz-Telles, 2015). Agents of chromoblastomycosis are traumatically inoculated from environmental sources such as plant thorns or wooden splinters carrying the respective opportunist (Salgado et al., 2004; De Hoog et al., 2007; Vicente et al., 2014). Those species are mainly found in *Fonsecaea* and *Cladophialophora*, of which *F. pedrosoi, F. monophora*, and *Cladophialophora carrionii* are recurrently recovered from patients in tropical and semi-arid climate zones, respectively around the globe (Xi et al., 2009; Queiroz-Telles, 2015). Recently, less common agents were described, such as *F. nubica* (Najafzadeh et al., 2010), *F. pugnacius* (de Azevedo et al., 2015b), and *C. samoensis* (Badali et al., 2010). The genera *Fonsecaea* and *Cladophialophora* are morphologically classified by differences in their conidial apparatus; however, DNA polymorphisms suggest that both genera are polyphyletic (De Hoog et al., 2007), as they are distributed within "bantiana-clade" and "carrionii-clade" groups of the family Herpotrichiellaceae (Chaetothyriales) (Vicente et al., 2014; de Azevedo et al., 2015b).

Closely related species of *Fonsecaea* differ significantly in their ecology and ability to cause infection in humans and animals (Vicente et al., 2014); virulence genes seem to be unequally distributed among members of the bantiana-clade. *Fonsecaea pedrosoi* and *F. nubica* are strictly associated to chromoblastomycosis, while *F. monophora* also causes primary brain disease (Surash et al., 2005; Takei et al., 2007; Koo et al., 2010). *Fonsecaea multimorphosa* and *F. brasiliensis* were isolated from disseminated infections in animal hosts (Najafzadeh et al., 2011; Vicente et al., 2012) and the environmental species *F. erecta* and *F. minima* were described from plants and no report from clinical cases (Vicente et al., 2014) has as yet been published.

Therefore, the central question of the present study concerns the difference in infectious potential between closely related members of *Fonsecaea*. Agents of chromoblastomycosis upon tissue invasion show dimorphism to muriform cells, while this behavior is not known from most plant debris-inhabiting siblings (Queiroz-Telles, 2015). Comparative genomic analysis of *Fonsecaea* pathogenic and non-pathogenic siblings was applied to highlight genes involved in fungal adaptation from a plant debris- to an animal-associated life style. To this aim, a *de novo* assembly of *F. erecta* and recently published black yeast genomes (Bombassaro et al., 2016; Costa et al., 2016; Leão et al., 2017; Teixeira et al., 2017) was included in the analysis.

MATERIALS AND METHODS

Genomic DNA Extraction, Sequencing, and *de Novo* Assembly of *Fonsecaea erecta* CBS 125763^T

A large-scale DNA extraction was conducted based on a method as described by Vicente et al. (2008). The strains were grown in Sabouraud broth for 7 days. The DNA was extracted by the cetyltrimethylammonium bromide (CTAB) method based and phenol-chloroform/isoamyl alcohol. Total DNA was purified with the Microbial DNA UltraClean™ kit. The genome was sequenced on MiSeq (Illumina™) sequencer using paired-end and mate-paired libraries and on Ion Proton (Thermo Fisher Scientific™) sequencer using single-end approaches. The library construction was done with Ion Plus Fragment Library Kit (Thermo Fisher Scientific™) and Nextera XT (Illumina™) following the manufacturer instructions. The read quality analysis was performed with FastQC and reads with quality below PHRED20 were removed (Andrews, 2016). The reads were assembled *de novo* using SPAdes v3.6.2 (Bankevich et al., 2012). The gap closure was performed with FGAP (Piro et al., 2014) and scaffolding with SSPACE (Boetzer et al., 2010). The mitochondrial genomes were assembled in *Fonsecaea* species by extracting reads using the complete mtDNA of *Exophiala dermatitidis* as reference. The reads were mapped using Bowtie2 (Langmead and Salzberg, 2012) and the mapped reads assembled with SPAdes v3.6.2 (Bankevich et al., 2012).

Gene Prediction and Annotation

Protein-coding genes were predicted with GeneMark-ES v4.39 (Besemer, 2001). The automatic annotation was done by

RAFTS3 (Vialle et al., 2016) best hits comparison with self-score cutoff of 0.5 using a black yeast protein database available on (www.broadinstitute.org/annotation/genome/Black_Yeasts/). Protein domain families and functional annotation was accessed using InterProScan5 (Quevillon et al., 2005). The tRNAs annotation used the ARAGORN software (Laslett and Canback, 2004). Putative enzymes and peptidases coding genes using CAZY (Cantarel et al., 2009) and peptidases coding genes using MEROPS database (Rawlings et al., 2015) and putative pathogen host interaction genes using PHI base (Winnenburg et al., 2007). Pathogen Host interacting (PHI) partners were identified by subjecting the predicted proteomes to BLASTp against the PHI database v4.2 with an *E*-value threshold of 10–5 with best hits.

Comparative Genomic Analysis of the Genus *Fonsecaea*

We compared the genome of *F. erecta* CBS 125763^T to 5 *Fonsecaea* species, including *F. monophora*, CBS 269.37^T (Bombassaro et al., 2016), *F. nubica* CBS 269.64^T (Costa et al., 2016), *F. multimorphosa* CBS 980.96^T (Leão et al., 2017), *Fonsecaea multimorphosa* CBS 102226 (Teixeira et al., 2017), and *F. pedrosoi* CBS 271.37^T (Teixeira et al., 2017) in addition to other 6 black yeast-like fungi belonging to the order Chaetothyriales (Teixeira et al., 2017): *Cladophialophora carrionii* CBS 160.54, *Cladophialophora yegresii, Capronia semiimmersa, Cladophialophora bantiana, Cladophialophora psammophila, Cladophialophora immunda,* and *Rhinocladiella mackenziei* (**Table 2**).

Protein sequences were compared using an all-vs.-all similarity search and self-score cutoff of 0.5 using RAFTS3 (Vialle et al., 2016). The clustering was done when at least one protein was shared amidst clusters. After the clustering verification step was done K-means and the cluster vectors where split into new clusters using the ratio of the cluster size and the number of organisms present in the analysis. For the resulting clusters it was calculated a centroid for each vector and chosen the best gene that represents each cluster based on the shortest distance. For both K-means and centroid analysis, a vectorial representation for the genes was created based on sparse *k*-mers sequences. A final clustering step was done using RAFTS all-vs.-all similarity searches with self-score of 90 (Vialle et al., 2016). The amino-acid sequences of each family were aligned with Muscle (Edgar, 2004) and poorly aligned regions were automatically removed using GBLOCKS (Talavera and Castresana, 2007). A maximum likelihood tree was done using PHYML (Guindon et al., 2005) and 1,000 bootstraps were used to infer branch support.

Genome Expansions and Contractions Based on Functional Domains

To identify functional expansions and contractions, InterPro domains were predicted using InterProScan5 (Quevillon et al., 2005) for 12 strains of black yeast species: 6 *Fonsecaea* species, 5 *Cladophialophora* species and 1 *Coniosporium apollinis* as outgroup (**Table 2**). Gene family evolution was estimated with CAFE version 3.0 (De Bie et al., 2006) using significance family-wide *p*-values threshold of <0.05 and VITERBI $p < 0.001$. To search for BIRTH (λ) values we run the program with the "-s" option. Two files were used as input in CAFE analyses: a table containing organism number of copies of each InterPro domain and an ultrametric tree.

Prediction of Genes Related to Pathogenicity

In order to research genes related to pathogenicity through analysis of the core, clusters and perform a correlation analysis, initially were rescued the 22 yeast genomes available at Broad Institute (http://www.broadinstitute.org/annotation/genome/Black_Yeasts/GenomesInde) and including the *Fonsecaea* sibling associated to (sub)cutaneous and systemic infection, totaling 26 genomes. They were all (re) annotated using toolbox RAFTS3 (Vialle et al., 2016). The next step was to vectorize and cluster each gene, which generated 28,355 gene clusters equal or bigger the 50% of identity between them. This analysis was sized in an array with 26 rows × 28,355 columns, the rows being the organisms and the columns all the genes of all clustered organisms.

To perform the correlation analysis between the clusters using Point-biserial correlation to each of 28,355 clusters, we selected a set of genes that was used as reference to access a set of already known pathogenic genes, being them: Cell Division Control Protein 42 (KIV82855.1), Cytochrome P450 (KIW97819.1), Thioredoxin (XP_013289847.1), HSP60-like protein (KIW92920.1), HSP90-like protein (AYO21_00238), Homogentisate 1,2-dioxygenase (KIW31930.1), and two hypothetical proteins (AYO21_05248 and KIW22607.1) which were present in the same clusters of paraoxonases.

The correlations of each cluster with the frequency of these pathogenic set genes in the organisms were calculated according to formula (**Figure 1**), which was filtered in 1,803 clusters of genes. Analyzing the gene families within organism related to systemic infection (*F. multimorphosa, C. bantiana, F. monophora,* and *R. mackenziei*) and subcutaneous infection (*F. pedrosoi, C. carrionii, F. monophora,* and *F. nubica*) only 280 showed positive correlation above 80% with 5.5×10^{-7} of max *e*-value.

$$r_{rp} = \frac{M_1 - M_0}{S_n} \sqrt{\frac{n_1 n_0}{n^2}}$$

FIGURE 1 | The point-biserial correlation coefficient: measure of the relationship between a continuous and a binary variable. For each protein of the 26 analyzed genomes, 0 and 1 scores correspond to the presence or absence of a protein of the binary variable, respectively. M1 is the mean of the presence of proteins and M0 is the mean of the missing proteins. The value "n" represents the total number of the proteins, where n1 is the total of proteins present and n0 are the total of the missing proteins. Sn is the standard deviation of the continuous variable.

Virulence Test of *Fonsecaea* Sibling Species Using *Galleria mellonella* Larvae As a Model

Fungal Strains, Growth Condition, and Inoculum Preparation

The strains *F. pedrosoi* ATCC 46428, *F. pedrosoi* CBS 271.37, *F. erecta* CBS 125763 and *F. monophora* CBS 102248 were selected for this study. The yeast strains were grown on Sabouraud Glucose Agar (SGA; Himedia, Mumbai, India) at 28°C for 7 days, transferred to Potato Dextrose Broth (PDB; Himedia) and incubated under agitation (150 rpm) at 37°C. After 5 days, the cultures were allowed to settle in order to decant the larger particles such as hyphae and conidia. Fungal cells were separated by filtration through a 40 μm cell strainer, (BD) washed with PBS 1× three times. Finally, the cells were re-suspended at 1×10^6 cells/mL for *F. pedrosoi* ATCC 46428, *F. pedrosoi* CBS 271.37, and *F. erecta* CBS 125763, or at 1×10^5 cells/mL for *F. monophora* CBS 102248.

Larvae Selection and Infection

Galleria mellonella larvae were selected using as criteria similar size and weight ranging 0.10–0.15 (g). For the survival experiments, each group consisted of 20 larvae. The selected larvae were inoculated by injecting 10 μL of the different inoculum in the last left pro-leg with a Hamilton syringe (0.75 mm diameter needle) according to Fuchs et al. (2010). The control group was inoculated with PBS and the same number of larvae. The following control groups were used in the experiment. The first group included the larvae that received 10 μL of PBS to monitoring survival mortality related to trauma. A second group of larvae (SHAM) received no injection and no injury. All larvae were placed in sterile Petri dishes and kept in the dark at 37°C. Mortality was monitored once per day. The death of the larvae was assessed by the lack of movement, no response to stimulation and discoloration of the cuticle. Melanization was checked every 24 h with a NIKON D3100 camera and images were analyzed. Survival curves were plotted and statistical analyses were performed using the Log-rank (Mantel-Cox) test with Graph Pad Prism software. Statistical differences were set at $p < 0.05$.

Histopathology

Larvae were fixed by immersion in Carnoy (60% methanol, 30% chloroform and 10% acetic acid) 7 days after infection. After 48 h the larvae were immersed in 70% ethanol. Then the sections were then embedded in paraffin wax, sectioned and stained with Periodic Acid-Schiff (PAS) for microscopic examination. The photomicrographs were obtained from Olympus BX41 microscope coupled with digital camera Olympus SC30.

Fungal Macrophage Co-culture

The strains *F. pedrosoi* CBS 271.37 and *F. erecta* CBS 125763 were cultivated on Sabouraud Glucose Agar (SGA, Himedia) supplemented with 100 mg/L^{-1} chloramphenicol at 37°C. To obtain purified conidia and hyphae, fungi propagules were grown in PDB supplemented with 100 mg/L^{-1} chloramphenicol, in a rotary shaker (120 rpm) at 30°C. Fungal purification was performed according to Siqueira et al. (2017). Briefly, 15 days suspension containing conidia and hyphal fragments was subjected to successive filtrations through 70 μm and 40 μm cell strainers (BD). Hyphae retained on the 40 μm cell strainer were re-suspended in phosphate buffered saline (PBS), centrifuged at 1,000 × g and re-suspended in PBS. This process was repeated twice. Ninety-eight percent of 98% of this suspension consisted of hyphae. The 40 μm cell strainer filtrate containing conidia and small hyphal fragments was subjected to a filtration through 14 μm filter paper (J. Prolab, Brazil), washed twice in PBS, and recovered by centrifugation at 3,000 × g. This fraction contained conidia more than 98% pure.

Macrophage infection assays were adapted from Hayakawa et al. (2006), Palmeira et al. (2008) and Siqueira et al. (2017). Mouse macrophages (J774 cell line) were plated in DMEM (Dulbecco's Modified Eagle's medium, Sigma) supplemented with 10% heat-inactivated fetal bovine serum (Gibco) and infected with conidia or hyphae of the *Fonsecaea* species at a multiplicity of infection (MOI) of 1. After 3 h of infection, non-phagocytized fungi were washed, fresh medium was added and co-culture was allowed to proceed for 24 h. For fungal burden determination (number of fungal cells in macrophages), macrophages were lysed with 0.05% SDS solution. Intracellular fungi were quantified by plating serial dilutions of cell lysates onto SDA medium, supplemented with 100 mg/L^{-1} chloramphenicol and cultivated at 30°C for 7 days. Fungal burden was then measured by counting fungi colony-forming units (CFU). The cell culture supernatants were used to determine tumor necrosis factor-α (TNF-α) levels by enzyme-linked immunosorbent assay (ELISA), in accordance with manufacture's (eBioscience) instructions. As positive control to TNF-α production, 500 ng/mL LPS (*Escherichia coli* serotype 0111:B, Sigma-Aldrich) was used. Results were expressed as number of CFU or pg/mL of cytokine ± standard deviation (SD).

Mice Infection

BALB/c mice were maintained under standard laboratory conditions. Mice (10–12 weeks old males) were inoculated by injecting 50 μL (per hind footpad) of PBS containing 1×10^6 *F. pedrosoi* or *F. erecta* propagules obtained by mixing the purified hyphae and conidia in the proportion of 3:1, respectively. Five animals per group were euthanized with CO_2 in an appropriate chamber at 7 and 14 days post-infection. The mice footpad were photographed, removed, weighed and thereafter homogenized in tubes with steel beads on a Precellys homogenizer. For fungal burden determination, homogenized tissue were diluted and plated as above mentioned. Results were expressed as number of CFU ± standard error of mean (SEM) per gram of fresh tissue. Cytokine production was measured from homogenized tissue obtained from infected and non-infected animals (healthy) by ELISA. The cytokines interleukin-1β (IL-1β), TNF-α, interleukin-6 (IL-6) and monocyte chemoattractant protein-1 (MCP-1/Ccl2) were measured with kits purchased from eBioscience and used according the manufacturer's instructions. Results were expressed as pg of cytokine ± standard error of mean (SEM) per 100 milligrams of tissue. All animal experimentation in this study were approved by the Federal University of Paraná Ethics Committee (approval

certificate 1002) and performed according to the Committee's recommendations.

RESULTS

De Novo Assembly of *Fonsecaea erecta* and Genome Contents of *Fonsecaea* Siblings

Whole genome sequencing of *Fonsecaea erecta* CBS 125763^T was performed using Illumina Hiseq 2000 and yielded 1,534,038 paired-end reads with average insert size of 1 Kb ± 1 Kb and 3,133 mate-paired reads with average insert size of 5 Kb ± 4 Kb. To increase sequence coverage, two additional Ion Torrent shotgun libraries were sequenced generating 5.4 Gb and 25,219,375 single reads. The final high quality draft genome of *Fonsecaea erecta* comprised 57 scaffolds. The genome size was estimated to be 34.75 Mb, with average coverage of 60X and G+C content of 53%. Protein coding regions account for 18,279,031 bp, corresponding to 12,327 genes. A total of 12,090 proteins encoding genes, one rRNA multi-copy segment and 30 tRNA genes were predicted (**Table 1**).

Comparing *F. erecta* with related species of Chaetotryriales it was observed that all genomes used in this study including the reference species are similar in size. The genome size of *Fonsecaea* species varied between 33.39 and 35.23 Mb. The *F. monophora* genome is nearly 1.84 Mb larger in size following of the plant associate species *F. erecta* with 34.75, while the reference genome of the species plant-associated *Cladophialophora yegresii* presented a reduced size of 27.9 Mb. The total number of initial predicted genes in *Fonsecaea* varied between 11,681 in *F. nubica* to 12,527 in *F. pedrosoi*; between 10,944 (93.69%) and 11,948 (96.59%) of the genes identified as conserved hypothetical proteins. In addition, repetitive element identification was considered to be low in *Fonsecaea* siblings, ranging from 1.06 to 1.13% in *F. multimorphosa* to 1.93% in *F. monophora* (**Table 2**).

Mitochondrial Genomes

Fonsecaea erecta CBS 125763^T and *F. pedrosoi* CBS 271.37^T mtDNA was assembled in one contig, measuring 25.7 and 25 Kb, respectively. The mtDNA of *F. monophora* assembled into eight contigs comprising 24.7 Kb, the mtDNA of *F. nubica* resulted in a single contig with 24.5 Kb and the mtDNA of *F. multimorphosa* CBS 980.96^T resulted in seven contigs with a size of 26.4 Kb. Although the gene composition of all

TABLE 1 | *Fonsecaea erecta* genome data assembly and quality.

Information	Value
Genome size (Mb)	34.75
DNA coding (bp)	18,279,031
DNA G+C (%)	53
DNA scaffolds	57
Coverage	60X
tRNA	30

TABLE 2 | Genome studied.

Species	Strains	Source	Geography	GeneBank genome	Genome size (Mb)	G+C content (%)	Repetitive elements	Hypothetical proteins
Capronia semiimmersa	CBS 27337	Human chromoblastomycosis	Brazil	JYCC00000000.1	31.62	53.7	0.71	92,23
Cladophialophora bantiana	CBS 173.52	Human chromoblastomycosis	USA	JYBT00000000.1	36.72	51.3	4.47	93,10
Cladophialophora carrionii	CBS 160.54	Human chromoblastomycosis	Australia	PRJNA185784	28.99	54.3	1.15	91,98
Cladophialophora immunda	CBS 834.96	Human skin lesion	USA	JYBZ00000000.1	43.03	52.8	2.24	93,00
Cladophialophora psammophila	CBS 110553	Gasolin-polluted soil	Netherlands	AMGX00000000.1	39.42	50.6	6.92	82,89
Cladophialophora yegresii	CBS 114405	*Stenocereus griseus* cactus	Venezuela	AMGW00000000.1	27.90	54	1.13	79,56
Coniosporium apollinis	CBS 100218	Pentelic marble	Greece	AJKL00000000.1	28.65	52.1	–	85,72
Fonsecaea erecta	CBS 125763	Living plant	Brazil	LVYI00000000.1	34.75	53	1.74	90,54
Fonsecaea monophora	CBS 269.37	Human chromoblastomycosis	South America	LVKK00000000.1	35.23	52.22	1.93	93,88
Fonsecaea multimorphosa	CBS 980.96	Cat brain abcess	Australia	LVCI00000000.1	33.39	52.64	1.06	96,34
Fonsecaea multimorphosa	CBS 102226	Decaying trunk palm tree	Brazil	PRJNA233317	33.45	52.6	1.13	96,59
Fonsecaea nubica	CBS 269.64	Human chromoblastomycosis	Cameroon	LVCJ00000000.1	33.79	52.46	1.59	93,69
Fonsecaea pedrosoi	ATCC 46428	Human chromoblastomycosis	South America	PRJNA233314	34.69	52.4	1.5	92,87
Fonsecaea pedrosoi	CBS 271.37	Human chromoblastomycosis	South America	PRJNA233314	34.69	52.4	1.5	92,87
Rhinocladiella mackenziei	CBS 650.93	Human cerebral phaeohyphomycosis	Saudi Arabia	JYBU00000000.1	32.47	50.4	3.49	92,48

mitochondrial genomes analyzed shared 16 protein coding genes involved in the respiratory chain and ATP synthesis, the synteny of these genes is not conserved, showing rearrangements when compared between *Fonsecaea* species and with the reference sequence of *E. dermatitidis* (**Figure 2**).

Orthologous Gene Comparison among *Fonsecaea* Siblings

In order to study gene family evolution in *Fonsecaea*, we identified 20,713 orthologous gene clusters across 17 fungal genomes of environmental species and agents of subcutaneous and disseminated infection in animals and humans, including 9 species from the bantiana-clade and 2 from the carrionii-clade using *Coniosporium apollinis, Exophiala aquamarina,* and *Phialophora attae* as outgroup. The comparison showed a total of 5,727 of gene family clusters shared among *Fonsecaea* species, which was used to build a phylogenomic tree (**Figure 3A**).

The analysis showed strong support for published phylogenetic relationships between bantiana-and carrionii-clades in the order Chaetothyriales. Agents of chromoblastomycosis were distributed in the separate clades, with species associated with vertebrate infection clearly being distinct from environmental siblings. *Fonsecaea pedrosoi* and *F. nubica* causing chromoblastomycosis were closely affiliated with *F. monophora* involved in the same disease and as well as in brain infection. The plant-associated *F. erecta* is distinct from the clinical species. In addition, *F. multimorphosa*, an environmental species that once caused a feline cerebral

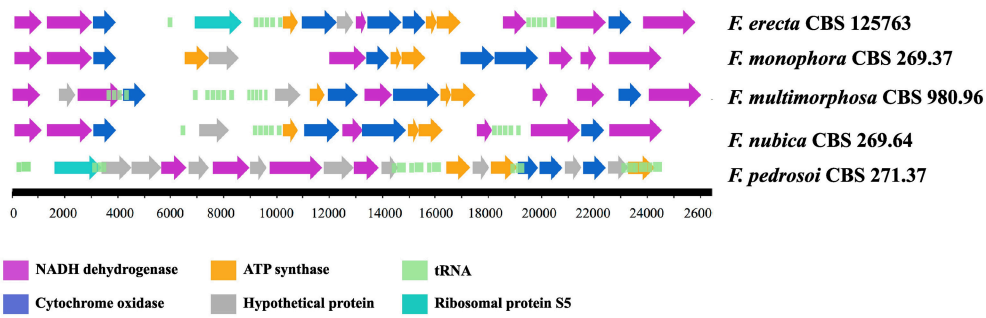

FIGURE 2 | Mitochondrial genomes of *Fonsecaea* sibling species.

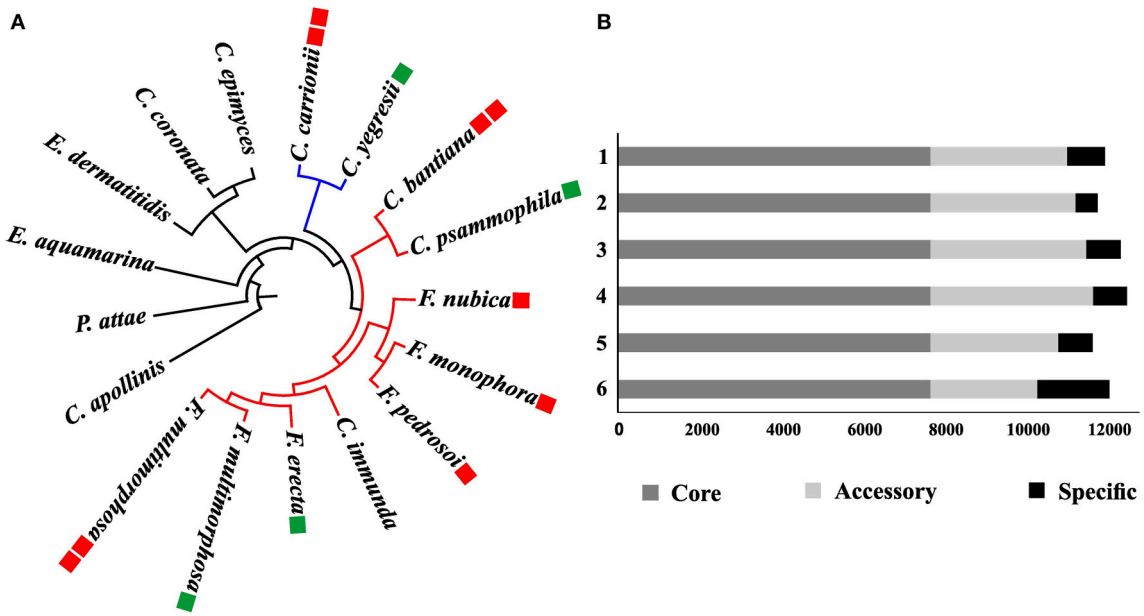

FIGURE 3 | Phylogenomic analysis among *Fonsecaea* sibling species. **(A)** Phylogenetic tree based on the orthologous gene clusters. The bantiana-clade is indicated by a red line and the carrionii-clade by a blue line. Species names in green boxes are environmental strains, in red boxes agents of chromoblastomycosis and cerebral infection. **(B)** Gene cluster distribution in *Fonsecaea* siblings. Clusters of orthologous genes are showed in colors: dark gray core genes; light gray accessory genes, black specific genes. 1. *F. monophora* CBS 269.37, 2. *F. multimorphosa* CBS 980.96. 3. *F. multimorphosa* CBS 102226, 4. *F. pedrosoi* CBS 271.37, 5. *F. nubica* CBS 269.64, 6. *F. erecta* CBS 125763.

abscess, formed a separate cluster with an environmental sibling (**Figure 3A**).

Cluster analysis was performed in the protein set of four *Fonsecaea* species: *F. erecta* CBS 125763^T, *F. multimorphosa* CBS 980.96^T (Leão et al., 2017), *F. monophora* CBS 269.37^T (Bombassaro et al., 2016) and *F. nubica* CBS 269.64^T (Costa et al., 2016). The core genome comprised almost 70% (∼8,000) of the genes (Table S1); the number of accessory genes (Table S2) in *F. erecta* was less than 20%, with specific genes (Table S3) lower than 10% (∼2,000) (**Figure 3B**).

The gene core set was annotated with Eukaryotic Orthologous Group (Table S1). A total of 6,775 genes families clusters were redundantly assigned into KOG classifications, of which 2,259 genes were annotated as poorly characterized proteins, 1,382 assignments were in the category of Information Storage and Processing, 2,128 in the Cellular Processes and Signaling category and 3,265 in the Metabolism category (**Figure 4**). Of the eight KOG sub-classifications allocated in the Metabolism category, 718 genes were annotated to the Secondary Metabolites Biosynthesis, Transport and Catabolism [Q], 566 genes annotated to Lipid Transport and Metabolism [I] and 552 genes annotated to Energy Production and Conversion [C], composing the three more relevant classifications in this category. Moreover, in the Cellular Process and Signaling category, 631 genes were annotated with 51% proteins distributed in the Post-translational Modification Protein Turnover Chaperones class [O] with 450 genes annotated and the class Signal Transduction Mechanisms [T] and 326 genes in the Intracellular Trafficking Secretion and Vesicular Transport [U], composing the top three classifications in this category to each species analyzed (**Figures 5A,B**).

In the Q class (**Figure 4**) significant domains were identified as being common among *Fonsecaea* clinical and plant-associated species. The catalytic domain related to zinc-containing alcohol dehydrogenase (ADH) (IPR002328, IPR013149, IPR013154) is the most abundant domain in the *Fonsecaea* siblings which has been implicated in many biochemical pathways with a role in pathogenicity, stress and intoxication and were previously reported to be expanded in black yeast species (Das and Vasudevan, 2007; Grahl et al., 2011; Strommer, 2011; Teixeira et al., 2017). In addition, flavin-containing monooxygenases (FMOs) (IPR000960) constitute a family of xenobiotic-metabolizing enzymes that are widely present in *Fonsecaea* species. Moreover, related to metabolic processes, some protein domains in Q class were related to the biosynthesis of melanin and were widely found among *Fonsecaea* siblings: IPR011141, IPR019587, and IPR004235 with a role in DHN-melanin pathway, IPR002227 related to DOPA-melanin pathway, and IPR005708, IPR005955, and IPR005956 related to L-tyrosine degradation pathway. Some key enzymes involved in melanin biosynthesis were observed, including the family multicopper oxidases (MCOs) (IPR011706, IPR011707, and IPR001117). This family includes laccases, ferroxidases, bilirubin oxidases and ascorbate oxidases (Hoegger et al., 2006). Likewise, the superfamily aldehyde dehydrogenase (ALDH) (IPR015590, IPR008274) represents a divergently related group of enzymes that metabolize a wide variety of endogenous and exogenous aldehydes (Vasiliou et al., 2000).

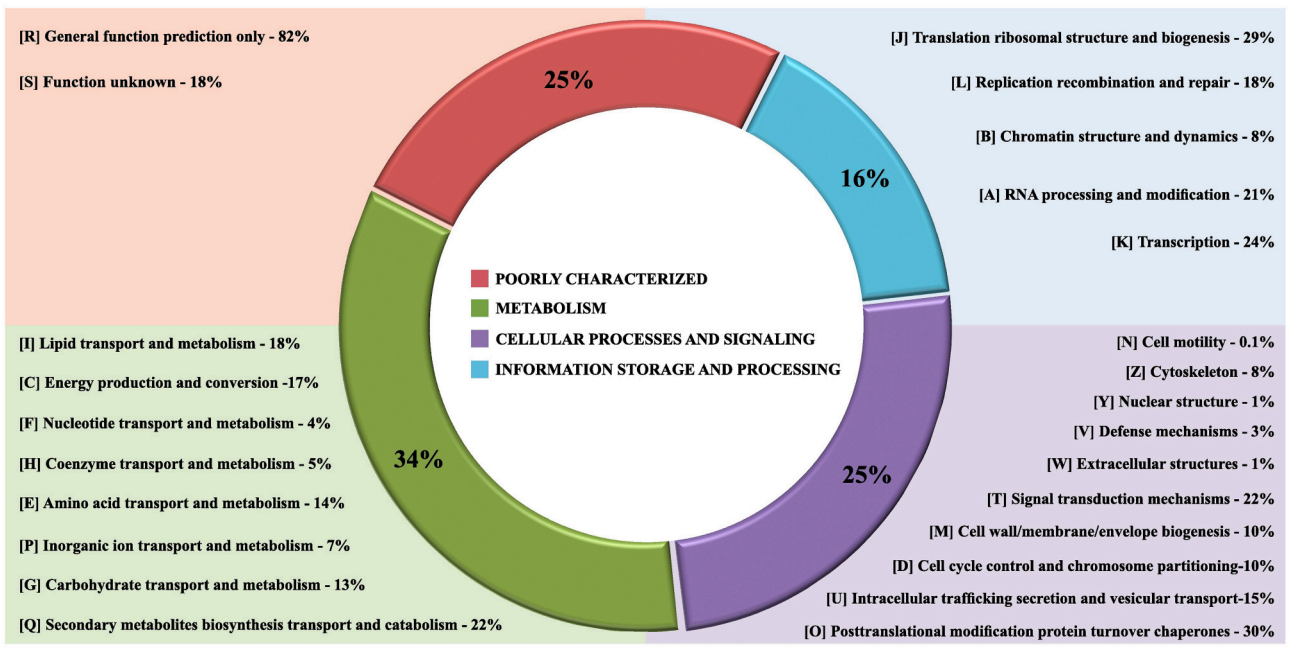

FIGURE 4 | The core gene annotation from Eukaryotic Orthologous Group (KOG) in *Fonsecaea* species. KOG annotation by categories: In red poorly characterized proteins; in green metabolism category, in purple cellular processes and signaling category and processing and in blue category of information storage.

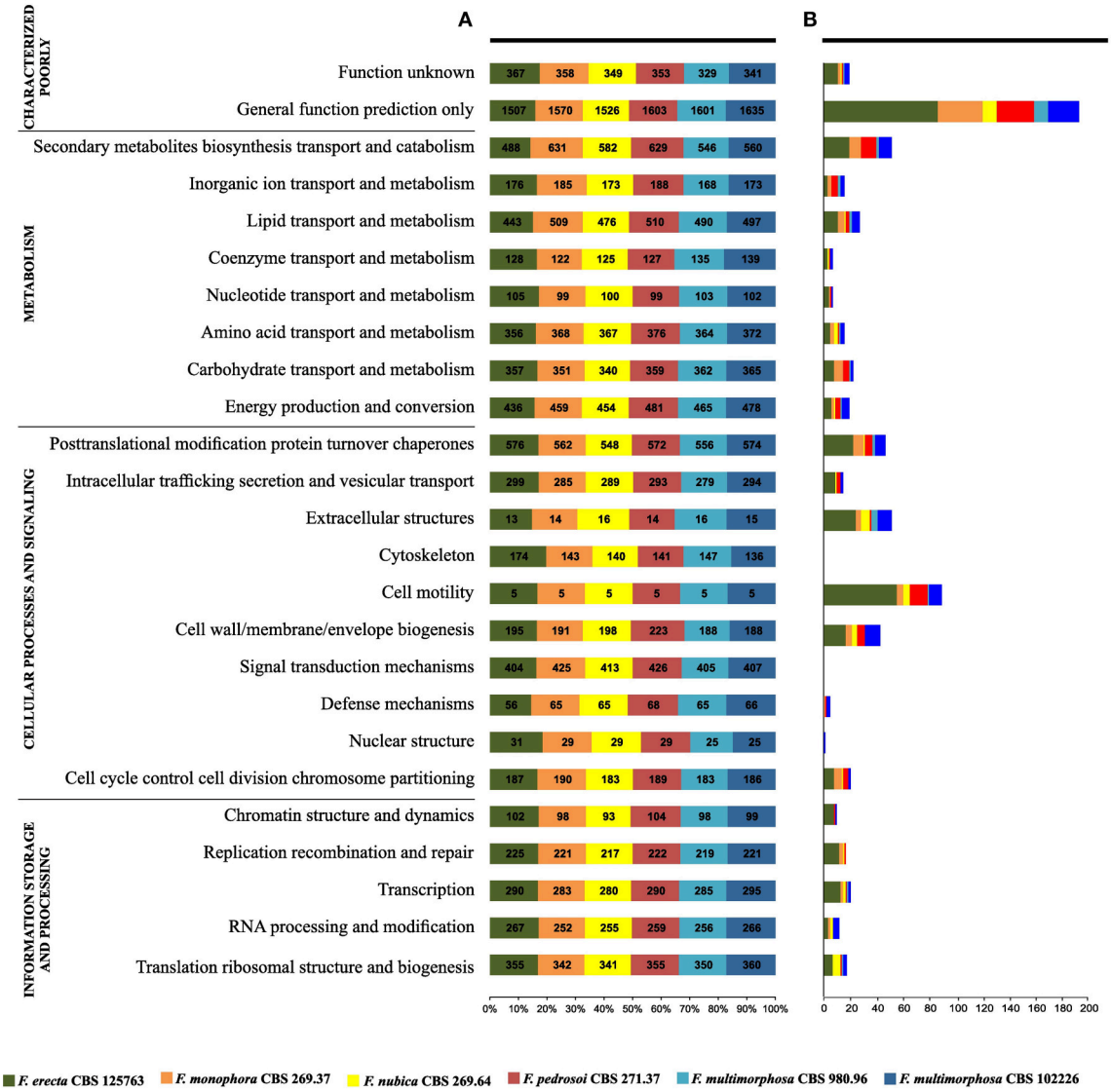

FIGURE 5 | Gene families shared between *Fonsecaea* siblings based on annotation from Eukaryotic Orthologous Group (KOG). **(A)** The siblings are summarized in colored boxes. **(B)** Specific gene annotation among *Fonsecaea* siblings.

In the T class (**Figure 4**) a caspase-like domain (IPR029030) and peptidase C14A, caspase non-catalytic subunit p10 (IPR002138), which are broadly classified as cysteine peptidases, were identified among the *Fonsecaea* species studied. Cysteine-dependent aspartyl-specific protease is mainly involved in mediating cell death processes, while caspases also have roles other than in apoptosis, e.g., caspase-1 (interleukin-1 beta convertase), which is involved in inflammatory processes (Abraham and Shaham, 2004; Lamkanfi et al., 2007). In the T class, small GTPases family (IPR001806), an independent superfamily within the larger class of regulatory GTP hydrolases (Bourne et al., 1990), was observed in *Fonsecaea* siblings ARF type (IPR02456), SAR1 type (IPR006687), ARF/SAR1 type (IPR006689) and Small GTPase, Ras type (IPR020849).

Within class O, post-translational modification protein turnover chaperones are involved in folding, maintenance, intracellular transport and degradation of proteins as well as in facilitating cell signaling. Many heat shock protein (Hsp) families have been identified in this study, such as Hsp20-like chaperone (IPR008979), Hsp40/DnaJ peptide-binding (IPR008971), Heat shock protein Hsp90, N-terminal (IPR020575), Heat shock protein Hsp90 family (IPR001404), Heat shock protein Hsp90, conserved site (IPR019805).

Likewise, using the functional annotation based on Gene Ontology (GO), a total of 7,392 genes were assigned (Figure S1). Of these genes, 409 were redundantly assigned into Cellular Component Ontology, 4,752 into Molecular Function Ontology and 2,231 into Biological Process Ontology. Most of the

genes were annotated to binding (434) and oxyreductase (277) and methyltransferase (187) activity in the Molecular Function Ontology. In the Biological Process the overrepresented functions were metabolic processes (495), transport (239), and biosynthetic processes (195). The less represented ontology classes were membrane (87), protein complex (69) and chromosome (32) in Cellular Component Ontology.

Judging from these analyses, the presence and abundance of these functional domains could be related to the ecology of this agents, i.e., Siderophore iron transporter (GO:0015892, IPR010573) recovered by cells either by the reductive system or by specific transporters able to internalize the siderophore-iron complex (Itoh et al., 2000) and the Quinoprotein amine dehydrogenase (IPR011044), which is related to extremotolerance, this domain has been shown to interact with series of metal ions in anhydrous organic media (Matthews and Sunde, 2002).

In addition, GO enrichment analyses were used to determine the functional characteristics in the studied species (Table S4). It was observed that *F. erecta* presents a mechanism to regulate the use of nitrogen (GO: 0006808), a feature that may favor its survival in plants. Likewise, *F. erecta* and *C. yegresii* shared GO enrichments related to degradation of phenolic compounds such as L-phenylalanine catabolic process (GO: 0006559), tyrosine catabolic process (GO: 0006572) and homogentisate 1,2-dioxygenase activity (GO: 0004411). On the other hand, *C. carrionii* and *F. pedrosoi* exhibited an overrepresentation of the following GO terms: cellular response to iron ion starvation (GO: 0010106), siderophore biosynthetic process (GO: 0019290) and ferric triacetylfusarinine C transport (GO: 0015686) that are involved in iron metabolism.

Species-Specific Genes

The gene families deduced by KOG annotations for each *Fonsecaea* species studied were presented in the **Figure 5A**. Considering the specific genes observed in each species (**Figure 5B**), the plant-associated *F. erecta* presented the largest number of genes related to General function prediction and Secondary metabolites biosynthesis transport and catabolism. The species had a Leucine-rich repeat variant (IPR004830, PF13855) and Universal stress protein signature (USP) (PF00582) domains. Moreover, the family fungal Fucose-specific lectin (IPR012475) and the domain Jacalin-type lectin domain profile (IPR001229) involved in metabolism of lectins also were found in this specie (Table S3). Zinc finger domains (Znf) are shared by *Fonsecaea* sibling, but some domains are present in specific proteins to some species (Table S3). The Znf are relatively small protein motifs, which contain multiple finger-like protrusions that make tandem contacts with their target molecules. There are many superfamilies of Znf motifs, varying in both sequence and structure (Matthews and Sunde, 2002).

Virulence-Related Genes

Using PHI (Pathogen Host Interactions data base) (Winnenburg et al., 2007), genes of species belonging to the bantiana- and carrionii-clades were classified into categories considering virulence and pathogenicity. In total 3,865 genes were divided into 3 categories: Lethal 2,801 genes, Increased virulence (hypervirulence) 1,013 genes and Effector (plant avirulence determinant) 51 genes (Table S5). According to this analysis, 3,614 genes were present in all species studied that includes different transcription factors. On the other hand, 251 genes were limited to one or more species such as *Xeg1* observed in *F. erecta* and *Gr-VAP* gene in *C. yegresii* and *F. erecta.* In the class hypervirulence, all the analyzed species share the transcription factor *Amr1*, a gene described in *Alternaria brassicicola* this is an obligate plant pathogen as an inducer of melanin biosynthesis and associated with pathogenesis, suggesting that it is an important gene for the species to be a competitive saprophytic and also as a parasite (Cho et al., 2012). Moreover, the *RpfF* gene involved in pathogenesis of opportunistic pathogens (Suppiger et al., 2016) was observed in *F. multimorphosa*, *F. pedrosoi*, *F. monophora,* and *F. nubica* from the bantiana-clade and it was absent in the species from carrionii-clade (**Table 3**).

Fungal Lifestyles Expressed in Peptidases and Carbohydrate-Active Enzymes

The bantiana-and carrionii-clades were annotated with carbohydrate-active enzymes (CAZymes) database resulting in 5,058 genes encoding putative CAZymes, comprising 723 auxiliary activities (AA), 155 carbohydrate binding module (CBM), 1,318 carbohydrate esterases (CE), 1,800 glycoside hydrolases (GH), 1,061 glycosyl transferases (GT) and 1 polysaccharide lyase (**Figure 6**). The phylogenomic tree showing the carbohydrate and peptidase metabolism content in bantiana-and carrionii-clades was presented in the **Figure 6A**.

In both clades CAZymes associated with degradation of polysaccharides such as chitin, hemicellulose, glucans and pectin were the largest enzyme families. The number of glycoside hydrolase 43 (GH43) enzyme family related to pectin and hemicellulose degradation was higher in *F. erecta* than the other species (Table S6). In addition, in the bantiana-clade the activity carbohydrate esterase (CE) was higher than in the carrionii-clade, while no polysaccharide lyase (PL) was identified in *Fonsecaea* sibling genomes, only one in *C. carrionii* (**Figure 6B**).

Peptidase-encoding genes were predicted using the MEROPS database (Rawlings et al., 2015) (Table S7). The bantiana- and carrionii-clades were predicted to produce a wide repertoire of different endo- and exopeptidases. We identified for both clades 5,266 peptidases, of which the largest families were serine peptidases (2,549), metallo peptidases (1,155) and cysteine peptidases (912), wherein peptidase family S1 containing Serine endopeptidase was higher in the bantiana-clade (**Figure 6C**). The relation between CAZY and MEROPS) in bantiana- and carrionii-clades is shown in **Figure 6** (family-specific classification shown in Tables S6, S7). The species in bantiana- and carrionii-clades showed similarity in gene contents, sharing different carbohydrate metabolism and peptidase genes ($p = 0.00398$; Mann-Whitney U test), suggesting that these fungi are able to degrade plant and animal substrates.

Protein Family Expansion and Contraction

Protein domain expansions and contractions were inferred from the abundance of protein domains predicted by InterProScan searches and statistically tested by CAFE v3.0 (De Bie et al.,

TABLE 3 | *Fonsecaea* and *Cladophialophora* specific genes annotated in the PHI base.

Species	Genes	Accession	Function in pathogenicity
F. erecta	*Xeg1*	OAP56881.1	Triggered defense responses including cell death Ma et al., 2015
F. erecta	*GzHOMEL040*	OAP56314.1	Transcription factor Son et al., 2011
F. erecta	*GzZC062*	OAP64706.1	Transcription factor Son et al., 2011
F. nubica	*GzC2H089*	OAL38924.1	Transcription factor Son et al., 2011
F. pedrosoi	*RSc1356*	XP013280599.1	Gene effector in plant infection Pensec et al., 2015
F. monophora	*RSc1356*	OAG34226.1	
F. nubica	*RSc1356*	OAL31073.1	
*F. multimorphosa**	*TcGALE*	OAL25194.1	Responsible for conidiation and mycelial development El-Ganiny et al., 2010
*F. multimorphosa***	*COS1*	XP_016633043.1	Function as a transcriptional regulator controlling genes responsible for conidiation Zhou et al., 2009
F. erecta	*Gr-Vap1*	OAP625883.1	Defense-related programmed cell death in plant cells Lozano-Torres et al., 2012
C. yegresii	*Gr-Vap1*	XP_007761267.1	
F. monophora	*RpFf*	OAG36832.1	Regulation of biofilm formation, colony morphology, proteolytic activity, and virulence Suppiger et al., 2016
F. pedrosoi	*RpFf*	XP_013286584.1	
F. nubica	*RpFf*	OAL34548.1	
*F. multimorphosa**	*RpFf*	OAL19303.1	
*F. multimorphosa***	*RpFf*	XP_016628078.1	
C. yegresii	*AMR1*	XP_007752625.1	Inducer of melanin biosynthesis Cho et al., 2012
C. carrionii	*AMR1*	KIW73572.1	
F. monophora	*AMR1*	OAG33974.1	
F. pedrosoi	*AMR1*	XP_013282497.1	
F. nubica	*AMR1*	OAL32231.1	
*F. multimorphosa**	*AMR1*	OAL18751.1	
*F. multimorphosa***	*AMR1*	XP_016627577.1	
F. erecta	*AMR1*	OAP58408.1	
C. immunda	*AMR1*	XP_016244825.1	
C. bantiana	*AMR1*	XP_016622751.1	
C. psammophila	*AMR1*	XP_007742386.1	

**CBS 980.69 isolated form brain disseminated infection in cat.*
***CBS 102226 environmental isolate.*

2006) (Table S8); letters indicating values for ancestors are shown in **Figure 7** and Table S8. The adaptive functions of organism gene contents were evaluated by expansion and contraction of the protein family in *Fonsecaea* siblings in the bantiana-clade compared with species from the carrionii-clade. Several domains were expanded in the bantiana-clade, while in the carrionii-clade there is contraction demonstrating that different clades related to chromoblastomycosis are evolved in different directions due to ecological preferences (**Figure 7**).

Many domains and sites (IPR015590, IPR016161, IPR016163, IPR029510, and IPR016160) related to superfamily aldehyde dehydrogenase (ALDH) and alcohol dehydrogenase zinc type conserved site (IPR002328) showed an expansion in the ancestor of *F. pedrosoi*, *F. monophora* and *F. nubica*. Similarly, expansions in *F. erecta* and *C. bantiana* were observed in the protein family peptidase M20 (IPR002933 and IPR011650) and in the CHAT domain (IPR024983) related to caspases (**Figure 7**, Table S8).

Moreover, two domains associated with the glyoxal pathway, the glyoxalase I (IPR018146) and the glyoxalase/fosfomycin resistance/dioxygenase (IPR004360) are expanded in the ancestor of *F. pedrosoi*, *F. monophora,* and *F. nubica*. This enzyme catalyzes the first step of the glyoxal pathway, and in addition to its role in detoxifying glyoxal it may have other roles in stress response (Kim et al., 1993; Yim et al., 2001). Further this ancestor showed expansion in the aminoglycoside phosphotransferase (IPR002575) domain (**Figure 7**, Table S8); this domain consists of bacterial antibiotic resistance proteins, which confers resistance to various aminoglycosides (Trower and Clark, 1990; Chow, 2000).

Virulence of *Fonsecaea* Siblings

Survival tests using *Galleria mellonella* larvae as a model infected with *F. pedrosoi* ATCC 46428 and CBS 271.37^T, *F. erecta* CBS 125763^T, and *F. monophora* CBS 102248 showed a low larvae survival rate when compared to control groups. Larvae infected with *F. erecta* had a lower survival rate (**Figure 8A**). The infected larvae from the tested groups developed varying degrees of melanization, whereas the controls (PBS and SHAM) (Thomaz et al., 2013) did not present any melanization (**Figure 8B1–6**). Melanization could be observed from the first day post-inoculation in all tested groups. Histopathology (**Figure 8C**) showed the presence of pigmented nodules and granulomata in the tissue of infected larvae. Based on these results it was concluded that *F. erecta* CBS 125763^T is potentially able to infect animal hosts. In order to find out how *F. pedrosoi* and *F. erecta* conidia and hyphae trigger macrophage activation, microbicidal activity and TNF-α production was measured. *Fonsecaea erecta* hyphae are more resistant to macrophage destruction than *F. pedrosoi* after 24 h of co-culturing with macrophages *in vitro* (**Figure 9**). No difference was observed when macrophages were co-cultured with conidia from both *Fonsecaea* species (**Figure 9A**). Only hyphae from both *Fonsecaea* species were able to induce TNF-α secretion (**Figure 9B**).

In vivo assay using BALB/c mice as a model infected by pathogenic species *F. pedrosoi* and plant associated species *F. erecta* showed ulcerative and plaque type lesions. However, the *F. pedrosoi* infected mice showed lesions with dark plaque while *F. erecta* infected mice presented higher areas of edema (**Figure 10A**). All groups showed high levels of fungal burden at 7 dpi followed by reduction of viable fungi in the injured area (**Figure 10B**). The levels of cytokines were similar in both groups, except to IL-1β levels in *F. erecta* infected mice that increase lately when compared with *F. pedrosoi* infected mice (**Figures 10C–F**).

Potential Virulence Genes Related to Human Infection

An analysis of common genes related to the casual agents of disease showed 43 gene clusters shared by agents of systemic

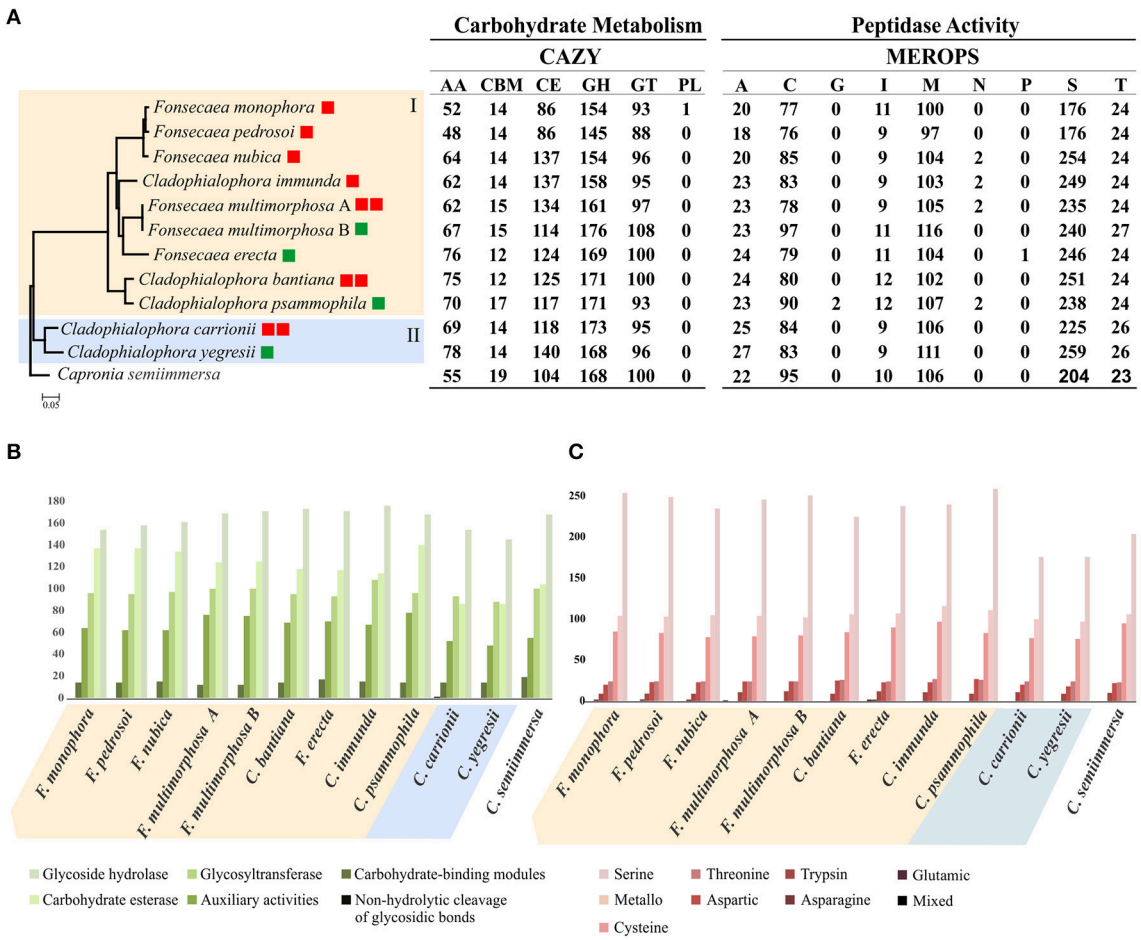

FIGURE 6 | Analysis of carbohydrate and peptidase metabolism content in bantiana-and carrionii-clades. **(A)** Phylogenomic tree of bantiana- (I) and carrionii-clades (II) *Fonsecaea multimorphosa* **(A)** CBS 980.69. *Fonsecaea multimorphosa.* **(B)** CBS 102.226. All nodes on the phylogeny were supported by bootstrap values of 100% and the letters indicate ancestors. Species names followed by boxes: in green environmental strains, in red agents of chromoblastomycosis and cerebral infection. The ratio of MEROPS enzymes to CAZY enzymes for each genome is shown in the last column. **(B)** CAZY annotation: categories include AA (auxiliary activities), CBM (carbohydrate-binding modules), CE (carbohydrate esterase), GH (glycoside hydrolase), GT (glycosyltransferase) and PL (non-hydrolytic cleavage of glycosidic bonds). **(C)** MEROPS annotation: categories include A (aspartic), C (cysteine), G (glutamic), I (trypsin), M (metallo), N (asparagine), P (mixed), S (serine), and T (threonine).

infection and 32 gene clusters related to (sub)cutaneous infection. Annotation of these clusters in *Fonsecaea* revealed 33 domains related to disseminated infection and 24 domains related to subcutaneous infection (**Table 4**).

In the agents of systemic infection a high frequency was noted of the domains DJ-1/PfpI family (IPR002818) and glyoxalase/fosfomycin resistance protein/dioxygenase superfamily (IPR004360) related to glyoxal pathway, which have important roles in detoxifying glyoxals (Lee et al., 2013) and domains related to flavin proteins, such as monooxygenase-like flavin-binding (IPR020946) and flavin-containing amine oxidoreductase (IPR002937), and the family multicopper oxidases (MCOs) (IPR011706, IPR011707, and IPR001117) that includes laccases, ferroxidases, bilirubin oxidases and ascorbate oxidases (Hoegger et al., 2006).

The subcutaneous agents shared a number of domains related to enzymes and transporters (**Table 4**), such as major facilitator, sugar transporter-like (IPR005828) and major facilitator superfamily IPR011701), aggregating several families of transporters. Among them a siderophore transporter, RhtX/FptX family and the yellow-like family is a gene class characterized by the presence of a major royal jelly protein (MRJP) domain (Ferguson et al., 2011) with multiple physiological and development functions in insects (Drapeau et al., 2003), such as synthesis of melanin pigments and sex-specific reproductive maturation. A large variety of enzymes such as acyltransferases (IPR002656), hydrolases (IPR013094 and IPR000757), proteases, lipases, permeases (IPR004841) and dehydrogenases (IPR002347) were observed. Nevertheless, also domains related to invasion of the plant tissue were observed, such as cutinase (IPR000675) (Dickman et al., 1989) and LysM domain related to chitinase (IPR018392) (Gruber and Seidl-Seiboth, 2012).

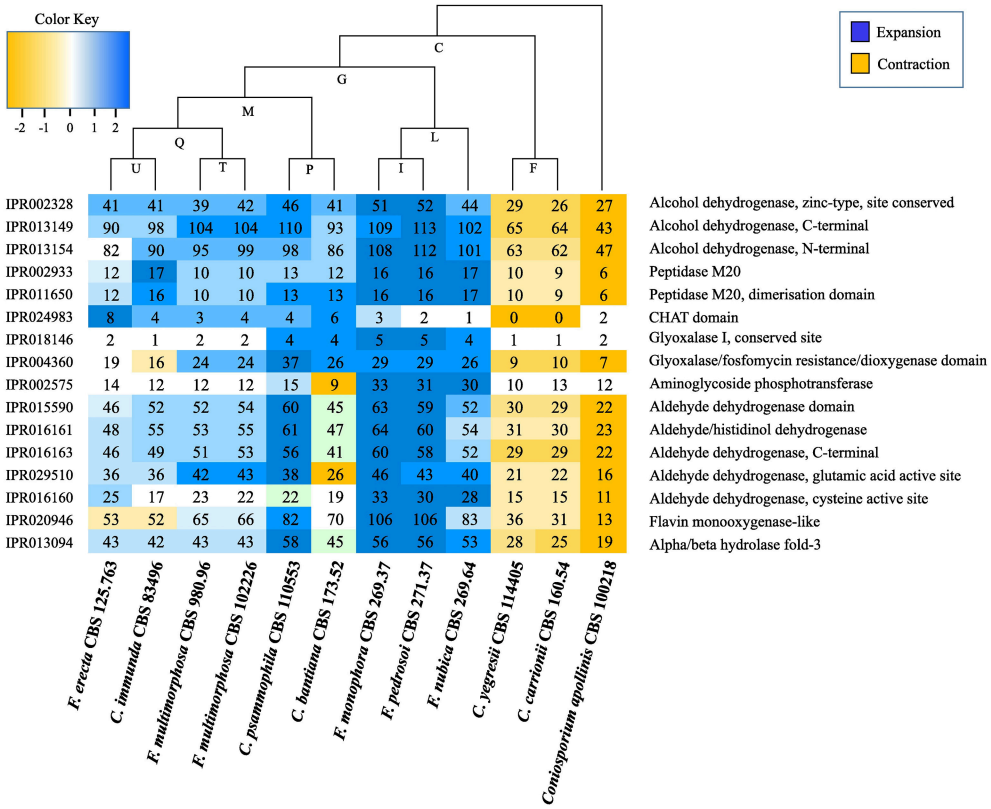

FIGURE 7 | Interpro domains in *Fonsecaea* siblings. The letters indicate values for ancestry. The species are organized in phylogenetic order.

DISCUSSION

The genus *Fonsecaea* is located in the Chaetothyriales, family Herpotrichiellaceae and contains species of environmental saprobes on plants or plant debris and pathogenic species, associated with subcutaneous and deep infections in human and animal hosts. The environmental species are consistently distinct from the *Fonsecaea* spp. commonly founded as agents of disease. The same phenomenon of environmental next to pathogenic species is known in *Cladophialophora* (Vicente et al., 2014).

Phylogenomic analysis shows that *Fonsecaea* is intermingled with some *Cladophialophora* species, while *Cladophialophora* agents of chromoblastomycosis are located in a separate carrionii-clade (**Figure 3A**). The invasive potential of black yeast-like fungi is known to differ significantly between species (Badali et al., 2008; Seyedmousavi et al., 2011). Both clades with agents of chromoblastomycosis also contain non-pathogenic representatives. Formation of muriform cells in host tissue is considered as the hallmark of the disease, but some environmental species are able to produce such cells *in vitro* (Badali et al., 2008).

Genomes of species of *Fonsecaea* under study are quite similar. An abundance of domains related to zinc-containing alcohol dehydrogenase (ADH) was observed (**Figure 4**), which have multiple biological functions such as detoxification. Similar results have been reported for other black yeasts (Teixeira et al., 2017), suggesting that tolerance of extreme and toxic environmental habitats is a mainstay in the ecology of black yeast-like fungi. Likewise, the superfamily ALDH represents enzymes that metabolize a wide variety of endogenous and exogenous aldehydes (Lindahl, 1992; Vasiliou et al., 2000). The expansion of ALDH in the ancestor of *Fonsecaea* (**Figure 7**) indicates metabolic plasticity explaining a dual ecological ability, surviving hostile environments as well as mammal host tissue. Also Flavin-containing monooxygenases (FMOs) play a role in a wide variety of processes such as the detoxification of drugs, biodegradation of aromatic compounds, siderophore biosynthesis and biosynthesis of antibiotics (van Berkel et al., 2006), which could thus be further key executors in processes related to extremotolerance.

Gene Ontology (GO) annotation indicated presence of siderophore iron transporters in the core genome of *Fonsecaea* (Figure S1). Most fungi are able to produce and utilize intracellular siderophores as an iron storage compound (Eisendle et al., 2006). In *Candida albicans* siderophore transporter-defective mutants were clearly compromised in invading keratinocyte layers suggesting that siderophore uptake is required to epithelial invasion and penetration (Leon-Sicairos et al., 2015). The clinical species *C. carrionii* and *F. pedrosoi* show gene enrichment in cellular response to siderophore biosynthetic

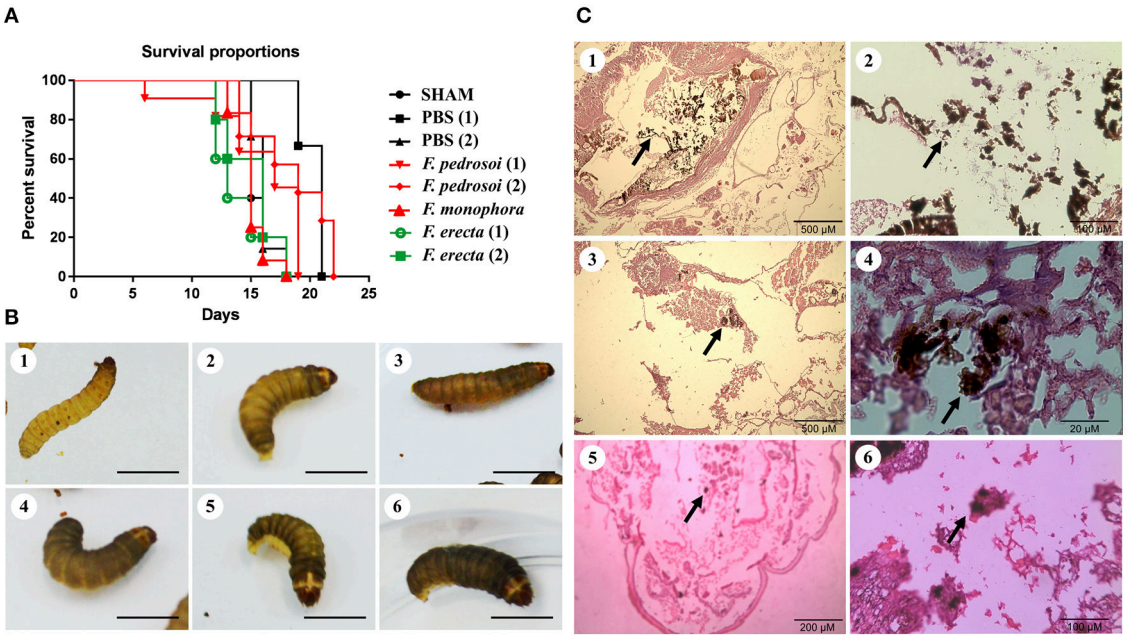

FIGURE 8 | Virulence of *Fonsecaea* siblings using *Galleria mellonella* larvae. **(A)** Survival of *G. mellonella* larvae infected with *Fonsecaea* species. **(B)** Melanization of *G. mellonella* larvae infected with *Fonsecaea* species: (1, 2). Controls: SHAM and PBS; (3). *Fonsecaea erecta* CBS 125763; (4). *Fonsecaea monophora*; (5). *Fonsecaea pedrosoi* CBS 271.37; (6). *Fonsecaea pedrosoi* ATCC 46428. **(C)** Histology of infected tissue of *G. mellonella* with *Fonsecaea* species. The internal structures were fixed, embedded in paraffin and stained with PAS. Black arrows show hyphae spreading through the larva tissue. (1, 2). *Fonsecaea erecta* CBS 125763; (3, 4). *Fonsecaea pedrosoi* CBS 271.37; (5, 6). *Fonsecaea monophora* CBS 102248.

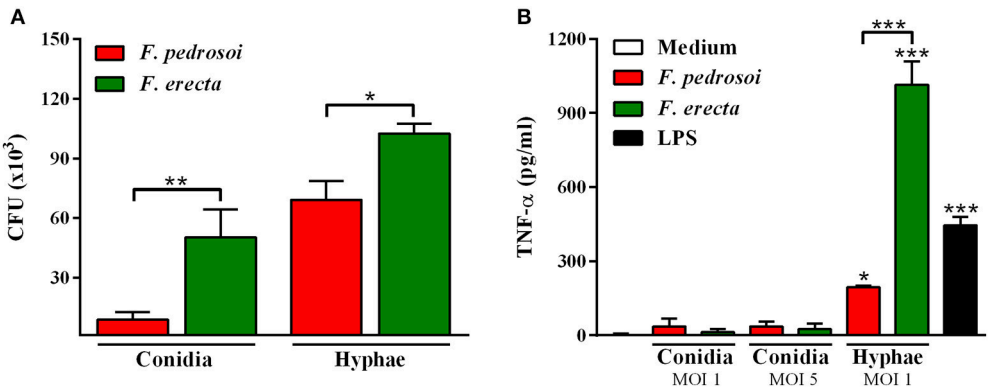

FIGURE 9 | Fungal burden and production of pro-inflammatory cytokines of *F. pedrosoi* and *F. erecta*. **(A)** J774 murine macrophages (J774) were co-cultured with conidia or hyphal fragments, in the MOI 1 during 24 h. CFU data showed faster clearance of inoculated conidia from *F. pedrosoi* than *F. erecta*. **(B)** High levels of TNF-α were observed in macrophage co-culture with hypha, but not with conidia. Data were analyzed by one-way ANOVA with Tukey's *post-hoc* test. $^{*}p < 0.05$, $^{**}p < 0.01$, and $^{***}p < 0.001$ compared with *F. pedrosoi*; or compared with non-infected macrophages.

process and ferric triacetylfusarinine C transport which might play a role in virulence of these agents, as these genes were not enriched in the environmental species (Table S4).

Fonsecaea siblings produce melanin via different pathways demonstrating that in these fungi the pathways are conserved (Chen et al., 2014; Teixeira et al., 2017). Melanin and carotenoids deposited in the cell walls are considered a putative virulence factor in established human pathogens such as *Histoplasma capsulatum*, *Sporothrix schenckii*, and *Cryptococcus neoformans*. Melanin is associated to the survival and competitive abilities of fungi in hostile environments (Nosanchuk et al., 2002; Mednick et al., 2005; Nosanchuk, 2005; Taborda et al., 2008) and also enhances tolerance of oxygenic burst in macrophages. Key enzymes involved in melanin biosynthetic pathways belong to the family Multicopper oxidases (MCOs) including laccases, ferroxidases, bilirubin, oxidases and ascorbate oxidases that

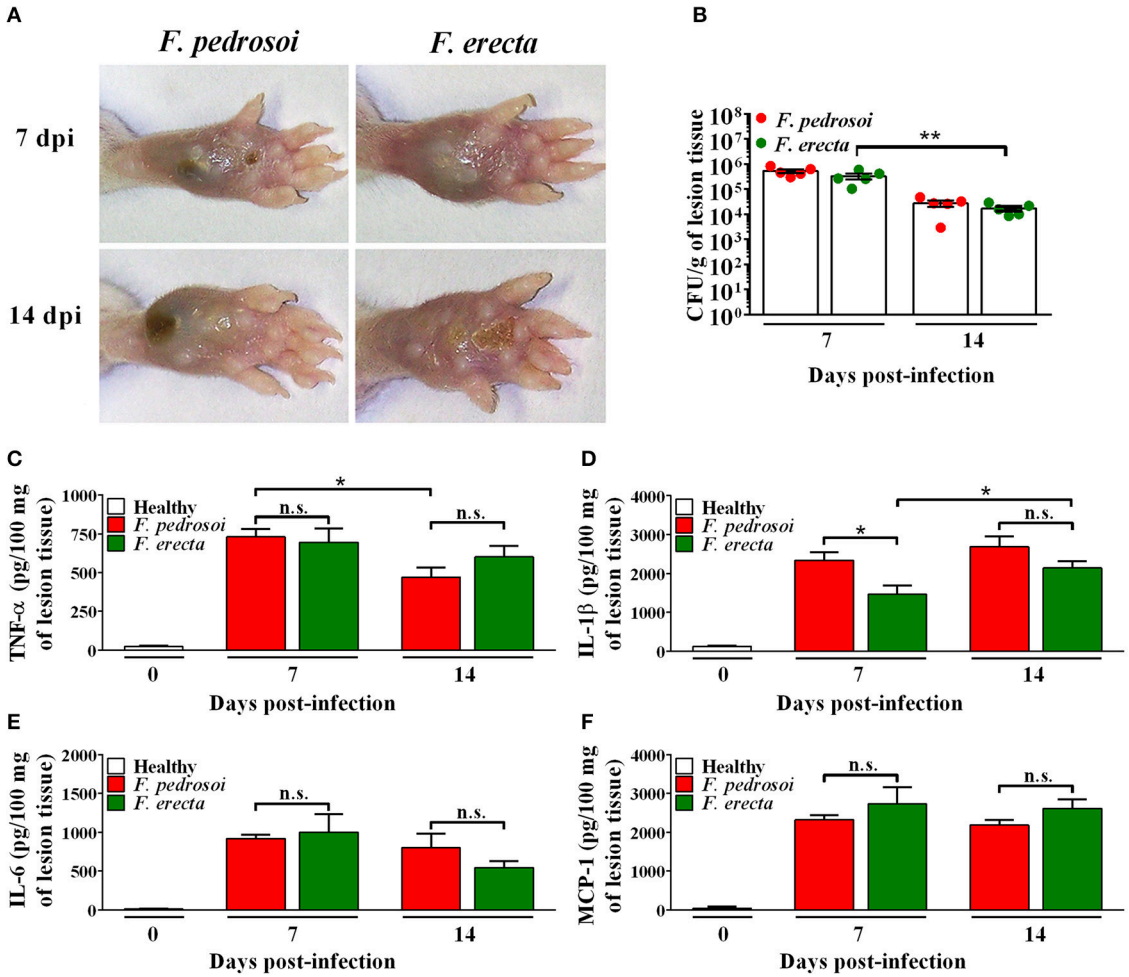

FIGURE 10 | Virulence and immunostimulatory potential test of *Fonsecaea* sibling species using BALB/c mice as a model. **(A)** Macroscopic aspect of the disease. **(B)** CFU data showed a high tissue fungal burden of *F. erecta* which decline over the course of the infection. **(C–F)** At 7 and 14 days post-infection, high levels of TNF-α, IL-1β, IL-6 and MCP-1 were observed similarly in the footpad of mice infected with *F. pedrosoi* or *F. erecta*. Data were analyzed by two-way ANOVA with Tukey's post-hoc test. *$p < 0.05$ and **$p < 0.01$ between groups indicated by brackets; n.s.: not significantly.

catalyze the oxidation of a variety of substrates and mainly aromatic compounds (Hoegger et al., 2006). Laccases form the largest subgroup and are considered key enzymes of the DOPA melanin pathway (Walton et al., 2005). They are abundant in fungal genomes, related to their divergent physiological roles and differential regulation upon changing environmental conditions (Cañero and Roncero, 2008; Giardina et al., 2010). Teixeira et al. (2010) suggested that melanin pigments protect the fungus from the mammalian host's innate immune responses providing resistance to oxidizing agents and fungal cell death during phagocytosis. Melanin is important because has a role in the protection against antifungal drugs (van den Sande et al., 2007) and is significant in differentiation of the muriform cell, the invasive form of chromoblastomycosis.

The glyoxalase system consists of two consecutive enzymatic reactions (Glyoxalase I and II) with the terminal product D-lactate by metabolism of the physiological substrate methylglyoxal. The widespread distribution of glyoxalase in prokaryotic and eukaryotic cells suggests it fulfills a function of fundamental importance to life. Inhibition of the glyoxalase system leads to methylglyoxal accumulation to toxic levels. It has been implicated in control of cell growth and proliferation, and detoxification of methylglyoxal (Thornalley, 1993). Glyoxalase enzymes are modified during phagocytosis, and the enzymatic reaction has been implicated as a virulence factor for neutralization of the immune response during invasion (Gillespie, 1978, 1981). It has been reported in sugar-limited environments, the fungus relies on fatty acid metabolism for growth (Sexton and Howlett, 2006). Accumulation of lipid in thick-walled resting cells at the expense of sugars is a key mechanism in yeast-to-mold conversion in black yeasts (Oujezdsky et al., 1973). Glyoxalase might thus play a central role in the response to varying conditions. In *Fonsecaea* the

TABLE 4 | Prediction of virulence domains related to systemic and (sub)cutaneous infection.

Systemic infection domains (Domain/ID access)	Function	(Sub)cutaneous infection (Domain/ID access)	Function
AhpC/TSA Family/IPR000866	Antioxidant activity	Acyltransferase family/IPR002656	Transferase activity
Alpha/beta hydrolase fold/IPR000866	Catalytic activity	Alpha/beta hydrolase fold/IPR013094	Hydrolase activity
Amidase/IPR023631	Hydrolase activity	Amino acid permease/IPR004841	Transmembrane transport
Amidohydrolase Family/IPR006680	Hydrolase activity	Asp/Glu/Hydantoin racemase/IPR015942	Nitrogen compound metabolic process
C-terminal of 1-Cys peroxiredoxin/IPR019479	Peroxiredoxin activity	Cutinase/IPR000675	Hydrolase activity
DJ-1/PfpI Family/IPR002818	Glyoxalase	Flavin-binding monooxygenase-like/IPR020946	NADP binding
Unknown function (DUF1772)/IPR013901	Anthrone oxygenases	Fungal specific transcription factor/IPR007219	Zinc ion binding
Eukaryotic aspartyl protease/IPR033121	Proteolytic enzymes	Fungal Zn(2)-Cys(6) binuclear cluster/IPR001138	Zinc ion binding
FAD binding domain/IPR003953	Catalytic activity	Glutathione-dependent formaldehyde activating enzyme/IPR006913	Carbon-sulfur lyase activity
Flavin-binding monooxygenase-like/IPR020946	Metabolize xenobiotics	Glycosyl hydrolases family 16/IPR000757	Hydrolase activity
Flavin amine oxidoreductase/IPR002937	Oxidoreductase activity	LysM domain/IPR018392	Binding chitin
Fumarylacetoacetate (FAA) hydrolase Family/IPR011234	Catalytic activity	Major Facilitator Superfamily/IPR011701	Transmembrane transport
Fungal N-terminal of STAND proteins/IPR031348	Function is not known	Major intrinsic protein/IPR000425	Transporter activity
Fungal specific transcription factor/IPR007219	Zinc ion binding	Major royal jelly protein/IPR017996	Function is not known
Fungal specific transcription factor/IPR021858	Transcription factor	NAD dependent epimerase/dehydratase family/IPR001509	Catalytic activity
Fungal Zn(2)-Cys(6) binuclear cluster/IPR001138	Zinc ion binding	NADP oxidoreductase coenzyme F420-dependent/IPR028939	Catalytic activity
Glyoxalase/fosfomycin resistance protein/Dioxygenase superfamily/IPR004360	Catalytic activity	OTT_1508-like deaminase/IPR027796	Chromatin function
GMC oxidoreductase/IPR000172	Oxidoreductase activity	Oxidoreductase family, NAD-binding Rossmann fold/IPR000683	Oxidoreductase activity
GMC oxidoreductase/IPR007867	Oxidoreductase activity	Phosphotransferase enzyme family/IPR002575	Antibiotic resistance
Heterokaryon incompatibility protein (HET)/IPR010730	Preserve genetic individuality	Putative oxidoreductase C terminal/IPR013944	Oxidoreductase activity
Major Facilitator Superfamily/IPR011701	Transmembrane transport	Putative threonine/serine exporter/IPR010619	Catalytic activity
Multicopper oxidase/IPR001117	Oxidation-reduction	Pyrroline-5-carboxylate reductase dimerization/IPR029036	Dimerization domain
Multicopper oxidase/IPR011707	Copper ion binding	Sugar (and other) transporter/IPR005828	Transmembrane transporter
Multicopper oxidase/IPR011706	Oxidoreductase activity	Short chain dehydrogenase/IPR002347	Catalytic activity
NAD(P)H-binding/IPR016040	Catalytic activity	Threonine/Serine exporter, ThrE/IPR024528	Transmembrane transporter
NMT1-like Family/IPR011852	Protein receptors	—	—
Phenazine biosynthesis-like protein/IPR003719	Catalytic activity	—	—
Prion-inhibition and propagation IPR029498	Prion-inhibitory and propagation effect	—	—
Unknown function (DUF4243)/IPR025337	Function is not known	—	—
Sugar (and other) transporter/IPR005828	Transmembrane transporter activity	—	—
X-Pro dipeptidyl-peptidase C-terminal non-catalytic/IPR013736	Dipeptidyl-peptidase activity	—	—
X-Pro dipeptidyl-peptidase (S15 family)/IPR000383	Hydrolase activity	—	—

pathway is expanded in the clinical species of the bantiana-clade (**Figure 7**) suggesting that the glyoxal pathway cycle might be required for virulence during invasion, in addition to its role in surviving extreme environmental conditions (Teixeira et al., 2017).

Caspases occur in the *Fonsecaea* core genome where they are synthesized as pro-proteins, possessing weak proteolytic activity (Madeo et al., 2002; Cheng et al., 2003; Abraham and Shaham, 2004) and also induce apoptosis enhancing pathogenesis (Douglas et al., 2015). Activation of apoptosis

may lead to caspase-1 activation, providing a link between apoptosis and inflammation (Schumann et al., 1998; Lamkanfi et al., 2007). In the T class, a small GTPase family and an independent superfamily of GTP-binding proteins share enzymatic activity and play pivotal roles in cell division, protein synthesis and signaling (Paduch et al., 2001). Small GTPase—Ras type (IPR020849) is the most represented domain regulating cell growth, proliferation and differentiation (Table S1). The Ras family of GTPase proteins has been shown to control morphogenesis in many organisms, including pathogenic fungi such as *Cryptococcus neoformans* (RAS1) (Alspaugh et al., 2000), *Candida albicans* (CaRAS1 and CaRSR1) (Leberer et al., 2001) and *Aspergillus fumigatus* (rhbA) (Panepinto et al., 2003).

Heat shock proteins (Hsp) in the core genome (Table S1) are essential eukaryotic molecular chaperones, being first proteins that are up-regulated under conditions of elevated temperature (Lund, 2001). Especially, Hsp90 chaperones are unique in their ability to regulate a specific subset of cellular signaling proteins that have been implicated in disease, including intracellular protein kinases, steroid hormone receptors and growth factor receptors (Tamayo et al., 2013), which are likely mechanism of mammal infection where elevated temperature is an essential condition (Vicente et al., 2012).

The above discussed domains may explain the capacity to survive extreme conditions, of which living mammal tissue is one, but do not explain differences between species of the same clade. The significant predisposition observed in agents of chromoblastomycosis (Vicente et al., 2001, 2008, 2014) probably rests upon diversity enzymatic reactions. CAFE analysis of *Fonsecaea pedrosoi* and *Cladophialophora carrionii*, both causing this disease, evolve in opposite directions, as several domains expanded in the bantiana-clade appeared to be contracted in the carrionii-clade (**Figure 7**). This may demonstrate that members of different clades causing chromoblastomycosis have evolved in different directions due to clade-specific ecological preferences, or perhaps more likely that the displayed domains *in toto* reflect phylogeny rather than ecology.

The CAZy Database is a powerful reporter of fungal lifestyles once the fungi degrade an enormous functional and structural diversity of complex plant polysaccharides. Zhao et al. (2013) revealed that most fungi that lack PL and tend to lose CE8, CE11, GH6, GH73, GH80, and GH82 families are saprobes; these were also observed in bantiana- and carrionii-clades. A wide variety of extracellular peptidases is produced to degrade a gamut of environmental substrate complexes, indicative for a less specialized nutritional status (da Silva et al., 2006; Sriranganadane et al., 2010). Species of the bantiana- and carrionii-clades produce enzymes involved in plant cell wall pectin and hemicellulose degradation. Besides, in both clades a significant similarity was observed among gene content related to carbohydrate metabolism and peptidase (**Figure 6**). It suggests that these fungi are able to degrade plant and animal substrates demonstrating a duality in lifestyle that could enable Chaetothyriales pathogenic species to transfer from environmental niches to animal material. The similarity of carbohydrate-active and protein degrading enzymes associated to the occurrence of additional virulence factors, which may support the tolerance to extreme environmental niches of the fungus (Teixeira et al., 2017), suggests an opportunistic tendency of *Fonsecaea* sibling species.

Primary fungal pathogens attempt to disrupt host cell homeostasis while avoiding and/or suppressing host recognition. In opportunists these mechanisms are not sophisticated and probably have emerged due to flexibility in nutrient acquisition (Dickman and Figueired, 2011) and extremotolerance (Moreno et al., 2017). Prenafeta-Boldú et al. (2006) and Casadevall (2007) suggested that this unfocused virulence explains the "dual use" determinants in unexpected agents of disease. It is likely that this principle also holds true for most black yeast-like fungi. However, as some common agents of chromoblastomycosis seem to have a significant predilection for this disease and are rarely found in the environment (Vicente et al., 2014) a certain degree of pathogenic adaptation cannot be excluded.

The subcutaneous infections by *Fonsecaea* and *Cladophialophora* species frequently result from a trauma from environmental sources. The muriform cell, considered to be a chromoblastomycosis-specific tissue form in humans, has been observed in cactus thorns infected with *C. yegresii* (De Hoog et al., 2007) and also *in vitro* in several environmental species (Badali et al., 2008). The *RSc1356* effector is involved in plant infection (Pensec et al., 2015) and its presence in *Fonsecaea* might support this hypothesis, although plant- and human-pathogenicity are almost mutually exclusive (De Hoog et al., 2000). The use of nitrogen and degradation of phenolic compounds that are also enriched in environmental *F. erecta* and *C. yegresii* (Table S7) are more likely causes of opportunism. The class of protein lectins (Table S3), which is implicated in many essential cellular and molecular recognition processes (Varrot et al., 2013) was present *F. erecta* isolated from plant material. De Hoog et al. (2004) stated that pathology on humans is coincidental, humans not being the primary hosts of these fungi.

The above hypothesis is partially supported by results of virulence testing using *G. mellonella* larvae as a model. Larvae infected by environmental *F. erecta* had a lower survival than those infected by clinical strains of *F. pedrosoi* (ATCC 46428 and CBS 271.37^{T}) and *F. monophora* (CBS 102248). In addition, *F. erecta* hyphae induced high levels of TNF-α (**Figure 9**), contributing to macrophage activation after phagocytosis. Macrophages activated by TNF-α increase their ability to control intracellular fungal growth, stimulate recruitment of inflammatory cells and stimulate the formation and maintenance of granulomata (Algood et al., 2005; Juhász et al., 2013; Gyurkovska and Ivanovska, 2016). Although *F. erecta* hyphae induced high levels of TNF-α, hyphal death was not observed, suggesting a higher level of extremotolerance. The higher virulence of strictly environmental *Fonsecaea* species does however not explain which the species which are commonly found on human hosts show lower virulence in the *Galleria* model.

Furthermore, based on PHI database the genes classified as lethal are mostly transcription factors (TFs) that orchestrate gene expression which determines life and functionality of the cell

(Shelest, 2008) by controlling cellular signaling pathways and thus are key mediators of cellular function of fungi (Shelest, 2008; Wang et al., 2011).

The high number of domains related to enzymes and transporters reveals important mechanisms of nutrient acquisition and extremotolerance, constituting a genomic machinery that allows hydrolysis of recalcitrant components present in plant debris and suggests multiple survival strategies including mammal infection. Explanation of the observed differences in prevalence in the human host between closely related species appeared nevertheless impossible, as illustrated by the lower *Galleria* survival rate after infection with the non-pathogenic *F. erecta*. The large number of proteins (**Figure 4**, **Table 4**) with unknown function demands further investigation of these genes and their potential role in survival; small but crucial differences between these closely related fungi may have been concealed in the present set of proteins studied. Despite the close relationship in classical marker genes, *Fonsecaea* species are surprisingly different in their mitochondrial genomes, which in most fungi are highly conserved (Torriani et al., 2014; Jelen et al., 2016). Differences in routes of transmission allowing passage of properties acquired in the host to a next generation and thus, allowing evolutionary adaptation (Queiroz-Telles et al., 2017) are not easily revealed.

AUTHOR CONTRIBUTIONS

Conceived and designed the experiments: VV, VW, LM, RR, ALB, SA, ES, SDH. Generation sequence data: HF, MZTS, VB, EB. Performed the experiments: GF, ALB, RdC, SA, SDS, MMFdN. Analyzed the data: VV, VW, AB, LM, FC, RR, AL. Contributed reagents/materials/analysis tools: RR, VV, FP, ES. Contributed to preparing the manuscript and revising it critically: VV, VW, AB, FC, AL, RG. Annotation and analysis of data; preparation, creation and/or presentation of the tables; graphics and figures: VW, AB, LM, FC, RR, AL, RG. Strains offered and/or Substantial contributions to the work FQ, ALB, SA, MMFN, SDH. Conceived and revised paper: JS, MT, MSF, MS, DA, MJN, VV, ES, SDH. Conception and design of the work and writing the manuscript. VV, VW, AB, ES, SDH.

FUNDING

This work was supported by Brazilian Federal Agency for Support and Evaluation of Graduate: Education Coordination for the Improvement of Higher Education Personnel—CAPES (PVE project grant number 0592012) (www.capes.gov.br) and National Counsel of Technological and Scientific Development (http://cnpq.br/), Brazil; and by The National Institute of Science and Technology of Biological Nitrogen Fixation/CNPq/MCT (grant number 573828/2008-3). VV received fellowships from National Council for Scientific and Technological Development (CNPq), Brasilia, Brazil.

ACKNOWLEDGMENTS

This work was developed in collaboration with the Broad Institute and the Bioinformatics Laboratory from Federal University of Parana. The authors are grateful to the INCT-BNF for providing computing resources.

SUPPLEMENTARY MATERIAL

The Supplementary Material for this article can be found online at: https://www.frontiersin.org/articles/10.3389/fmicb.2017.01924/full#supplementary-material

REFERENCES

Abraham, M. C., and Shaham, S. (2004). Death without caspases, caspases without death. *Trends Cell Biol.* 14, 184–193. doi: 10.1016/j.tcb.2004.03.002

Algood, H. M., Lin, P. L., and Flynn, J. L. (2005). Tumor necrosis factor and chemokine interactions in the formation and maintenance of granulomas in tuberculosis. *Clin. Infect. Dis.* 1(Suppl. 3), S189–S193. doi: 10.1086/429994

Alspaugh, J. A., Cavallo, L. M., Perfect, J. R., and Heitman, J. (2000). RAS1 regulates filamentation, mating and growth at high temperature of *Cryptococcus neoformans*. *Mol. Microbiol.* 36, 352–365. doi: 10.1046/j.1365-2958.2000.01852.x

Andrews, S. (2016). *FastQC: A Quality Control Tool for High Throughput Sequence Data; 1.* Available online at: from: http://www.bioinformatics.babraham.ac.uk/projects/fastqc.

Badali, H., de Hoog, G. S., Curfs-Breuker, I., Klaassen, C. H. W., and Meis, J. F. (2010). Use of amplified fragment length polymorphism to identify 42 *Cladophialophora* strains related to cerebral phaeohyphomycosis with *in vitro* antifungal susceptibility. *J. Clin. Microbiol.* 48, 2350–2356. doi: 10.1128/JCM.00653-10

Badali, H., Gueidan, C., Najafzadeh, M. J., Bonifaz, A., Gerrits van den Ende, A. H., and de Hoog, G. S. (2008). Biodiversity of the genus *Cladophialophora*. *Stud. Mycol.* 61, 175–191. doi: 10.3114/sim.2008.61.18

Bankevich, A., Nurk, S., Antipov, D., Gurevich, A. A., Dvorkin, M., Kulikov, A. S., et al. (2012). SPAdes: a new genome assembly algorithm and its applications to single-cell sequencing. *J. Comput. Biol.* 19, 455–477. doi: 10.1089/cmb.2012.0021

Besemer, J. (2001). GeneMarkS: a self-training method for prediction of gene starts in microbial genomes. Implications for finding sequence motifs in regulatory regions. *Nucleic Acids Res.* 29, 2607–2618. doi: 10.1093/nar/29.12.2607

De Bie, T., Cristianini, N., Demuth, J. P., and Hahn, M. W. (2006). CAFE: a computational tool for the study of gene family evolution. *Bioinformatics*. 22, 1269–1271. doi: 10.1093/bioinformatics/btl097

Boetzer, M., Henke, C. V., Jansen, H. J., Butler, D., and Pirovano, W. (2010). Scaffolding pre-assembled contigs using SSPACE. *Bioinformatics*. 27, 578–579. doi: 10.1093/bioinformatics/btq683

Bombassaro, A., de Hoog, S., Weiss, V. A., Souza, E. M., Leão, A. C. R., Costa, F. F., et al. (2016). Draft genome sequence of *Fonsecaea monophora* strain CBS 269.37, an agent of human chromoblastomycosis. *Genome Announc.* 4, 731–716. doi: 10.1128/genomeA.00731-16

Bourne, H. R., Sanders, D. A., and McCormick, F. (1990). The GTPase superfamily: a conserved switch for diverse cell functions. *Nature* 348, 125–132. doi: 10.1038/348125a0

Cañero, D. C., and Roncero, M. I. (2008). Functional analyses of laccase genes from *Fusarium oxysporum*. *Phytopathology* 98, 509–518. doi: 10.1094/PHYTO-98-5-0509

Cantarel, B. L., Coutinho, P. M., Rancurel, C., Bernard, T., Lombard, V., and Henrissat, B. (2009). The Carbohydrate-Active EnZymes database (CAZy): an expert resource for glycogenomics. *Nucleic Acids Res.* 37, D233–D238. doi: 10.1093/nar/gkn663

Casadevall, A. (2007). Determinants of virulence in the pathogenic fungi. *Fung. Biol. Rev.* 21, 130–132. doi: 10.1016/j.fbr.2007.02.007

Chen, Z., Martinez, D. A., Gujja, S., Sykes, S. M., Zeng, Q., Szaniszlo, P. J., et al. (2014). Comparative genomic and transcriptomic analysis of *Wangiella dermatitidis*, a major cause of phaeohyphomycosis and a model black yeast human pathogen. *G3* 4, 561–578. doi: 10.1534/g3.113.009241

Cheng, J., Park, T. S., Chio, L. C., Fischl, A. S., and Ye, X. S. (2003). Induction of apoptosis by sphingoid long-chain bases in *Aspergillus nidulans*. *Mol. Cell. Biol.* 23, 163–177. doi: 10.1128/MCB.23.1.163-177.2003

Cho, Y., Srivastava, A., Ohm, R. A., Lawrence, C. B., Wang, K. H., Grigoriev, I. V., et al. (2012). Transcription factor amr1 induces melanin biosynthesis and suppresses virulence in *Alternaria brassicicola*. *PLoS Pathog.* 8:e1002974. doi: 10.1371/journal.ppat.1002974

Chow, J. W. (2000). Aminoglycoside resistance in enterococci. *Clin. Infect. Dis.* 31, 586–589. doi: 10.1086/313949

Costa, F. F., de Hoog, S., Raittz, R. T., Weiss, V. A., Leão, A. C., Bombassaro, A., et al. (2016). Draft genome sequence of *Fonsecaea nubica* strain CBS 269.64, causative agent of human chromoblastomycosis. *Genome Announc.* 4, 735–716. doi: 10.1128/genomeA.00735-16

Das, S. K., and Vasudevan, D. M. (2007). Alcohol-induced oxidative stress. *Life Sci.* 81, 177–187. doi: 10.1016/j.lfs.2007.05.005

de Azevedo, C. M., Gomes, R. R., Vicente, V. A., Santos, D. W., Marques, S. G., do Nascimentob, M. M., et al. (2015b). *Fonsecaea pugnacius*, a novel agent of disseminated chromoblastomycosis. *J. Clin. Microbiol.* 53, 2674–2685. doi: 10.1128/JCM.00637-15

de Azevedo, C. M., Marques, S. G., Santos, D. W., Silva, R. R., Silva, N. F., Santos, D. A., et al. (2015a). Squamous cell carcinoma derived from chronic chromoblastomycosis in Brazil. *Clin. Infect. Dis.* 60, 1500–1504. doi: 10.1093/cid/civ104

De Hoog, G. S., Attili-Angelis, D., Vicente, V. A., Gerrits van den Ende, A. H., and Queiroz-Telles, F. (2004). Molecular ecology and pathogenic potential of *Fonsecaea* species. *Med. Mycol.* 42, 405–416. doi: 10.1080/13693780410001661464

De Hoog, G. S., Nishikaku, A. S., Fernandez-Zeppenfeldt, G., Padín-González, C., Burger, E., Badali, H., et al. (2007). Molecular analysis and pathogenicity of the *Cladophialophora carrionii* complex, with the description of a novel species. *Stud. Mycol.* 58, 219–234. doi: 10.3114/sim.2007.58.08

De Hoog, G. S., Queiroz-Telles, F., Haase, G., Fernandez-Zeppenfeldt, G., Attili Angelis, D., Gerrits van den Ende, A. H., et al. (2000). Black fungi: clinical and pathogenic approaches. *Med. Mycol.* 38(Suppl. 1), 243–250. doi: 10.1080/mmy.38.s1.243.250

Dickman, M. B., and Figueired, P. (2011). Comparative pathobiology of fungal pathogens of plants and animals. *PLoS Pathog.* 7:e1002324. doi: 10.1371/journal.ppat.1002324

Dickman, M. B., Podila, G. K., and Kolattukudy, P. E. (1989). Insertion of cutinase gene into a wound pathogen enables it to infect intact host. *Nature* 342, 446–448. doi: 10.1038/342446a0

Douglas, T., Champagne, C., Morizot, A., Lapointe, J. M., and Saleh, M. (2015). The inflammatory caspases-1 and−11 mediate the pathogenesis of dermatitis in sharpin-deficient mice. *J. Immun.* 195, 2365–2373. doi: 10.4049/jimmunol.1500542

Drapeau, M. D., Radovic, A., Wittkopp, P. J., and Long, A. D. (2003). A gene necessary for normal male courtship, yellow, acts downstream of fruitless in the *Drosophila melanogaster* larval brain. *J. Neurobiol.* 55, 53–72. doi: 10.1002/neu.10196

Edgar, R. C. (2004). Muscle: a multiple sequence alignment method with reduced time and space complexity. *BMC Bioinformatics* 5:113. doi: 10.1186/1471-2105-5-113

Eisendle, M., Schrett, M., Krag, C., Muller, D., Illmer, P., and Haas, H. (2006). The intracellular siderophore ferricrocin is involved in iron storage, oxidative-stress resistance, germination, and sexual development in *Aspergillus nidulans*. *Eukaryot Cell.* 5, 1596–1603. doi: 10.1128/EC.00057-06

El-Ganiny, A. M., Sheoran, I., Sanders, D. A., and Kaminskyi, S. G. (2010). *Aspergillus nidulans* UDP-glucose-4-epimerase UgeA has multiple roles in wall architecture, hyphal morphogenesis, and asexual development. *Fungal Genet. Biol.* 47, 629–635. doi: 10.1016/j.fgb.2010.03.002

Ferguson, L. C., Green, J., Surridge, A., and Jiggins, C. D. (2011). Evolution of the insect yellow gene family. *Mol. Biol. Evol.* 28, 257–272. doi: 10.1093/molbev/msq192

Fuchs, B. B., Eby, J., Nobile, C. J., El Khoury, J. B., Mitchell, A. P., and Mylonakis, E. (2010). Role of filamentation in *Galleria mellonella* killing by *Candida albicans*. *Microbes Infect.* 12, 488–496. doi: 10.1016/j.micinf.2010.03.001

Giardina, P., Faraco, V., Pezzella, C., Piscitelli, A., Vanhulle, S., and Sannia, G. (2010). Laccases: a never-ending story. *Cell. Mol. Life Sci.* 67, 369–385. doi: 10.1007/s00018-009-0169-1

Gillespie, E. (1978). Concanavalin A increases glyoxalase enzyme activities in polymorphonuclear leukocytes and lymphocytes. *J. Immunol.* 121, 923–925.

Gillespie, E. (1981). The tumor promoting phorbol diester, 12-O-tetradecanoylphorbol-13-acetate (TPA) increases glyoxalase I and decreases glyoxalase II activity in human polymorphonuclear leucocytes. *Biochem. Biophys. Res. Commun.* 98, 463–470. doi: 10.1016/0006-291X(81)90862-7

Grahl, N., Puttikamonkul, S., Macdonald, J. M., Gamcsik, M. P., Ngo, L. Y., Hohl, T. M., et al. (2011). *In vivo* hypoxia and fungal alcohol dehydrogenase influence the pathogenesis of invasive pulmonary Aspergillosis. *PLoS Pathog.* 7:e1002145. doi: 10.1371/journal.ppat.1002145

Gruber, S., and Seidl-Seiboth, V. (2012). Self versus non-self: fungal cell wall degradation in *Trichoderma*. *Microbiology* 158, 26–34. doi: 10.1099/mic.0.052613-0

Guindon, S., Lethiec, F., Duroux, P., and Gascuel, O. (2005). PHYML Online-a web server for fast maximum likelihood-based phylogenetic inference. *Nucleic Acids Res.* 33, 557–559. doi: 10.1093/nar/gki352

Gyurkovska, V., and Ivanovska, N. (2016). Distinct roles of TNF-related apoptosis-inducing ligand (TRAIL) in viral and bacterial infections: from pathogenesis to pathogen clearance. *Inflamm. Res.* 65, 427–437. doi: 10.1007/s00011-016-0934-1

Hayakawa, M., Ghosn, E. E., da Gloria Teixeria de Sousa M., and Ferreira, K. S. (2006). Phagocytosis, production of nitric oxide and pro-inflammatory cytokines by macrophages in the presence of dematiaceous fungi that cause chromoblastomycosis. *Scand. J. Immunol.* 64, 382–387. doi: 10.1111/j.1365-3083.2006.01804.x

Hoegger, P. J., Kilaru, S., James, T. Y., Thacker, J. R., and Kües, U. (2006). Phylogenetic comparison and classification of laccase and related multicopper oxidase protein sequences. *FEBS J.* 273, 2308–2326. doi: 10.1111/j.1742-4658.2006.05247.x

Itoh, S., Taniguchi, M., Takada, N., Nagatomo, S., Kitagawa, T., and Fukuzumi, S. (2000). Effects of metal ions on the electronic, redox, and catalytic properties of cofactor TTQ of quinoprotein amine dehydrogenases. *J. Am. Chem. Soc.* 122, 12087–12097. doi: 10.1021/ja0020207

Jelen, V., de Jonge, R., Van de Peer, Y., Javornik, B., and Jakše, J. (2016). Complete mitochondrial genome of the *Verticillium*-wilt causing plant pathogen *Verticillium nonalfalfae*. *PLoS ONE* 11:e0148525. doi: 10.1371/journal.pone.0148525

Juhász, K., Buzás, K., and Duda, E. (2013). Importance of reverse signaling of the TNF superfamily in immune regulation. *Expert Rev. Clin. Immunol.* 9, 335–348. doi: 10.1586/eci.13.14

Kim, N. S., Umezawa, Y., Ohmura, S., and Kato, S. (1993). Human glyoxalase I: cDNA cloning, expression, and sequence similarity to glyoxalase I from *Pseudomonas putida*. *J. Biol. Chem.* 268, 11217–11221.

Koo, S., Klompas, M., and Marty, F. M. (2010). *Fonsecaea monophora* cerebral phaeohyphomycosis: case report of successful surgical excision and voriconazole treatment and review. *Med. Mycol.* 48, 769–774. doi: 10.3109/13693780903471081

Lamkanfi, M., Kanneganti, T. D., Franchi, L., and Núñez, G. (2007). Caspase-1 inflammasomes in infection and inflammation. *J. Leukoc. Biol.* 82, 220–225. doi: 10.1189/jlb.1206756

Langmead, B., and Salzberg, S. L. (2012). Fast gapped-read alignment with Bowtie 2. *Nat. Methods.* 9, 357–359. doi: 10.1038/nmeth.1923

Laslett, D., and Canback, B. (2004). ARAGORN, a program to detect tRNA genes and tmRNA genes in nucleotide sequences. *Nucleic Acids Res.* 32, 11–16. doi: 10.1093/nar/gkh152

Leão, A. C. R., Weiss, V. A., Vicente, V. A., Costa, F. F., Bombassaro, A., Raittz, R. T., et al. (2017). Genome sequence of type strain *Fonsecaea multimorphosa* CBS 980.96T, a causal agent of feline cerebral phaeohyphomycosis. *Genome Announc.* 5, 1–2. doi: 10.1128/genomeA.01666-16

Leberer, E., Harcus, D., Dignard, D., Johnson, L., Ushinsky, S., Thomas, D. Y., et al. (2001). Ras links cellular morphogenesis to virulence by regulation of the MAP kinase and cAMP signaling pathways in the pathogenic fungus *Candida albicans*. *Mol. Microbiol.* 42, 673–687. doi: 10.1046/j.1365-2958.2001.02672.x

Lee, C., Kim, I., and Park, C. (2013). Glyoxal detoxification in *Escherichia coli* K-12 by NADPH dependent aldo-keto reductases. *J. Microbiol.* 51, 527–530. doi: 10.1007/s12275-013-3087-8

Leon-Sicairos, N., Reyes-Cortes, R., Guadrón-Llanos, A. M., Madueña-Molina, J., Leon-Sicairos, C., and Canizalez-Román, A. (2015). Strategies of intracellular pathogens for obtaining iron from the environment. *Biomed Res. Int.* 2015, 1–17. doi: 10.1155/2015/476534

Lindahl, R. (1992). Aldehyde dehydrogenases and their role in carcinogenesis. *Crit. Rev. Biochem. Mol. Biol.* 27, 283–335. doi: 10.3109/10409239209082565

Lozano-Torres, J. L., Wilbers, R. H., Gawronski, P., Boshoven, J. C., Finkers-Tomczak, A., Cordewener, J. H., et al. (2012). Dual disease resistance mediated by the immune receptor Cf-2 in tomato requires a common virulence target of a fungus and a nematode. *Proc. Natl. Acad. Sci. U.S.A.* 109, 10119–10124. doi: 10.1073/pnas.1202867109

Lund, P. A. (2001). Microbial molecular chaperones. *Adv. Microb. Physiol.* 44, 93–140. doi: 10.1016/S0065-2911(01)44012-4

Ma, Z., Song, T., Zhu, L., Ye, W., Wang, Y., Shao, Y., et al. (2015). A *Phytophthora sojae* Glycoside hydrolase 12 protein is a major virulence factor during soybean infection and is recognized as a PAMP. *Plant Cell.* 27, 2057–2072. doi: 10.1105/tpc.15.00390

Madeo, F., Herker, E., Maldener, C., Wissing, S., Lächelt, S., Herlan, M., et al. (2002). A caspase-related protease regulates apoptosis in yeast. *Mol. Cell.* 9, 911–917. doi: 10.1016/S1097-2765(02)00501-4

Matthews, J. M., and Sunde, M. (2002). Zinc fingers—folds for many occasions. *IUBMB Life* 54, 351–355. doi: 10.1080/15216540216035

Mednick, A. J., Nosanchuk, J. D., and Casadevall, A. (2005). Melanization of *Cryptococcus neoformans* affects lung inflammatory responses during cryptococcal infection. *Infect. Immun.* 73, 2012–2019. doi: 10.1128/IAI.73.4.2012-2019.2005

Moreno, L. F., Feng, P., Weiss, V. A., Vicente, V. A., Stielow, J. B., et al. (2017). Phylogenomic analyses reveal the diversity of laccase-coding genes in *Fonsecaea* genomes. *PLoS ONE* 12:e0171291. doi: 10.1371/journal.pone.0171291

Najafzadeh, M. J., Sun, J., Vicente, V. A., Xi, L., van den Ende, A. H., and de Hoog, G. S. (2010). *Fonsecaea nubica* sp. nov, a new agent of human chromoblastomycosis revealed using molecular data. *Med. Mycol*. 48, 800–806. doi: 10.3109/13693780903503081

Najafzadeh, M. J., Vicente, V. A., Sun, J., Meis, J. F., and de Hoog, G. S. (2011). *Fonsecacea multimorphosa* sp. nov, a new species of Chaetothyriales isolated from a feline cerebral abscess. *Fungal Biol.* 115, 1066–1076. doi: 10.1016/j.funbio.2011.06.007

Nosanchuk, J. D. (2005). Protective antibodies and endemic dimorphic fungi. *Curr. Mol. Med.* 5, 435–442. doi: 10.2174/1566524054022530

Nosanchuk, J. D., Gomez, B. L., Youngchim, S., Diez, S., Aisen, P., Zancopé-Oliveira, R. M., et al. (2002). *Histoplasma capsulatum* synthesizes melanin-like pigments *in vitro* and during mammalian infection. *Infect. Immun.* 70, 5124–5131. doi: 10.1128/IAI.70.9.5124-5131.2002

Oujezdsky, K. B., Grove, S. N., and Szaniszlo, P. J. (1973). Morphological and structural changes during the yeast-to-mold conversion of *Phialophora dermatitidis. J. Bact.* 113, 468–477.

Paduch, M., Jelen, F., and Otlewski, J. (2001). Structure of small G proteins and their regulators. *Acta Biochimic Pol*. 48, 829–850.

Palmeira, V. F., Kneipp, L. F., Rozental, S., Alviano, C. S., and Santos, A. L. (2008). Beneficial effects of HIV peptidase inhibitors on *Fonsecaea pedrosoi*: promising compounds to arrest key fungal biological processes and virulence. *PLoS ONE* 3:e3382. doi: 10.1371/journal.pone.0003382

Panepinto, J. C., Oliver, B. G., Fortwendel, J. R., Smith, D. L., Askew, D. S., and Rhodes, J. C. (2003). Deletion of the *Aspergillus fumigatus* gene encoding the Ras-related protein RhbA reduces virulence in a model of invasive pulmonary aspergillosis. *Infect. Immun.* 71, 2819–2826. doi: 10.1128/IAI.71.5.2819-2826.2003

Pensec, F., Lebeau, A., Daunay, M. C., Chiroleu, F., Guidot, A., and Wicker, E. (2015). Towards the identification of type III effectors associated with *Ralstonia solanacearum* virulence on tomato and eggplant. *Phytopathology* 105, 1529–1544. doi: 10.1094/PHYTO-06-15-0140-R

Piro, V. C., Faoro, H., Weiss, V. A., Steffens, M. B., Pedrosa, F. O., Souza, E. M., et al. (2014). FGAP: an automated gap closing tool. *BMC Res. Notes*. 7:371. doi: 10.1186/1756-0500-7-371

Prenafeta-Boldú, F. X., Summerbell, R., and de Hoog, S. G. (2006). Fungi growing on aromatics hydrocarbons: biotechnology's unexpected encounter with biohazard? *FEMS Microbiol. Rev.* 30, 109–130 doi: 10.1111/j.1574-6976.2005.00007.x

Queiroz-Telles, F. (2015). Chromoblastomycosis: a neglected tropical disease. *Rev. Inst. Med. Trop.* 57, 46–50. doi: 10.1590/S0036-46652015000700009

Queiroz-Telles, F., de Hoog, S. G., Santos, D. W. C. L., Salgado, C. G., Vicente, V. A., Bonifaz, A., et al. (2017). Chromoblastomycosis. *Clin. Microbiol. Rev.* 30, 233–276. doi: 10.1128/CMR.00032-16

Quevillon, E., Silventoinen, V., Pillai, S., Harte, N., Mulder, N., Apweiler, R., et al. (2005). InterProScan: protein domains identifier. *Nucleic Acids Res.* 33, 116–120. doi: 10.1093/nar/gki442

Rawlings, N. D., Barrett, A. J., and Finn, R. (2015). Twenty years of the MEROPS database of proteolytic enzymes, their substrates and inhibitors. *Nucleic Acids Res.* 44, 343–350. doi: 10.1093/nar/gkv1118

Salgado, C. G., da Silva, J. P., Diniz, J. A., Silva, M. B., Costa, P. F., Teixeira, C., et al. (2004). Isolation of *Fonsecaea pedrosoi* from thorns of *Mimosa pudica*, a probable natural source of chromoblastomycosis. *Rev. Inst. Med. Trop*. 46, 33–36. doi: 10.1590/S0036-46652004000100006

Schumann, R. R., Belka, C., Reuter, D., Lamping, N., Kirschning, C. J., et al. (1998). Lipopolysaccharide activates caspase-1 (interleukin-1–converting enzyme) in cultured monocytic and endothelial cells. *Blood* 91, 577–584.

Sexton, A. C., and Howlett, B. J. (2006). Parallels in fungal pathogenesis on plant and animal hosts. *Eukaryotic Cell* 5, 1941–1949. doi: 10.1128/EC.00277-06

Seyedmousavi, S., Badali, H., Chlebicki, A., Zhao, J., Prenafeta-Boldú, F. X., and De Hoog, G. S. (2011). *Exophiala sideris*, a novel black yeast isolated from environments polluted with toxic alkyl benzenes and arsenic. *Fung. Biol.* 115, 1030–1037. doi: 10.1016/j.funbio.2011.06.004

Shelest, E. (2008). Transcriptional factors in fungi. *FEMS Microbiol. Lett.* 286, 145–151. doi: 10.1111/j.1574-6968.2008.01293.x

da Silva, B. A., dos Santos, A. L., Barreto-Bergter, E., and Pinto, M. R. (2006). Extracellular peptidase in the fungal pathogen *Pseudallescheria boydii*. *Curr. Microbiol.* 53, 18–12. doi: 10.1007/s00284-005-0156-1

Siqueira, I. M., de Castro, R. J. A., Leonhardt, L. C. M., Jerônimo, M. S., Soares, A. C., Raiol, T., et al. (2017). Modulation of the immune response by *Fonsecaea pedrosoi* morphotypes in the course of experimental chromoblastomycosis and their role on inflammatory response chronicity. *PLoS Negl. Trop. Dis.* 11:e0005461. doi: 10.1371/journal.pntd.0005461

Son, H., Sep, Y. S., Min, K., Park, A. R., Lee, J., Jin, J. M., et al. (2011). A phenome-based functional analysis of transcription factors in the cereal head blight fungus, *Fusarium graminearum*. *PLoS Pathog.* 7:e1002310. doi: 10.1371/journal.ppat.1002310

Sriranganadane, D., Waridel, P., Salamin, K., Reichard, U., Grouzmann, E., Neuhaus, J. M., et al. (2010). *Aspergillus* protein degradation pathways with different secreted protease sets at neutral and acidic pH. *J. Proteome Res.* 9, 3511–3519. doi: 10.1021/pr901202z

Strommer, J. (2011). The plant ADH gene family. *Plant J.* 66, 128–142. doi: 10.1111/j.1365-313X.2010.04458.x

Sudhadham, M., Prakitsin, S., Sivichai, S., Chaiyarat, R., Dorrestein, G. M., Menken, S. B. J., et al. (2008). The neurotropic black yeast *Exophiala dermatitidis* has a possible origin in the tropical rain forest. *Stud. Mycol.* 61, 145–155. doi: 10.3114/sim.2008.61.15

Suppiger, A., Eshwar, A. K., Stephan, R., Kaever, V., Eberl, L., and Lehner, A. (2016). The DSF type quorum sensing signalling system RpfF/R regulates diverse phenotypes in the opportunistic pathogen *Cronobacter*. *Sci. Rep.* 6:18753. doi: 10.1038/srep18753

Surash, S., Tyagi, A., de Hoog, G. S., Zeng, J. S., Barton, R. C., and Hobson, R. P. (2005). Cerebral phaeohyphomycosis caused by *Fonsecaea monophora*. *Med. Mycol.* 43, 465–472. doi: 10.1080/13693780500220373

Taborda, C. P., da Silva, M. B., Nosanchuk, J. D., and Travassos, L. R. (2008). Melanin as a virulence factor of *Paracoccidioides brasiliensis* and other dimorphic pathogenic fungi: a minireview. *Mycopathologia* 165, 331–339. doi: 10.1007/s11046-007-9061-4

Takei, H., Goodman, J. C., and Powell, S. Z. (2007). Cerebral phaeohyphomycosis caused by *Cladophialophora bantiana* and *Fonsecaea monophora*: report of three cases. *Clin. Neuropathol.* 26, 21–27. doi: 10.5414/NPP26021

Talavera, G., and Castresana, J. (2007). Improvement of phylogenies after removing divergent and ambiguously aligned blocks from protein sequence alignments. *Systemat Biol.* 56, 564–577. doi: 10.1080/10635150701472164

Tamayo, D., Muñoz, J. F., Torres, I., Almeida, A. J., Restrepo, A., McEwen, J. G., et al. (2013). Involvement of the 90 kDa heat shock protein during adaptation of *Paracoccidioides brasiliensis* to different environmental conditions. *Fungal Genet. Biol.* 51, 34–41. doi: 10.1016/j.fgb.2012.11.005

Teixeira, M. M., Moreno, L. F., Stielow, B. J., Muszewska, A., Hainaut, M., Gonzaga, L., et al. (2017). Exploring the genomic diversity of black yeasts and relatives (Chaetothyriales, Ascomycota). *Stud. Mycol.* 86, 1–28. doi: 10.1016/j.simyco.2017.01.001

Teixeira, P. A., De Castro, R. A., Ferreira, F. R., Cunha, M. M., Torres, A. P., Penha, C. V., et al. (2010). L-DOPA accessibility in culture medium increases melanin expression and virulence of *Sporothrix schenckii* yeast cells. *Med. Mycol.* 48, 687–695. doi: 10.3109/13693780903453287

Thomaz, L., Garcia-Rodas, R., Guimarães, A. J., Taborda, C. P., Zaragoza, O., and Nosanchuk, J. D. (2013). *Galleria mellonella* as a model host to study *Paracoccidioides lutzii* and *Histoplasma capsulatum*. *Virulence* 4:2. doi: 10.4161/viru.23047

Thornalley, P. J. (1993). The glyoxalase system in health and disease. *Elsevier* 14, 287–371. doi: 10.1016/0098-2997(93)90002-U

Torriani, S. F., Penselin, D., Knogge, W., Felder, M., Taudin, S., Platzer, M., et al. (2014). Comparative analysis of mitochondrial genomes from closely related *Rhynchosporium* species reveals extensive intron invasion. *Fung. Genet. Biol.* 62, 34–42. doi: 10.1016/j.fgb.2013.11.001

Trower, M. K., and Clark, K. G. (1990). PCR cloning of a streptomycin phosphotransferase (aphE) gene from *Streptomyces griseus* ATCC 12475. *Nucleic Acids Res.* 18:4615. doi: 10.1093/nar/18.15.4615

van Berkel, W. J., Kamerbeek, N. M., and Fraaije, M. W. (2006). Flavoprotein monooxygenases, a diverse class of oxidative biocatalysts. *J. Biotechnol.* 124, 670–689. doi: 10.1016/j.jbiotec.2006.03.044

van den Sande, W. W., de Kat, J., Coppens, J., Ahmed, A. O., Fahal, A., Verbrugh, H., et al. (2007). Melanin biosynthesis in *Madurella mycetomatis* and its effect on susceptibility to itraconazole and ketoconazole. *Microb. Infect.* 9, 1114–1123. doi: 10.1016/j.micinf.2007.05.015

Varrot, A., Basheer, S. M., and Imberty, A. (2013). Fungal lectins: structure, function and potential applications. *Curr. Opin. Struct. Biol.* 23, 678–685. doi: 10.1016/j.sbi.2013.07.007

Vasiliou, V., Pappa, A., and Petersen, D. R. (2000). Role of aldehyde dehydrogenases in endogenous and xenobiotic metabolism. *Chem. Biol. Interact.* 129, 1–19. doi: 10.1016/S0009-2797(00)00211-8

Vialle, R. A., Pedrosa, F. O., Weiss, V. A., Guizelini, D., Tibaes, J. H., Marchaukoski, J. N., et al. (2016). RAFTS3: Rapid alignment-free tool for sequence similarity search. *BioRxiv*. 1–32. doi: 10.1101/055269

Vicente, V. A., Atilli-Angellis, D., Pie, M. R., Queiroz-Telles, F., Cruz, L. M., Najafzadeh, M. J., et al. (2008). Environmental isolation of black yeast-like fungi involved in human infection. *Stud. Mycol.* 61, 137–144. doi: 10.3114/sim.2008.61.14

Vicente, V. A., Attili-Angelis, D., Queiróz-Telles, F., and Pizzirani-Kleiner, A. A. (2001). Isolation of herpotrichiellacious fungi from the environment. *Br. J. Microbiol.* 32, 47–51. doi: 10.1590/S1517-83822001000100011

Vicente, V. A., Najafzadeh, M. J., Sun, J., Gomes, R. R., Robl, D., Marques, S. G., et al. (2014). Environmental siblings of black agents of human chromoblastomycosis. *Fung. Div.* 65, 47–63. doi: 10.1007/s13225-013-0246-5

Vicente, V. A., Orélis-Ribeiro, R., Najafzadeh, M. J., Sun, J., Guerra, R. S., Miesch, S., et al. (2012). Black yeast-like fungi associated with Lethargic Crab Disease (LCD) in the mangrove-land crab, *Ucides cordatus* (Ocypodidae). *Vet. Microbiol.* 158, 109–122. doi: 10.1016/j.vetmic.2012.01.031

Walton, F. J., Idnurm, A., and Heitman, J. (2005). Novel gene functions required for melanization of the human pathogen *Cryptococcus neoformans*. *Mol. Microbiol.* 57, 1381–1396. doi: 10.1111/j.1365-2958.2005.04779.x

Wang, Y., Liu, W., Hou, Z., Wang, C., Zhou, X., Jonkers, W., et al. (2011). A novel transcriptional factor important for pathogenesis and ascosporogenesis in *Fusarium graminearum*. *Mol. Plant Microbe Interact.* 24, 118–128. doi: 10.1094/MPMI-06-10-0129

Winnenburg, R., Urban, M., Beacham, A., Baldwin, T. K., Holland, S., Lindeberg, M., et al. (2007). PHI-base update: additions to the pathogen host interaction database. *Nucleic Acids Res.* 36, 572–576. doi: 10.1093/nar/gkm858

Xi, L., Sun, J., Lu, C., Liu, H., Xie, Z., Fukushima, K., et al. (2009). Molecular diversity of *Fonsecaea* (Chaetothyriales) causing chromoblastomycosis in southern China. *Med. Mycol.* 47, 27–33. doi: 10.1080/13693780802468209

Yim, M. B., Yim, H. S., Lee, C., Kang, S. O., and Chock, P. B. (2001). Protein glycation: creation of catalytic sites for free radical generation. *Ann. N.Y. Acad. Sci.* 928, 48–53. doi: 10.1111/j.1749-6632.2001.tb05634.x

Zhao, Z., Liu, H., Wang, C., and Xu, J. R. (2013). Comparative analysis of fungal genomes reveals different plant cell wall degrading capacity in fungi. *BMC Genomics*. 14:274. doi: 10.1186/1471-2164-14-274

Zhou, Z., Li, G., Lin, C., and He, C. (2009). Conidiophore stalk-less1 encodes a putative zinc-finger protein involved in the early stage of conidiation and mycelial infection in *Magnaporthe oryzae*. *Mol. Plant Microbe Interact.* 22, 402–410. doi: 10.1094/MPMI-22-4-0402

Conflict of Interest Statement: The authors declare that the research was conducted in the absence of any commercial or financial relationships that could be construed as a potential conflict of interest.

frontiers in Microbiology

ORIGINAL RESEARCH
published: 09 October 2018
doi: 10.3389/fmicb.2018.02211

A Model for Trans-Kingdom Pathogenicity in *Fonsecaea* Agents of Human Chromoblastomycosis

Gheniffer Fornari[1], Renata Rodrigues Gomes[1], Juliana Degenhardt-Goldbach[2], Suelen Silvana dos Santos[3], Sandro Rogério de Almeida[3], Germana Davila dos Santos[1], Marisol Dominguez Muro[4], Cleusa Bona[5], Rosana Herminia Scola[6], Edvaldo S. Trindade[7], Israel Henrique Bini[7], Lisandra Santos Ferreira-Maba[7], Daiane Rigoni Kestring[2], Mariana Machado Fidelis do Nascimento[1], Bruna Jacomel Favoreto de Souza Lima[1], Morgana F. Voidaleski[1], Douglas André Steinmacher[8], Bruna da Silva Soley[9], Shuwen Deng[10], Anamelia Lorenzetti Bocca[11], Moises B. da Silva[12], Claudio G. Salgado[11], Conceição Maria Pedroso e Silva de Azevedo[13], Vania Aparecida Vicente[1] and Sybren de Hoog[1,9,14,15]**

[1] Microbiology, Parasitology and Pathology Post-graduation Program, Department of Basic Pathology, Federal University of Paraná, Curitiba, Brazil, [2] Embrapa Forestry, Brazilian Agricultural Research Corporation (EMBRAPA), Colombo, Brazil, [3] Department of Clinical and Pharmacological Analysis, College of Pharmaceutical Sciences, University of São Paulo, São Paulo, Brazil, [4] Support and Diagnosis Unit, Mycology Laboratory, Hospital of Clinics, Federal University of Paraná, Curitiba, Brazil, [5] Department of Botany, Federal University of Paraná, Curitiba, Brazil, [6] Hospital of Clinics, Federal University of Paraná, Curitiba, Brazil, [7] Department of Cell Biology, Federal University of Paraná, Curitiba, Brazil, [8] Vivetech Agrociências, Paraná, Brazil, [9] Department of Pharmacology, Federal University of Paraná, Curitiba, Brazil, [10] Department of Medical Microbiology, People's Hospital of Suzhou National New & Hi-Tech Industrial Development Zone, Jiangsu, China, [11] Dermato-Immunology Laboratory, Institute of Biological Sciences, Federal University of Para, Marituba, Brazil, [12] Department of Cell Biology, University of Brasília (UnB), Brasília, Brazil, [13] Department of Medicine, Federal University of Maranhão, São Luís, Brazil, [14] Westerdijk Fungal Biodiversity Institute, Utrecht, Netherlands, [15] Center of Expertise in Mycology Radboudumc/CWZ, Nijmegen, Netherlands

OPEN ACCESS

Edited by:
Orazio Romeo,
Università degli Studi di Messina, Italy

Reviewed by:
Peiying Feng,
Sun Yat-sen University, China
Gil Benard,
Universidade de São Paulo, Brazil

***Correspondence:**
Vania Aparecida Vicente
vaniava63@gmail.com
Sybren de Hoog
s.hoog@westerdijkinstitute.nl

Specialty section:
This article was submitted to Fungi and Their Interactions, a section of the journal Frontiers in Microbiology

Received: *01 April 2018*
Accepted: *29 August 2018*
Published: *09 October 2018*

Citation:
Fornari G, Gomes RR, Degenhardt-Goldbach J, Santos SSd, Almeida SRd, Santos GDd, Muro MD, Bona C, Scola RH, Trindade ES, Bini IH, Ferreira-Maba LS, Kestring DR, Nascimento MMFd, Lima BJFdS, Voidaleski MF, Steinmacher DA, Soley BdS, Deng S, Bocca AL, da Silva MB, Salgado CG, de Azevedo CMPS, Vicente VA and de Hoog S (2018) A Model for Trans-Kingdom Pathogenicity in Fonsecaea Agents of Human Chromoblastomycosis. Front. Microbiol. 9:2211. doi: 10.3389/fmicb.2018.02211

The fungal genus *Fonsecaea* comprises etiological agents of human chromoblastomycosis, a chronic implantation skin disease. The current hypothesis is that patients acquire the infection through an injury from plant material. The present study aimed to evaluate a model of infection in plant and animal hosts to understand the parameters of trans-kingdom pathogenicity. Clinical strains of causative agents of chromoblastomycosis (*Fonsecaea pedrosoi* and *Fonsecaea monophora*) were compared with a strain of *Fonsecaea erecta* isolated from a living plant. The clinical strains of *F. monophora* and *F. pedrosoi* remained concentrated near the epidermis, whereas *F. erecta* colonized deeper plant tissues, resembling an endophytic behavior. In an invertebrate infection model with larvae of a beetle, *Tenebrio molitor*, *F. erecta* exhibited the lowest survival rates. However, *F. pedrosoi* produced dark, spherical to ovoidal cells that resembled muriform cells, the invasive form of human chromoblastomycosis confirming the role of muriform cells as a pathogenic adaptation in animal tissues. An immunologic assay in BALB/c mice demonstrated the high virulence of saprobic species in animal models was subsequently controlled via host higher immune response.

Keywords: *Fonsecaea*, chromoblastomycosis, virulence, *Mimosa pudica*, *Bactris gasipaes*, *Tenebrio molitor*, animal model, plant model

INTRODUCTION

The fungal genus *Fonsecaea* comprises several etiologic agents of human chromoblastomycosis, a severely mutilating skin disease. The genus belongs to the family Herpotrichiellaceae, which consists of numerous species potentially causing a wide range of recalcitrant infections. Among these are cerebral and disseminated diseases which if untreated mostly lead to the death of the patient (Najafzadeh et al., 2011; Doymaz et al., 2015; Gomes et al., 2016). In general, immunocompromised individuals are more susceptible to fungal infections; however, in black fungi infection is also observed in apparently healthy individuals. Vertebrate hosts other than humans include fish and amphibians, other host animals being very rare (de Hoog et al., 2011).

Chromoblastomycosis is characterized by a chronic involvement of cutaneous and subcutaneous tissues containing the fungal invasive form, the muriform cell embedded in microabscesses and fibrosis. The infection often shows skin tissue proliferation, leading to clinically recognizable nodular, tumoral (cauliflower-like), verrucous, scarring, or plaque-like lesions (Queiroz-Telles et al., 2017). The prevalent agents of the disease include *Fonsecaea pedrosoi*, *Fonsecaea monophora*, *Cladophialophora carrionii* (Badali et al., 2008; Doymaz et al., 2015), and *Rhinocladiella aquaspersa* (Badali et al., 2010; González et al., 2013). *Cladophialophora carrionii* is found in arid and semi-arid climates (Lavelle, 1980), while *Fonsecaea* species are endemic to the areas with a warm and humid climate (Najafzadeh et al., 2011).

The causative fungal species seem to be implanted into the host skin through sharp specimens of plant debris, such as thorns, carrying the respective opportunistic agent. In this regard, a report indicated their isolation from plant debris, while non-pathogenic relatives were occasionally derived from living plants (Vicente et al., 2008). Epidemiological data provided evidence of traumatic infection by puncture of plant material (Rubin et al., 1991; Fernández-Zeppenfeldt et al., 1994; Queiroz-Telles et al., 2017). Marques et al. (2006) isolated *Fonsecaea*-like fungi from the shells of babassu coconuts of the palm tree, *Orbignya phalerata* and Salgado et al. (2004) found a species morphologically resembling *Fonsecaea* on the thorns of a *Mimosa pudica* plant, which the patient identified as the possible source of his disease.

However, molecular studies have demonstrated that the major part of the environmental strains morphologically that are similar to clinical strains do not necessarily belong to the same species (Crous et al., 2006; Mostert et al., 2006; Vicente et al., 2013). Sequence data of the clinical strains of *C. carrionii* and of a *Cladophialophora* species isolated from cactus thorns surrounding the cottage of a patient demonstrated them to belong to a different species, *C. yegresii*, which had never been observed to infect a human host (de Hoog et al., 2007). Upon environmental sampling to recover the clinical species (Marques et al., 2006; Vicente et al., 2008, 2013), *F. pedrosoi* and *F. monophora* were only rarely encountered, while the majority of environmental species were not known from human infections. Vicente et al. (2013) described the environmental *Fonsecaea* sibling species as novel taxa, named *F. minima* and *F. erecta*.

The apparent selection by human tissue of *F. monophora* and *F. pedrosoi* remains unexplained. The disease is characterized by the presence of muriform cells inside host tissues, which can also be reproduced *in vitro* in non-pathogenic species (Badali et al., 2008). de Hoog et al. (2007) demonstrated that both the clinical species, *C. carrionii* and the environmental, *C. yegresii* could produce muriform cells upon their artificial inoculation into cactus plants, which seemed to contradict the observed predilections for animal hosts (Vicente et al., 2013). In addition, more detailed understanding of the natural ecology and environmental niches of chromoblastomycosis agents is required to monitor the possible routes of infection (Gümral et al., 2014). Adequate infection models in animal and plant hosts are required to build up plausible evolutionary hypotheses.

Therefore, the present study compared plant and animal models to evaluate the associations of hosts with clinical and environmental *Fonsecaea* strains to understand the mechanisms involved in the adaptation of fungal animal and plant disease to elucidate routes of infection of this implantation disease.

MATERIALS AND METHODS

Strains

The fungal strains were acquired from the reference collection of Centraalbureau voor Schimmelcultures (CBS; housed at the Westerdijk Fungal Biodiversity Institute, Utrecht, Netherlands) and Microbiological Collections of Paraná Network (CMRP, Curitiba, Brazil), i.e., *F. pedrosoi* (CBS 271.37) and *F. monophora* (CBS 102248), both isolated from human chromoblastomycosis, and the environmental species, *F. erecta* (CBS 125763) isolated from a living plant (Vicente et al., 2013). In addition, an endophyte, *Colletogloeopsis dimorpha* (CMRP 1417) isolated from *M. pudica* and a strain of *Cladosporium tenuissimum* (CMRP 1441) isolated as endophyte from *Bactris gasipaes* were utilized as controls. The cultures were maintained on 2% malt extract agar (MEA) and Sabouraud's glucose agar (SGA) at 28°C.

Plant Inoculum Preparation

The fungal strains were grown on potato dextrose agar (PDA) at 28°C for 7 days. Conidial production was enhanced by passing the cells through a liquid PDA medium in a shaker at 200 rpm at 30°C. After 5 days, the cells were allowed to settle; hyphae and conidia were decanted, and the supernatant was filtered through a cell strainer membrane with 40 μm pore size. After repeated washings with phosphate buffered saline (PBS), the inocula were adjusted to the concentration tested and the cell viability was determined by plating of the suspensions on Mycosel agar followed by incubation for 7 days at 28 and 37°C for *Fonsecaea* species, while the control strains were incubated on PDA at 28°C for 7 days.

In vitro and in Vessel Assays Using *M. pudica* and *B. gasipaes*

Seeds of *M. pudica* were provided by the Brazilian Agricultural Research Corporation-EMBRAPA (Manaus, Brazil). Seeds were

washed by keeping them for 30 min in flasks under running tap water, then surface sterilized inside a laminar flow chamber with 70% ethanol for 1 min and 5% sodium hypochlorite (NaOCl) for 10 min followed by rinsing thrice with autoclaved distilled water. The seeds were incubated in concentrated sulfuric acid for 15–20 min followed by rinsing thrice in autoclaved distilled water (Souza Filho et al., 2001; Paiva and Aloufa, 2009). Subsequently, the seeds were cultured in agar-solidified Murashige and Skoog (MS) medium (Murashige and Skoog, 1962) containing 3% sucrose for germination. The seeds began to germinate after 48 h under aseptic conditions. An *in vitro* cultured palm plant (*B. gasipaes*) was provided by Vivetech Agrociências using the protocols based on Steinmacher et al. (2011).

In the *in vitro* and in vessel assays, both plants tested were inoculated with three *Fonsecaea* species (*F. pedrosoi* "Fp", *F. monophora* "Fm", and *F. erecta* "Fe"), The endophyte, *C. dimorpha* (CMRP 1417) was utilized as the positive control and sterile saline (NaCl 0.85%) was utilized as negative control. The experiments were performed in duplicate with groups of four plants per evaluated strain.

In vitro Plant Inoculation

Plants of *M. pudica* were inoculated with 10 μL of the strains culture solutions at concentrations of 10^2, 10^3, 10^4, 10^5, and 10^6 cells/mL, whereas the plants of *B. gasipaes* were inoculated at concentrations of 10^2 and 10^5 cells/mL. Positive and negative controls had equal volumes. The experiments were performed in duplicate with groups of four plants per evaluated strain The inocula were applied at five different points on the plant stem using 10 μL containing 10^2 cells/mL of each tested strain according to three protocols: (I) direct injection into the stem, (II) stem injury followed by micropipette inoculation, and (III) suspension of culture medium around the root (**Figure 1A**). The plants were maintained *in vitro* under controlled temperature at 28°C. Plant detected with fungal inside the tissues was transferred to the vessel (IV).

Vessel Plant Inoculation

The *M. pudica* plants previously inoculated *in vitro* were transplanted to vessels with soil substrate (**Figure 1A**) and maintained at a temperature of 30°C with 85% humidity in a Versatile Environmental Test Chamber (VETC; Panasonic MLR-352). Additionally, 61 plants of *M. pudica* obtained by a micropropagation protocol and maintained under aseptic conditions during 60 days were transplanted to the substrate soil containing loam/vermiculite (2:1). In addition, 24 plants of *B. gasipaes* were maintained in soil vessels at a temperature of 30°C with 85% humidity in a VETC at the EMBRAPA forest facility. After 15 days of incubation, inoculations were performed following three protocols: (I) direct injection into the stem, (II) injury associated with injection in the stem, and (III) suspension of 250 mL of liquid culture of each strain tested containing 1×10^6 cells/mL (**Figure 1B**). The experiments were performed in duplicate with groups of four plants per evaluated strain.

Plant Sample Microscopy

Histological sections were obtained at days 15, 30, 45, and 60 after infection. Plant samples were fixed and stained based on Bernal et al. (2015). The slides were observed and photomicrographs were captured using an Olympus microscope equipped with an SC30 camera.

Identification of Fungal Colony Recovered From Plant Tissue Artificially Inoculated

The re-isolation of fungi from plant tissues was performed by culturing in Sabouraud's medium for 2 weeks at 28°C and by flotation technique in mineral oil (Vicente et al., 2008). The fungal ID was confirmed by rDNA internal transcribed spacer (ITS) sequencing (Vicente et al., 2013).

Virulence Testing With *Tenebrio molitor*

The assessment of survival after fungal infection was done with larvae of *Tenebrio molitor* of approximately 100–200 mg using a total of 10 larvae per strains tested: Fp, Fm and Fe (**Figure 1C**). The inocula of 1×10^6 cells/mL in sterile PBS in aliquots of 5 μL were injected using a Hamilton syringe with a 0.75 mm diameter needle into the hemocoel, the second or third sternite visible above the legs, and the ventral portion. Negative controls included sterile PBS and control sham without physical damage (no treatment). The larvae were placed in sterile Petri dishes and kept in darkness at 37°C. Mortality was monitored once a day for 10 days. The pupae were omitted from the calculation. To detect melanization, the hemolymph of each larva was collected at 4, 24 h, 3, 7, and 10 days postinfection (Scorzoni et al., 2013) and the melanization was determined according to Perdoni et al. (2014). Each hemolymph sample was measured thrice independently. The experiments were performed in triplicate with groups of ten animals, with a total of 30 larvae per group. Survival curves were plotted and statistical analyses were performed according to Maekawa et al. (2015) using the Log-rank (Mantel-Cox), with a *p*-value 0.05 and two-way ANOVA, indicating statistical significance, according to test survival GraphPad Prism 5.

Tenebrio molitor Tissue Burden and Histopathology

Three caterpillars per group (Fp, Fm, and Fe) were weighed and homogenized in 1 mL sterile PBS with a TissueLyser (Qiagen), plated on Mycosel agar, and incubated at 30°C for 14 days. Fungal growth from caterpillars was measured by the number of colony forming units (CFUs) per mL of solution and the re-isolated fungi were sequenced. The samples were embedded in adracanth gum (7 g adracanth in 100 mL of distilled water, 1 drop of formaldehyde), immersed in liquid nitrogen, and sectioned (8 μm) using steel blades in a cryostat (Leica CM 1850). The samples were stained with hematoxylin and eosin (HE) and observed using an Axio Imager Z2 (Carl Zeiss; Jena, Germany) equipped with Metafer 4/VSlide automated capture software (MetaSystems; Altlußheim, Germany) and a CoolCube 1 (MetaSystems) camera.

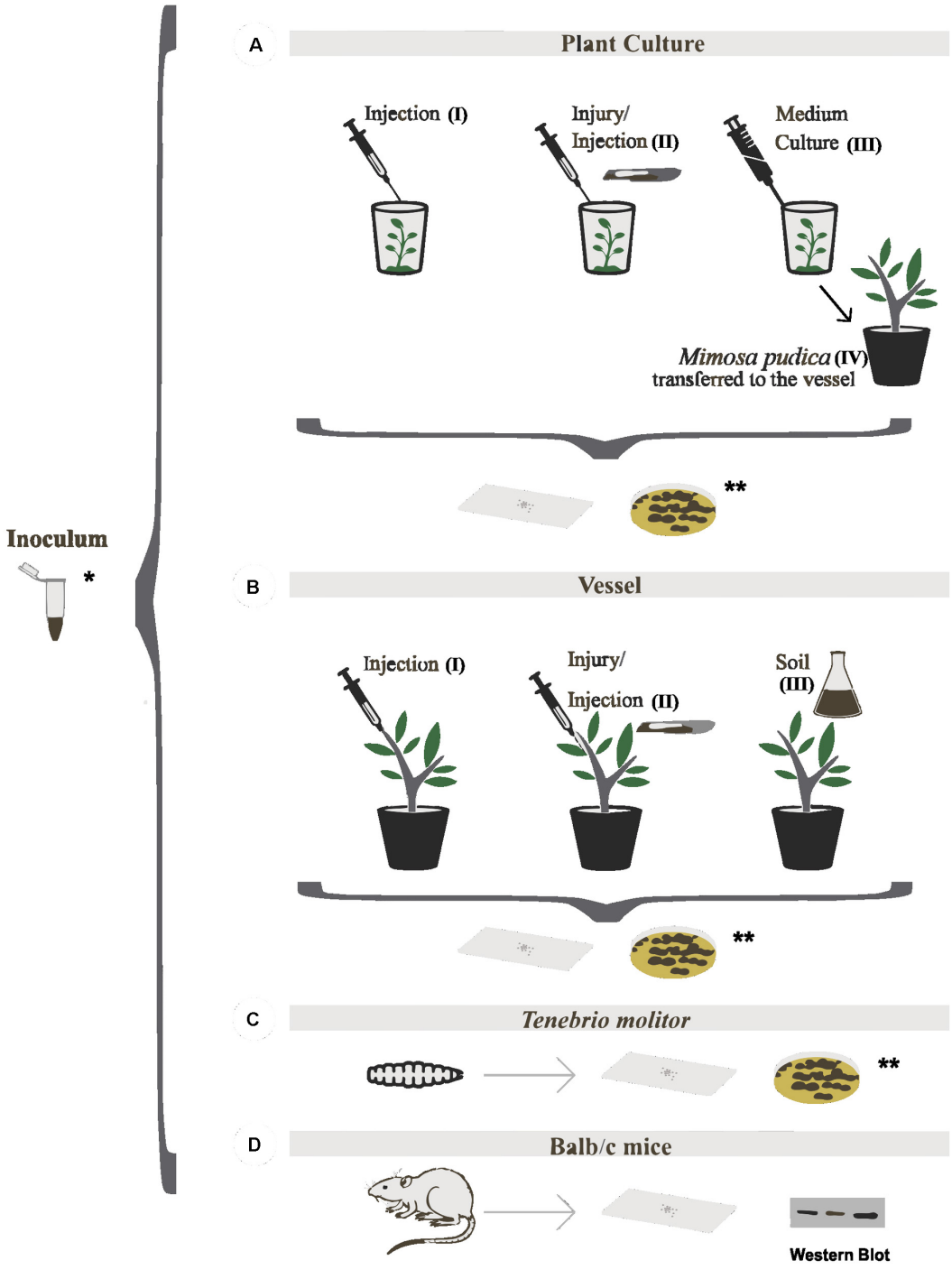

FIGURE 1 | Virulence models tested in *Fonsecaea* sibling species. **(A)** *In vitro* inoculation of plants [**(1AI)** injection, **(1AII)** injury/injection and **(1AIII)** medium culture] and *M. pudica* transferred to the vessel previously *in vitro* infected **(1AIV)**; **(B)** Inoculation of plants in vessel (injection, injury/injection, and soil); **(C)** tests in *Tenebrio molitor*; **(D)** tests in BALB/c mice. *Inoculum of the studied strains and **all experiments were monitored by the slides and re-isolation in culture in the plate.

Immunogenic Testing in Murine Model

Immunocompetent BALB/c male mice (SPF, 6- to 8-week-old) were maintained under standard laboratory conditions (**Figure 1D**). Inocula of Fp, Fm, and Fe were adjusted to 5×10^7 cells/mL using sterile PBS as the negative control. A volume of 100 μL was injected subcutaneously into the abdomen of the mice. The mice were monitored weekly for up to 30 days postinoculation, on which day histopathological

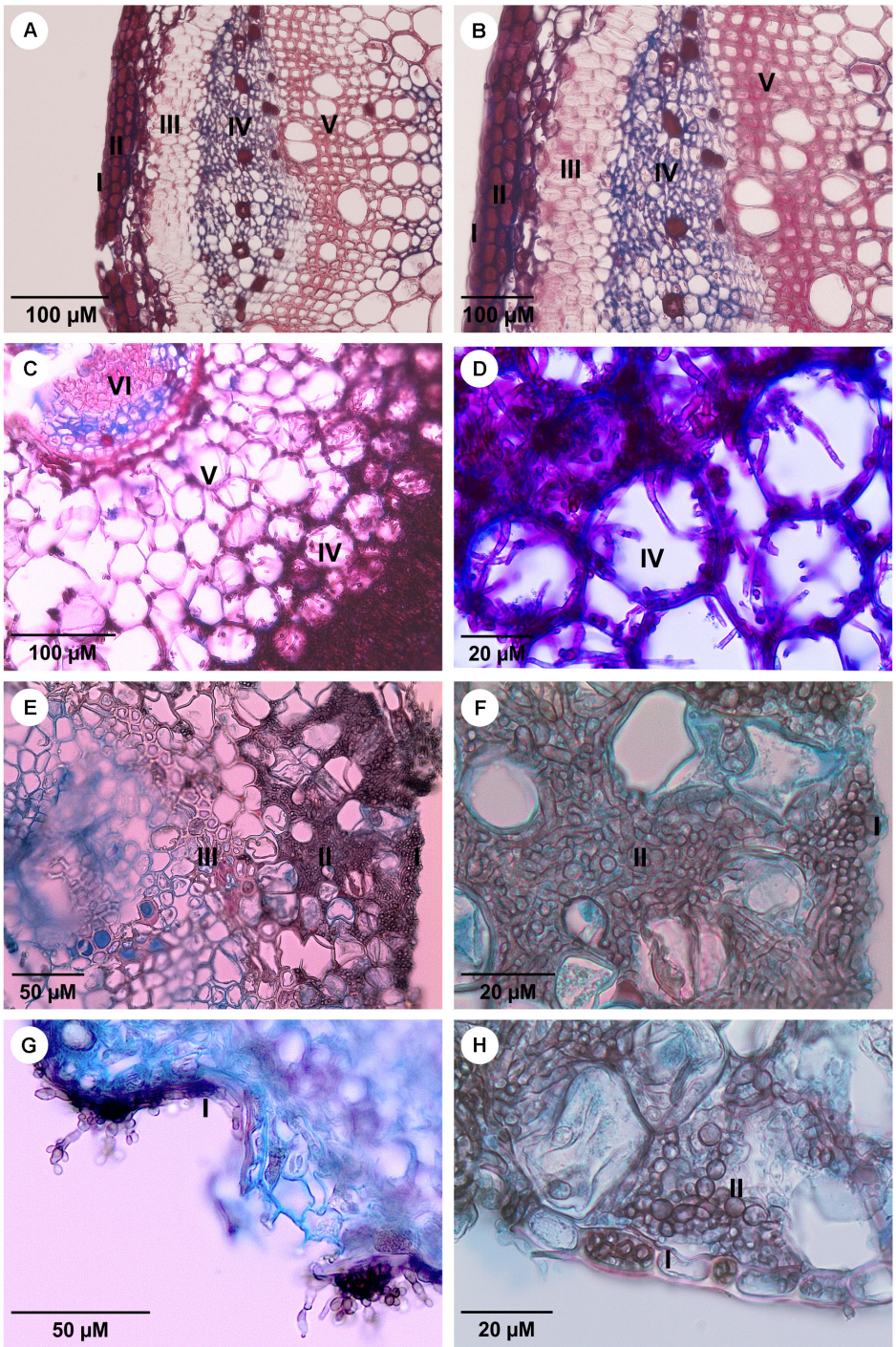

FIGURE 2 | The sections of *Mimosa pudica* micropropagate under histological prudish with Astra Blue and 1% safranin. **(A,B)** Stem histological sections of the control plant without presence of fungus; **(C,D)** root inoculated with *F. erecta* upright; **(E,F)** root inoculated with *F. monophora*; **(G,H)** root inoculated with *F. pedrosoi*. I-Epidermis; II-cortex; III-fiber sheath; IV-phloem; V-xylem; and VI-medulla. The inoculum was applied at five different points on the plant stem using 10 µL with 10^2 cells/mL of each tested strain.

examination of spleen tissue was performed. Western blot analysis was performed using crude protein extracts of the test species obtained by maceration of mycelia using liquid nitrogen based on Almeida et al. (2015). The experiments were performed in triplicate. The animal experiments were performed in accordance with the recommendations on animal welfare by the Institutional Ethics Committee of the Federal University of Paraná (approval certificate no. 1002).

Murine Tissue Histopathology

Histopathological samples obtained from mice were fixed in ALFAC solution containing 80% ethanol, 40% formalin, and glacial acetic acid for 16 h. Subsequently, the samples were subjected to serial dehydration, embedded in paraffin, sectioned into 5 μm slices, and stained with hematoxylin and eosin (H&E) stain (Cardona-Castro et al., 1996) followed by mounting of the samples with Entellan™. The samples were observed and photomicrographs were captured using an Olympus microscope BX51 equipped with capture software cellSens (2008, Olympus Soft Imaging Solutions, Münster, Germany) and coupled with a camera model DP72.

RESULTS

Virulence in the Plant Model

The environmental species, *F. erecta* and the clinical strains of *F. pedrosoi* and *F. monophora* were inoculated into plant hosts using *M. pudica* and *B. gasipaes*. A total of 152 plants were used, of which 112 were inoculated *in vitro* and 40 were transplanted into the vessels containing autoclaved soil as the substrate. The average height of *in vitro* plants varied from 5 to 12 cm and that of vessel plants varied from 30 to 45 cm. The plants of the *M. pudica in vitro* model were small in height, with structures too delicate to injury or injection demonstrating that the infection was evident when conducted by the culture medium inoculation (**Figure 1AIII**). In both plant models, the inocula with densities above 10^2 cells/mL proved to be quite invasive, leading to weakened and deteriorated plants which did not survive. In other words, at this concentration of the inoculum, all studied fungal strains could grow inside *in vitro* plant tissues (**Figure 2** and **Supplementary Figure S1**), while the host plants did not exhibit any visible external lesions during the assay period.

The *in vitro* plants of *M. pudica* and *B. gasipaes* infected with the clinical species, *F. monophora* and *F. pedrosoi*, presented pseudomycelial cells within the epidermal and cortical tissues, mainly in the intercellular spaces. Hyphae and pseudomycelial cells were concentrated in the parenchyma close to the sclerenchymatic sheath; however, they were absent in the vascular tissue (**Figures 2F,H** and **Supplementary Figures S1H,J**). The invasive property of the fungi was demonstrated by their ability to penetrate the epidermis, reaching the cortical region and consequently leading to the separation of parenchymal cells, with the formation of intercellular spaces that were subsequently colonized by the fungus (**Figures 2E,F,H**). No colonization of the vascular tissue was observed in the plants infected by the strains of the clinical species; reproductive structures of *F. pedrosoi* were observed to grow on the surface of the plant (**Figure 2G**).

In the *in vitro* plants infected with *F. erecta*, smooth, pale brown hyphae with some septa and pseudomycelial cells forming a dense mass in the stalk primary cortex were observed at the location of application of the inoculum (**Figure 2C** and **Supplementary Figure S1F**). The fungus was present inside the vascular tissue, while the endoderm served as an internal barrier (**Figure 2C** and **Supplementary Figure S1F**). The developments were similar in both *M. pudica* and *B. gasipaes* plant models. The endophytic fungi, *Colletogloeopsis dimorpha* and *Cladosporium tenuissimum* utilized as the positive controls in *M. pudica*, and *B. gasipaes*, respectively (**Supplementary Figures S1C,D**), demonstrated similar growth patterns in plant tissues as *F. erecta* (**Supplementary Figures S1E,F**).

Plants of the *in vitro* infected with *M. pudica* demonstrated root invasion by all fungi analyzed after 30 days of culture followed by their transfer to vessels (**Figure 1AIV**). After 60 days, both clinical and environmental strains were observed in the root and stalk tissues; epidermal regions and cortical cells contained large fungal concentrations (**Supplementary Figures S2C,E–G,I**) with the cells of *F. erecta* in the vascular tissue (**Supplementary Figure S2E**).

The plants of *M. pudica* previously produced *in vitro* and transferred to vessels for later inoculation by the injection and/or injury, respectively, (**Figures 1BI,II**) also did not display fungal presence in the histological sections of stalk tissue. In contrast, fungi were observed in the stalk tissues of *B. gasipaes* in the vessels infected by both methods (**Supplementary Figures S3C,E,G,I**).

In the plants of *M. pudica* and *B. gasipaes* produced *in vitro* and transferred to the vessel and infected via soil (**Figure 1BIII**), pseudomycelial cells and hyphae were observed only in the roots of the plants infected by *F. erecta*, which grew as an endophyte similar to the controls (**Supplementary Figures S2D,F**, **S3D,F**). The clinical species were unable to invade the plants by this infection route during the test period of 60 days (**Supplementary Figures S2H,J**, **S3H,J**), implying their ability to invade the plants by this route only during early growth phases via small roots. In contrast, the environmental species could invade the plants through the soil route during all growth phases, indicating a higher ability of invasion and adaptation of these species to living plant tissue (**Supplementary Table S1**)

Virulence in the *Tenebrio molitor* Larvae Model

This study is the first of *Fonsecaea* virulence testing using *T. molitor* as an infection model. In all species analyzed, the larvae were successfully infected with inoculum concentrations of 1×10^6 cells/mL. During the 10 days of monitoring, the infected larvae displayed lower survival rates than compared to those in the control groups (**Figure 3B**). The larvae infected with *F. erecta* exhibited the lowest survival rates, followed by *F. monophora* and *F. pedrosoi*, demonstrating that all species evaluated were able to survive inside the animal host. The infection rates were significant (F: 33.50; d_f: 4; $p < 0.01$), with larval survival rates ranging from 35 to 69% (control: 5%; **Figure 3C**). According to the histological sections of larvae all species produced yeast cells and hyphae inside the tissues. However, in larvae infected with *F. pedrosoi*, at 120 h postinoculation, was observed spherical or ovoidal cells, 5–20 μm in diameter, with a dark, and thick, multilayered cell wall resembling muriform cells (**Figure 3F**).

Larvae melanization is an intracellular and key defense response to microbial infection. The larvae inoculated with all *Fonsecaea* species presented a gradual increase in the concentration of melanin (pigmentation) within 24 h after inoculation, as assessed both by visual observation and detection

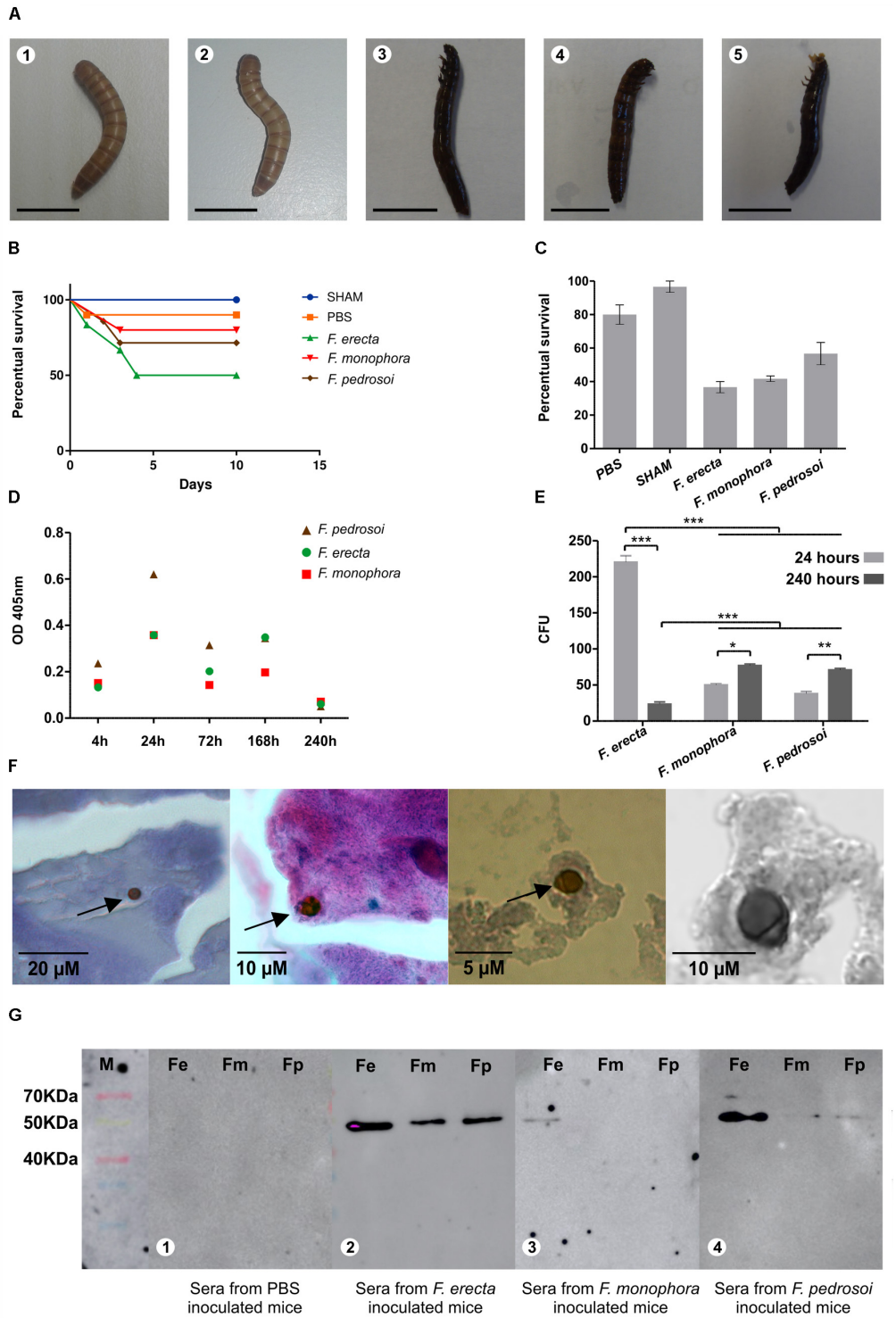

FIGURE 3 | The virulence test using *Tenebrio molitor* and detection of antigenic components using BALB/c mice infected with *Fonsecaea pedrosoi*, *Fonsecaea erecta*, and *Fonsecaea monophora*; **(A)** inoculated larvae with PBS, SHAM **(1,2)** and infected larvae with *F. erecta* **(3)**; *F. monophora* **(4)**; and *F. pedrosoi* **(5)**. It was used 10 larvae per group; **(B)** the survival curves of the larvae are shown. For each experiment, two different controls were used: untouched larvae (SHAM) and larvae injected with PBS; **(C)** percentage survival of larvae infected with *F. pedrosoi*, *F. erecta*, and *F. monophora* (Fm) is shown; **(D)** the melanization of the hemolymph is demonstrated by measuring the OD_{405} nm of the hemolymph at 4, 24, 72, 168 and 240 h after infection; **(E)** larvae were homogenized in PBS at 4, 24, 72, 168, and 240 h after infection with *Fonsecaea* for CFU determination; **(F)** occasional muriform cells observed in tissues larvae infected with *F. pedrosoi*; **(G)** Western blot analysis of total proteins from *F. erecta*, *F. monophora*, and *F. pedrosoi* against serum from mice infected with the same species. Panel **(G)** depicts that a band of approximately 50 kDa was recognized by the sera. Serum was collected from BALB/c mice 30 days postinfection.

of melanization in the hemolymph using spectrophotometry (**Figure 3A**). The pigmentation could be observed during the entire 10-day period of analysis (**Figure 3D**).

The fungal burden inside the larvae was assessed 24 h postinoculation. Significantly higher CFUs of *F. erecta* in the culture medium than that of *F. monophora* and *F. pedrosoi* were observed (**Figure 3E**). The environmental species of *F. erecta* yielded 220 CFUs/mL, while the clinical species, *F. monophora* and *F. pedrosoi* yielded 50 and 38 CFUs/mL, respectively. These results were confirmed by an increase in the number of cells after 72 h, again with *F. erecta* presenting the highest number of 495 CFUs/mL, followed by *F. monophora* with 97 CFUs/mL and *F. pedrosoi* with 101 CFUs/mL. However, after 240 h, the infected larvae that had survived exhibited a significant reduction in the growth of *F. erecta* with 23 CFUs/mL, while those infected with *F. monophora* and *F. pedrosoi* yielded 77 CFUs/mL and 71 CFUs/mL, respectively, suggesting that the environmental species could survive inside the animal (**Supplementary Table S1**) which were demonstrated by the statistical analysis.

Virulence in Murine Model

The plant-associated species, *F. erecta*, appeared to be more immunogenic in mice than the clinical species, as evident by the recognition of the fungal antigens in the serum of infected mice. The sera obtained from mice 30 days postinfection with *F. pedrosoi*, *F. monophora*, and *F. erecta* were incubated with the total proteins obtained from the same fungi to detect the antigenic components. In **Figure 3G** depicts that a band of approximately 50 kDa was recognized by the sera. This reaction was more evident when mice were infected with *F. erecta* against all protein extracts. More intense reaction was obtained with *F. erecta* protein extract (**Figures 3G, 4**). At 30 days after inoculation of *F. pedrosoi*, *F. monophora*, and *F. erecta*, were spleen tissue analysis was performed to check for systemic infection (**Supplementary Table S1**). However, no change in the sectioned spleen tissues was observed (**Supplementary Figure S4**).

DISCUSSION

The rationale of the present study was to establish the degree to which the etiologic agents of chromoblastomycosis could reside in plant material. *F. pedrosoi* and *F. monophora* are endemic in humid climates (Badali et al., 2008; Najafzadeh et al., 2011; Gomes et al., 2016), particularly tropical areas, such as the Amazon rainforest (Vicente et al., 2013). Two plant hosts with similar distribution were selected. *M. pudica* is a creeping annual or perennial herb belonging to the pea family, *Fabaceae*; it is native to South and Central America and currently considered a pantropical weed that is also prevalent in the Asian countries (Souza Filho et al., 2001). It has been associated with thorn trauma, leading to chromoblastomycosis (Salgado et al., 2004; Salgado, 2010). *B. gasipaes* is a palm native to the tropical forests of South and Central America. It is a long-living perennial plant, which on average is productive for 50–75 years. Species of *Palmaceae* have been reported as a habitat of the melanized fungi (Gezuele et al., 1972; Caligiorne et al., 2005). Silva et al. (1995) reported patients presenting with chromoblastomycosis lesions on the buttocks due to an exposure to palm debris while processing babassu coconuts, a common activity in the Maranhão state of Brazil considered the main endemic area in this country (Gomes et al., 2016).

Our data demonstrated that both clinical and plant-associated *Fonsecaea* species were able to growth inside the two tissues plant models, *M. pudica* and *B. gasipaes* (**Figure 2** and **Supplementary Figure S1**, **S2**, **S3**) using both *in vitro* and vessel plants as hosts. *M. pudica* represents an attractive model for *in vitro* analysis because of its rapid growth. It was invaded when the fungus was inoculated via culture medium *in vitro*; however, the vessel invasion only occurred when it was previously infected *in vitro* (**Supplementary Figures S2C,E,G,I**), although, there are a previously reports of this plant colonized by the fungus related to the disease (Salgado et al., 2004; Salgado, 2010). The fine stems of the plant are difficult to manipulate, which interferes with the *in vitro* inoculation. The palm tree, *B. gasipaes*, our second model, with a long life cycle serves as an excellent model once the plant has a more robust stalk, which makes handling easier; the plant could be infected by different methods of inoculation both in vessels and *in vitro*. Moreover, its fruit pulp was already used as substrate for culture media in order to produce sclerotic cells *in vitro* (Silva et al., 2008). We believe that the method of inoculation may have influenced our results. The observation that the inoculum in the *in vitro* culture medium applied around the root allowed invasion of several tissues in both plants used (**Figure 2** and **Supplementary Figure S1**) could be the way in order to investigate the route of this implantation disease.

The current hypothesis is that patients suffering from chromoblastomycosis acquire the infection via injury from plant material (Queiroz-Telles and Santos, 2013; Queiroz-Telles et al., 2017). This may be considered a possibility; however, it fails to provide the explanation behind the different isolation rates between the species from humans and plant material. The species must differ significantly in predilection for either host (de Hoog et al., 2007; Vicente et al., 2013). According to the comparative genomics of sibling species of *Fonsecaea* associated with human chromoblastomycosis (Vicente et al., 2017) these fungi are able to degrade plant and animal substrates demonstrating a duality in lifestyle that might allow host shifts in Chaetothyriales from environmental niches to animal tissue.

In the present study, we expected low invasion rates of plants by the clinical species and low animal virulence in the plant species. However, we found *F. erecta* to have the largest CFUs in the larvae model suggesting to be the most immunogenic in mice (**Figure 3G**). It was also observed to be the most invasive in the used plant models, where it developed as an endophyte with deep invasion.

The above-mentioned finding led us to formulate an alternative hypothesis to explain the observed etiology of chromoblastomycosis by *Fonsecaea* species (Queiroz-Telles et al., 2017). The clinical species, *F. monophora* and *F. pedrosoi* were seen to remain in the epidermis of the stem in the inoculated plants. The epidermis is responsible for the formation of the

thorn, and thus might provide an explanation of the thorn acting as the vehicle of transmission of the "clinical" species, rather than of *F. erecta* that invaded the deeper tissues with a colonizing profile similar to that of the endophyte controls. The larvae initially displayed no defense against this uncommon invader, but later developed an immune response, also observed in murine model (**Figure 3G**), that could control the infection, which was not observed for the clinical species that survived into the host tissues. Besides, we also reported morphologic structures similar to the muriform cells inside the tissues larvae infected by *F. pedrosoi* (**Figure 3F**). Likewise, others studies with animal host, e.g., in mice, already have shown production by muriform cells conidia by *F. pedrosoi* (Sousa Mda et al., 2011; Siqueira et al., 2017; Vicente et al., 2017).

After transcutaneous implantation into a human host, propagules of the agents of chromoblastomycosis become meristematic and form muriform cells (Queiroz-Telles et al., 2017); this is considered to be the pathogenic form of the fungus (Esterre and Queiroz-Telles, 2006). Muriform cells can also be produced *in vitro* by the environmental relatives of the agents of chromoblastomycosis, which has never been reported from this disease (Badali et al., 2008). In the present study, we observed swollen, dark and thick-walled cells that could be considered as a structure similar to the true muriform cells observed in human tissues, where they occasionally have transverse and longitudinal walls.

The mealworm beetle, *T. molitor* is a non-vertebrate animal model that has been used earlier, e.g., in *Candida albicans*, *Cryptococcus neoformans*, and *Madurella mycetomatis* (Mylonakis et al., 2005; Fuchs et al., 2010; Mowlds et al., 2010; Kloezen et al., 2015; Souza et al., 2015). The larvae infected by *F. erecta* reported the lowest survival rates, but in 240 h, the survived larvae could destroy more *F. erecta* cells than that of *F. pedrosoi*. This suggested that due the fact that *F. erecta* promoted lower survival rates after prolonged periods of infection, higher fungal reduction was achieved, which may be attributed to an increased immune response.

In the virulence test using a murine model was observed that all sera from the infected animals reacted with a 50 kDa molecule (**Figure 3G**). These results indicate that possibly this protein is envolved in the pathogenesis of chromoblastomycosis and it should be better clarified.

In conclusion, the plant infection models employed suggested that all *Fonsecaea* species were saprobic; considering the fact that all agents have to be traumatically inoculated to cause disease, it may be speculated that no primary animal pathogenicity is present in these species. Unexpectedly, *F. erecta* demonstrated to be a virulent species in the animal model, confirming earlier data by Vicente et al. (2017), who concluded the same using *Galleria mellonella* as the animal model. However, *T. molitor* represented a good model to reproduce the disease. The larvae of *T. molitor* have a longer cycle life than those of *G. mellonella*, and we observed for the first time structures similar to muriform cells produced during infection of human tissue in a larvae model. Assuming that all species concerned are opportunists rather than primary pathogens, we might hypothesize that lower virulence is an indication of higher adaptation to the animal host. The results confirm the role of muriform cells as a pathogenic adaptation in animal tissues.

AUTHOR CONTRIBUTIONS

GF, VV, SH, and RG conceived and designed the experiments. GF, BS, MV, IB, MN, GS, and BS performed the experiments. GF, VV, RG, JD-G, CB, LM, DK, GS, and BS analyzed the data. JD-G, VV, DS, RS, ET, CA, and MM contributed reagents, materials, and analysis tools. GF, VV, SH, RG, CB, SS, and SA contributed to preparing the manuscript and revising it critically. GF, RG, and VV contributed to annotation and analysis of data; preparation, creation, and/or presentation of the tables, graphics, and figures. VV, CA, ET, DS, AB, SD, CS, and MdS offered strains and/or substantial contributions to the work. VV, RG, SH, SS, and SA conceived and revised the paper. VV, GF, SH, and RG conceived and designed the work and wrote the manuscript.

FUNDING

This work was supported by Brazilian government by financial support (Special Visiting Researcher Project; Grant No. 059/2012PVE-CAPES) from the Brazilian Federal Agency of Support and Evaluation of Graduate: Education Coordination for the Improvement of Higher Education Personnel–CAPES (www.capes.gov.br). The authors VV and SH were supported by fellowship from National Council of Technological and Scientific Development (http://cnpq.br/), Brasilia, Brazil. The author GF received fellowship from Araucaria Foundation/CAPES/CNPq and GRR received it from the PNPD/CAPES.

ACKNOWLEDGMENTS

We thank Janaina Cassia Campos and Álvaro Figueredo dos Santos from the Brazilian Agricultural Research Corporation (EMBRAPA)-Embrapa Forestry, Nilson Belem Filho from the Department of Botany, Daniela Cabrini de Almeida and Vanessa Vaccari for technical assistance.

SUPPLEMENTARY MATERIAL

The Supplementary Material for this article can be found online at: https://www.frontiersin.org/articles/10.3389/fmicb.2018.02211/full#supplementary-material

FIGURE S1 | Sections of *Bactris gasipaes* plants under histological prudish with 0.5% toluidine blue and safranin. **(a,b)** Sections of stalk and root in the control plant without the presence of fungus; **(c,d)** the stalk and root inoculated with the positive control (*Cladosporium tenuissimum*) upright; **(e,f)** the stalk and root inoculated with *F. erecta*; **(g,h)** stalk and root inoculated with *F. monophora* (the plant structures and fungus are demonstrated by arrow); and **(i,j)** stalk and root inoculated with *F. pedrosoi*. I-Epidermis; II-cortex; III-fiber sheath; IV-phloem; V-xylem; and VI-medulla.

FIGURE S2 | The vessel sections of *Mimosa pudica* under histological prudish with 0.5% toluidine blue and safranin. **(a,b)** Cortes stalk and root of the control plant without the presence of fungus; **(c,d)** stalk and root inoculated with

Colletogloeopsis dimorpha (positive control); **(e,f)** stalk and root inoculated *F. erecta* (the plant structures and fungus are demonstrated by arrow); **(g,i)** stalk inoculated with *F. monophora* (the plant structures and fungus are demonstrated by arrow) and *F. pedrosoi*; **(h,j)** root of the plant inoculated with *F. monophora* and *F. pedrosoi* without the presence of fungus. I- Epidermis; II-cortex; III-fiber sheath; IV-phloem; V-xylem; VI-medulla.

FIGURE S3 | The vessel sections of *Bactris gasipaes* under histological prudish with 0.5% toluidine blue and safranin. **(a,b)** The sections of stem and root in control plant without the presence of fungus; **(c,d)** stalk and root inoculated with *Cladosporium tenuissimum* (positive control); **(e,g,i)** stalk inoculated with *F. erecta*, *F. monophora*, and *F. pedrosoi*; **(f,h,j)** the plant root inoculated with *F. erecta*, *F. monophora*, and *F. pedrosoi* without the presence of fungus. I-Epidermis; II-cortex; III-fiber sheath; IV-phloem; V-xylem; and VI-medulla. The plant structures and fungus are demonstrated by arrow.

FIGURE S4 | Histologic analysis of the infected tissue of BALB/c with *Fonsecaea* species, the samples were stained with hematoxylin and eosin (HE). **(a,b)** PBS; **(c,d)** *F. erecta*; **(e,f)** *F. monophora*; **(g,h)** *F. pedrosoi*.

TABLE S1 | Clinical and environmental strains of *Fonsecaea* sibling species in different infection models.

REFERENCES

Almeida, J. R. F., Kaihami, G. H., Jannuzzi, G. P., and Almeida, S. R. (2015). Therapeutic vaccine using a monoclonal antibody against a 70-kDa glycoprotein in mice infected with highly virulent *Sporothrix schenckii* and *Sporothrix brasiliensis*. *Med. Mycol.* 53, 42–50. doi: 10.1093/mmy/myu049

Badali, H., Bonifaz, A., Barrón-Tapia, T., Vázquez-González, D., Estrada-Aguilar, L., Oliveira, N. M., et al. (2010). *Rhinocladiella aquaspersa*, proven agent of verrucous skin infection and a novel type of chromoblastomycosis. *Med. Mycol.* 48, 696–703. doi: 10.3109/13693780903471073

Badali, H., Gueidan, C., Najafzadeh, M. J., Bonifaz, A., Gerrits van den Ende, A. H. G., and de Hoog, G. S. (2008). Biodiversity of the genus *Cladophialophora*. *Stud. Mycol.* 61, 175–191. doi: 10.3114/sim.2008.61.18

Bernal, A. A., Smidt, E. C., and Bona, C. (2015). Spiral root hairs in Spiranthinae (Cranichideae: Orchidaceae). *Braz. J. Bot.* 38, 1–5. doi: 10.1007/s40415-015-0141-2

Caligiorne, R. B., Licinio, P., Dupont, J., and de Hoog, G. S. (2005). Internal transcribed spacer rRNA gene-based phylogenetic reconstruction using algorithms with local and global sequence alignment for black yeasts and their relatives. *J. Clin. Microbiol.* 43, 2816–2823. doi: 10.1128/JCM.43.6.2816-2823.2005

Cardona-Castro, N., Agudelo-Florez, P., and Restrepo-Molina, R. (1996). Chromoblastomycosis murine model and in vitro test to evaluate the sensitivity of *Fonsecaea pedrosoi* to ketoconazole, itraconazole and saperconazole. *Mem. Inst. Oswaldo Cruz* 91, 779–784. doi: 10.1590/S0074-02761996000600026

Crous, P. W., Slippers, B., Wingfield, M. J., Rheeder, J., Marasas, W. F. O., Philips, A. J. L., et al. (2006). Phylogenetic lineages in the Botryosphaeriaceae. *Stud. Mycol.* 55, 235–253. doi: 10.3114/sim.55.1.235

de Hoog, G. S., Nishikaku, A. S., Fernandez-Zeppenfeldt, G., Padín-González, C., Burger, E., Badali, H., et al. (2007). Molecular analysis and pathogenicity of the *Cladophialophora carrionii* complex, with the description of a novel species. *Stud. Mycol.* 58, 219–234. doi: 10.3114/sim.2007.58.08

de Hoog, G. S., Vicente, V. A., Najafzadeh, M. J., Harrak, M. J., Badali, H., and Seyedmousavi, S. (2011). Waterborne exophiala species causing disease in cold-blooded animals. *Persoonia* 27, 46–72. doi: 10.3767/003158511X614258

Doymaz, M. Z., Seyithanoglu, M. F., Hakyemez, I., Gultepe, B. S., Cevik, S., and Aslan, T. (2015). A case of cerebral phaeohyphomycosis caused by *Fonsecaea monophora*, a neurotropic dematiaceous fungus, and a review of the literature. *Mycoses* 58, 187–192. doi: 10.1111/myc.12290

Esterre, P., and Queiroz-Telles, F. (2006). Management of chromoblastomycosis: novel perspectives. *Curr. Opin. Infect. Dis.* 19, 148–152. doi: 10.1097/01.qco.0000216625.28692.67

Fernández-Zeppenfeldt, G., Richard-Yegres, N., Yegres, F., and Hernández, R. (1994). *Cladosporium carrionii*: hongo dimórfico en cactáceas de la zona endémica para la cromomicosis en Venezuela. *Rev. Iberoam. Micol.* 11, 61–63.

Fuchs, B. B., O'Brien, E., Khoury, J. B. E., and Mylonakis, E. (2010). Methods for using *Galleria mellonella* as a model host to study fungal pathogenesis. *Virulence* 1, 475–482. doi: 10.4161/viru.1.6.12985

Gezuele, E., Mackinnon, J. E., and Conti-Diaz, I. A. (1972). The frequent isolation of *Phialophora verrucosa* and *Phialophora pedrosoi* from natural sources. *Sabouraudia* 10, 266–273. doi: 10.1080/00362177285190501

Gomes, R. R., Vicente, V. A., Azevedo, C. M. P. S., Salgado, C. G., Da Silva, M. B., Queiroz-Telles, F., et al. (2016). Molecular epidemiology of agents of human chromoblastomycosis in Brazil with the description of two novel species. *PLoS Negl. Trop. Dis.* 10:e0005102. doi: 10.1371/journal.pntd.0005102

González, G. M., Rojas, O. C., González, J. G., Kang, Y., and de Hoog, G. S. (2013). Chromoblastomycosis caused by *Rhinocladiella aquaspersa*. *Med. Mycol. Case Rep.* 31, 148–151. doi: 10.1016/j.mmcr.2013.08.001

Gümral, R., Tümgör, A., Saraçlı, M. A., Yıldıran, S. T., Ilkit, M., and de Hoog, G. S. (2014). Black yeast diversity on creosoted railway sleepers changes with ambient climatic conditions. *Microb. Ecol.* 68, 699–707. doi: 10.1007/s00248-014-0459-5

Kloezen, W., Poppel, M. V. H., Fahal, A. H., and Sande, W. W. J. V. (2015). A *Madurella mycetomatis* grain model in *Galleria mellonella* larvae. *PLoS Negl. Trop. Dis.* 9:e0003926. doi: 10.1371/journal.pntd.0003926

Lavelle, P. (1980). Chromoblastomycosis in Mexico. *Pan. Am. Health Organ. Sci. Publ.* 396, 235–247.

Maekawa, L. E., Rossoni, R. D., Barbosa, J. O., Jorge, A. O. C., Junqueira, J. C., and Valera, M. C. (2015). Different extracts of Zingiber officinale decrease Enterococcus faecalis infection in *Galleria mellonella*. *Braz. Dent. J.* 26, 105–109. doi: 10.1590/0103-6440201300199

Marques, S. G., Pedroso Silva, C. M., Saldanha, P. C., Rezende, M. A., Vicente, V. A., Queiroz-Telles, F., et al. (2006). Isolation of *Fonsecaea pedrosoi* from the shell of the babassu coconut (*Orbignya phalerata* Martius) in the amazon region of Maranhão Brazil. *Japan J. Med. Mycol.* 47, 305–311. doi: 10.3314/jjmm.47.305

Mostert, L., Groenewald, J. Z., Summerbell, R. C., Gams, W., and Crous, P. W. (2006). Taxonomy and pathology of *Togninia* (*Diaporthales*) and its *Phaeoacremonium* anamorphs. *Stud. Mycol.* 54, 1–113. doi: 10.3114/sim.54.1.1

Mowlds, P., Coates, C., Renwick, J., and Kavanagh, K. (2010). Dose-dependent cellular and humoral responses in *Galleria mellonella* larvae following beta-glucan inoculation. *Microbes Infect.* 12, 146–153. doi: 10.1016/j.micinf.2009.11.004

Murashige, T., and Skoog, F. (1962). A revised medium for rapid growth and bio assays with tobacco tissue cultures. *Phys. Plant.* 15, 473–497. doi: 10.1111/j.1399-3054.1962.tb08052.x

Mylonakis, E., Moreno, R., El Khoury, J. B., Idnurma Heitman, J., and Calderwood, S. B. (2005). *Galleria mellonella* as a model system to study *Cryptococcus neoformans* pathogenesis. *Infect. Immun.* 73, 3842–3850. doi: 10.1128/IAI.73.7.3842-3850.2005

Najafzadeh, M. J., Sun, J., Vicente, V. A., Klaassen, C. H., Bonifaz, A., Gerrits van den Ende, A. H. G., et al. (2011). Molecular epidemiology of *Fonsecaea* species. *Emerg. Infect. Dis.* 17, 464–469. doi: 10.3201/eid1703.100555

Paiva, A. M. S., and Aloufa, M. A. I. (2009). Estabelecimento in vitro de aroeira da praia (*Schinus terebinthifolius* Raddi) em diferentes concentrações de 6-benzilaminopurina (BAP). *Rev. Bras. Plantas Med.* 11, 300–304. doi: 10.1590/S1516-05722009000300011

Perdoni, F., Falleni, M., Tosi, D., Cirasola, D., Romagnoli, S., Braidotti, P., et al. (2014). A histological procedure to study fungal infection in the wax moth *Galleria mellonella*. *Eur. J. Histochem.* 58, 24–28. doi: 10.4081/ejh.2014.2428

Queiroz-Telles, F., de Hoog, S., Santos, D. W. C. L., Salgado, C. G., Vicente, V. A., Bonifaz, A., et al. (2017). Chromoblastomycosis. *Clin. Microbiol. Rev* 30, 233–276. doi: 10.1128/CMR.00032-16

Queiroz-Telles, F., and Santos, D. W. (2013). Challenges in the therapyof chromoblastomycosis. *Mycopathologia* 175, 477–488. doi: 10.1007/s11046-013-9648-x

Rubin, H. A., Bruce, S., Rosen, T., and Mcbrid, E. M. E. (1991). Evidence for percutaneous inoculation as the mode of transmission for chromoblastomycosis. *J. Am. Acad. Dermatol.* 25, 951–954. doi: 10.1016/0190-9622(91)70292-A

Salgado, C. G. (2010). Fungal x host interactions in chromoblastomycosis. *Virulence* 1, 3–5. doi: 10.4161/viru.1.1.10169

Salgado, C. G., da Silva, J. P., Diniz, J. A., da Silva, M. B., da Costa, P. F., Teixeira, C., et al. (2004). Isolation of *Fonsecaea pedrosoi* from thorns of *Mimosa pudica*, a probable natural source of chromoblastomycosis. *Rev. Inst. Med. Trop. São Paulo* 46, 33–36. doi: 10.1590/S0036-46652004000100006

Scorzoni, L., de Lucas, M. P., Mesa-Arango, A. C., Fusco-Almeida, A. M., Lozano, E., Cuenca-Estrella, M., et al. (2013). Antifungal efficacy during *Candida krusei* infection in non-conventional models correlates with the yeast *in vitro* susceptibility profile. *PLoS One* 8:e60047. doi: 10.1371/journal.pone.0060047

Silva, C. M., da Rocha, R. M., Moreno, J. S., Branco, M. R., Silva, R. R., Marques, S. G., et al. (1995). The coconut babaçu (*Orbignya phalerata* martins) as a probable risk of human infection by the agent of chromoblastomycosis in the State of Maranhão, Brazil. *Rev. Soc. Bras. Med. Trop.* 28, 49–52. PMID: 7724868. doi: 10.1590/S0037-86821995000100009

Silva, C. M., da Silva, J. P., Yamano, S. S. P., Salgado, I., Diniz, J. A. P., and Salgado, C. G. (2008). Development of natural culture media for rapid induction of *Fonsecaea pedrosoi* sclerotic cells in vitro. *J. Clin. Microbiol.* 46, 3839–3841. doi: 10.1128/JCM.00482-08

Siqueira, I. M., Castro, R. J. A., Leonhardt, L. C. M., Jeronimo, M. S., Soares, A. C., Raiol, T., et al. (2017). Modulation of the immune response by *Fonsecaea pedrosoi* morphotypes in the course of experimental chromoblastomycosis and their role on inflammatory response chronicity. *PLoS Negl. Trop. Dis.* 11:e0005461. doi: 10.1371/journal.pntd.0005461

Sousa Mda, G., Reid, D. M., Schweighoffer, E., Tybulewicz, V., Ruland, J., Langhorne, J., et al. (2011). Restoration of pattern recognition receptor costimulation to treat chromoblastomycosis, a chronic fungal infection of the skin. *Cell Host Microbe* 9, 436–443. doi: 10.1016/j.chom.2011.04.005.

Souza, P. C., Morey, A. T., Castanheira, M. G., Bocate, K. P., Panagio, L. A., Ito, F. A., et al. (2015). *Tenebrio molitor* (Coleoptera: Tenebrionidae) as an alternative host to study fungal infections. *J. Microbiol. Methods* 118, 182–186. doi: 10.1016/j.mimet.2015.10.004

Souza Filho, A. P. S., Alves, S. M., Figueiredo, F. J. C., and Dutra, S. (2001). Germinação de sementes de plantas daninhas de pastagens cultivadas: *Mimosa pudica* e *Ipomoea asarifolia*. *Planta Daninha* 19, 23–31. doi: 10.1590/S0100-83582001000100003

Steinmacher, D. A., Guerra, M. P., Saare-Surminski, K., and Lieberei, R. (2011). A temporary immersion system improvesin vitroregeneration of peach palm through secondary somatic embryogenesis. *Ann. Bot.* 108, 1463–1475. doi: 10.1093/aob/mcr033

Vicente, V. A., Attili-Angelis, D., Pie, M. R., Queiroz-Telles, F., Cruz, L. M., Najafzadeh, M. J., et al. (2008). Environmental isolation of black yeast-like fungi involved in human infection. *Stud. Mycol.* 61, 137–144. doi: 10.3114/sim.2008.61.14

Vicente, V. A., Najafzadeh, M. J., Sun, J., Gomes, R. R., Robl, D., Marques, S. G., et al. (2013). Environmental siblings of black agents of human chromoblastomycosis. *Fungal Divers.* 65, 47–63. doi: 10.1007/s13225-013-0246-5

Vicente, V. A., Weiss, V. A., Bombassaro, A., Moreno, L. F., Costa, F. F., Raittz, R. T., et al. (2017). Comparative genomics of sibling species of *Fonsecaea* associated with human chromoblastomycosis. *Front. Microbiol.* 8:1924. doi: 10.3389/fmicb.2017.01924

Conflict of Interest Statement: The authors declare that the research was conducted in the absence of any commercial or financial relationships that could be construed as a potential conflict of interest.

The handling Editor declared a co-authorship with one of the authors SH.

The reviewer GB declared a shared affiliation, with no collaboration, with several of the authors, SA and SS, to the handling Editor at time of review.

frontiers in Cellular and Infection Microbiology

ORIGINAL RESEARCH
published: 18 March 2022
doi: 10.3389/fcimb.2022.851769

Phylogeny, Antifungal Susceptibility, and Point Mutations of *SQLE* Gene in Major Pathogenic Dermatophytes Isolated From Clinical Dermatophytosis

Nasrin Pashootan[1], *Masoomeh Shams-Ghahfarokhi*[2], *Arash Chaichi Nusrati*[1], *Zahra Salehi*[3], *Mehdi Asmar*[1] *and Mehdi Razzaghi-Abyaneh*[3*]

[1] Department of Microbiology, Faculty of Basic Sciences, Lahijan Branch, Islamic Azad University, Lahijan, Iran, [2] Department of Mycology, Faculty of Medical Sciences, Tarbiat Modares University, Tehran, Iran, [3] Department of Mycology, Pasteur Institute of Iran, Tehran, Iran

OPEN ACCESS

Edited by:
Carlos Pelleschi Taborda,
University of São Paulo, Brazil

Reviewed by:
Rui Kano,
Nihon University, Japan
Anke Burmester,
University Hospital Jena, Germany

***Correspondence:**
Mehdi Razzaghi-Abyaneh
mrab442@yahoo.com;
mrab442@pasteur.ac.ir

Specialty section:
This article was submitted to Fungal Pathogenesis, a section of the journal Frontiers in Cellular and Infection Microbiology

Received: 10 January 2022
Accepted: 11 February 2022
Published: 18 March 2022

Citation:
Pashootan N, Shams-Ghahfarokhi M, Chaichi Nusrati A, Salehi Z, Asmar M and Razzaghi-Abyaneh M (2022) Phylogeny, Antifungal Susceptibility, and Point Mutations of SQLE Gene in Major Pathogenic Dermatophytes Isolated From Clinical Dermatophytosis. Front. Cell. Infect. Microbiol. 12:851769. doi: 10.3389/fcimb.2022.851769

Drug resistance is one of the major challenges to skin fungal infections, especially in tropical and subtropical infections caused by dermatophytes. This study aimed to determine the antifungal susceptibility of clinically dermatophytes and evaluate point mutations in terbinafine-resistant isolates. A total number of 123 clinical dermatophyte isolates in eight species were evaluated in terms of sensitivity to seven major antifungals. Furthermore, the point mutation in squalene epoxidase (*SQLE*) gene responsible for terbinafine resistance was studied. The dermatophytes species were identified by morphological characteristics and confirmed by the ITS sequencing. Also, the phylogenetic tree was drawn using the RAxML analyses for 123 dermatophytes isolates. A new XXIX genotype was also found in 4 *Trichophyton mentagrophytes* isolates. Based on the results obtained, terbinafine was the most effective antifungal drug followed by itraconazole and voriconazole. *Trichophyton rubrum* and *Trichophyton tonsurans* were the most susceptible species (MIC_{50} = 0.01, 0.09 μg/ml), and *T. mentagrophytes* was the most resistant species (MIC_{50} = 0.125 μg/ml) to terbinafine. Of the 123 dermatophytes isolates, six isolates showed reduced susceptibility to terbinafine, and only *Trichophyton indotineae* had a mutation in *SQLE* gene as a Phe397Leu substitution. Overall, the antifungal susceptibility test is necessary for managing dermatophytosis. These results help physicians to control the course of the disease and provide further insights to select effective drugs for patients with dermatophytosis, especially in tropical and subtropical regions of the world, where dermatophytosis is still a public health problem.

Keywords: dermatophytes, antifungal susceptibility testing, point mutation, terbinafine resistance, Phe397Leu substitution, *T. indotineae*, dermatophytosis, squalene epoxidase

1 INTRODUCTION

Dermatophytes are a group of keratinophilic fungi with considerable morphological and genetic similarities (Dabas et al., 2017; Salehi et al., 2021). They can attack keratinized tissue of humans and animals and create dermatophytosis (Zareshahrabadi et al., 2020). According to the new classification, dermatophytes are classified into *Trichophyton*, *Epidermophyton*, *Nannizzia*, *Paraphyton*, *Lophophyton*, *Microsporum*, and *Arthroderma* (de Hoog et al., 2017).

According to the WHO's evaluation, dermatophytosis affects 20%–25% of the world population (Ebert et al., 2020). In addition, studies have shown that dermatophyte species responses to antifungal drugs are not the same (Bhatia and Sharma, 2015). The confirmed therapeutic strategies for dermatophytosis infection include griseofulvin (GRI) drugs and systemic or topical triazole and allylamine drugs, which mostly include itraconazole (ITZ) and terbinafine (TRB). Currently, TRB is the first choice for the treatment of dermatophytosis given its stable clinical effect and fewer recurrence (Haugh et al., 2000; Niimi et al., 2010). On the other hand, therapeutic failure has become an alarming trend, and health systems around the world pay heavy costs to treat the disease every year (Siopi et al., 2021). In addition, there are an increased number of studies about resistance to antifungal drugs and TRB in particular in dermatophyte species (Haugh et al., 2000; Mukherjee et al., 2003; Osborne et al., 2005; Niimi et al., 2010; Singh et al., 2018; Nenoff et al., 2020; Siopi et al., 2021).

The TRB is a synthetic allylamine derivative that, by the activity of squalene epoxidase (*SQLE*), causes the accumulation of squalene and decreases ergosterol of the cell membrane, which leads to cellular death (Ghannoum et al., 2004; Osborne et al., 2005; Afshari et al., 2016).

The genetic basis of TRB resistance in fungi including *Aspergillus fumigatus*, *Aspergillus nidulans*, and *Trichophyton rubrum* has shown that the resistance may arise from the overexpression of *SQLE* gene, or it could result from mutations in other genes that indirectly affect antimycotic susceptibility (Rocha et al., 2002; Liu et al., 2004; Santos et al., 2018). It has been shown that resistance to TRB in dermatophyte species is related to the mutation of *salicylate 1-monooxygenase* (*sa1A*) and *SQLE* (Mukherjee et al., 2003; Yamada et al., 2017). Studies have shown that the resistance is more related to the substitutions at one of the amino acid positions of Leu393, Phe397, Phe415, and His440 in *SQLE* protein (Mukherjee et al., 2003; Osborne et al., 2005; Osborne et al., 2006). Furthermore, a recent study by Nenoff et al. (2020) identified two substitutions of amino acids at Ser395Pro and Ser443Pro positions of *SQLE* in *Trichophyton* strains resistant to TRB. It has been shown that replacement in the F397L position of *SQLE* is the most common type of substitution. There are reports of mutation in different positions of *SQLE* in *T. tonsurans*, *T. interdigitale*, *T. mentagrophytes,*, and *T. rubrum* isolates resistant to TRB (Rocha et al., 2002; Singh et al., 2018). In addition, Taghipour et al. showed that there was a relationship between *SQLE* mutation in the species resistant to TRB and ITS genotype. So the resistant strains of *T. mentagrophytes* are categorized only in VIII genotype, and resistant species of *T. interdigitale* are categorized in II genotype. On the other hand, according to the new classification of *T. mentagrophytes*, subtype VIII is considered as a separate species named *Trichophyton indotineae* (Kano et al., 2020).

However, the emergence of TRB-resistant dermatophyte strains in the south of Asia and an increase in resistance of the strains to antifungal drugs are survival mechanisms of dermatophyte fungi, which lead to failure of treatment and recurrence of disease (Ebert et al., 2020). Therefore, in this study, to accurately identify dermatophyte species, ITS region sequence was utilized, and ITS genotypes of *T. mentagrophytes* and *T. interdigitale* were determined. In addition, antifungal activity assessment of TRB drugs, ITZ, ketoconazole (KTZ), fluconazole (FLZ), posaconazole (PCZ), voriconazole (VCZ), and amphotericin B (AMB) was done through Clinical and Laboratory Standards Institute (CLSI) broth microdilution M38-A2 method against 123 clinical isolates and five standard isolates of dermatophyte. In addition, the point mutation in *SQLE* gene was investigated in TRB-resistant strains.

2 MATERIAL AND METHODS

2.1 Clinical Fungal Isolation

This experimental study included 123 dermatophyte isolates obtained from the patients visiting the Mycology Department, Pasteur Institute of Iran, between 2018 and 2019. The isolates were identified using microscope and culture, and for final confirmation, ITS sequence was used. In addition, five standard strains were provided from Persian Type Culture Collection (PTCC), Iranian Research Organization for Science and Technology (Karaj-Iran), including *T. mentagrophytes* PTCC 5054, *Microsporum canis* PTCC 5069, *Nannizzia gypsea* PTCC 130396, *Trichophyton verrucosum* PTCC 10694, and *T. rubrum* PTCC 5808, which were used as quality control. The species under study were *T. mentagrophytes/T. interdigitale* complex (include *T. indotineae*), *T. rubrum*, *T. tonsurans*, *Epidermophyton floccosum*, *T. verrucosum*, *N. gypsea*, *Nannizzia fulva*, and *M. canis* (**Table 1**).

2.2 Molecular Identification by ITS Region

All fungal strains were cultured on Mycobiotic agar (Merck, Darmstadt, Germany) and incubated at 27°C for 7 days (Osborne et al., 2005). In summary, fungal cell fragmentation was performed by liquid nitrogen and added to the extracted cells of DNA extraction buffer containing 200 M of Tris-HCl, pH 8, 25 mM of EDTA, SDS 0.5% W/V, and NaCl 250 mM. The DNA extraction method was based on phenol/chloroform/isoamyl alcohol (25:24:1) and proteinase K. After extraction, the resulting DNA was re-dissolved in 50 µl of Tris-EDTA (TE) buffer and stored at −20°C (Salehi et al., 2018a). The ITS region was PCR amplified using primers ITS1 (5′-TCCGT AGGTGAACCTGCGG-3′) and ITS4 (5′-TCCTCCGCTT ATTGATATGC-3′) (White et al., 1990). The final volume of PCRs was 25 µl, containing 12.5 µl of premix (Ampliqon, Odense, Denmark), 1 µl of DNA template, 0.5 µM of forward

TABLE 1 | Clinical features of the 123 clinical dermatophyte strains based on the infection body area.

Clinical manifestation	Etiologic agents, no. (%)										
	Trichophyton mentagrophytes	*Trichophyton interdigitale*	*Trichophyton indotineae*	*Trichophyton rubrum*	*Trichophyton tonsurans*	*Trichophyton verrucosum*	*Epidermophyton floccosum*	*Microsporum canis*	*Nannizzia gypsea*	*Nannizzia fulva*	Total no. (%)
Tinea cruris	2 (1.62)	11 (8.84)	5 (4.06)	5 (4.06)	3 (2.43)	–	14 (11.38)	1 (0.81)	–	–	41 (33.33)
Tinea pedis	2 (1.62)	9 (7.31)	3 (2.43)	7 (5.69)	–	–	3 (2.43)	–	–	–	24 (19.51)
Tinea corporis	1 (0.81)	1 (0.81)	2 (1.62)	–	2 (1.62)	–	1 (0.81)	5 (4.06)	–	–	12 (9.75)
Tinea capitis	–	2 (1.62)	–	–	8 (6.50)	–	–	4 (3.25)	2 (1.62)	–	16 (13.00)
Tinea unguium	–	–	–	–	–	–	–	–	4 (3.25)	2 (1.62)	6 (4.87)
Tinea faciei	–	–	–	–	3 (2.43)	5 (4.06)	–	–	–	–	8 (6.50)
Tinea manuum	1 (0.81)	5 (4.06)	–	3 (2.43)	–	2 (1.62)	1 (0.81)	4 (3.25)	–	–	16 (13.00)
Total	6	28	10	15	16	7	19	14	6	2	123

and reverse primers, and distilled water. The PCR cycling conditions were as follows: 5 min initial pre-incubation at 95°C, followed by 35 cycles consisting of denaturation at 94°C for 30 s, annealing at 58°C for 30 s, and extension at 72°C for 45 s, with a final extension at 72°C for 5 min (Salehi et al., 2020). Five microliters of the PCR products was electrophoresed on the 1% agarose gel in Tris/Borate/EDTA (TBE) buffer (Yurkov et al., 2012). The sequences of isolates were edited manually and subjected to ClustalW pairwise alignment using the MEGA10 software. The sequences deposited in GenBank are shown in **Table 2**. ITS genotyping determined *T. interdigitale/T. mentagrophytes* species complex according to the studies by Heidemann et al. (2010) and Taghipour et al. (2019). In addition to examining the relationship between the genotype and resistance to TRB, the ITS genotype of complex isolates *T. mentagrophytes/T. interdigitale/T. indotineae* was determined.

Then, the sequences were analyzed by RAxML version 8.2 (Stamatakis, 2014) running on CIPRES Science Gateway (Miller et al., 2010). Optimization in RAxML was carried out using the GTRCAT option. Bootstrap values for maximum likelihood were 1,000 replicates with one search replicate per bootstrap replicate and *Fusarium solani* as the outgroup.

2.3 Antifungal Susceptibility Testing

2.3.1 Chemical Antifungal Drugs

The drug susceptibility test was performed through minimum inhibitory concentration (MIC) microdilution broth. The drugs related to the MIC test were prepared according to the M38-A2 protocol for filamentous fungi (Wayne, 2008).

2.3.2 Drug Susceptibility Testing Using Microdilution Broth

The broth microdilution was used following M38-A2 CLSI protocol to examine and assess MIC in all strains (Wayne, 2008). According to the CLSI standard, drug stocks were prepared in dimethyl sulfoxide (DMSO). Different concentrations (100 µl) were poured into 96-well round-bottom microplates from the lowest concentration to the highest concentration. According to the CLSI standard, the range of antifungals was as follows: 0.001–32 µg/ml for TRB; 0.01–16 µg/ml for ITZ, KTZ, VCZ, PCZ, and AMB; and 0.06–64 µg/ml for FLZ. Then the prepared suspensions (100 µl) of each strain containing 1-3 × 10^3 ml/CFU spore were added to the wells. The plates were incubated at 35°C and visually assessed for fungal growth after 96 h. The MIC range, geometric mean, MIC_{50}, and MIC_{90} were calculated for all the isolates tested.

2.4 PCR Assay Targeting the SQLE Region

To investigate mutations in *SQLE* gene, the strains with less susceptibility to TRB were evaluated with the primers Drsq1 (5′-TTGCCAACGGGGTGTAAAG-3′) and Drsq2 (5′-GGGGCCATCTATAATTCAGACTC-3′) (Osborne et al., 2006). The primer for replacing amino acids in Leu393Phe, Leu393Ser, Phe397Leu, and Gln408Leu in *SQLE* was used. The length of the fragments for *Trichophyton* was 500 bp, while it was 520 bp for *Epidermophyton* and *Nannizzia*. According to CLSI, *T. rubrum* strains with MIC > 0.5 µg/ml and other strains with

TABLE 2 | Age and sex distribution of dermatophyte species isolated from clinical specimens.

Dermatophytes species	Sex (no.)		Age (no.)								Accession no.
	F	M	0–10	11–20	21–30	31–40	41–50	51–60	61–70	71–80	
Trichophyton mentagrophytes (n = 6)	4	2	1	–	2	1	1	1	–	–	MZ983790- MZ983485- MZ994488- MZ994650- MZ994652- MZ994491
Trichophyton interdigitale (n = 28)	12	16	1	–	3	11	5	6	2	–	OK 35221- OK 35220- OK 110565- OK 110585- OK 110591- OK 110574- OK 110568- OK 110566- OK 110586- OK 110567- OK 110580- OK 110572- OK 110578- OK 110576- OK 110577- OK 35231- OK 110583- OK 110570- OK 110569- OK 110589- OK 110571- OK 35266-o OK 110575- OK 110581- OK 110573- OK 110579- OK 110587-OK110582
Trichophyton indotineae (n = 10)	4	6	–	1	1	5	2	1	–	–	OM366332 to OM366341
Trichophyton rubrum (n = 15)	3	12	–	–	2	2	7	1	2	1	MT188699- MZ427314- MZ434885- MT188700- MT150739- MZ434887- MZ434886- MZ427316- MT191357- MT152325
Trichophyton tonsurans (n = 16)	3	13	4	6	3	1	2	–	–	–	MT041242- MT041041- MT041256- MT066197- MT051844
Trichophyton verrucosum (n = 7)	–	7	–	–	2	2	2	1	–	–	MT318679- MT318720
Epidermophyton floccosum (n = 19)	5	14	1	–	4	6	3	2	3	–	MT040969- MT040750- MT150728- MT040755- MZ363671- MT040763- MZ363673- MZ363722- MZ363721- MT040762- MZ363674
Microsporum canis (n = 14)	9	5	4	2	3	3	–	2	–	–	MT129526- MT067649- MT183698- Mz363857- MT136105- MT129500
Nannizzia gypsea (n = 6)	3	3	2	2	1	–	–	1	–	–	MT318651- MZ434959- MZ435310- MT394865
Nannizzia fulva (n = 2)	2	–	1	1	–	–	–	–	–	–	–

MIC > 0.25 μg/ml were selected as the strains with less sensitivity to TRB.

The PCRs were prepared with the final volume of 50 μl containing 25 μl of premix (Ampliqon, Denmark), 3 μl of DNA template, 0.6 μM of forward and reverse primers, and distilled water. The PCR cycling conditions were as follows: 5 min initial pre-incubation at 95°C, followed by 35 cycles consisting of denaturation at 94°C for 30 s, annealing at 58°C for 30 s, and extension at 72°C for 45 s, with a final extension at 72°C for 5 min (Salehi et al., 2018b). The PCR products of the *SQLE* region were sequenced by the ABI PRISM BigDye Terminator Cycle Sequencing Ready Reaction Kit. The forward and reverse sequences of isolates showing reduced susceptibility to TRB were subjected to ClustalW pairwise alignment using the MEGA10 software and edited manually to improve the alignment accuracy.

2.5 Statistical Analysis

The quantitative data from MIC, the geometric mean, MIC_{50}, and MIC_{90} were calculated using the SPSS statistical package.

3 RESULTS

3.1 Characteristics of the Studied Dermatophyte Isolates

Clinical data of 123 patients including 82 men (66.66%) and 41 women (33.33%) are listed in **Table 1**. In addition, the age range of the patients was 2–80 years with a mean age of 41. The most common clinical manifestations were tinea cruris (34.95%) followed by tinea pedis (17.88%), tinea manuum (19.51%), and tinea capitis (16.26%). The dominant species in tinea cruris, tinea pedis, and tinea capitis were *T. tonsurans*, *T. rubrum*, and *E. floccosum*, respectively. In addition, the isolated species from tinea faciei only included *T. tonsurans* and *T. verrucosum*. It is significant that *N. fulva* was only isolated from tinea unguium and that *T. verrucosum* was only isolated from the male cases.

3.2 Molecular Identification by ITS Region

All the dermatophyte species were identified by determining the sequence of ITS-rDNA regions. The results of the molecular method indicated species *T. mentagrophytes* (6), *T. interdigitale* (28), *T. indotineae* (10), *E. floccosum* (19), *T. tonsurans* (16), *T. rubrum* (15), *M. canis* (14), *T. verrucosum* (7), *N. gypsea* (6), and *N. fulva* (2). After manually editing and blast analysis, the sequences were deposited in GenBank (**Table 2**). In addition, ITS genotype examination results showed that out of 6 *T. mentagrophytes* isolates, there was one isolate in each of the V and III* genotypes. *T. indotineae* was located between genotypes V and III* of *T. mentagrophytes*. Also, a new genotype was found in four isolates of *T. mentagrophytes* (XXIX). *T. interdigitale* isolates were only seen in two genotypes II (n = 22) and II* (n = 6) (**Figure 1**).

The phylogenetic tree was drawn through RAxML analysis for all species (**Figure S1**). The tree illustrates the phylogenetic relationships between all isolates under study. Based on phylogenetic analysis, all isolates were placed in six clades (*T. mentagrophytes*, *T. interdigitale*, and *T. indotineae* were in

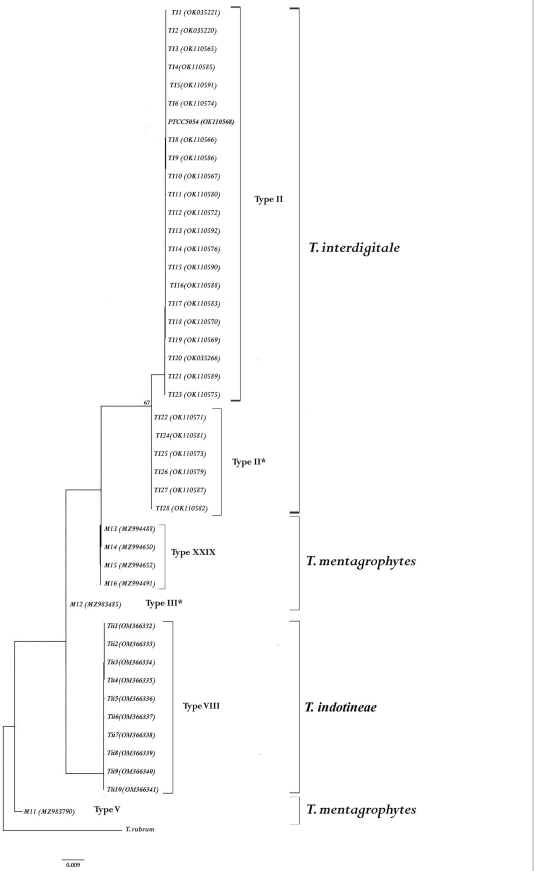

FIGURE 1 | The genotyping tree was constructed based on ITS region sequences by RAxML analysis from *Trichophyton mentagrophytes/ Trichophyton interdigitale* complex, and the accession numbers are given in parentheses. *Trichophyton rubrum* was used as an outgroup to root the dendrogram. The bootstrap value greater than 65% is shown above the branches.

separate clusters). In addition, *N. gypsea* and *N. fulva* were observed in one clade with high support. In addition, the *M. canis* clade was in the base position compared to other species (**Figure S1**). Supports of bootstrap higher than 85% were represented in RAxML analysis. In addition, the phylogenetic tree did not demonstrate a relationship between the isolates that showed a decrease in sensitivity to TRB.

3.3 Antifungal Susceptibility Testing

MIC range, geometric mean MIC, MIC_{50}, and MIC_{90} were computed for all dermatophyte strains (**Table 2**). In general, among all strains, the highest antifungal effects were observed with TRB followed by ITZ, VCZ, KTZ, FLZ, AMB, and PCZ. The most sensitive strains to TRB were *T. rubrum*, *T. tonsurans*, *T. interdigitale*, *M. canis*, *T. verrucosum*, *N. gypsea*, *N. fulva*, *T. mentagrophytes*, *E. floccosum*, and *T. indotineae* in a descending order. In addition, the results showed that *M. canis* (MIC_{50} = 0.12 μg/ml) had the highest MIC and *T. indotineae* (MIC_{50} = 1 μg/ml) had the lowest MIC against ITZ. In addition, KTZ had a low suppressive effect only against *E. floccosum* (G mean = 1.07 μg/ml). Also, among *T. mentagrophytes*, *T. interdigitale*, and *T. indotineae* species, the lowest and highest sensitivity to seven antifungal drugs tested was observed in *T. indotineae* and *T. interdigitale*, respectively. Furthermore, TRB had the highest antifungal effects against *T. indotineae*.

Moreover, VCZ had a high suppressive effect on *N. gypsea* species. The FLZ had a lower suppressive effect on *T. rubrum* and *T. mentagrophytes* species compared to other species. In general, the lowest suppressive effect on all dermatophyte species was observed with PCZ (**Table 3**).

A comparison of MIC_{50} in II and II* genotypes of *T. interdigitale* showed that genotype II had a higher MIC_{50} with all drugs. In addition, isolates of XXIX genotype of *T. mentagrophytes* had a higher MIC_{50} as compared to *T. indotineae*.

In general, a comparison of *Trichophyton*, *Epidermophyton*, *Microsporum*, and *Nannizzia* genera showed that TRB and ITZ had the highest effect as compared to other drugs. *Trichophyton* genus had the lowest G mean against all drugs followed by *Nannizzia*. On the other hand, for all the drugs under study, *Epidermophyton* had the highest MIC_{50}.

In *Nannizzia* genus, TRB and VCZ had a strong effect, KTZ had a weak effect, and AMB was inefficient (**Table 3**).

Among anthropophilic, geophilic, and zoophilic species, anthropophilic species had a high sensitivity to all drugs. In addition, the lowest and highest G mean in the anthropophilic group was observed in *T. rubrum* and *E. floccosum* isolates, respectively. On the other hand, AMB and PCZ had a low inhibitory effect against *E. floccosum* in the anthropophilic group. In general, geophilic and zoophilic species compared to anthropophilic species had a lower sensitivity to TRB and ITZ, respectively. Moreover, among zoophilic and geophilic species, *M. canis* and *N. gypsea* had a high level of sensitivity to TRB, respectively. Overall, azoles had the highest inhibitory effect against *T. tonsurans* species and the lowest inhibitory effect against *T. indotineae*.

Among all isolates, *T. indotineae* (n = 2), *T. mentagrophytes* (n = 1), *E. floccosum* (n = 1), *Trichophyton verrucosum* (n = 1), and *N. gypsea* (n = 1) demonstrated a decrease in sensitivity to TRB (MIC > 32 μg/ml). In addition, among all strains, two isolates (1.62%) were resistant to all drugs under study. The highest cross-resistance was observed between FLZ and ITZ (16.26%), and cross-resistance among azole antifungals was observed in 11 isolates (8.94%).

3.4 Point Mutation in *SQLE* Gene (Terbinafine-Resistant Strains)

To examine mutation in *SQLE* gene, all the six strains with a lower sensitivity to TRB were reproduced using Drsq primers and sequenced. The band length of the PCR product for *Trichophyton* was 500 bp, while it was 520 bp for *Epidermophyton* and *Nannizzia*. Forward and reverse sequences were edited using MEGA10 for each isolate, and then, the sequences were compared with sensitive strain

TABLE 3 | Antifungal susceptibility profile of 123 dermatophyte strains to seven antifungal agents by broth microdilution method.

Dermatophyte species	Antifungal drugs	MIC range (μg/ml)	MIC_{50}/ MIC_{90} (μg/ml)	G mean (μg/ml)	MIC (μg/ml)														
					64	32	16	8	4	2	1	0.5	0.25	0.125	0.06	0.03	0.015	0.007	0.003	0.001
Trichophyton mentagrophytes (n = 6)	TRB	0.015–16	0.09/–	0.13			1							2	1	1	1			
	ITZ	0.125–8	0.75/–	0.70				1			2	1	1	1						
	KTZ	0.06–8	1.25/–	1				1	1	1		1	1	1						
	FLZ	0.125–16	1.25/–	1.2			1		1	1		1	1	1						
	VCZ	0.125–8	0.3/–	0.5				1			1	1	1	2						
	PCZ	0.125–16	1.25/–	1.09			1	1		1		1	1	1						
	AMB	0.125–8	0.75/–	0.79				1			2	1	1	1						
Trichophyton interdigitale (n = 28)	TRB	0.003–0.025	0.06/0.125	0.04										7	8	6	4	2	1	
	ITZ	0.03–16	0.25/8.8	0.38			2	1	2	2	1	4	4	9	2	1				
	KTZ	0.03–16	0.5/8.8	0.37			2	1	2	1	3	6	2	7	2	2				
	FLZ	0.125–64	0.25/35.2	0.78	2	1	2	2	1	1	1	3	4	10						
	VCZ	0.125–16	0.37/16	0.70			4	3		1	2	4	6	8						
	PCZ	1–16	1.5/16	1.55			6	3	3	2	4	3	2	4	1					
	AMB	0.125–8	0.25/8	0.56				5	2		3	3	6	9						
Trichophyton indotineae (n = 10)	TRB	0.015–32	0.125/30.4	0.24		1	1							5	1	1	1			
	ITZ	0.06–16	1/15.2	0.9			1		1	1	2		1	3	1					
	KTZ	0.125–16	0.5/16	0.79			2		2			2	2	2						
	FLZ	0.125–16	0.75/14.8	0.93			1		3		1	1	2	2						
	VCZ	0.125–8	0.37/7.4	0.53				1		1	2	1	3	2						
	PCZ	0.125–16	0.75/16	1			2		1	1	1	1	2	2						
	AMB	0.125–16	0.5/15.2	0.81			1	1		1	1	2	3	1						
Trichophyton rubrum (n = 15)	TRB	0.003–0.006	0.015/0.06	0.01											3	2	3	2	5	
	ITZ	0.06–16	0.25/14	0.30			1			1	1	2	3	2	5					
	KTZ	0.125–16	0.25/16	0.75			2	2	1			2	4	4						
	FLZ	0.125–16	0.5/16	1.04			3	1	1	–	2	2	4	2						
	VCZ	0.06–8	0.25/5.6	0.39				1	1	1	1	3	2	5	1					
	PCZ	0.25–16	1/16	1.58			3	1	1	1	3	4	2							
	AMB	0.125–8	0.5/8	0.79				3	1	1	2	2	3	3						
Trichophyton tonsurans (n = 16)	TRB	0.003–0.125	0.09/0.125	0.07										8	5	3				
	ITZ	0.06–8	0.37/8	0.51				2	2	1	1	2	2	4	2					
	KTZ	0.125–16	0.5/10.4	0.64			1	2			2	4	5	2						
	FLZ	0.125–32	0.5/20.8	0.67		1	1			1	2	5	4	2						
	VCZ	0.06–16	0.25/16	0.49			3	1				2	3	5	2					
	PCZ	0.125–16	0.75/16	1.24			4	2			2	2	3	3						
	AMB	0.06–16	0.25/16	0.56			3	2				2	3	2	3	1				
Trichophyton verrucosum (n = 7)	TRB	0.06–4	0.125/–	0.16					1					4	2					
	ITZ	0.06–1	0.25/–	0.30							2	1	2	1	1					
	KTZ	0.125–1	0.5/–	0.37							2	2	1	2						
	FLZ	0.125–16	0.5/–	0.90			1	1		1		1	1	2						
	VCZ	0.03–16	0.5/–	0.40			1	1			2			1	1	1				
	PCZ	0.125–16	0.5/–	1.21			2		1			1	2	1						
	AMB	0.06–2	0.25/–	0.30						1	1	1	1	2	1					
Epidermophyton floccosum (n = 19)	TRB	0.06–16	0.125/0.25	0.17			1						6	9	3					
	ITZ	0.06–16	0.5/16	0.80			3	2		1	2	2	5	3	1					
	KTZ	0.125–16	0.5/16	1.07			4	2	1	1	1	3	3	5						
	FLZ	0.125–32	0.37/32	0.77		2	2			1	1	3	7	3						
	VCZ	0.03–8	0.5/8	0.80				5	1	2		3	3	4	1					
	PCZ	0.125–16	0.5/16	1			3	2	1	1	2	3	4	3						
	AMB	0.06–16	0.25/16	0.57			3	2				4	3	5	2					
Microsporum canis (n = 14)	TRB	0.03–0.125	0.09/0.125	0.07										7	5	2				
	ITZ	0.03–16	0.125/8.5	0.19			1				1	1	3	3	4	1				
	KTZ	0.125–16	0.5/20.5	0.93			2	1	1			3	3	4						
	FLZ	0.125–32	0.37/20	0.67		1		2		1	1	2	3	4						
	VCZ	0.125–16	0.5/16	0.86			2	1	1		1	3	5	1						
	PCZ	0.125–16	1.5/16	1.72			4	1	1	1	1	2	3	1						
	AMB	0.25–16	1/16	1.28			3		1	1	3	2	4							
Nannizzia gypsea (n = 6)	TRB	0.015–16	0.09/–	0.13			1							2	1	1	1			
	ITZ	0.125–8	0.37/–	0.70				2				1	1	2						

(Continued)

TABLE 3 | Continued

Dermatophyte species	Antifungal drugs	MIC range (μg/ml)	MIC_{50}/ MIC_{90} (μg/ml)	G mean (μg/ml)	MIC (μg/ml)													
					64	32	16	8	4	2	1	0.5	0.25	0.125	0.06	0.03	0.015	0.007	0.003	0.001
	KTZ	0.125–16	0.37/–	0.89			1	1				1	2	1						
	FLZ	0.125–16	0.62/–	0.62			1				1	1	2	1						
	VCZ	0.125–16	0.18/–	0.35			1						2	3						
	PCZ	0.25–16	1.25/–	1.58			3	1					2							
	AMB	0.125–8	0.37/–	0.70				1	1			1	2	1						
Nannizzia fulva (n = 2)	TRB	0.125–0.25	–/–	–									1	1						
	ITZ	0.25–0.5	–/–	–								1	1							
	KTZ	0.125–2	–/–	–						1				1						
	FLZ	0.25–1	–/–	–							1		1							
	VCZ	0.25–0.5	–/–	–								1	1							
	PCZ	0.5–1	–/–	–					1			1								
	AMB	0.5–1	–/–	–							1	1								

MIC, minimum inhibitory concentration; TRB, terbinafine; ITZ, itraconazole; KTZ, ketoconazole; FLZ, fluconazole; VCZ, voriconazole; PCZ, posaconazole; AMB, amphotericin B.

sequences in GenBank using BLASTn. Afterward, the nucleic acid sequence was converted into an amino acid sequence. Among the six strains with a lower sensitivity to TRB, a point mutation was seen only in one strain of *T. indotineae* with MIC > 32, so Phe397Leu replacement of *SQLE* protein was observed. Replacement of C with A in *SQLE* gene leads to the replacement of Phe with Leu (**Figure 2**). The DNA sequence of the TRB-resistant isolate was recorded with accession no. OM373652 of *T. indotineae* in GenBank.

4 DISCUSSION

In the light of continuing emergence of resistant dermatophytes to antifungal drugs around the world, monitoring drug resistance is essential (Siopi et al., 2021). In general, the identification of dermatophytes at the species level is a major issue for treating patients (Falahati et al., 2018). In this study, 123 clinical isolates of dermatophyte and five standard strains were examined. All the strains were identified by determining the ITS region sequence, and then the sensitivity pattern for seven antifungal drugs was determined using antifungal susceptibility testing (AFST). As the results showed, the number of men was twice the number of women, and tinea cruris was the dominant form. Other studies have reported tinea pedis and tinea capitis as the prevalent forms of dermatophytosis (Zareshahrabadi et al., 2020).

The current new taxonomy of dermatophytes separates *T. mentagrophytes* from its clonal offshoot *T. interdigitale* (Lipner and Scher, 2019). In fact, this classification is highly important from a clinical viewpoint, as *T. interdigitale* is only anthropophilic, and it is usually isolated from non-inflammatory cases such as tinea unguium and tinea pedis. In contrast, *T. indotineae* is mostly zoophilic and a cause of inflammatory symptoms, which mostly cause tinea corporis and tinea cruris. This is a key factor in selecting the right treatment (Taghipour et al., 2019; Siopi et al., 2021). In this study, *T. interdigitale* was the main causative agent of tinea pedis, while *E. floccosum* was responsible for most cases of tinea cruris. Siopi et al. reported that *T. interdigitale* species was mostly isolated from tinea pedis, which is similar to our results (Siopi et al., 2021).

In this study, the highest frequency of ITS genotypes of *T. interdigitale* and *T. mentagrophytes* belonged to II and VIII genotypes, respectively. Taghipour et al. showed that the VIII genotype was the most common in *T. mentagrophytes* species (Taghipour et al., 2019). In addition, a new XXIX genotype was found in *T. mentagrophytes* in this study. Dabas et al. showed that out of 123 dermatophyte isolates, 56% were *T. interdigitale*, which had been first mistakenly identified as *T. mentagrophytes*. Through determining the sequence of ITS regions, these two species were differentiated (Dabas et al., 2017), which is in accordance with our findings.

The phylogenetic tree using RAxML analysis showed that the sequence of ITS region can effectively differentiate dermatophyte species. Despite that Baert et al. failed to differentiate *Nannizzia* and *Epidermophyton* genera using the sequence of the ITS and BT2 regions, the results showed that the sequence of ITS regions can differentiate these two genera (Baert et al., 2020). Our results are consistent with Gräser et al. (1999).

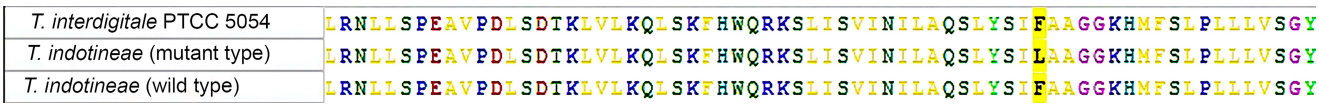

FIGURE 2 | Comparison of the amino acid sequence of squalene epoxidase in terbinafine-sensitive strain and terbinafine-resistant strain.

According to the therapeutic protocols, dermatophytosis TRB is the first choice as a systemic treatment. Also, the latest studies showed the number of resistant cases to TRB is increasing (Dogra et al., 2017). *SQLE* gene mutation changes the protein structure and interrupts the drug attachment to the target enzyme (Shankarnarayan et al., 2020; Shaw et al., 2020; Kong et al., 2021). Here, six strains showed a low sensitivity to TRB, and among them, only one isolate (*T. mentagrophytes*) had a mutation on the Phe397Leu amino acid position. The cause of resistance in other strains might be replacement in other areas of *SQLE* gene or other intervening mechanisms of resistance.

According to Hiruma et al., the highest TRB resistance was observed in *T. rubrum* with L393F replacement in *SQLE* gene (Hiruma et al., 2021). Salehi et al. examined mutation in *SQLE* gene and reported replacement in Phe397Leu amino acid in *T. tonsurans* and *T. rubrum* species (Salehi et al., 2018b). In addition, Rezaei-Matehkolaei et al. showed *SQLE* gene mutation in five strains of TRB-resistant *T. interdigitale* and *T. mentagrophytes* (Rezaei-Matehkolaei et al., 2013). Singh et al. reported a replacement in Phe397Leu and Leu393Phe positions in TRB-resistant *T. interdigitale* strains (Singh et al., 2018). On the other hand, Yamada et al. found the replacement of amino acid in Phe397Leu position of *SQLE* gene in TRB-resistant *T. rubrum* species (Yamada et al., 2017). A similar examination was conducted by Lagowski et al. on resistant strains of *T. mentagrophytes*, and four strains with a mutation at the Leu393Phe region were reported (Lagowski et al., 2020).

In a study by Taghipour et al. of 45 strains of *T. mentagrophytes*, 5 strains (11.11%) were TRB resistant and had substitutions in Ala448Thr, Leu393Ser, and Phe397Leu positions in *SQLE* protein (Dabas et al., 2017). All the TRB-resistant isolates of *T. mentagrophytes* in other studies belonged to the VIII type of ITS genotype. In our study, out of 16 *T. mentagrophytes*, 3 strains were less sensitive to TRB, of which only 1 strain had a mutation in *SQLE* gene. This finding can be explained by the low number of *T. mentagrophytes* isolates or the low number of the VIII type isolates (n = 10). Also, in this study, contrary to the report by Heidemann et al. (2010), no significant correlation was seen between ITS genotype and clinical data, which is in line with the results of Salehi et al. It seems that conclusions about these data require further studies and samples.

In addition to TRB, AFST was carried out on six antifungal drugs. In general, AFST results of all isolates showed that, despite the resistant strains, TRB still is the most efficient drug against dermatophyte species. In addition, the results indicated that *T. indotineae* and *E. floccosum* had the lowest sensitivity to TRB. This finding is consistent with Lagowski et al. (2020), Rezaei-Matehkolaei et al. (2013), Rudramurthy et al. (2018), and Taghipour et al. (2019). Furthermore, in studies by Pourpak et al. (Pourpak and Firooz, 2021) and Kano et al. (2020), low sensitivity against TRB was reported in *T. indotineae*. Moreover, Taghipour et al. (2019) and Salehi et al. (2018b) showed that *T. interdigitale* species were more sensitive to TRB than *T. mentagrophytes* and *T. indotineae*, which is also consistent with our study.

In addition to TRB, ITZ is also prescribed for systemic treatment of dermatophytosis (Siopi et al., 2021). Here, ITZ had the highest and lowest effects on *M. canis* (G mean = 0.19 μg/ml) and *T. indotineae* (G mean = 0.9 μg/ml), respectively. On the other hand, FLZ demonstrated high levels of MIC, which is also consistent with Curatolo et al. (2020) and Barros et al. (2006). Curatolo et al. (2020) showed that TRB and ITZ had a good suppressive effect, which is consistent with the findings of the present study.

Aneke et al. (2018) reported that TRB and VCZ had the highest resistance effect on dermatophyte species and *M. canis* species in particular. This is not consistent with our finding of VCZ. It has been shown that in *T. mentagrophytes*/*T. interdigitale* complex, genotype XXIX of *T. mentagrophytes* and genotype II of *T. interdigitale* had a higher MIC_{50} with all drugs under study. This finding indicates that specific genotypes of this complex species had a higher MIC than others. Further examination of this topic can lead to the identification of more important species.

Among all tested isolates in our study, three strains were resistant to all drugs. In five strains (4.06%) out of all species, cross-resistance between TRB and other azoles drugs was observed, which is expected given that both groups of drugs suppress *SQLE* and cytochrome on the ergosterol biosynthesis path. It is suggested that in addition to major point mutations in *SQLE* gene (L393S, L393F, F397L, and Q408L), which were examined in the present study, other less frequent mutations including F415S, H440Y, and A448T are further investigated. Likewise, selecting more isolates from less frequent dermatophyte species of different geographic regions will help to provide more accurate data about antifungal susceptibility and genotype variations within the population.

5 CONCLUSION

With respect to the increasing prevalence of dermatophytosis and the growing numbers of antifungal drug resistance in dermatophyte species, precise identification of the etiologic species by molecular methods is believed to be crucial to achieve more effective treatments. In addition, epidemiological changes and lack of drug susceptibility testing have led to the failure of treatment and subsequent recurrence of the infection. Determining genotypes can improve our epidemiological information because specific genotypes have higher and different AFST and MIC results, which can help us to have a better diagnosis and treatment. Apparently, determining choice-effective drugs and drug-resistant strains through AFST can bring us closer to more efficient therapeutic goals. Given that TRB is the frontline defense against dermatophytosis, the growing resistance to TRB is a considerable challenge. Altogether, our results showed that precise identification of etiologic dermatophyte species and prescribing antifungal drugs with more caution can prevent resistance in strains, effectively reducing frequently recurrent infections, and prevent the distribution of the infection within the population.

DATA AVAILABILITY STATEMENT

The original contributions presented in the study are included in the article/**Supplementary Material**. Further inquiries can be directed to the corresponding author.

ETHICS STATEMENT

The studies involving human participants were reviewed and approved by IR.PII.REC.1397.021. Written informed consent to participate in this study was provided by the participants' legal guardian/next of kin.

AUTHOR CONTRIBUTIONS

NP performed the experiments, contributed to the analysis of the data, and drafted the manuscript. MS-G, ACN, MA and ZS assisted in the interpretation of the molecular data, data analysis and editing the manuscript. MR-A supervised the study, participated in the study design and data analysis, and approved the final draft. All authors have read and approved the final version of the manuscript.

FUNDING

This work was supported financially by the Pasteur Institute of Iran.

ACKNOWLEDGMENTS

The authors gratefully thank the personnel of the Mycology Department of the Pasteur Institute of Iran for helpful assistance in isolate preparation.

SUPPLEMENTARY MATERIAL

The Supplementary Material for this article can be found online at: https://www.frontiersin.org/articles/10.3389/fcimb.2022.851769/full#supplementary-material

REFERENCES

Afshari, M., Shams-Ghahfarokhi, M., and Razzaghi-Abyaneh, M. (2016). Antifungal Susceptibility and Virulence Factors of Clinically Isolated Dermatophytes in Tehran, Iran. *Iran J. Microbiol.* 8 (1), 36–46.

Aneke, C. I., Otranto, D., and Cafarchia, C. (2018). Therapy and Antifungal Susceptibility Profile of *Microsporum canis*. *J. Fungi* 4 (3). doi: 10.3390/jof4030107

Baert, F., De Hoog, G. S., Packeu, A., and Hendrickx, M. (2020). Updating the Taxonomy of Dermatophytes of the BCCM/IHEM Collection According to the New Standard: A Phylogenetic Approach. *Mycopathologia* 185 (1), 161–168. doi: 10.1007/s11046-019-00338-7

Barros, M. E. S., Santos, D. D. A., and Hamdan, J. S. (2006). *In Vitro* Methods for Antifungal Susceptibility Testing of Trichophyton spp. *Mycol Res.* 110 (11), 1355–1360. doi: 10.1016/j.mycres.2006.08.006

Bhatia, V. K., and Sharma, P. C. (2015). Determination of Minimum Inhibitory Concentrations of Itraconazole, Terbinafine and Ketoconazole Against Dermatophyte Species by Broth Microdilution Method. *Indian J. Med. Microbiol.* 33, 533–537. doi: 10.4103/0255-0857.167341

Curatolo, R., Juricevic, N., Leong, C. H., and Bosshard, P. P. (2020). Antifungal Susceptibility Testing of Dermatophytes: Development and Evaluation of an Optimized Broth Microdilution Method. *Mycoses* 64 (3), 282–291. doi: 10.1111/myc.13202

Dabas, Y., Xess, I., Singh, G., Pandey, M., and Meena, S. (2017). Molecular Identification and Antifungal Susceptibility Patterns of Clinical Dermatophytes Following CLSI and EUCAST Guidelines. *J. Fungi* 3 (2), 17. doi: 10.3390/jof3020017

de Hoog, G. S., Dukik, K., Monod, M., Packeu, A., Stubbe, D., Hendrickx, M., et al. (2017). Toward a Novel Multilocus Phylogenetic Taxonomy for the Dermatophytes. *Mycopathologia* 182, 5–31. doi: 10.1007/s11046-016-0073-9

Dogra, S., Kaul, S., and Yadav, S. (2017). Treatment of Dermatophytosis in Elderly, Children, and Pregnant Women. *Indian Dermatol. Online J.* 8 (5) , 310–318. doi: 10.4103/idoj.IDOJ-169-17

Ebert, A., Monod, M., Salamin, K., Burmester, A., Uhrlaß, S., Wiegand, C., et al. (2020). Alarming India-Wide Phenomenon of Antifungal Resistance in Dermatophytes: A Multicentre Study. *Mycoses* 63 (7), 717–728. doi: 10.1111/myc.13091

Falahati, M., Fateh, R., Nasiri, A., Zaini, F., Fattahi, A., and Farahyar, S. H. (2018). Specific Identification and Antifungal Susceptibility Pattern of Clinically Important Dermatophyte Species Isolated From Patients With Dermatophytosis in Tehran, Iran. *Arch. Clin. Infect. Dis.* 13 (3), e63104. doi: 10.5812/archcid.63104

Ghannoum, M., Chaturvedi, V., Espinel-Ingroff, A., Pfaller, M., Rinaldi, M., Lee-Yang, W., et al. (2004). Intra and Inter Laboratory Study of a Method for Testing the Antifungal Susceptibilities of Dermatophytes. *J. Clin. Microbiol.* 42, 2977–2979. doi: 10.1128/JCM.42.7.2977-2979.2004

Gräser, Y., El Fari, M., Vilgalys, R., Kuijpers, A. F. A., De Hoog, G. S., Presber, W., et al. (1999). Phylogeny and Taxonomy of the Family Arthrodermataceae (Dermatophytes) Using Sequence Analysis of the Ribosomal ITS Region. *Med. Mycol.* 37 (2), 105–114. doi: 10.1080/02681219980000171

Haugh, M., Helou, S., Boissel, J. P., and Cribier, B. J. (2000). Terbinafine in Fungal Infections of the Nails: A Meta-Analysis of Randomized Clinical Trials. *Br. J. Dermatol.* 147 (1), 118–121. doi: 10.1046/j.1365-2133.2002.04825.x

Heidemann, S., Monod, M., and Graser, Y. (2010). Signature Polymorphisms in the Internal Transcribed Spacer Region Relevant for the Differentiation of Zoophilic and Anthropophilic Strains of *Trichophyton nterdigitale* and Other Species of *T. mentagrophytes* Sensu Lato. *Br. J. Dermatol.* 162 (2), 282–295. doi: 10.1111/j.1365-2133.2009.09494.x

Hiruma, J., Noguchi, H., Hase, M., Tokuhisa, Y., Shimizu, T., Ogawa, T., et al. (2021). Epidemiological Study of Terbinafine-Resistant Dermatophytes Isolated From Japanese Patients. *J. Dermatol.* 48 (4), 564–567. doi: 10.1111/1346-8138.15745

Kano, R., Kimura, U., Kakurai, M., Hiruma, J., Kamata, H., Suga, Y., et al. (2020). *Trichophyton indotineae* sp. Nov.: A New Highly Terbinafine-Resistant Anthropophilic Dermatophyte Species. *Mycopathologia* 185, 947–958. doi: 10.1007/s11046-020-00455-8

Kong, X., Tang, C. H., Singh, A., Ahmed, S. A., Al-Hatmi, A. M. S., Chowdhary, A., et al. (2021). Antifungal Susceptibility and Mutations in the Squalene Epoxidase Gene in Dermatophytes of the *Trichophyton mentagrophytes* Species Complex. *Antimicrob. Agents Chemother.* 1665 (8), e0005621. doi: 10.1128/AAC.00056-21

Lagowski, D., Gnat, S., Nowakiewicz, A., Osinska, M., and Dyląg, M. (2020). Intrinsic Resistance to Terbinafine Among Human and Animal Isolates of *Trichophyton m entagrophytes* Related to Amino Acid Substitution in the Squalene Epoxidase. *Infection* 48 (6), 889–897. doi: 10.1007/s15010-020-01498-1

Lipner, S. R., and Scher, R. K. (2019). Onychomycosis: Treatment and Prevention of Recurrence. *J. Am. Acad. Dermatol.* 80 (4), 853–867. doi: 10.1016/j.jaad.2018.05.1260

Liu, W., May, G. S., Lionakis, M. S., Levis, R. E., and Kontoyiannis, D. P. (2004). Extra Copies of the *Aspergillus fumigatus* Squalene Epoxidase Gene Confer Resistance to Terbinafine: Genetic Approach to Studying Gene Dose-Dependent Resistance to Antifungals in *A. fumigatus*. *Antimicrob. Agent Chemother.* 48 (7), 2490–2496. doi: 10.1128/AAC.48.7.2490-2496

Miller, M. A., Pfeiffer, W., and Schwartz, T. (2010). Creating the CIPRES Science Gateway for Inference of Large Phylogenetic Trees. *Gateway Computing Environments Workshop (GCE)*, 1–8. doi: 10.1109/GCE.2010.5676129

Mukherjee, P., Leidich, S., Isham, N., Leitner, I., Ryder, N., and Ghannoum, M. (2003). Clinical *Trichophyton Rubrum* Strain Exhibiting Primary Resistance to Terbinafine. *Antimicrob. Agents Chemother.* 47 (1), 82–86. doi: 10.1128/AAC.47.1.82-86.2003

Nenoff, P., Verma, S. B., Ebert, A., Süß, A., Fischer, E., Auerswald, E., et al. (2020). Spread of Terbinafine-Resistant *Trichophyton mentagrophytes* Type VIII (India) in Germany–"The Tip of the Iceberg. *J. Fungi* 6 (4), 207. doi: 10.3390/jof6040207

Niimi, M., Firth, N. A., and Cannon, R. (2010). Antifungal Drug Resistance of Oral Fungi. *Odontology* 98 (1), 15–25. doi: 10.1007/s10266-009-0118-3

Osborne, C., Leitner, I., Favre, B., and Ryder, N. (2005). Amino Acid Substitution in *Trichophyton rubrum* Squalene Epoxidase Associated With Resistance to Terbinafine. *Antimicrob. Agents Chemother.* 49 (7), 2840–2844. doi: 10.1128/AAC.49.7.2840-2844.2005

Osborne, C., Leitner, I., Hofbauer, B., Fielding, C., Favre, B., and Ryder, N. (2006). Biological, Biochemical, and Molecular Characterization of a New Clinical *Trichophyton rubrum* Isolate Resistant to Terbinafine. *Antimicrob. Agents Chemother.* 50, 2234–2236. doi: 10.1128/AAC.01600-05

Pourpak, Z., and Firooz, A. (2021). Multidrug-Resistant *Trichophyton mentagrophytes* Genotype VIII in an Iranian Family With Generalized Dermatophytosis: Report of Four Cases and Review of Literature. *Int. J. Dermatol.* 60 (6), 686–692. doi: 10.1111/ijd.15226

Rezaei-Matehkolaei, A., Makimura, K., De Hoog, S., Shidfar, M. R., Zaini, F., Eshraghian, M., et al. (2013). Molecular Epidemiology of Dermatophytosis in Tehran, Iran, a Clinical and Microbial Survey. *Med. Mycol.* 51 (2), 203–207. doi: 10.3109/13693786.2012.686124

Rocha, E. M. F., Almeida, C. B., and Martinez-Rossi, N. M. (2002). Identification of Genes Involved in Terbinafine Resistance in *Aspergillus nidulans*. *Lett. Appl. Microbiol.* 35 (3), 228–232. doi: 10.1046/j.1472-765x.2002.01174.x

Rudramurthy, S. H. M., Shankarnarayan, S. H. A., Dogra, S., Shaw, D., Mushtaq, K. H., Paul, R. A., et al. (2018). Mutation in the Squalene Epoxidase Gene of *Trichophyton Interdigitale* and *Trichophyton rubrum* Associated With Allylamine Resistance. *Antimicrob. Agents Chemother.* 62 (5), e02522–e02517. doi: 10.1128/AAC.02522-17

Salehi, Z., Shams-Ghahfarokhi, M., Fattahi, A., Ghazanfari, M., and Yazdanparast, S. A. (2018a). A Head-to-Head Comparison of Four Cryopreservation Protocols of Dermatophyte Species. *Infect. Epidemiol* 4 (3), 109–114.

Salehi, Z., Shams-Ghahfarokhi, M., and Razzaghi-Abyaneh, M. (2021) Molecular Epidemiology, Genetic Diversity, and Antifungal Susceptibility of Major Pathogenic Dermatophytes Isolated From Human Dermatophytosis. *Front. Microbiol.* 4. doi: 10.3389/fmicb.2021.643509

Salehi, Z., Shams-Ghahfarokhi, M., and Razzaghi-Abyaneh, M. (2018b). Antifungal Drug Susceptibility Profile of Clinically Important Dermatophytes and Determination of Point Mutations in Terbinafine-Resistant Isolates. *Eur. J. Clin. Microbiol. Infect. Dis.* 37 (10), 1841–1846. doi: 10.1007/s10096-018-3317-4

Salehi, Z., Shams-Ghahfarokhi, M., and Razzaghi-Abyaneh, M. (2020). Internal Transcribed Spacer rDNA and *TEF-1α* Gene Sequencing of Pathogenic Dermatophyte Species and Differentiation of Closely Related Species Using PCR-RFLP of the *Topoisomerase II*. *Cell J.* 22 (1), 85–91. doi: 10.22074/cellj.2020.6372

Santos, H. L., Lang, E. A. S., Fernando Segato, F., Rossi, A., and Martinez-Rossi, N. M. (2018). Terbinafine Resistance Conferred by Multiple Copies of the Salicylate 1-Monooxygenase Gene in *Trichophyton rubrum*. *Med. Mycol.* 56 (3), 378–381. doi: 10.1093/mmy/myx044

Shankarnarayan, S. H. A., Shaw, D., Sharma, A., Chakrabarti, A., Dogra, S., Kumaran, M. S., et al. (2020). Rapid Detection of Terbinafine Resistance in *Trichophyton* Species by Amplified Refractory Mutation System Polymerase Chain Reaction. *Sci. Rep.* 10, 1297. doi: 10.1038/s41598-020-58187-0

Shaw, D., Singh, S., Dogra, S., Jayaraman, J., Bhat, R., Panda, S., et al. (2020). MIC and Upper Limit of Wild-Type Distribution for 13 Antifungal Agents Against a *Trichophyton mentagrophytes- Trichophyton interdigitale* Complex of Indian Origin. *Antimicrob. Agents Chemother.* 64 (4), e01964–e01919. doi: 10.1128/AAC.01964-19

Singh, A., Masih, A., Khurana, A., Singh, P., Gupta, M., Hagen, F., et al. (2018). High Terbinafine Resistance in *Trichophyton interdigitale* Isolates in Delhi, India Harbouring Mutations in the *Squalene Epoxidase* (*SQLE*) Gene. *Mycoses* 61 (7), 477–484. doi: 10.1111/myc.12772

Siopi, M., Efstathiou, I., Theodoropoulos, K., Pournaras, S., and Meletiadis, J. (2021). Molecular Epidemiology and Antifungal Susceptibility of *Trichophyton* Isolates in Greece: Emergence of Terbinafine-Resistant *Trichophyton mentagrophytes* Type VIII Locally and Globally. *J. Fungi* 7 (6), 419. doi: 10.3390/jof7060419

Stamatakis, A. (2014). RAxML Version 8: A Tool for Phylogenetic Analysis and Post-Analysis of Large Phylogenies. *Bioinformatics* 3, 1312–1313. doi: 10.1093/bioinformatics/btu033

Taghipour, S., Pchelin, I. M., Mahmoudabadi, A. Z., Ansari, S., Katiraee, F., Rafiei, A., et al. (2019). *Trichophyton mentagrophytes* and *T. interdigitale* Genotypes Are Associated With Particular Geographic Areas and Clinical Manifestations. *Mycoses* 62 (11), 1084–1091. doi: 10.1111/myc.12993

Wayne, P. A. (2008). "CLSI Reference Method for Broth Dilution Antifungal Susceptibility Testing of Filamentous Fungi. Approved Standard", in *CLSI Document M38–A2*, *2nd ed* (Wayne PA 19087 USA:Clinical and Laboratory Standards Institute).

White, T. J., Bruns, T., Lee, S., and Taylor, J. (1990). Amplification and Direct Sequencing of Fungal Ribosomal RNA Genes for Phylogenetics. PCR protocols: a guide to methods and applications. In: *PCR Protocols*, pp. 315–22. New York: Academic Press, Inc., Harcourt Brace Jovanovich Publishers. doi: 10.1016/B978-0-12-372180-8.50042-1

Yamada, T., Maeda, M., Alshahni, M., Tanaka, R., Yaguchi, T., Bontems, O., et al. (2017). Terbinafine Resistance of *Trichophyton* Clinical Isolates Caused by Specific Point Mutations in the Squalene Epoxidase Gene. *Antimicrob. Agents Chemother.* 61 (7), e00115–e00117. doi: 10.1128/AAC.00115-17

Yurkov, A., Krüger, D., Begerow, D., et al. (2012). Basidiomycetous Yeasts From Boletales Fruiting Bodies and Their Interactions With the Mycoparasite *Sepedonium chrysospermum* and the Host Fungus *Paxillus*. *Microb. Ecol.* 63 (2), 295–303. doi: 10.1007/s00248-011-9923-7

Zareshahrabadi, Z., Totonchi, A., Rezaei-Matehkolaei, A., Ilkit, M., Ghahartars, M., Arastehfar, A., et al. (2020). Molecular Identification and Antifungal Susceptibility Among Clinical Isolates of Dermatophytes in Shiraz, Iran (2017-2019). *Mycoses* 64 (4), 385–393. doi: 10.1111/myc.13226

Conflict of Interest: The authors declare that the research was conducted in the absence of any commercial or financial relationships that could be construed as a potential conflict of interest.

Publisher's Note: All claims expressed in this article are solely those of the authors and do not necessarily represent those of their affiliated organizations, or those of the publisher, the editors and the reviewers. Any product that may be evaluated in this article, or claim that may be made by its manufacturer, is not guaranteed or endorsed by the publisher.

frontiers | Frontiers in Immunology

CASE REPORT
published: 26 April 2022
doi: 10.3389/fimmu.2022.881352

Case Report: Invasive Cryptococcosis in French Guiana: Immune and Genetic Investigation in Six Non-HIV Patients

Jeanne Goupil de Bouillé[1,2*], *Loïc Epelboin*[3,4], *Fanny Henaff*[3], *Mélanie Migaud*[5], *Philippe Abboud*[3], *Denis Blanchet*[3,4], *Christine Aznar*[3,4], *Felix Djossou*[3,4], *Olivier Lortholary*[6], *Narcisse Elenga*[3,4], *Anne Puel*[5,6,7], *Fanny Lanternier*[5,6,8] *and Magalie Demar*[3,4]

[1] Avicenne Hospital, Assistance Publique des Hôpitaux de Paris, Bobigny, France, [2] Laboratoire Éducation et Pratique de Santé, University of Sorbonne Paris Nord, Bobigny, France, [3] Cayenne Hospital, Cayenne, French Guiana, [4] University of French Guiana, Cayenne, French Guiana, [5] Imagine Institute, Paris Cité University, Paris, France, [6] Laboratory of Human Genetics of Infectious Diseases, Necker Branch, Institut national de la santé et de la recherche médicale U1163, Necker Hospital, Assitance Publique des hôpitaux de Paris (APHP), Paris, France, [7] St. Giles Laboratory of Human Genetics of Infectious Diseases, Rockefeller University, New York, NY, United States, [8] Unité Mixte de Recherche 2000, Pasteur Institute Paris, University of Paris, Paris, France

OPEN ACCESS

Edited by:
Sergio Rosenzweig, National Institutes of Health (NIH), United States

Reviewed by:
Alexandra Freeman, National Institutes of Health (NIH), United States
Som G. Nanjappa, University of Illinois at Urbana-Champaign, United States

***Correspondence:**
Jeanne Goupil de Bouillé
jeanne.goupildebouille@aphp.fr

Specialty section:
This article was submitted to Microbial Immunology, a section of the journal Frontiers in Immunology

Received: 22 February 2022
Accepted: 28 March 2022
Published: 26 April 2022

Citation:
Goupil de Bouillé JG, Epelboin L, Henaff F, Migaud M, Abboud P, Blanchet D, Aznar C, Djossou F, Lortholary O, Elenga N, Puel A, Lanternier F and Demar M (2022) Case Report: Invasive Cryptococcosis in French Guiana: Immune and Genetic Investigation in Six Non-HIV Patients. Front. Immunol. 13:881352. doi: 10.3389/fimmu.2022.881352

Objectives: We describe the clinical, mycological, immunological, and genetic characteristics of six HIV-negative patients presenting with invasive cryptococcosis.

Methods: Patients with cryptococcosis without any of the classical risk factors, such as HIV infection, followed at Cayenne Hospital, were prospectively included. An immunologic and genetic assessment was performed.

Results: Five male patients and one female patient, 5 adults and one child, were investigated. All presented a neuromeningeal localization. *Cryptococcus neoformans* var. *gattii* and *C. neoformans* var. *grubii* were isolated in two and three patients, respectively, whereas one patient could not be investigated. Overall, we did not observe any global leukocyte defect. Two patients were found with high levels of circulating autoantibodies against Granulocyte macrophage-colony stimulating factor (GM-CSF), and none had detectable levels of autoantibodies against Interferon gamma (IFN-γ) Sequencing of *STAT1* exons and flanking regions performed for four patients was wild type.

Conclusion: To better understand cryptococcosis in patients with cryptococcosis but otherwise healthy, further explorations are needed with repeated immune checkups and strain virulence studies.

Keywords: cryptococcosis, immunocompetent, STAT1 gene, autoantibodies against GM-CSF, antibodies against IFN-γ, fungal infection

HIGHLIGHTS

- Invasive cryptococcosis in otherwise healthy individuals is rare.
- This study presents the clinical manifestations and the immune and genetic explorations performed in six of such patients.

INTRODUCTION

Cryptococcosis is a life-threatening fungal infection of immunosuppressed patients, well described in HIV-infected patients. More rarely, it occurs in patients without any of the known classical risk factors. The mechanism of the infection of these patients remains unclear, and we could hypothesize that otherwise healthy individuals with cryptococcosis carry a rare inborn error of immunity affecting specifically their immune response to *Cryptococcus* spp. The particular virulence of certain strains of *Cryptococcus* could also be involved.

The current classification based on its capsule immunologic and molecular analysis reports three varieties, five serotypes, and eight molecular types (1). *Cryptococcus neoformans* var. *grubii* has a worldwide distribution and is mainly responsible for cryptococcosis in patients with acquired immunosuppression (e.g., AIDS), whereas *Cryptococcus gattii*, mainly found in tropical and subtropical areas, usually strikes otherwise healthy individuals (2–4). In addition, anti-GM-CSF antibodies (5, 6) and primary immune deficiencies have been previously associated with crypotococcosis [STAT1 Gain of Function (GOF) (7, 8), STAT3 deficiency (9, 10), CD40 ligand deficiency (11)].

Few cases of cryptococcosis have been reported in French Guiana, a French overseas territory located on the northeastern coast of South America, supposedly in patients who were otherwise healthy. In the current study, we assessed the clinical, epidemiological, mycological, immunological, and genetic characteristics of patients from French Guiana with invasive cryptococcosis without known underlying causes. A better understanding of these features should help for an earlier and better diagnosis, preventing complicated forms of cryptococcal infections, and should bring new insights into the pathogenesis of the disease.

MATERIALS AND METHODS

Study Site

The study was performed at the Cayenne Hospital in French Guiana, a French overseas territory of 250,000 inhabitants, located between Brazil and Suriname in the Amazonian region.

Study Design

A prospective analysis was carried out on all consecutive non-HIV patients who were admitted to the Cayenne Hospital from 2011 to 2018 and diagnosed with cryptococcosis.

Case Definition

In accordance with the European Organisation for Research and Treatement of Cancer (ORTC) criteria for invasive fungal infections (12), invasive cryptococcosis was defined by at least one of the following criteria:

i) Histopathologic, cytopathologic, or direct microscopic examination of *Cryptococcus* obtained by needle aspiration or biopsy from a normally sterile site showing yeast cells.

ii) Recovery of a yeast by culture of a sample obtained by a sterile procedure from a normally sterile site showing a clinical or radiological abnormality consistent with an infectious disease process.

iii) Blood culture that yields yeast and cryptococcal antigen in cerebrospinal fluid (CSF).

iv) Amplification of cryptococcal DNA by PCR combined with DNA sequencing.

Immune Investigation

After inclusion, the patients were evaluated for their immune profile, including the following: i) lymphocyte immunophenotyping, immunoglobulin (IgG, IgA, IgM) levels, complement (CH50, C3, C4) levels, autoimmunity investigation by evaluating the presence of antinuclear antibodies (ANAs), anti-cardiolipin antibodies (ACAs), anti-β2-glycoprotein I antibodies, lupus anticoagulant; ii) the Interleukin (IL)-12/IFN-γ axis exploration, the presence of autoantibodies (auto-Abs) against GM-CSF and IFN-γ; iii) *STAT1* exons and flanking intronic regions were sequenced in four patients.

Data Collection

Data were collected from patient medical records: i) general demographic data; ii) laboratory data including biochemistry, hematology, immunology, and microbiology; iii) radiology variables and additional investigations depending on the findings; iv) the clinical and therapeutic management; v) the outcome of the patients.

All patients and/or relatives gave informed written consents.

The study received the agreement of the Committee of Protection of the Persons of the University Paris II on September 6, 2010 and of the AFFSAPS under the number B100712-40.

RESULTS

Description of Cases

During the study period, six patients were included. Clinical, epidemiological, and fungal characteristics are reported in **Table 1**. Most were male patients (5/6), with a median (minimum–maximum) age of 23.5 years (4–55 years) at the time of inclusion in the study. They were from various origins; one Creole Haitian male patient, one Creole French Guianese male patient, one Hmong male patient (refugee people from Vietnam war), two Brazilian citizens, and an Amerindian male patient. None of the patients had significant past medical history (cf **Table 1**).

TABLE 1 | Clinical, epidemiological, fungal characteristics of the 6 *Cryptococcosis* cases.

	Case 1	Case 2	Case 3	Case 4	Case 5	Case 6	MedianIQR
Age (years)	17	15	37	30	55	4	23.5 (15.5–35.2)
Sex	Male	Male	Male	Female	Male	Male	
Biotope of the usual residency	Urban	Semi-natural forest	Urban	Urban	Rural	Primary forest	
Cultural group	Haitian	Hmong	French Guianese Creole	Brazilian	Brazilian	Amerindian	
Medical history	None	None	Meningitis Steatosis Hypothyroiditis Polyglobulia	Thyroid nodules	None	Asthma	
Time to diagnosis since the onset of the symptoms (days)	89	16	57	11	3	30	23 (12.2–50.2)
Location of infection	Meningo encephalitis Pulmonary nodule Skin	Meningoencephalitis Hematologic	Meningitis	Meningoencephalitis Cerebral nodules Pulmonary infection	Meningoencephalitis	Meningoencephalitis Pulmonary Nodules	
Symptoms	Headache Neck pain Fever	Headache Quadriplegia Blindness Bilateral Hypoacusis Intracranious hypertension	Headaches Vomiting Intracranial hypertension Homonymous hemianopsia	Pulmonary infection Meningitis Intracranious hypertension Blindness Diplopia Scotomas	Fever Headaches Vomiting Intracranious hypertension Confusion Motor deficit Upper right limb Left ptosis	Loss of weigh Cough, Headache, Vomiting, Intracranious hypertension hydrocephalus	
Sequelae	None	Blindness Hearing loss Psychomotor retardation	Persistent headaches	Blindness Loss of the sense of smell	Ideomotor slowdown	None	
Lumbar punction pressure	Not done	85 mmHg	Not done	25 mmHg	110 mmHg	49 mmHg	67 mmHg (43–91))
Brain MRI Abnormalities	Nodular lesions (temporal, frontal, parieto-occipital), Peripheral ring signal Enhancement and Perilesional edema	Periventricular bilateral FLAIR hypersignal	Hyperintensities in the brain's white matter (supratentorial, cerebellar), ventricular dilatation	Multiple diffuse nodular brain lesions, Perilesional edema	Pachymeningitis Diffuse high-intensity signal	Periventricular hyperintensity, tetra ventricular dilatation	
Chest CT abnormalities	Pulmonary nodules of right basal pyramid excavated	None	None	Nodules	None	Pulmonary intraparenchymal cystic formations Parenchymal condensation Excavated nodules	
CSF Leukocytes (/mm3) and lymphocyte count (%)	74 92%	180 99%	130 100%	135 70%	236 60%	10 Not realized	132.5 (88–168.7) 92 (70–99)
CSF sugar (mmol/l) Blood sugar (mmol/l) CSF proteins (g/l)	2,2 5,8 1,5	2.1 4.3 0.6	0.2 3.9 1.5	3,3 3.3 6.5	1.9 6.5 6.1	1.7 4.5 0.5	2.0 (1.7–2.2) 4.4 (4–5.5) 1.5 (0.8–4.9)
CSF Antigen titer	1:10	1:100	1:120	1:10	1:100	Not done	
CSF culture and identification	*C. gattii*	*C. neoformans* var. *grubii*	*C. neoformans* var. *grubii*	*Cryptococcus* sp.	*C. neoformans* var. *grubii*	*C. gattii*	3 *C. neoformans* var. grubii *2 C. gattii* 1 *Cryptococcus* Sp.

(Continued)

TABLE 1 | Continued

	Case 1	Case 2	Case 3	Case 4	Case 5	Case 6	Median|IQR
Blood antigen titer at diagnosis	1:20	1:100	1:100	1:10	1:1000	1:640	
Induction treatment	Amphotericin B + Flucytosine 31 days	Amphothericin B + Flucytosine 31 days	Amphotericin B + Flucytosine 15 days	Amphotericin B + Flucytosine Duration not known	Amphotericin B + Flucytosine 15 days	Amphotericin B + Flucytosine 15 days	
Neurosurgery management	No	Yes	No	No	No	Yes	
Corticotherapy	Yes	Yes	No	No	No	Yes	
Consolidation treatment	Fluconazole 800 mg/day	Fluconazole 800 mg/day + Flucytosine	Fluconazole 800 mg/day	Fluconazole 800 mg/day	Fluconazole 400 mg/day	Fluconazole 12 mg/kg/day	

MRI, magnetic resonance imaging; CT, computed tomography; CSF, cerebrospinal fluid; sp., species; IQR, Interquartile range; CRP, C reactive protein; NK, Natural Killer; BCG, Bacillus Calmette Guerin; IDSA, Infectious Diseases Society America..

All patients had neurological involvement, mostly meningoencephalitis. One patient was reported with brain cryptococcoma. Another patient suffered from an isolated meningitis without encephalitis. The neurological presentation manifested either as an uncomplicated symptom type (headache or neck stiffness) or in a more severe form as motor deficit, confusion. One patient had vigilance disorders requiring intensive care monitoring. Clinical signs of intracranial hypertension were present for all patients except one. Ophthalmologic disorders such as blindness or diplopia were found in four patients. The median (IQR) CSF opening pressure was 67 mmHg (43–91 mmHg). Median cellularity of CSF was 132.5 (88.0–168.7) leukocytes/mm^3 with lymphocytic predominance. Five patients presented abnormalities on their brain imaging (MRI and/or CT scan) when included (**Figure 1**). Three cases presented, in addition, pulmonary involvement with nodules (**Figure 2**). Pulmonary symptomatology was often absent, and the lesions were revealed during complimentary tests. Only one patient had a cough.

All patients received induction therapy with amphotericin and flucytosine, 3 received corticosteroid therapy, and 2 had neurosurgical management. Consolidation therapy always included fluconazole. One of the patients also had flucytosine.

Neurological sequelae were common (four out of six patients) ranging from chronic headaches to blindness and deafness.

The serotyping led to the identification of three *C. neoformans* var. *grubii* and two *C. gattii.* The identification of *Cryptococcus* serotype could not be specified for one patient. The time to diagnosis was longer for *C. gattii* vs. *C. grubii* serotypes. One microbiological sampling was performed to isolate *Cryptococcus* in the lung (case 1) and was positive. Pulmonary lesions were found only *for C. gattii* species.

Immune Exploration

Immune explorations of the cases are reported in **Table 2**. None of the patients presented any remarkable increase of inflammatory markers in their serum with a median (IQR) CRP of 5.8 mg/L (2.7–9.4 mg/L). All patients were HIV and HTLV1 seronegative, and none received any immunosuppressive therapy. Immunoglobulin levels were normal in all patients. All patients had normal global lymphocyte immunophenotyping, except case 2, who showed a transient low NK cell count at the time of infection, which was fully restored a few months after the acute episode.

Anti-nuclear factors were found in only one patient, with titers in the upper limit of normal values (1/80). Circulating anticoagulants were found to be transiently positive in one patient but became negative on a second test. Two patients had anti-cardiolipin antibodies. Complement (C4, CH50, C3) levels were consistently normal. Whole blood activation from four patients with BCG without or with IL-12 or IFN-γ showed normal production of IFN-γ or IL-12, respectively, suggesting a normal IL-12/IFN-γ axis. Two out of five patients tested showed high titers of neutralizing auto-Abs against GM-CSF. All *STAT1* exons were sequenced for four patients and were found to be wild type.

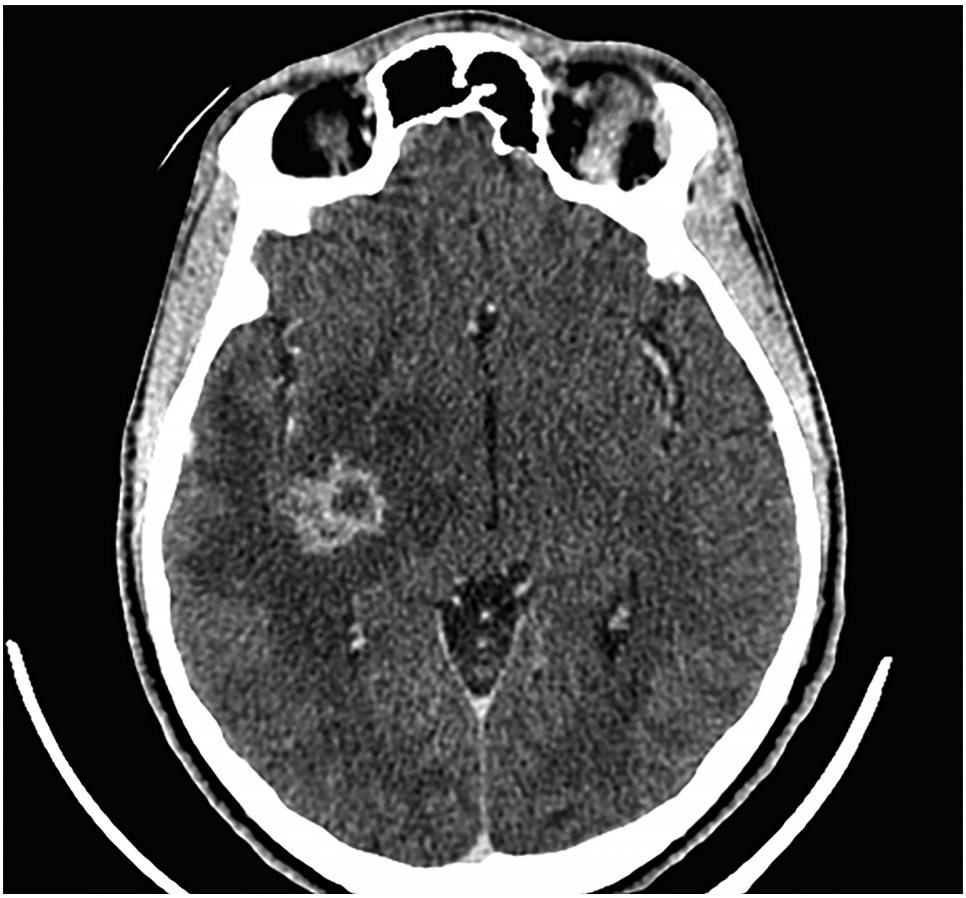

FIGURE 1 | Brain Computed Tomography-scan with nodular, right insular lesion with cocoon enhancement and peri-lesional edema.

DISCUSSION

Cryptococcosis is a well-known fungal infection in French Guiana. A retrospective study, conducted between 1998 and 2008, identified 43 patients with cryptococcosis admitted to hospitals in French Guiana (13). Fourteen cases (32.6%) were not infected with HIV, and of these 14 patients, only 2 (4.7%) had another detected cause of immunosuppression (corticotherapy alone or associated with diabetes mellitus). Whereas the sex ratio (M/F) was equal to 1 in the HIV-negative group, M/F ratio was 2.63 among the 29 HIV-positive patients. Patients of the HIV-negative group were older (51.6 ± 23.9) than those of the HIV-positive group (41.8 ± 12.5). The average incidence of cryptococcosis was estimated at 22.6 cases/million inhabitants/year during the period 1998–2008, about 10 times higher than in metropolitan France (14).

The clinical presentations of our patients were similar to those of cases reported in the literature. Unlike patients with immunodeficiency, cerebral and pulmonary forms are predominant in patients with cryptococcosis but otherwise healthy (13, 15–18). They frequently present as indolent forms of meningitis, and visual symptoms are the most frequent manifestations (13). In rare cases, the neurologic symptomatology can be very noisy and be associated with high and recurrent neurological morbidities, including shunt requirements, serial lumbar punctures, and pressure-related complications (19). The mean time at diagnosis is significantly longer. CSF white blood cell counts are usually higher, and meningeal enhancement on CT scan of the brain is more frequently observed (16, 19). Cryptococcaemia and other extraneural, extrapulmonary (digestive, ganglionic, oropharyngeal, dermatologic, hematologic, or bone) manifestations are much more associated with immunodeficiency and poorer prognosis (18, 20–23).

In this study, we identified three patients with *C. neoformans* var. *grubii* and two patients with *C. gattii*. A French Guianese study showed an epidemiology for *Cryptococcus* composed mainly with A (77.3%) and B (22.7%); no types C and D were revealed. This differs from a study performed in France, especially for types B and D showing respectively 1.8% and 22.9%. *C. neoformans* var. *gattii* usually invades more frequently the brain and pulmonary parenchyma and causes multiple granuloma (24–26). Cryptococcomas can appear in any region of the lung and can have different sizes. Visual alterations are also more frequent in *C. gattii* (27).

We found anti-GM-CSF auto-Abs in two patients, as previously reported in otherwise healthy patients with cryptococcal meningitis

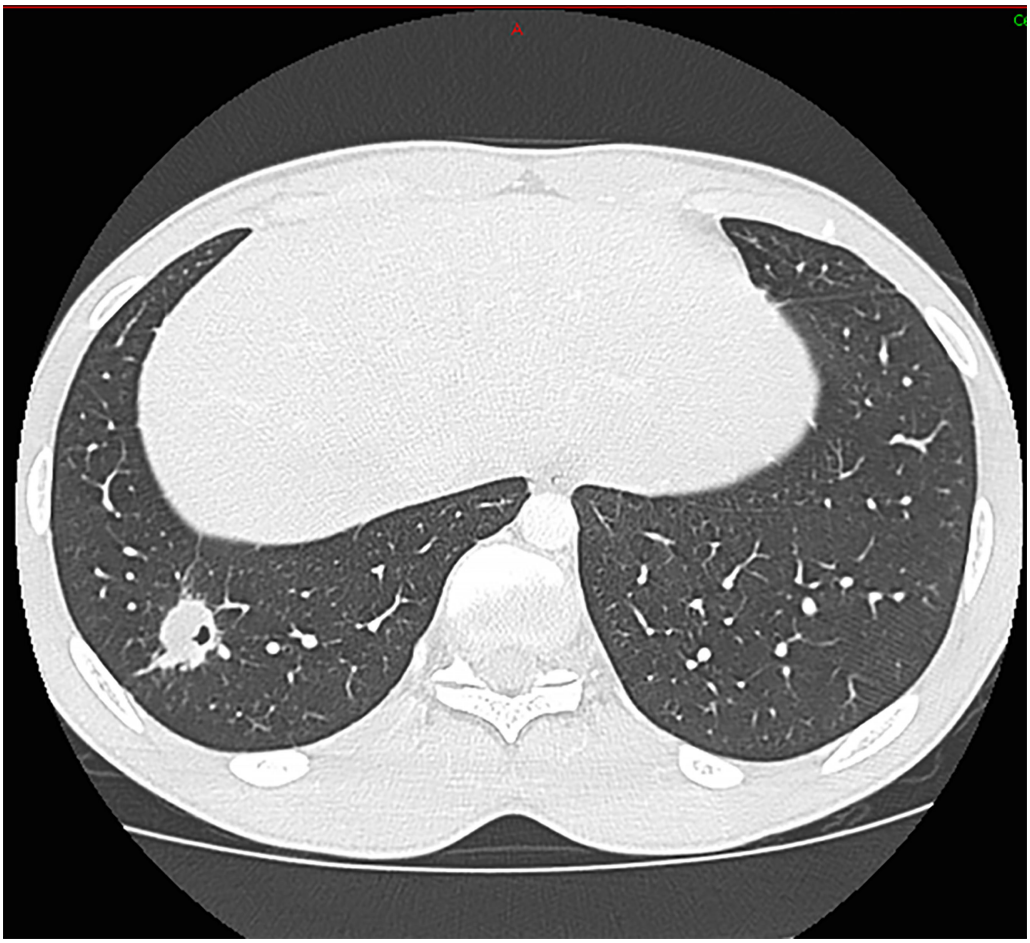

FIGURE 2 | Pulmonary Computed Tomography–scan with pulmonary nodule of the right basad pyramid excavated.

caused by *C. gattii* (5, 6). One of the patients was infected with *C. gattii*, whereas we could not test the strain in the other one. These auto-Abs were neutralizing, as shown *in vitro*, with an abolished STAT5 phosphorylation upon GM-CSF stimulation of control peripheral blood mononuclear cells (PBMCs) in the presence of 10% of patients' plasma, but not in the presence of 10% of healthy individuals' plasma, probably inhibiting macrophage function *in vivo*. We also tested for the presence of anti-IFN-γ auto-Abs, as some patients with cryptococcosis were also reported with such auto-Abs (28–30); none of the 6 patients tested displayed anti-IFN-γ auto-Abs.

In addition, few inborn errors of immunity have been associated with increased susceptibility to cryptococcosis [CD4

TABLE 2 | Immune exploration of the *Cryptococcosis* cases.

	Case 1	Case 2	Case 3	Case 4	Case 5	Case 6
HTLV1 serology	Negative	Negative	Negative	Negative	Negative	Negative
Lymphocyte immunophenotyping (CD4/CD8/B/NK)	Normal	NK lymphopenia Re-controlled Normal	Normal	Normal	Normal	Normal
Immunoglobulin (g/g/L)	Normal	Normal	Normal	Normal	Normal	Normal
Study of IL12/Interferon gamma production (in comparison with a healthy individual)	Normal	Normal	Normal	Not done	Not done	Normal
Anti-GM-CSF antibodies	Positive with positive neutralizing activity	Negative	Negative	Positive with positive neutralizing activity	Not done	Negative
Anti-IFN γ antibodies	Negative	Negative	Negative	Not done	Not done	Negative
STAT1 gene	Not done	Wild type	Wild type	Wild type	Not done	Wild type

***Author Bio**: Dr. Jeanne Goupil is an infectious disease specialist. She is currently practicing in the suburbs of Paris. Her research interests include tropical diseases, HIV, and public health.*

lymphopenia (31), X-linked CD40L deficiency (11), STAT3 mutated hyper-IgE syndrome (9, 10)]. Among them, some patients carrying heterozygous STAT1 GOF mutations (7, 8) were found with cryptococcosis (32). However, none of the four patients tested in our cohort carried any rare variants of *STAT1*. In our studies, no ethnic group was overrepresented such as aborigines in Australia (33) suggesting that genetic factors may be important.

Some limitations should be considered in this study. Due to logistical difficulties in delivering immunoassay and lost to follow-up, the study has missing data. Genetic studies have only screened rare variants of *STAT1*. A particular virulence of the strain could be evoked (24, 34, 35). Unfortunately, this parameter could not be studied in this study.

Our study highlights the difficulty of determining the causal agent of cryptococcosis in patients. It thus opens up different avenues for consideration. The immune status of the host and a particular virulence of the *Cryptococcus* strain are the two main hypotheses.

The immune status of the host is a key issue, since, as notified in IDSA Guidelines (25), treatment depends on it. A comprehensive immune and genetic exploration, in our opinion, is the first step in answering the various questions. To our knowledge, the present study is the first that proposes a standardized and detailed immunological assessment for so-called "immunocompetent" patients suffering from cryptococcal disease (**Figure 3**). It seems unclear whether these patients have phenotypic or genetic deficits. Genetic analyses are not easy to carry out routinely but must be integrated into research programs. It could also be assumed that cryptococcosis is the cause of immunosuppression. In case 2, a dosage of lymphocyte NK was abnormal during the infection. A control was performed a few months later with normal proportion of lymphocyte NK. This suggests that *Cryptococcus* infection can suppress the immune system, and its elimination contributes to the reestablishment of an immune equilibrium. French Guiana is known for its specificities in terms of tropical infections, and we could evoke the virulence of a specific strain in our patients. Further *in vivo* investigation is essential to understand the basic mechanism of virulence of *C. gattii* and *C. grubii* especially in tropical areas where epidemiology is different from the other areas (36–40).

CONCLUSION

This study describes the clinical, biological, immunological, and genetic characteristics of six non-HIV patients in French Guiana suffering from cryptococcosis. Clinical presentations can be devious, and they highlight the particularities of this infection according to the *gattii* or *grubii* serotype. Cryptococcosis is a potentially emerging disease. Two out of the six patients tested had high titers of neutralizing auto-Abs against GM-CSF, and this consequent percentage deserves further studies on these antibodies. None of the four patients tested carry rare variants of *STAT1*, the only candidate gene tested yet. Studying patients with cryptococcosis but otherwise healthy should help to progressively

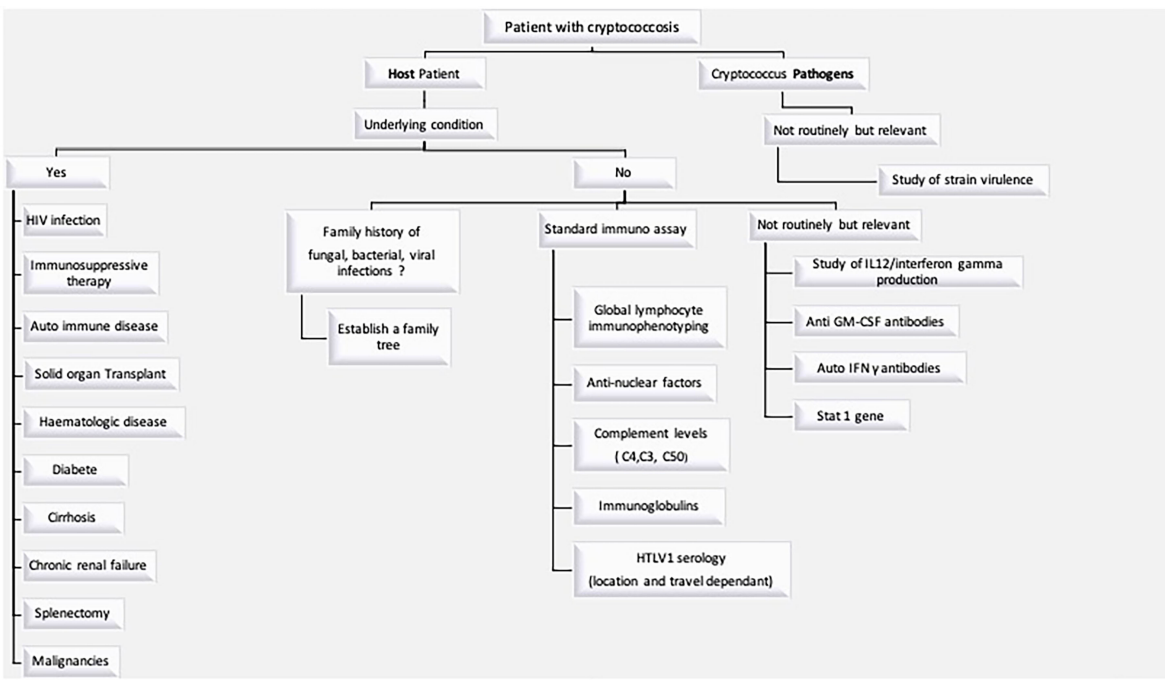

FIGURE 3 | Investigation to be performed in a patient with cryptococcosis.

decipher the crucial physiopathological mechanisms underlying this disease.

DATA AVAILABILITY STATEMENT

The original contributions presented in the study are included in the article/supplementary material. Further inquiries can be directed to the corresponding author.

ETHICS STATEMENT

The studies involving human participants were reviewed and approved by the Committee of Protection of the Persons of the University Paris II on 2010-06-09 and of the AFFSAPS under the number B100712-40. Written informed consent to participate in this study was provided by the participants' legal guardian/next of kin.

AUTHOR CONTRIBUTIONS

Conceptualization: JGdB and MD. Formal analysis: JGdB. Investigation: JGdB, LE, FH, MM, FL, PA, DB, AP, CA, and OL. Methodology: JGdB and MD. Supervision: MD. Writing—original draft: JGdB. Writing—review and editing: JGdB, LE, FH, MM, PA, DB, CA, FD, NE, AP, FL, and MD. All authors have read and approved the final article.

FUNDING

The work was funded by the French National Research Agency (ANR) under the "Investments for the future" program (ANR-10-IAHU-01), the ANR-FNS LTh-MSMD-CMCD (ANR-18-CE93-0008-01), the Integrative Biology of Emerging Infectious Diseases Laboratory of Excellence (ANR-10-LABX-62-IBEID), and the National Institute of Allergy and Infectious Diseases of the NIH (grant no. R01AI127564).

REFERENCES

1. Desnos-Ollivier M, Patel S, Raoux-Barbot D, Heitman J, Dromer F. Cryptococcosis Serotypes Impact Outcome and Provide Evidence of Cryptococcus Neoformans Speciation. *mBio* (2015) 6(3):4. doi: 10.1128/mBio.00311-15
2. De Vroey C, Gatti F. Cryptococcus Neoformans Var. Gattii Vanbreuseghem and Takashio, 1970. *Mycoses* (1989) 32(12):675. doi: 10.1111/j.1439-0507.1989.tb02200.x
3. Dixit A, Carroll SF, Qureshi ST. Cryptococcus Gattii: An Emerging Cause of Fungal Disease in North America. *Interdiscip Perspect Infect Dis* (2009) 2009:840452. doi: 10.1155/2009/840452
4. Sorrell TC. Cryptococcus Neoformans Variety Gattii. *Med Mycol* (2001) 39 (2):155–68. doi: 10.1080/714031012
5. Rosen LB, Freeman AF, Yang LM, Jutivorakool K, Olivier KN, Angkasekwinai N, et al. Anti-GM-CSF Autoantibodies in Patients With Cryptococcal Meningitis. *J Immunol Baltim Md 1950* (2013) 190(8):3959–66. doi: 10.4049/jimmunol.1202526
6. Saijo T, Chen J, Chen SC-A, Rosen LB, Yi J, Sorrell TC, et al. Anti-Granulocyte-Macrophage Colony-Stimulating Factor Autoantibodies Are a Risk Factor for Central Nervous System Infection by Cryptococcus Gattii in Otherwise Immunocompetent Patients. *mBio* (2014) 5(2):e00912–00914. doi: 10.1128/mBio.00912-14
7. Leopold Wager CM, Hole CR, Wozniak KL, Olszewski MA, Mueller M, Wormley FL. STAT1 Signaling Within Macrophages Is Required for Antifungal Activity Against Cryptococcus Neoformans. *Infect Immun* (2015) 83(12):4513–27. doi: 10.1128/IAI.00935-15
8. Zhang W, Chen X, Gao G, Xing S, Zhou L, Tang X, et al. Clinical Relevance of Gain- and Loss-Of-Function Germline Mutations in STAT1: A Systematic Review. *Front Immunol 11 mars* (2021) 12. doi: 10.3389/fimmu.2021.654406
9. Chandesris M-O, Melki I, Natividad A, Puel A, Fieschi C, Yun L, et al. Autosomal Dominant STAT3 Deficiency and Hyper-IgE Syndrome: Molecular, Cellular, and Clinical Features From a French National Survey. *Med (Baltimore)* (2012) 91(4):e1–19. doi: 10.1097/MD.0b013e31825f95b9
10. Odio CD, Milligan KL, McGowan K, Rudman Spergel AK, Bishop R, Boris L, et al. Endemic Mycoses in Patients With STAT3 Mutated Hyperimmunoglobulin E (Job's) Syndrome. *J Allergy Clin Immunol* (2015) 136(5):1411–3.e2. doi: 10.1016/j.jaci.2015.07.003
11. Winkelstein JA, Marino MC, Ochs H, Fuleihan R, Scholl PR, Geha R, et al. The X-Linked Hyper-IgM Syndrome: Clinical and Immunologic Features of 79 Patients. *Med (Baltimore)* (2003) 82(6):373–84. doi: 10.1097/01.md.0000100046.06009.b0
12. Donnelly JP, Chen SC, Kauffman CA, Steinbach WJ, Baddley JW, Verweij PE, et al. Revision and Update of the Consensus Definitions of Invasive Fungal Disease From the European Organization for Research and Treatment of Cancer and the Mycoses Study Group Education and Research Consortium. *Clin Infect Dis Off Publ Infect Dis Soc Am* (2020) 71(6):1367–76. doi: 10.1093/cid/ciz1008
13. Debourgogne A, Iriart X, Blanchet D, Veron V, Boukhari R, Nacher M, et al. Characteristics and Specificities of Cryptococcus Infections in French Guiana, 1998-2008. *Med Mycol* (2011) 49(8):864–71. doi: 10.3109/13693786.2011.584198
14. Gangneux JP. *An Estimation of Burden of Serious Fungal Infections in France*. NCBI (2016). Available at: https://www-ncbi-nlm-nih-gov.gate2.inist.fr/pubmed/?term=An+estimation+of+burden+of+serious+fungal+infections+in+France.
15. Dromer F, Mathoulin-Pélissier S, Launay O, Lortholary O. French Cryptococcosis Study Group. Determinants of Disease Presentation and Outcome During Cryptococcosis: The CryptoA/D Study. *PloS Med* (2007) 4 (2):e21.
16. Pappas PG. Cryptococcal Infections in Non-HIV-Infected Patients. *Trans Am Clin Climatol Assoc* (2013) 124:61–79. doi: 10.1371/journal.pmed.0040021
17. Jongwutiwes U, Sungkanuparph S, Kiertiburanakul S. Comparison of Clinical Features and Survival Between Cryptococcosis in Human Immunodeficiency Virus (HIV)-Positive and HIV-Negative Patients. *Jpn J Infect Dis* (2008) 61 (2):111–5.
18. Lui G, Lee N, Ip M, Choi KW, Tso YK, Lam E, et al. Cryptococcosis in Apparently Immunocompetent Patients. *QJM Mon J Assoc Phys* (2006) 99 (3):143–51. doi: 10.1093/qjmed/hcl014
19. Marr KA, Sun Y, Spec A, Lu N, Panackal A, Bennett J, et al. A Multicenter, Longitudinal Cohort Study of Cryptococcosis in HIV-Negative People in the United States. *Clin Infect Dis Off Publ Infect Dis Soc Am* (2019) 70(2):252–61. doi: 10.1093/cid/ciz193
20. Pappas PG, Perfect JR, Cloud GA, Larsen RA, Pankey GA, Lancaster DJ, et al. Cryptococcosis in Human Immunodeficiency Virus-Negative Patients in the Era of Effective Azole Therapy. *Clin Infect Dis Off Publ Infect Dis Soc Am* (2001) 33(5):690–9. doi: 10.1086/322597
21. Speed B, Dunt D. Clinical and Host Differences Between Infections With the Two Varieties of Cryptococcus Neoformans. *Clin Infect Dis* (1995) 21(1):28–34. doi: 10.1093/clinids/21.1.28
22. Hoang LMN, Maguire JA, Doyle P, Fyfe M, Roscoe DL. Cryptococcus Neoformans Infections at Vancouver Hospital and Health Sciences Centre (1997-2002): Epidemiology, Microbiology and Histopathology. *J Med Microbiol* (2004) 53(Pt 9):935–40. doi: 10.1099/jmm.0.05427-0

23. Jean S-S, Fang C-T, Shau W-Y, Chen Y-C, Chang S-C, Hsueh P-R, et al. Cryptococcaemia: Clinical Features and Prognostic Factors. *QJM Mon J Assoc Phys* (2002) 95(8):511–8. doi: 10.1093/qjmed/95.8.511
24. Chen SC-A, Meyer W, Sorrell TC. Cryptococcus Gattii Infections. *Clin Microbiol Rev* (2014) 27(4):980–1024. doi: 10.1128/CMR.00126-13
25. Perfect JR, Dismukes WE, Dromer F, Goldman DL, Graybill JR, Hamill RJ, et al. Clinical Practice Guidelines for the Management of Cryptococcal Disease: 2010 Update by the Infectious Diseases Society of America. *Clin Infect Dis Off Publ Infect Dis Soc Am* (2010) 50(3):291–322. doi: 10.1086/649858
26. Voelz K, May RC. Cryptococcal Interactions With the Host Immune System. *Eukaryot Cell* (2010) 9(6):835–46. doi: 10.1128/EC.00039-10
27. Zhu L-P, Wu J-Q, Xu B, Ou X-T, Zhang Q-Q, Weng X-H. Cryptococcal Meningitis in Non-HIV-Infected Patients in a Chinese Tertiary Care Hospital, 1997–2007. *Med Mycol* (2010) 48(4):570–9. doi: 10.3109/13693780903437876
28. Wongkulab P, Wipasa J, Chaiwarith R, Supparatpinyo K. Autoantibody to Interferon-Gamma Associated With Adult-Onset Immunodeficiency in Non-HIV Individuals in Northern Thailand. *PloS One* (2013) 8(9):1–6. doi: 10.1371/journal.pone.0076371
29. Rujirachun P, Sangwongwanich J, Chayakulkeeree M. Triple Infection With Cryptococcus, Varicella-Zoster Virus, and Mycobacterium Abscessus in a Patient With Anti-Interferon-Gamma Autoantibodies: A Case Report. *BMC Infect Dis* (2020) 20(1):232. doi: 10.1186/s12879-020-4949-4
30. Browne SK, Burbelo PD, Chetchotisakd P, Suputtamongkol Y, Kiertiburanakul S, Shaw PA, et al. Adult-Onset Immunodeficiency in Thailand and Taiwan. *N Engl J Med* (2012) 367(8):725–34. doi: 10.1056/NEJMoa1111160
31. Zonios DI, Falloon J, Huang C-Y, Chaitt D, Bennett JE. Cryptococcosis and Idiopathic CD4 Lymphocytopenia. *Med (Baltimore)* (2007) 86(2):78–92. doi: 10.1097/md.0b013e31803b52f5
32. Toubiana J, Okada S, Hiller J, Oleastro M, Lagos Gomez M, Aldave Becerra JC, et al. Heterozygous STAT1 Gain-of-Function Mutations Underlie an Unexpectedly Broad Clinical Phenotype. *Blood* (2016) 127(25):3154–64. doi: 10.1182/blood-2015-11-679902
33. Chen S, Sorrell T, Nimmo G, Speed B, Currie B, Ellis D, et al. Epidemiology and Host- and Variety-Dependent Characteristics of Infection Due to Cryptococcus Neoformans in Australia and New Zealand. Australasian Cryptococcal Study Group. *Clin Infect Dis Off Publ Infect Dis Soc Am* (2000) 31(2):499–508. doi: 10.1086/313992
34. Herkert PF, Hagen F, Pinheiro RL, Muro MD, Meis JF, Queiroz-Telles F. Ecoepidemiology of Cryptococcus Gattii in Developing Countries. *J Fungi* (2017) 3(4):62. doi: 10.3390/jof3040062
35. Favalessa OC, Lázera M dos S, Wanke B, Trilles L, Takahara DT, Tadano T, et al. Fatal Cryptococcus Gattii Genotype AFLP6/VGII Infection in a HIV-Negative Patient: Case Report and a Literature Review. *Mycoses* (2014) 57(10):639–43. doi: 10.1111/myc.12210
36. Escandón P, Lizarazo J, Agudelo CI, Castañeda E. Cryptococcosis in Colombia: Compilation and Analysis of Data From Laboratory-Based Surveillance. *J Fungi Basel Switz* (2018) 4(1):8. doi: 10.3390/jof4010032
37. Epelboin L, Nacher M, Mahamat A, Pommier de Santi V, Berlioz-Arthaud A, Eldin C, et al. Q Fever in French Guiana: Tip of the Iceberg or Epidemiological Exception? *PloS Negl Trop Dis* (2016) 10(5):e0004598. doi: 10.1371/journal.pntd.0004598
38. Mosnier E, Martin N, Razakandrainibe R, Dalle F, Roux G, Buteux A, et al. Cryptosporidiosis Outbreak in Immunocompetent Children From a Remote Area of French Guiana. *Am J Trop Med Hyg* (2018) 98(6):1727–32. doi: 10.4269/ajtmh.17-0609
39. Eldin C, Mahamat A, Demar M, Abboud P, Djossou F, Raoult D. Q Fever in French Guiana. *Am J Trop Med Hyg* (2014) 91(4):771–6. doi: 10.4269/ajtmh.14-0282
40. Blaizot R, Nabet C, Blanchet D, Martin E, Mercier A, Dardé M-L, et al. Pediatric Amazonian Toxoplasmosis Caused by Atypical Strains in French Guiana, 2002-2017. *Pediatr Infect Dis J* (2019) 38(3):e39–42. doi: 10.1097/INF.0000000000002130

Conflict of Interest: The authors declare that the research was conducted in the absence of any commercial or financial relationships that could be construed as a potential conflict of interest.

Publisher's Note: All claims expressed in this article are solely those of the authors and do not necessarily represent those of their affiliated organizations, or those of the publisher, the editors and the reviewers. Any product that may be evaluated in this article, or claim that may be made by its manufacturer, is not guaranteed or endorsed by the publisher.

frontiers | Frontiers in Immunology

ORIGINAL RESEARCH
published: 09 May 2022
doi: 10.3389/fimmu.2022.868523

Three Models of Vaccination Strategies Against Cryptococcosis in Immunocompromised Hosts Using Heat-Killed *Cryptococcus neoformans* Δ*sgl1*

Tyler G. Normile[1] *and Maurizio Del Poeta*[1,2,3*]

[1] Department of Microbiology and Immunology, Stony Brook University, Stony Brook, NY, United States, [2] Division of Infectious Diseases, School of Medicine, Stony Brook University, Stony Brook, NY, United States, [3] Veterans Administration Medical Center, Northport, NY, United States

OPEN ACCESS

Edited by:
Rajko Reljic,
St George's, University of London, United Kingdom

Reviewed by:
Amariliz Rivera,
Rutgers, The State University of New Jersey, United States
Carolina Coelho,
University of Exeter, United Kingdom

***Correspondence:**
Maurizio Del Poeta
maurizio.delpoeta@stonybrook.edu

Specialty section:
This article was submitted to Vaccines and Molecular Therapeutics, a section of the journal Frontiers in Immunology

Received: *02 February 2022*
Accepted: *11 April 2022*
Published: *09 May 2022*

Citation:
Normile TG and Del Poeta M (2022) Three Models of Vaccination Strategies Against Cryptococcosis in Immunocompromised Hosts Using Heat-Killed Cryptococcus neoformans Δsgl1. Front. Immunol. 13:868523. doi: 10.3389/fimmu.2022.868523

Vaccines are one of the greatest medical accomplishments to date, yet no fungal vaccines are currently available in humans mainly because opportunistic mycoses generally occur during immunodeficiencies necessary for vaccine protection. In previous studies, a live, attenuated *Cryptococcus neoformans* Δ*sgl1* mutant accumulating sterylglucosides was found to be avirulent and protected mice from a subsequent lethal infection even in absence of $CD4^+$ T cells, a condition most associated with cryptococcosis (e.g., HIV). Here, we tested three strategies of vaccination against cryptococcosis. First, in our preventative model, protection was achieved even after a 3-fold increase of the vaccination window. Second, because live *C. neoformans* Δ*sgl1*-vaccinated mice challenged more than once with WT strain had a significant decrease in lung fungal burden, we tested *C. neoformans* Δ*sgl1* as an immunotherapeutic. We found that therapeutic administrations of HK *C. neoformans* Δ*sgl1* post WT challenge significantly improves the lung fungal burden. Similarly, therapeutic administration of HK *C. neoformans* Δ*sgl1* post WT challenge resulted in 100% or 70% survival depending on the time of vaccine administration, suggesting that HK Δ*sgl1* is a robust immunotherapeutic option. Third, we investigated a novel model of vaccination in preventing reactivation from lung granuloma using *C. neoformans* Δ*gcs1*. Remarkably, we show that administration of HK Δ*sgl1* prevents mice from reactivating Δ*gcs1* upon inducing immunosuppression with corticosteroids or by depleting $CD4^+$ T cells. Our results suggest that HK Δ*sgl1* represents a clinically relevant, efficacious vaccine that confers robust host protection in three models of vaccination against cryptococcosis even during CD4-deficiency.

Keywords: *Cryptococcus neoformans*, cryptococcosis, sterylglucosides, heat-killed vaccine, reactivation, immunotherapeutics, granuloma, immunocompromised host

INTRODUCTION

Invasive fungal infections are primarily caused by environmental fungi that mainly infect immunocompromised individuals resulting in ~1.5 million deaths a year that account for ~50% of all AIDS-related deaths (1, 2). Individuals most at risk include HIV/AIDS patients (3–5), cancer patients receiving chemotherapy (6, 7), solid organ transplant recipients (8–10), or patients taking medication to control chronic diseases (11–14). Unlike most fungi that do not infect humans, the pathogenicity of invasive fungal species begins with the ability to grow and replicate at human body temperature (15, 16), which suggests that climate change, particularly global warming, may play a role in increasing infections from environmental fungi in more temperate climates (17–19). The incidence of invasive fungal infections is expected to further increase as the global immunocompromised population continues to rise due to novel immunosuppressive therapies or comorbidities, such as the current COVID-19 pandemic (20–25).

One of these fungal pathogens is *Cryptococcus neoformans*, a basidiomycetous yeast ubiquitously found in environmental sources such as avian habitation, trees, and soil (3, 5, 26). *C. neoformans* is a main etiological agent of cryptococcosis, a life-threatening invasive fungal infection that originates in the respiratory tract (27–29). Upon inhalation of the environmental fungal propagules, immunocompetent hosts often remain asymptomatic while they either clear the initial infection eliminating the yeast from the lungs or control fungal proliferation by enclosing the persistent yeast in lung granulomas where the fungal cells remain dormant (30–32). Conversely, immunocompromised individuals lacking a necessary component of the immune system, namely $CD4^+$ T cells as seen with HIV/AIDS, generally fail to control the initial infection or maintain the integrity of the lung granulomas containing latent cryptococcal cells leading to host pathology (11, 33). These individuals may experience uncontrolled fungal replication and dissemination of the fungus to the central nervous system potentially leading to life-threatening meningoencephalitis (9, 33) accounting for ~220,000 new cryptococcal cases and ~180,000 deaths a year (34, 35).

Vaccines are considered to be one of the greatest medical accomplishments to date (36). Although the high mortality rate upon extrapulmonary cryptococcosis in at-risk individuals can be partly attributed to the poor efficacy, host toxicity, and pathogen-acquired resistance of current antifungal therapeutics (37–39), the absence of fungal vaccines is a major constraint in overcoming invasive fungal infections in humans (40). While there has been ample research into the development of a vaccine against *C. neoformans* [reviewed in (41–43)], none have advanced past the pre-clinical research stage. The lack of vaccine advancement is chiefly due to the fact this pathogen infects mostly immunocompromised individuals with low $CD4^+$ T cell counts (3, 28), and the majority of current cryptococcal vaccine research lack host protective efficacy in this immunodeficiency. As such, vaccine formulations exhibiting high efficacy in animal models that resemble immunodeficiencies associated with cryptococcosis (e.g., lacking $CD4^+$ T cells) are in high demand (42, 44).

Exposure to *C. neoformans* may result in the yeast being cleared or safely contained within lung granulomas in immunocompetent hosts (31, 33). In addition to the necessity of vaccine studies being carried out in immunodeficient conditions, the literature currently contains only cryptococcal vaccines used in a prophylactic manner. However, there are no reports of vaccination strategies against the reactivation of dormant *C. neoformans* from lung granuloma breakdown due to immunosuppressive occurrences [reviewed in (44)]. This disparity is mainly attributed to the lack of tools to evaluate vaccines against infection by the reactivation of latent fungal cells in mouse models since mice do not form lung granulomas to wild-type (WT) *C. neoformans* and remains a major understudied bottleneck in the advancement of a clinically available anti-cryptococcal vaccine.

Our lab has previously engineered a mutant strain of *C. neoformans* (Δ*sgl1*) that accumulates large amounts of sterylglucosides (SGs) and provided the first evidence on the key role of sterylglucosidase 1 (Sgl1) on fungal virulence (45). SGs have been previously shown to possess immunological functions [reviewed in (46)]. The use of the plant SG, β-sitosterol, increased T cell proliferation and Th1 polarization (47, 48), significantly prolonged survival of mice infected with *Candida albicans* (49, 50), and promoted the recovery of patients with pulmonary tuberculosis in combination with regular anti-tuberculosis treatment (48). However, our work provided the first physio-pathological studies with fungal-derived SGs, and our recent structural studies will enable the rational design of new antifungal agents targeting Sgl1 (51).

Prior studies in our lab have shown that *C. neoformans* Δ*sgl1* induces a proinflammatory lung cytokine environment with robust effector cell recruitment to the lungs as well as confers complete host protection to lethal WT challenge under immunodeficiencies most associated with cryptococcosis (e.g., lacking $CD4^+$ T cells) (52). Interestingly, we found that protection required SGs in combination to the immunosuppressive glucuronoxylomannan (GXM)-based capsule since an acapsular mutant strain (Δ*cap59*Δ*sgl1*) was no longer protective (53) nor induce a protective cytokine response to *ex vivo* stimulated γδ T cells (T.G. Normile, T.H. Chu, B.S. Sheridan, and M. Del Poeta, submitted for publication), suggesting that SGs may act as an immunoadjuvant to GXM to induce host protection. Most recently, we uncovered the immune-mechanism of protection involved TLR2-mediated production of IFNγ and IL-17A by γδ T cells resulting in a robust $CD4^+$ or $CD8^+$ T cell response for complete host protection to subsequent WT infection (T.G. Normile, T.H. Chu, B.S. Sheridan, and M. Del Poeta, submitted for publication). Overall, these studies suggest that *C. neoformans* Δ*sgl1* represents a viable live, attenuated vaccine.

In the present study, we validate three different models of successful vaccination strategies against cryptococcosis using heat-killed (HK) *C. neoformans* Δ*sgl1* in condition of $CD4^+$ T cell deficiency. In the canonical prevention model of vaccination, we found that two subsequent administrations of HK *C. neoformans* Δ*sgl1* conferred complete host protection to a WT challenge even when $CD4^+$ T cells were depleted, mimicking the results obtained with the live, attenuated mutant. Host

protection in immunocompetent and CD4-deficient mice was still found after increasing the time of the vaccination window from 30 to 90 days or after challenging vaccinated mice 3 subsequent times, suggesting our vaccine strategy induces long term host immunity and protection against the WT strain. Interestingly, vaccinated mice receiving multiple WT challenges showed a significant decrease in lung fungal burden compared to vaccinated mice that were challenged only once. Because of these findings, we tested whether *C. neoformans* Δ*sgl1* could be used in a therapeutic manner. We found that administration of HK *C. neoformans* Δ*sgl1* post WT challenge in naïve mice significantly prolonged survival compared to untreated mice. In previously vaccinated mice, administration of HK *C. neoformans* Δ*sgl1* post WT challenge significantly decreased the lung fungal burden post challenge, even during $CD4^+$ T cell deficiency. Finally, we tested HK *C. neoformans* Δ*sgl1* in a model of cryptococcal granuloma to study whether our vaccination strategy would prevent fungal reactivation upon immunosuppression. We found that *C. neoformans* Δ*sgl1*-vaccinated mice exhibited significantly enhanced survival and control of fungal proliferation from latent granuloma-contained fungal cells upon inducing immunosuppression with either corticosteroid administration or $CD4^+$ T cell depletion.

In conclusion, our results suggest that HK *C. neoformans* Δ*sgl1* represents a clinically relevant vaccine candidate and confers robust host protection in three models of vaccination against cryptococcosis during host conditions most associated with clinical cases of cryptococcosis in humans.

MATERIALS AND METHODS

Fungal Strains and Heat Killed Yeast

The fungal strains used in this study were wild-type (WT) *C. neoformans* var. *grubii* strain H99, *C. neoformans* Δ*sgl1*, a mutant strain accumulating sterylglucosides developed by our group (45), and *C. neoformans* Δ*gcs1*, a mutant strain lacking glucosylceramide synthase (54). For all experiments, fungal strains were freshly recovered from a -80°C freezer stock on YPD agar at 30°C for 3-4 days. An isolated colony was added to 10ml of YPD broth and grown for 16-18hr with shaking, washed three times in sterile PBS, counted with a hemocytometer, and resuspended in sterile PBS at the desired concentration. For HK strains, the desired concentration of live yeast was resuspended in PBS and added to an 80°C heat block for 1hr. All HK strains were confirmed to be fully dead by plating the mixture on YPD plates at 30°C for 4 days and observing no growth.

Mice and Ethical Statement

Both male and female CBA/J mice were purchased from Envigo. All animals were housed under specific pathogen free conditions and had access to food and water *ad libitum*. Mice were allowed one week to acclimate upon arrival before any procedures began. All animal procedures were approved by the Stony Brook University Institutional Animal Care and Use Committee (protocol no. 341588) and followed the guidelines of American Veterinary Medical Association.

In vivo Infections and Organ Fungal Burden

All primary infections and immunizations were carried out in both male and female CBA/J mice 4-6 weeks old. Mice were first intraperitoneally (IP) anesthetized with a ketamine/xylazine solution (95mg of ketamine and 5mg of xylazine per kg of animal body weight). Anesthetized mice were then intranasally (IN) injected with the desired concentration of the specified yeast cells in 20µl of PBS. For fungal burden analysis, mice were euthanized *via* CO_2 inhalation on pre-determined timepoints. The lungs, brain, spleen, kidneys, and liver were removed, homogenized in 10ml of sterile PBS using a Stomacher 80 blender (Seward, UK), and serial dilutions were grown on YPD plates at 30°C for 3-4 days before being counted and total organ burden calculated.

Immunosuppression Treatments

Cortisone 21-acetate (CA) (Sigma; cat # C3130) was used to induce leukopenia. Mice were sub-cutaneously administered 250mg/kg/mouse CA in PBS every other day for a set timeline. IP administration of anti-CD4 monoclonal antibody (clone: GK1.5; BioXCell) was used to deplete mice of $CD4^+$ T cells. Antibody dilutions were prepared from the stock solution in PBS each time. Mice were administered 400µg/100µl every 4 days for the duration of the experiment to maintain cell depletion as previously validated in this infection model (52). Control group mice were administered isotype-matched antibody at the same concentration and administration timeline.

Vaccination Strategies and Survival Studies

Three different vaccination models were used in this study. For survival studies, any animal that appeared to be moribund, exhibited labored breathing or neurological infection, or had lost more than 20% body weight was euthanized *via* CO_2.

i) For the prevention model, mice were IN injected with $5x10^5$ live *C. neoformans* Δ*sgl1* in 20µl of PBS, $5x10^5$, $5x10^6$, or $5x10^7$ HK *C. neoformans* Δ*sgl1* in 20µl of PBS, or 20µl of sterile PBS (unvaccinated controls) 30 days prior to WT challenge unless stated otherwise in the figure caption. Mice were challenged with $5x10^5$ *C. neoformans* WT in 20µl of PBS unless stated otherwise in the figure caption and monitored daily until the pre-determined experimental endpoint.

ii) For the therapeutic model, live or HK *C. neoformans* Δ*sgl1* was used to treat vaccinated or unvaccinated mice post WT challenge. In vaccinated mice, immunocompetent or CD4-deficient mice were administered two subsequent doses of $5x10^7$ HK *C. neoformans* Δ*sgl1* on days -30 and -15, and mice were challenged with the WT strain on day 0. Mice were administered additional doses of $5x10^7$ HK *C. neoformans* Δ*sgl1* on days 30 and 45 to reduce WT cells that persist in the lungs of vaccinated mice. In unvaccinated mice, mice were first challenged with $1x10^5$ *C. neoformans* WT strain on day 0. WT challenged mice were treated with $5x10^5$ live *C. neoformans* Δ*sgl1* in 20µl of PBS, $5x10^7$ HK *C. neoformans* Δ*sgl1* in 20µl of PBS, or 20µl of sterile PBS (controls) on either day 3 or day 7 post challenge and assessed for survival until day 30.

iii) For the reactivation model, we assessed whether vaccination with *C. neoformans* Δ*sgl1* could protect mice from

lethal reactivation infection from latent fungal cells. First, mice were IN injected with $5x10^5$ *C. neoformans* Δ*gcs1*, an avirulent mutant that has been shown to induce lung granuloma formation that recapitulates a human pulmonary granuloma (54), on day -60. After 30 days, mice were IN injected with $5x10^5$ live *C. neoformans* Δ*sgl1*, $5x10^7$ HK *C. neoformans* Δ*sgl1*, or 20μl of sterile PBS (unvaccinated controls) on day -30 (and a second dose of $5x10^7$ HK *C. neoformans* Δ*sgl1* on day -15). To induce reactivation of latent *C. neoformans* Δ*gcs1*, mice were immunosuppressed *via* administration of either corticosteroids (cortisone 21-acetate) or depleted of $CD4^+$ T cells *via* IP injection of a monoclonal antibody at set timelines beginning on day 0. Mice were monitored for survival over 30 days.

Statistical Analysis

All analyses were performed using GraphPad Prism 9 software. The sample size, statistical analysis, and statistical significance is described in each figure caption. The Mantel-Cox log-rank test was used to calculate significance for survival studies. A two-tailed unpaired *t* test was used to calculate statistical significance between two samples, and either an ordinary one-way ANOVA using Tukey's multiple comparisons test for *P* value adjustment or a two-way ANOVA using Šídák's multiple comparisons test for *P* value adjustment was used to calculate statistical significance between more than two samples.

RESULTS

Vaccination With HK *C. neoformans* Δsgl1 Confers Concentration-Dependent Host Protection

We have recently found that murine splenocytes robustly produced the essential protective cytokines IFNγ and IL-17A when stimulated with HK *C. neoformans* Δ*sgl1 ex vivo*, and in fact *ex vivo* stimulation of splenocytes produced significantly greater quantities of these cytokines compared to live-cell stimulation at the same concentration and on the same timeline (T.G. Normile, T.H. Chu, B.S. Sheridan, and M. Del Poeta, submitted for publication). From this observation, we asked if administration of HK *C. neoformans* Δ*sgl1* would provide the same host protection to lethal WT challenge as with the live, attenuated mutant.

Since vaccination with HK mutant strains is notoriously known to elicit a weaker immune response than live, attenuated strains (55), mice were administered increasing concentrations of HK *C. neoformans* Δ*sgl1* 30 days prior to WT challenge. As expected, mice vaccinated with live *C. neoformans* Δ*sgl1* were fully protected while unvaccinated mice fully succumbed to infection (**Figure 1A**). Interestingly, we observed a concentration-dependent survival rate in mice with the increasing concentrations of HK *C. neoformans* Δ*sgl1*. Mice administered $5x10^5$ HK *C. neoformans* Δ*sgl1* fully succumbed to the WT infection in a similar timeline to unvaccinated mice (**Figure 1A**). There was a significant increase in median survival time for mice administered $5x10^6$ HK *C. neoformans* Δ*sgl1*, although all mice still succumbed to infection. Remarkably, mice administered $5x10^7$ HK *C. neoformans* Δ*sgl1* exhibited a 70% survival rate at the endpoint of the experiment that was not statistically different from the complete protection seen with live *C. neoformans* Δ*sgl1* (**Figure 1A**).

Surviving mice visually appeared healthy with normal weight gain, and endpoint organ fungal burden analysis confirmed no extrapulmonary dissemination had occurred (**Figure 1B**). Nevertheless, mice vaccinated with $5x10^7$ HK *C. neoformans* Δ*sgl1* displayed a significantly greater lung fungal burden compared to mice vaccinated with live *C. neoformans* Δ*sgl1* (**Figure 1B**). These data suggest that mice vaccinated with HK *C. neoformans* Δ*sgl1* exhibited concentration-dependent partial protection with $5x10^7$ HK *C. neoformans* Δ*sgl1* being the most efficacious.

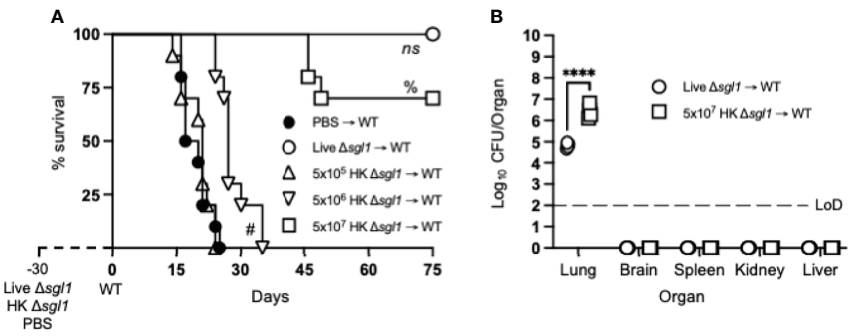

FIGURE 1 | Vaccination with heat-killed (HK) *C. neoformans* Δ*sgl1* confers concentration-dependent partial host protection. **(A)** CBA/J mice (n=10 mice/group) were administered $5x10^5$ Live Δ*sgl1*, $5x10^5$, $5x10^6$, or $5x10^7$ HK Δ*sgl1*, or PBS. After 30 days, mice were challenged with $5x10^5$ *C. neoformans* wild-type (WT) (day 0) and monitored for survival. **(B)** Endpoint organ fungal burden was quantified in the lungs, brain, spleen, kidney, and liver in surviving mice (n=4 mice/group). Dotted line represents the limit of detection (LoD) of CFU quantification. Graphed data represent the survival percentage of WT challenged mice **(A)** or the mean +/- SD **(B)** and are representative of two independent experimental replicates. Significance was determined using a two-tailed unpaired t-test **(B)** and significance is denoted as $^{****}P < 0.001$. Survival significance was determined by the Mantel-Cox log-rank test **(A)** and denoted on graph A: *ns*, not significant ($P > 0.05$) for Live Δ*sgl1* → WT vs. $5x10^7$ HK Δ*sgl1* → WT; %, $P < 0.001$ for $5x10^7$ HK Δ*sgl1* → WT vs. $5x10^6$ HK Δ*sgl1* → WT; #, $P < 0.001$ for $5x10^6$ HK Δ*sgl1* → WT vs. $5x10^5$ HK Δ*sgl1* → WT.

Two Administrations of HK *C. neoformans* Δsgl1 Confers Complete Host Protection Even During CD4$^+$ T Cell Immunodeficiency

We have unveiled that administration of a single dose of 5x10^7 HK *C. neoformans* Δ*sgl1* conferred similar host protection compared to vaccination with live *C. neoformans* Δ*sgl1*, although complete protection was not achieved (**Figure 1A**), and the endpoint lung fungal burden was significantly greater than the live mutant vaccinated mice (**Figure 1B**). However, due to the decreased length of antigen encounter, vaccination with HK mutants offer less host cell stimulation of protective cytokines, decreased naïve T cell expansion, and attenuated memory T cell formation (36, 55).

Since we have previously reported that either CD4$^+$ or CD8$^+$ T cells are required for *C. neoformans* Δ*sgl1*-mediated host protection (52), we hypothesized that repeated immunization with this HK mutant dose may negate the negative facets of HK vaccination and promote stronger adaptive T cell-mediated immunity as seen with other HK mutant vaccine studies (56, 57). We tested this hypothesis by administering two subsequent doses of 5x10^7 HK *C. neoformans* Δ*sgl1* (HK2d Δ*sgl1*) on days -30 and -15 prior to the WT challenge. Indeed, mice that received two administrations of 5x10^7 HK *C. neoformans* Δ*sgl1* exhibited complete host protection (100% survival) at the experimental endpoint (**Figure 2A**). Endpoint organ fungal burden analysis showed that HK2d Δ*sgl1*-vaccinated mice displayed no extrapulmonary dissemination and a significantly lower lung fungal compared to live *C. neoformans* Δ*sgl1*-vaccinated mice (**Figure 2B**). In fact, 1 of the 7 HK2d Δ*sgl1*-vaccinated mice fully cleared the WT yeast from the lungs. These data suggest that vaccination with two subsequent doses of 5x10^7 HK *C. neoformans* Δ*sgl1* confers complete host protection and aids in pulmonary clearance of the WT fungal cells.

To assess if vaccination with HK *C. neoformans* Δ*sgl1* possessed clinical relevance, CD4-deficient mice were also vaccinated with two subsequent doses of 5x10^7 HK *C. neoformans* Δ*sgl1* and challenged mice with the WT strain. Interestingly, 100% host protection was achieved in HK2d Δ*sgl1*-vaccinated mice depleted of CD4$^+$ T cells (**Figure 2C**), and endpoint organ fungal burden analysis revealed no extrapulmonary dissemination of the WT strain (**Figure 2D**). There was a significantly greater fungal burden in the lungs of HK2d Δ*sgl1*-vaccinated mice depleted of CD4$^+$ T cells compared

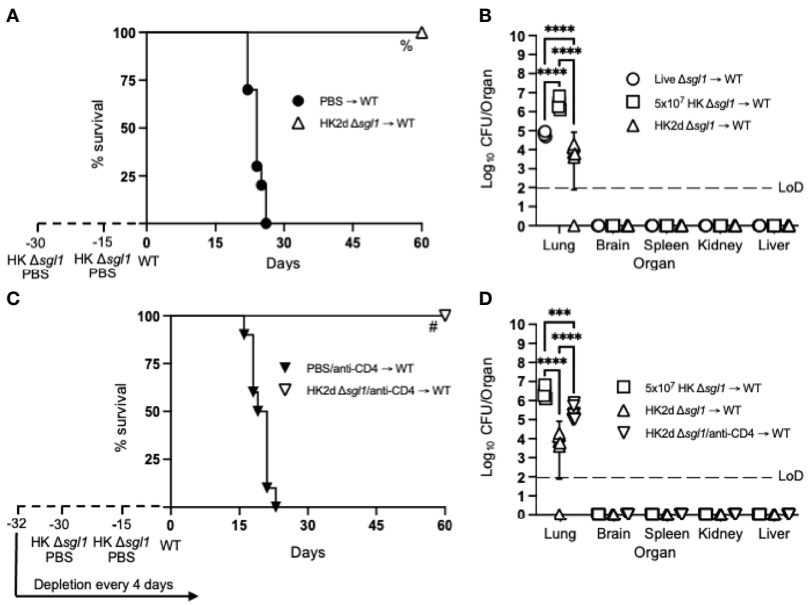

FIGURE 2 | Two doses of heat-killed (HK2d) **(C)** *neoformans* Δ*sgl1* confers complete host protection even in the absence of CD4$^+$ T cells. **(A)** CBA/J mice (n=10 mice/group) were administered two identical doses of 5x10^7 HK Δ*sgl1* or PBS (days -30 and -15), challenged with 5x10^5 *C. neoformans* wild-type (WT) (day 0), and monitored for survival. **(B)** Endpoint organ fungal burden was quantified in the lungs, brain, spleen, kidney, and liver from HK2d Δ*sgl1* → WT and compared to the endpoint fungal burden in Live Δ*sgl1* → WT and 5x10^7 HK Δ*sgl1* → WT from **Figure 1B** (n=4-7 mice/group). **(C)** CBA/J mice (n=10 mice/group) were depleted of CD4$^+$ T cells prior to administration of two identical doses of 5x10^7 HK Δ*sgl1* or PBS (days -30 and -15), challenged with 5x10^5 **(C)** *neoformans* WT (day 0), and monitored for survival. **(D)** Endpoint organ fungal burden was quantified in the lungs, brain, spleen, kidney, and liver in HK2d Δ*sgl1*/anti-CD4 → WT mice and compared to the endpoint fungal burden from 5x10^7 HK Δ*sgl1* → WT and HK2d Δ*sgl1* → WT from Figure 2B (n=4-7 mice/group). Graphed data represent the survival percentage of WT challenged mice **(A, C)** or the mean +/- SD **(B, D)** and are representative of two independent experimental replicates. Dotted lines represent the limit of detection (LoD) of CFU quantification **(B, D)**. Significance was determined by a two-way ANOVA using Šídák's multiple comparisons test for *P* value adjustment **(B, D)** and significance is denoted as ***$P < 0.005$; ****$P < 0.001$. Survival significance was determined by the Mantel-Cox log-rank test **(A, C)** and denoted on each graph: A: %, $P < 0.001$ for HK2d Δ*sgl1* → WT vs. PBS → WT; C: #, $P < 0.001$ for HK2d Δ*sgl1*/anti-CD4 → WT vs. PBS/anti-CD4 → WT.

to HK2d Δ*sgl1*-vaccinated immunocompetent mice. However, there was a significantly lower lung fungal burden in HK2d Δ*sgl1*-vaccinated mice depleted of $CD4^+$ T cells compared to live *C. neoformans* Δ*sgl1*-vaccinated immunocompetent mice (**Figure 2D**). Overall, these data indicate that vaccination with two subsequent administrations of $5x10^7$ HK *C. neoformans* Δ*sgl1* confers host protection from WT challenge in both immunocompetent and CD4-deficient mice, and the HK vaccination strategy may provide a greater efficacy in host clearance of the WT strain from the lungs compared to live vaccination strategy.

Vaccination With Live or HK *C. neoformans* Δsgl1 Confers Long-Lasting Host Immunity to Lethal WT Infection

Because administration of 2 subsequent doses of $5x10^7$ HK *C. neoformans* Δ*sgl1* also conferred complete host protection to the WT strain even during CD4-deficiency (**Figure 2**), we sought to investigate the efficacy of host protection after vaccination with either live or HK *C. neoformans* Δ*sgl1 via* alternations to our preventative vaccination model during immunocompetency and CD4-deficiency.

To assess the longevity of the vaccine-induced host protection, we increased the time between the administration of the vaccine and WT challenge. Immunocompetent or CD4-deficient mice were administered either live *C. neoformans* Δ*sgl1* or PBS and challenged with the WT strain 90 days later (a 3-fold increase between vaccination and WT challenge). Interestingly, all vaccinated mice survived the WT challenge, while all unvaccinated mice succumbed to the WT infection (**Figure 3A**). Endpoint organ fungal burden in surviving mice showed that no extrapulmonary dissemination was observed (**Figure 3B**). Similar to our previous studies, the lung fungal burden in CD4-deficient vaccinated mice was significantly greater than in immunocompetent vaccinated mice. These data show that vaccination with live *C. neoformans* Δ*sgl1* confers long term host immunity to lethal WT challenge, which strongly suggests long-lived memory T cells even during CD4-deficiency.

Because vaccination with live *C. neoformans* Δ*sgl1* promoted long term immunity resulting in complete host protection to the

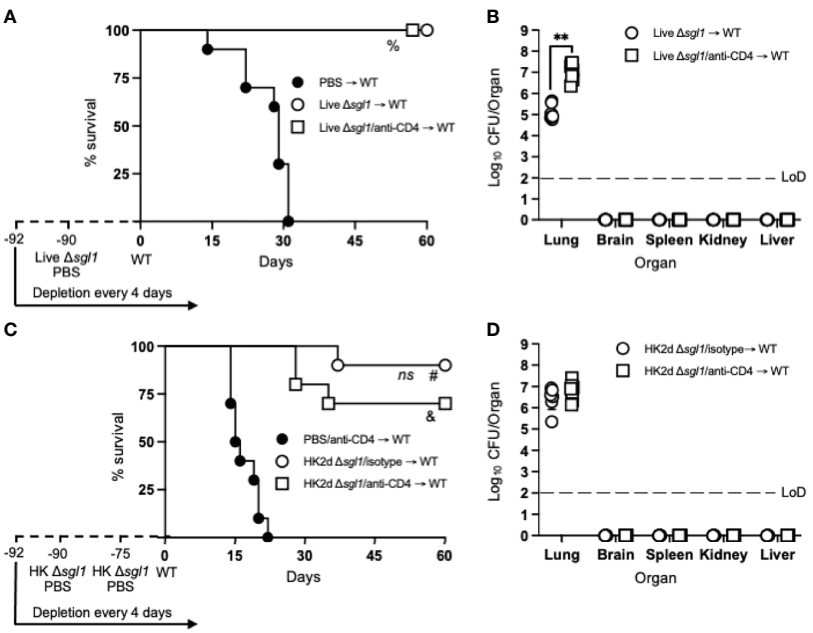

FIGURE 3 | Vaccination with live or heat-killed (HK) *C. neoformans* Δ*sgl1* confers long-lasting host protection. **(A)** CBA/J mice (n=10 mice/group) were administered anti-CD4 antibody or left untreated prior to vaccination with $5x10^5$ Live Δ*sgl1* or PBS controls, and the depletions continued for the entirety of the experiment at noted intervals. Mice were given an extended 90-day rest period where vaccinated and unvaccinated mice were then challenged with $5x10^6$ *C. neoformans* wild-type (WT) (day 0) and monitored for survival. **(B)** Endpoint organ fungal burden was quantified in the lungs, brain, spleen, kidney, and liver in surviving mice (n=8 mice/group). **(C)** CBA/J mice (n=10 mice/group) were administered either isotype or anti-CD4 antibodies prior to vaccination with two identical doses of $5x10^7$ HK Δ*sgl1* or PBS controls on days -90 and -75, and the depletions continued for the entirety of the experiment at noted intervals. Mice were given an extended 90-day rest period where vaccinated and unvaccinated mice were then challenged with $5x10^6$ *C. neoformans* WT (day 0) and monitored for survival. **(D)** Endpoint organ fungal burden was quantified in the lungs, brain, spleen, kidney, and liver in surviving mice (n=7 mice/group). Graphed data represent the survival percentage of WT challenged mice **(A, C)** or the mean +/- SD (B, D). Dotted lines represent the limit of detection (LoD) of CFU quantification **(B, D)**. Significance was determined by a two-tailed unpaired t-test **(B, D)** and significance is denoted as $^{**}P < 0.01$. Survival significance was determined by the Mantel-Cox log-rank test **(A, C)** and denoted on each graph: A: %, $P < 0.001$ for Live Δ*sgl1* → WT or Live Δ*sgl1*/anti-CD4 → WT vs. PBS → WT; C: *ns*, not significant ($P > 0.05$) for HK2d Δ*sgl1*/isotype → WT vs. HK2d Δ*sgl1*/anti-CD4 → WT; #, $P < 0.001$ for HK2d Δ*sgl1*/isotype → WT vs. PBS/anti-CD4 → WT; &, $P < 0.001$ for HK2d Δ*sgl1*/anti-CD4 → WT vs. PBS/anti-CD4 → WT.

WT strain, we then asked if HK *C. neoformans* Δ*sgl1* provided the same protection. Immunocompetent or CD4-deficient mice were administered 2 subsequent doses of either HK *C. neoformans* Δ*sgl1* or PBS on days -90 and -75 and challenged with the WT strain on day 0. We observed a 90% and 70% survival rate in immunocompetent and CD4-deficient mice, respectively (**Figure 3C**). Nonetheless, the difference between the median survival time for immunocompetent mice and CD4-deficient mice was not statistically different, the endpoint lung fungal burdens were nearly identical, and no extrapulmonary dissemination of the WT yeast was observed in either group (**Figure 3D**). Altogether, these data suggest that vaccination with live or HK *C. neoformans* Δ*sgl1* provides long-lived host protection and robust lung containment even after a 3-fold increase of the vaccination window.

Vaccination With *C. neoformans* Δsgl1 Confers Complete Host Protection to Multiple WT Challenges Even in the Absence of CD4$^+$ T cells

During chronic infections following an antigen encounter, T cells may become tolerant and non-responsive but remain alive for extended periods of time in a hyporesponsive state (58). Because we observe persistent fungal cells in the lungs post WT challenge, T cell anergy may potentially occur after the contraction phase post WT challenge. Since we have now shown that vaccination with either live or HK *C. neoformans* Δ*sgl1* provides long term immunity, we then wanted to investigate the possibility of induced T cell anergy in our model since T cell-mediated immunity is an essential facet to host vaccine protection in our model (52) (T.G. Normile, T.H. Chu, B.S. Sheridan, and M. Del Poeta, submitted for publication).

To test for induced T cell anergy, immunocompetent or CD4-deficient *C. neoformans* Δ*sgl1*-vaccinated mice underwent multiple WT challenges, monitored for survival, and lung fungal burden was assessed at the end of each WT challenge period (experimental design schematic: **Figure 4A**). Very interestingly, *C. neoformans* Δ*sgl1*-vaccinated mice completely survived for a total of 105 days after three subsequent lethal WT challenges on days 0, 45, and 75 (**Figure 4B**). Endpoint lung fungal burden analysis showed that there was a significant decrease of persistent WT yeast in the lungs of mice that were WT challenged a second time (**Figure 4C**). This decrease in lung burden did not further decrease after a third challenge. In addition, the decrease in the persistent lung fungal burden from the subsequent WT challenge resulted in no statistical difference between the lung burden in isotype-treated and CD4-deficient mice (**Figure 4C**). Overall, these data indicate that

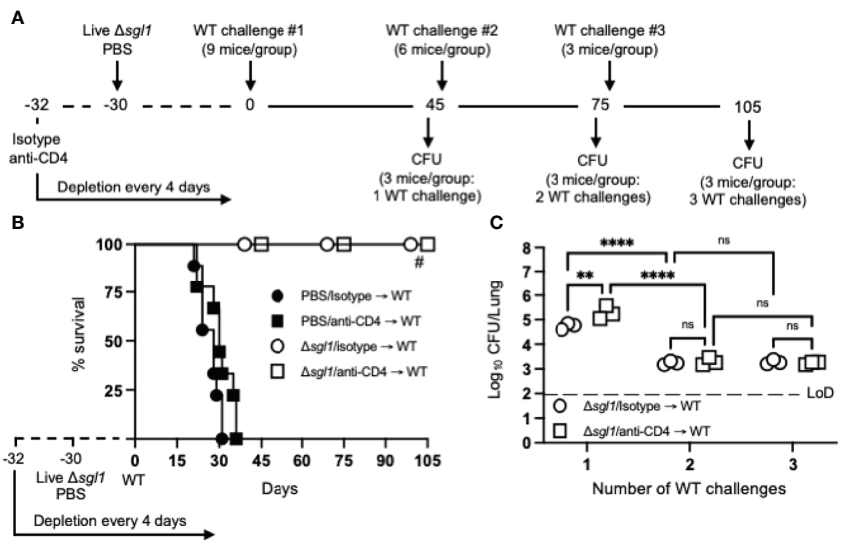

FIGURE 4 | Vaccination with **(C)** *neoformans* Δ*sgl1* confers complete host protection to multiple subsequent wild-type (WT) challenges even in the absence of CD4$^+$ T cells. **(A)** Experimental design schematic. **(B)** CBA/J mice (n=9 mice/group) were administered either isotype or anti-CD4 antibody prior to vaccination with 5x10^5 Live Δ*sgl1* or PBS controls, and the depletion continued for the entirety of the experiment at noted intervals. After 30 days, vaccinated and unvaccinated mice were challenged with 5x10^5 *C. neoformans* WT on day 0 (WT challenge #1). Only vaccinated mice remained on day 45 post WT challenge #1, and 3 mice/group were sacrificed for organ fungal burden while the remaining mice were all challenged a second time with 5x10^5 *C. neoformans* WT on day 45 (WT challenge #2). 30 days later on day 75, 3 mice/group were sacrificed for organ fungal burden while the remaining mice were all challenged a third time with 5x10^5 *C. neoformans* WT on day 75 (WT challenge #3). Finally, 30 days later on day 105, the remaining 3 mice/group were sacrificed for organ fungal burden. **(C)** Endpoint organ fungal burden was quantified in the lungs for mice sacrificed on days 45 (1 WT challenge), 75 (2 WT challenges), and 105 (3 WT challenges) (n=3 mice/group). Graphed data represent the survival percentage of WT challenged mice **(B)** or the mean +/- SD **(C)**. Dotted line represents the limit of detection (LoD) of CFU quantification. Significance was determined by a two-way ANOVA using Šídák's multiple comparisons test for *P* value adjustment **(C)** and significance is denoted as *ns*, not significant ($P > 0.05$); $^{**}P < 0.01$; $^{****}P < 0.001$. Survival significance was determined by the Mantel-Cox log-rank test **(B)** and denoted on graph B: #, $P < 0.001$ for Δ*sgl1*/isotype → WT vs PBS/isotype → WT or Δ*sgl1*/anti-CD4 → WT vs. PBS/anti-CD4 → WT.

immunocompetent and CD4-deficient *C. neoformans* Δ*sgl1*-vaccinated mice are protected from at least three subsequent lethal WT challenges resulting in fewer persisting WT cells in the lungs strongly suggesting that vaccination produces memory T cells that do not undergo anergy due to chronic infection.

Therapeutic Administration of HK *C. neoformans* Δsgl1 Post WT Challenge Reduces WT Cells in the Lungs of Vaccinated Mice

From our previous studies and present work, complete host protection in either immunocompetent or immunocompromised *C. neoformans* Δ*sgl1*-vaccinated mice has always been associated with persistent WT fungal cells remaining in the lungs post WT challenge (52) (T.G. Normile, T.H. Chu, B.S. Sheridan, and M. Del Poeta, submitted for publication). In those studies, we showed that the lung fungal burden at days 45, 75, and 105 post WT challenge was nearly identical at all timepoints, and histopathology at these timepoints displayed a decreased percentage of inflamed lung tissue and increased formation isolated nodules of contained yeast cells (52). In this study, we found for the first time that vaccination with two subsequent doses of HK *C. neoformans* Δ*sgl1* results in a significant decrease of lung fungal burden compared to live *C. neoformans* Δ*sgl1*-vaccination for both immunocompetent and CD4-deficient mice (**Figure 2D**). Moreover, vaccinated mice that received more than one WT challenge displayed a significant reduction in the lung fungal burden compared to mice that were received only one WT challenge (**Figure 4C**). Because subsequent WT challenges decreased the lung fungal burden, we asked if administration of our vaccine could be used as a therapeutic strategy and administered after the WT challenge.

To investigate the therapeutic potential of HK *C. neoformans* Δ*sgl1* administration in *C. neoformans* Δ*sgl1*-vaccinated mice, immunocompetent and CD4-deficient mice were challenged with the WT strain first and then received either 1 or 2 subsequent administrations of HK *C. neoformans* Δ*sgl1* (experimental design schematic: **Figure 5A**). We found a significant decrease in the lung fungal burden after therapeutic administration of HK *C. neoformans* Δ*sgl1* in both immunocompetent and CD4-deficient mice (**Figure 5B**). From the baseline lung fungal burden on day 30 post challenge, there was a significantly greater lung burden in CD4-deficient mice compared to the isotype-treated as we have seen previously. In addition, the lung fungal burden in mice that were treated with either 1 or 2 administrations of PBS (control groups) on days 30 and 45, respectively, was nearly identical to the baseline lung fungal burden (**Figure 5B**). Interestingly, there was a significant decrease in the lung burden in mice that received 1 or 2 administrations of HK *C. neoformans* Δ*sgl1* post WT challenge compared to the PBS-treated groups at those timepoints as well

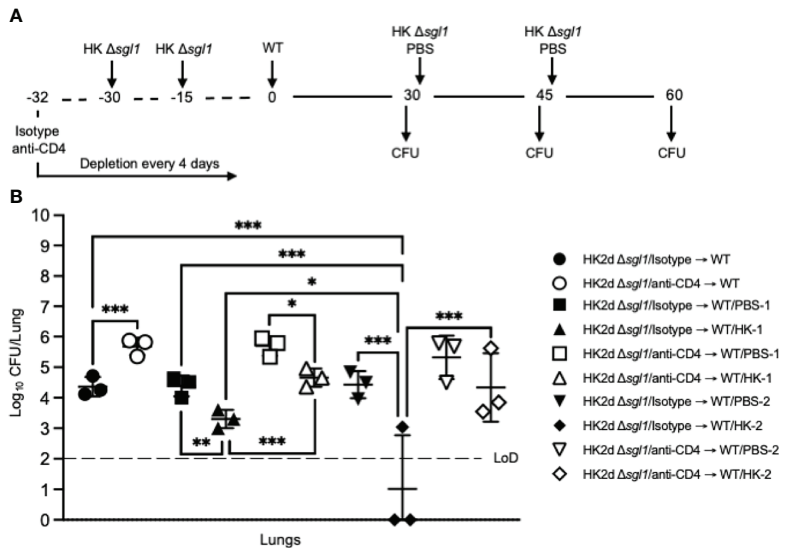

FIGURE 5 | Administration of heat-killed (HK) *C. neoformans* Δ*sgl1* post wild-type (WT) challenge significantly reduces persistent WT yeast from the lungs of vaccinated mice. **(A)** Experimental design schematic. CBA/J mice (n=9 mice/group) were administered either isotype or anti-CD4 antibody prior to vaccination with two identical doses of $5x10^7$ HK Δ*sgl1* on days -30 and -15, and all mice were challenged with $5x10^5$ *C. neoformans* WT on day 0. After 30 days post WT challenge, 3 mice/group (HK2d Δ*sgl1*/isotype → WT and HK2d Δ*sgl1*/anti-CD4 → WT) were sacrificed for lung fungal burden determination, and the remainder of the mice were then administered either $5x10^7$ HK Δ*sgl1* or PBS. Fifteen days later on day 45, 3 mice/group were sacrificed for lung fungal burden determination (HK2d Δ*sgl1*/isotype → WT/PBS-1, HK2d Δ*sgl1*/isotype → WT/HK-1, HK2d Δ*sgl1*/anti-CD4 → WT/PBS-1, and HK2d Δ*sgl1*/anti-CD4 → WT/HK-1), and the remainder of the mice were then administered either $5x10^7$ HK Δ*sgl1* or PBS. Fifteen days later on day 60, 3 mice/group were sacrificed for lung fungal burden determination (HK2d Δ*sgl1*/isotype → WT/PBS-2, HK2d Δ*sgl1*/isotype → WT/HK-2, HK2d Δ*sgl1*/anti-CD4 → WT/PBS-2, and HK2d Δ*sgl1*/anti-CD4 → WT/HK-2). **(B)** Endpoint organ fungal burden was quantified in the lungs for mice sacrificed on days 30, 45, and 60 (n=3 mice/group/timepoint). Dotted line represents the limit of detection (LoD) of CFU quantification. Graphed data represent the mean +/- SD **(B)**. Significance was determined by an Ordinary one-way ANOVA using Tukey's multiple comparisons test for *P* value adjustment and is denoted as $^*P < 0.05$; $^{**}P < 0.01$; $^{***}P < 0.005$.

as in the lung burdens between mice that received 1 or 2 administrations of HK *C. neoformans* Δ*sgl1* (**Figure 5B**). Together, these data suggest that therapeutic administration of HK *C. neoformans* Δ*sgl1* post WT challenge significantly reduces the number of persistent WT yeast in the lungs of vaccinated mice.

Therapeutic Administration of Live or HK *C. neoformans* Δsgl1 Post WT Challenge Significantly Prolongs Survival in Unvaccinated Mice

Because we observed the efficacious therapeutic potential of HK *C. neoformans* Δ*sgl1* administration post WT challenge in vaccinated mice, we then asked if therapeutic administration of HK *C. neoformans* Δ*sgl1* post WT challenge was useful in naïve, unvaccinated mice.

We tested this hypothesis by challenging naive mice with the WT strain and then administered HK *C. neoformans* Δ*sgl1*, live *C. neoformans* Δ*sgl1*, or PBS on either day 3 or day 7 and monitored for survival (experimental design schematic: **Figure 6A**). While all mice administered PBS fatally succumbed to infection, all mice administered HK *C. neoformans* Δ*sgl1* or live *C. neoformans* Δ*sgl1* on day 3 post WT challenge survived to the experimental endpoint (**Figure 6B**). In addition, mice administered HK *C. neoformans* Δ*sgl1* or live *C. neoformans* Δ*sgl1* on day 7 post WT challenge exhibited a 70% and 60% survival rate at the experimental endpoint, respectively. Nevertheless, there were no differences in the lung fungal burden between any of the surviving groups (**Figure 6B**). Of note, all surviving mice displayed extrapulmonary dissemination of the WT strain to the brain. Interestingly, mice that received therapeutic administration of live or HK *C. neoformans* Δ*sgl1* on day 3 had fewer brain CFU compared to mice administered on day 7 (**Figure 6C**). Overall, these data suggest that live or HK *C. neoformans* Δ*sgl1* aids to significantly prolong the survival of mice from fatal WT infection.

Vaccination With Live or HK *C. neoformans* Δsgl1 Protects Mice From Fatal Infection by Reactivation of Latent Cryptococcosis *via* Immunosuppression

We have now shown that live or HK *C. neoformans* Δ*sgl1* can be effectively used both preventatively (**Figures 2**–**4**) and therapeutically (**Figures 5**, **6**) to elicit robust host protection. However, *C. neoformans* is not only a primary pathogen since fungal cells can be contained within lung granulomas in immunocompromised hosts for extensive periods of time but immunosuppressive conditions, such as CD4-lymphopenic HIV/AIDS patients, can cause granuloma breakdown, latent fungal cell proliferation, and brain dissemination potentially resulting in fatal meningoencephalitis (11, 31). Thus, we investigated the ability of *C. neoformans* Δ*sgl1* to protect mice from cryptococcal reactivation from a lung granuloma.

To test this, mice were intranasally inoculated with *C. neoformans* Δ*gcs1*, a mutant strain lacking glucosylceramide synthase, that has been previously reported to induce pulmonary granuloma formation in mice over 30 days. At 30 days post Δ*gcs1* administration, we administered live *C. neoformans* Δ*sgl1*, HK *C. neoformans* Δ*sgl1*, or PBS. After another 30 days, all groups of mice underwent either corticosteroid-induced immunosuppression to induce

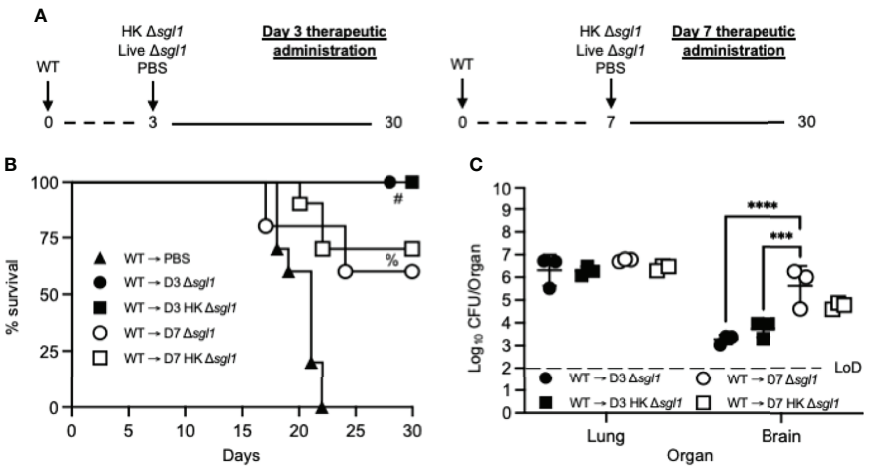

FIGURE 6 | Therapeutic administration of live or heat-killed (HK) *C. neoformans* Δ*sgl1* significantly prolongs host survival to lethal WT infection. **(A)** Experimental design schematic. **(B)** CBA/J mice (n=10 mice/group) were challenged with $1x10^5$ *C. neoformans* WT on day 0. WT challenged mice were administered $5x10^7$ HK Δ*sgl1*, $5x10^5$ Live Δ*sgl1*, or PBS on either day 3 (D3) or day 7 (D7) and monitored for survival until the experimental endpoint. **(C)** Endpoint organ fungal burden was assessed in the lungs and brains of surviving mice (n=3 mice/group). Dotted line represents the limit of detection (LoD) of CFU quantification. Graphed data represent the survival percentage of WT challenged mice **(B)** or the mean +/- SD **(C)**. Significance was determined by a two-way ANOVA using Šídák's multiple comparisons test for *P* value adjustment **(C)** and significance is denoted as ***$P < 0.005$; ****$P < 0.001$. Survival significance was determined by the Mantel-Cox log-rank test **(B)** and denoted on graph B: #, $P < 0.001$ for WT → D3 Δ*sgl1* or WT → D3 HK Δ*sgl1* vs. WT → PBS; %, $P < 0.001$ for WT → D7 Δ*sgl1* or WT → D7 HK Δ*sgl1* vs. WT → PBS.

leukopenia or $CD4^+$ T cell depletion to induce CD4 lymphopenia, and mice were monitored for survival (simplified experimental design schematic: **Figure 7A**; detailed experimental design schematic: **Supplementary Figure 1**). Extraordinarily, we observed that mice administered live *C. neoformans* Δ*sgl1* or HK *C. neoformans* Δ*sgl1* exhibited a 75% and 62.5% survival rate, respectively, at the experimental endpoint post corticosteroid-induced immunosuppression, while all PBS-treated mice fully succumbed to fatal reactivation (**Figure 7B**). Similarly, mice administered live *C. neoformans* Δ*sgl1* or HK *C. neoformans* Δ*sgl1* exhibited a 100% and 87.5% survival rate, respectively, at the experimental endpoint post $CD4^+$ T cell depletion, which were significantly greater than the PBS-treated mice that displayed a 37.5% survival rate (**Figure 7C**). These data suggest that vaccination with live or HK *C. neoformans* Δ*sgl1* can be used to protect the host from cryptococcal reactivation from a lung granuloma in the event that they become immunocompromised.

To examine the efficacy of our vaccine strategy in the experimental reactivation model, the endpoint lung fungal burden in mice pre-immunosuppression (day 0) was compared to the fungal burden in the lungs of mice that survived until the experimental endpoint post-immunosuppression (day 30). We first observed there were no differences in the lung fungal burdens between any of the groups pre-immunosuppression (**Figure 7D**). Interestingly, there were no statistical differences between the

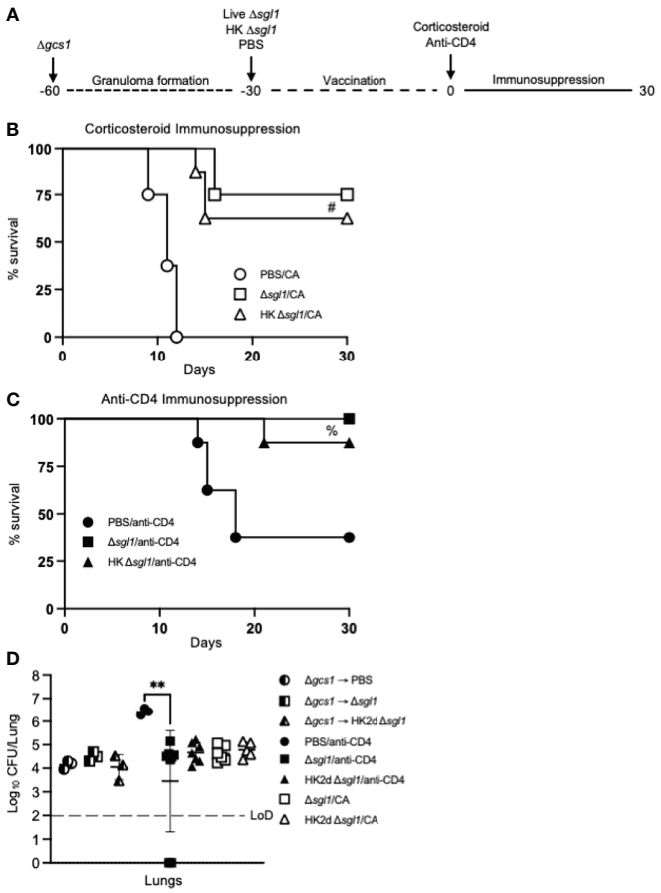

FIGURE 7 | Vaccination with either live or heat-killed (HK) *C. neoformans* Δ*sgl1* protects mice from lethal reactivation infection post immunosuppression. **(A)**. Experimental design schematic (a more detailed schematic can be found in **Supplementary Figure S1**). **(B, C)**. CBA/J mice were infected with $5x10^5$ *C. neoformans* Δ*gcs1* on day -60 to induce lung granuloma formation. After 30 days, mice were administered either $5x10^5$ Live Δ*sgl1* or PBS on day -30 or $5x10^7$ HK Δ*sgl1* on days -30 and -15. Finally on day 0, all groups of mice underwent continuous immunosuppressive treatment with either the corticosteroid cortisone acetate (CA) **(B)** or anti-CD4 antibody **(C)** to cause reactivation of the latent *C. neoformans* Δ*gcs1* yeast contained within the lung granulomas and assessed for survival over 30 days. **(D)** Endpoint lung fungal burden comparison in mice pre-immunosuppression on day 0 (Δ*gcs1* → PBS and Δ*gcs1* → Δ*sgl1*) (n=3 mice/group) and post-immunization on day 30 for CA-treated mice (Δ*sgl1*/CA and HK2d Δ*sgl1*/CA) (n=6-7 mice/group) and anti-CD4-treated mice (PBS/anti-CD4, Δ*sgl1*/anti-CD4, and HK2d Δ*sgl1*/anti-CD4) (n=9-10 mice/group). Dotted line represents the limit of detection (LoD) of CFU quantification. Graphed data represent the survival percentage of mice **(B, C)** and the mean +/- SD **(D)**. Significance was determined by an Ordinary one-way ANOVA using Tukey's multiple comparisons test for *P* value adjustment **(D)** and is denoted as $^{**}P < 0.01$. The Mantel-Cox log-rank test was used to determine survival significance **(B, C)** and denoted on each graph: B: #, $P < 0.001$ for either Δ*sgl1*/CA or HK Δ*sgl1*/CA vs. PBS/CA; C: %, $P < 0.01$ for Δ*sgl1*/anti-CD4 or HK Δ*sgl1*/anti-CD4 vs. PBS/anti-CD4.

endpoint lung fungal burdens post-immunosuppression in *C. neoformans* Δ*sgl1*-vaccinated mice or between the endpoint lung fungal burdens in mice pre-immunosuppression compared to in mice post-immunosuppression. In fact, the only observed statistically significant difference was between the surviving PBS-treated CD4-deficient mice and live *C. neoformans* Δ*sgl1*-vaccinated mice, which further supports that vaccination with *C. neoformans* Δ*sgl1* protects mice from lethal reactivation upon immunosuppression (**Figure 7D**). Comparably, all surviving PBS-treated mice displayed significantly greater brain dissemination compared to vaccinated mice, which were almost fully absent of any brain fungal burden (**Supplementary Figure 2**). Overall, these data suggest that administration of live or HK *C. neoformans* Δ*sgl1* inhibits the proliferation of dormant fungal cell in the lung granuloma and protects from extrapulmonary dissemination upon immunosuppression.

DISCUSSION

In the current study, we have presented ample evidence on the highly efficacious use of HK *C. neoformans* Δ*sgl1* in conferring robust host protection in three separate models of vaccination against cryptococcosis during immunosuppression. More specifically, we have shown that: i) preventative vaccination with 2 doses of HK *C. neoformans* Δ*sgl1* conferred complete host protection to lethal challenge with decreased endpoint lung fungal burden compared to live cell vaccination; ii) therapeutic administration of HK *C. neoformans* Δ*sgl1* post WT challenge resulted in a continual decrease in the lung fungal burden with each subsequent vaccine administration, conferring significantly increased survival rate; and iii) our vaccination strategy prevented cryptococcal reactivation from a lung granuloma, by inhibiting proliferation of latent fungal cells and improving survival upon immunosuppression.

Host protection was both concentration- and dose-dependent requiring 2 subsequent administrations of $5x10^7$ HK *C. neoformans* Δ*sgl1*. The requirement for multiple doses has been seen with other HK vaccine-inducing mutant strains (56, 57), while others required only one dose (59, 60). Because all these studies including our current work use a similar vaccine concentration between $1x10^7$ and $5x10^7$, the only difference for the single dose requirement was the use of the KN99 WT strain compared to the H99 WT strain. Nevertheless, all studies on HK vaccine-inducing mutants, including this current work, report 100% protection to the lethal WT challenge. However, the true standout characteristic for a clinically relevant vaccine formulation is the ability to induce protection in a model most associated with a disease, which is CD4-deficiency for cryptococcosis (36, 40).

In comparison to our present findings where we report 100% protection in CD4-deficiency with HK *C. neoformans* Δ*sgl1* vaccination, the only other HK vaccine-inducing mutant to demonstrate protection during CD4-deficiency was from Wang and colleagues using a HK F-box protein (Δ*fbp1*) mutant strain (56). Similarly, both HK *C. neoformans* Δ*sgl1* and the HK Δ*fbp1* mutants demonstrated complete protection in both immunocompetent and CD4-deficient CBA/J mice, although differences between the two are noteworthy. First, our present work with HK *C. neoformans* Δ*sgl1* resulted in a ~1 log lower endpoint lung fungal burden for isotype-treated mice compared to isotype-treated mice in the report by Wang and colleagues (although the endpoint lung fungal burden for CD4-deficient mice was nearly identical) (56) (**Figure 2**). Second, we observed a complete lack of any extrapulmonary dissemination in mice vaccinated with HK *C. neoformans* Δ*sgl1*, while several mice displayed fungal CFU in the brain and spleen in the study by Wang and colleagues (56). Finally, the WT challenge dose used in our work was 15x greater than used by Wang and colleagues.

With regards to our vaccine, we aimed to test the rigor and robustness of *C. neoformans* Δ*sgl1* in the preventative model of vaccination *via* functional alterations to our experimental design. Since T cell mediated immunity is a well-established keystone of anti-cryptococcal immunity (61, 62), the need for either $CD4^+$ or $CD8^+$ T cells in *C. neoformans* Δ*sgl1* host protection (52), and our recent findings that show memory T cell recall responses of IFNγ- and IL-17A-producing subsets in *C. neoformans* Δ*sgl1*-vaccinated mice to the WT strain (T.G. Normile, T.H. Chu, B.S. Sheridan, and M. Del Poeta, submitted for publication), these functional alterations focused upon memory T cells. The first alteration involved a 3-fold increase in the time between vaccination and WT challenge, where vaccination began 90 days prior to WT challenge for both live and HK *C. neoformans* Δ*sgl1*. All immunocompetent and CD4-deficient mice vaccinated with live *C. neoformans* Δ*sgl1* survived the lethal WT challenge, and a respective 90% and 70% survival was observed in mice vaccinated with HK *C. neoformans* Δ*sgl1* (**Figures 3A, C**). The protection observed in the extended rest period suggests the induction of long-lived memory T cells post vaccination with *C. neoformans* Δ*sgl1*. Future immunophenotyping assays will be aimed to define the type of circulating memory T cells, such as central memory, tissue-resident memory, or effector memory.

Complete host protection was not observed in 100% of the $CD4^+$ deficient mice when they were vaccinated with HK *C. neoformans* Δ*sgl1* 90 days prior to WT challenge. This suggests that the immunological memory induced was either less robust or shorter-lived compared to vaccination with the live cell strain. It is noteworthy to mention that the WT challenge dose was doubled in this experimental design due to the increased age of the mice at the time of challenge. However, the decreased length of antigen encounter using HK mutant strains may have potentially resulted in less robust naïve T cell stimulation and fewer memory T cells following the contraction phase (55, 63). Optimization of the dosing regimen will be required in future studies. Potential adjustments could include increasing the number of doses, increasing the time between the first and second dose, or altering the concentrations to induce more robust immunity with a lower first dose and a greater second dose.

The second functional alteration to the preventative vaccination model experimental design was to increase the number of WT challenges administered to vaccinated mice. During chronic infections, such as when fungal cells are

persisting in the lungs, T cells may become tolerized to antigens remaining alive for extended periods of time in a hyporesponsive state known as T cell anergy (58, 64). Mice vaccinated with *C. neoformans* Δ*sgl1* exhibited the opposite, however. First, all mice that received two or three subsequent WT challenges exhibited 100% survival even during $CD4^+$ T cell deficiency (**Figure 4B**). Second, the endpoint lung fungal burden in mice that received at least 2 WT challenges displayed a ~2 log decrease compared to mice that received only 1 WT challenge (**Figure 4C**). This suggests the efficacy observed with the functional alterations in the preventative model during vaccination with *C. neoformans* Δ*sgl1* elicits long-lived, non-exhaustive T cell memory with increasing clonal functionality upon subsequent WT encounters. Future work will address a phenotypic and functional characterization comparing T cells from mice administered one WT challenge with mice administered more than one challenge.

Persistent fungal cells remaining in the lungs post WT challenge in *C. neoformans* Δ*sgl1*-vaccinated mice have been an observable facet in all experimental variations in this study and previous work from our lab. Moreover, fungal cell persistence post WT challenge in vaccinated mice has been reported in other cryptococcal vaccine studies as well (56, 57, 59, 60, 65, 66). Because we observed a decrease in the lung fungal burden after a second WT challenge (**Figure 4C**), we investigated the immunotherapeutic ability of HK *C. neoformans* Δ*sgl1* to decrease further WT fungal cells remaining in the lungs. The first administration of HK *C. neoformans* Δ*sgl1* significantly decreased the persistent fungal burden to a similar degree as mice that received a second WT challenge (**Figure 5B** and **Figure 4C**). Interestingly, mice that received a second administration of HK *C. neoformans* Δ*sgl1* significantly decreased the remaining fungal cells to an even further extent compared to mice that were administered PBS or mice that received only 1 therapeutic dose of HK *C. neoformans* Δ*sgl1* (**Figure 5B**). In fact, 2 of the 3 mice fully cleared the WT fungal cells from the lungs. Thus, HK *C. neoformans* Δ*sgl1* exhibits robust immunotherapeutic potential in previously vaccinated immunocompetent mice.

Collectively, the therapeutic potential of HK *C. neoformans* Δ*sgl1* administration has demonstrated highly efficacious host protection in both previously vaccinated (**Figure 5**) and unvaccinated mice (**Figure 6**). While this adds an entirely new dimension to our vaccine, immunotherapeutic administration is scarce in the literature with only a few other reports. The first immunotherapeutic study utilized P13, an antigenic peptide mimotope of the cryptococcal capsular GXM conjugated to either tetanus toxoid or diphtheria toxoid (67, 68). Immunization with P13 after an otherwise lethal challenge significantly prolonged survival, yet all mice soon succumbed to fatal infection (67). Similarly, Datta and colleagues established a model of chronic infection in mice and administration of P13 significantly prolonged host survival compared to control mice, but again all mice soon succumbed to fatal infection (68). In addition to the P13 conjugate vaccine, a TNFα-expressing adenoviral vector was also utilized post lethal WT challenge (69). Although survival was not assessed, the authors reported a significant decrease in lung fungal burden, increased IFNγ levels, and a significant increase in macrophage and neutrophil recruitment to the lungs. Overall, in addition to the robust efficacy in the preventative model of vaccination, *C. neoformans* Δ*sgl1* has now been shown to possess unrivaled immunotherapeutic potential adding to the clinical significance of our vaccine.

Although both the prevention and therapeutic models increase the novelty and translational potential of our vaccine, we have demonstrated vaccine-induced host protection against lethal infection due to reactivation of latent fungal cells upon immunosuppressive treatments (**Figures 7B, C**). To our knowledge, this is the first time a vaccine against the reactivation infection has been reported in the literature. Previous work in our lab had shown that mice treated with FTY720, a prescribed treatment for relapsing remitting multiple sclerosis, was linked to granuloma breakdown with a disorganization of the peripheral macrophages with a shift towards an M2 polarized state (11). In addition, our findings also validate the reactivation model, as it showed that the *C. neoformans* Δ*gcs1*-induced granuloma in mice can lose integrity upon immunosuppression resulting in fungal proliferation in the lungs, brain dissemination, and ultimately death.

In fact, clinical cases can occur due to the reactivation of granuloma-contained fungal cells from either immunosuppression or comorbidities (HIV/AIDS progression) (27, 70). Because of this, we tested our vaccination strategy in this mouse model during prolonged corticosteroid-induced immunosuppression as well as CD4-deficiency. We observed a 70% and 60% survival rate in mice vaccinated with live or HK *C. neoformans* Δ*sgl1*, respectively, at the endpoint after corticosteroid-induced immunosuppression with cortisone acetate (**Figure 7B**), and a 100% and 90% survival rate in mice vaccinated with live or HK *C. neoformans* Δ*sgl1* at the endpoint after depletion of $CD4^+$ T cells (**Figure 7C**). Interestingly, the corticosteroid-induced immunosuppression was more lethal than the depletion of $CD4^+$ T cells, which may be attributed to the mechanism of immunosuppression. Corticosteroid-induced immunosuppression induces leukopenia, inhibits phagocytosis, and decreases antigen presentation capabilities (71, 72), while depletion of $CD4^+$ T cells ablates circulating $CD4^+$ lymphocytes. So, we speculate that the difference in lethality of the infection may be the speed at which the immunosuppression took effect.

Although there was an observed difference in survival between the two modes of immunosuppression, the endpoint lung fungal burden between the two modes of immunosuppression were nearly identical (**Figure 7D**). In fact, there were also no differences between the endpoint lung fungal burden of mice pre-immunosuppression and *C. neoformans* Δ*sgl1*-vaccinated mice post-immunosuppression. This suggests that vaccination with either live or HK *C. neoformans* Δ*sgl1* controls the proliferation of the latent fungal cells in the lungs even after the immunosuppressive regime. This is further supported from the endpoint lung fungal burden in unvaccinated CD4-deficient mice being significantly

greater than the lung fungal burden in the vaccinated mice, which indicate that fungal cells extensively proliferate in unvaccinated mice upon immunosuppression. The same was observed for extrapulmonary dissemination to the brain (**Supplementary Figure 2**). While there were only 1-2 C. *neoformans* Δ*sgl1*-vaccinated mice that displayed fungal dissemination, all the surviving unvaccinated mice had significant fungal burden in the brain. Overall, vaccination with either live or HK *C. neoformans* Δ*sgl1* demonstrated remarkable efficacy in this cryptococcal model of reactivation.

In conclusion, we have shown here that HK *C. neoformans* Δ*sgl1* demonstrates a highly efficacious vaccine candidate that goes beyond the canonical preventative model of primary disease prevention. We have expanded not only to a more clinically relevant HK formulation but also to additional models of vaccine strategies to protect against cryptococcosis during CD4-deficiency, including using our vaccine as a therapeutic mean and using our vaccine to prevent reactivation of a latent infection upon immunodepression. Here forth, the tools for investigation into the protective immunity against fungal reactivation from pulmonary granulomas in mice are now available, which greatly opens future possibilities to significantly add to this completely absent portion of the literature.

DATA AVAILABILITY STATEMENT

The original contributions presented in the study are included in the article/**Supplementary Material**. Further inquiries can be directed to the corresponding author.

ETHICS STATEMENT

The animal study was reviewed and approved by Stony Brook University Institutional Animal Care and Use Committee (protocol no. 341588).

AUTHOR CONTRIBUTIONS

TGN and MDP took part in the conceptualization of this study as well as the writing and finalization of the manuscript. TGN performed all animal and experimental procedures, statistical analysis, and figure generation. All authors contributed to the article and approved the submitted version.

FUNDING

This work was supported by the National Institute of Health (NIH) grants AI136934 (MDP), AI116420 (MDP), and AI125770 (MDP), and by a Merit Review Grant I01BX002924 (MDP) from the Veterans Affairs (VA) Program. MDP is a recipient of the Research Career Scientist (RCS) Award (IK6 BX005386) and a Burroughs Welcome Investigator in Infectious Diseases.

SUPPLEMENTARY MATERIAL

The Supplementary Material for this article can be found online at: https://www.frontiersin.org/articles/10.3389/fimmu.2022.868523/full#supplementary-material

REFERENCES

1. Fierer J. Invasive Endemic Fungi of the Western Hemisphere. *Virulence* (2019) 10(1):832–4. doi: 10.1080/21505594.2019.1664719
2. Firacative C. Invasive Fungal Disease in Humans: Are We Aware of the Real Impact? *Mem Inst Oswaldo Cruz* (2020) 115:e200430. doi: 10.1590/0074-02760200430
3. Akhtar S, Aggarwal N, Demkowicz R, Andreatos N, Gupta M. Cryptococcus and HIV. *QJM* (2020) 113(5):347–8. doi: 10.1093/qjmed/hcz299
4. Armstrong-James D, Meintjes G, Brown GD. A Neglected Epidemic: Fungal Infections in HIV/AIDS. *Trends Microbiol* (2014) 22(3):120–7. doi: 10.1016/j.tim.2014.01.001
5. Chang CC, Chen SC. Colliding Epidemics and the Rise of Cryptococcosis. *J Fungi (Basel)* (2015) 2(1):1–11. doi: 10.3390/jof2010001
6. Elsegeiny W, Marr KA, Williamson PR. Immunology of Cryptococcal Infections: Developing a Rational Approach to Patient Therapy. *Front Immunol* (2018) 9:1–9. doi: 10.3389/fimmu.2018.00651
7. Brown GD, Denning DW, Gow NA, Levitz SM, Netea MG, White TC, et al. Hidden Killers: Human Fungal Infections. *Sci Transl Med* (2012) 4 (165):165rv13. doi: 10.1126/scitranslmed.3004404
8. Henao-Martinez AF, Beckham JD. Cryptococcosis in Solid Organ Transplant Recipients. *Curr Opin Infect Dis* (2015) 28(4):300–7. doi: 10.1097/QCO.0000000000000171
9. Saha DC, Goldman DL, Shao X, Casadevall A, Husain S, Limaye AP, et al. Serologic Evidence for Reactivation of Cryptococcosis in Solid-Organ Transplant Recipients. *Clin Vaccine Immunol* (2007) 14(12):1550–4. doi: 10.1128/CVI.00242-07
10. Zafar H, Altamirano S, Ballou ER, Nielsen K. A Titanic Drug Resistance Threat in Cryptococcus Neoformans. *Curr Opin Microbiol* (2019) 52:158–64. doi: 10.1016/j.mib.2019.11.001
11. Bryan AM, You JK, McQuiston T, Lazzarini C, Qiu Z, Sheridan B, et al. FTY720 Reactivates Cryptococcal Granulomas in Mice Through S1P Receptor 3 on Macrophages. *J Clin Invest* (2020) 130(9):4546–60. doi: 10.1172/JCI136068
12. Grebenciucova E, Reder AT, Bernard JT. Immunologic Mechanisms of Fingolimod and the Role of Immunosenescence in the Risk of Cryptococcal Infection: A Case Report and Review of Literature. *Mult Scler Relat Disord* (2016) 9:158–62. doi: 10.1016/j.msard.2016.07.015
13. Ward MD, Jones DE, Goldman MD. Cryptococcal Meningitis After Fingolimod Discontinuation in a Patient With Multiple Sclerosis. *Mult Scler Relat Disord* (2016) 9:47–9. doi: 10.1016/j.msard.2016.06.007
14. Del Poeta M, Ward BJ, Greenberg B, Hemmer B, Cree BAC, Komatireddy S, et al. Cryptococcal Meningitis Reported With Fingolimod Treatment: Case Series. Neurology, Neuroimmunology, & Neuroinflammation. (2022) 9:e1156.
15. Casadevall A. Immunity to Invasive Fungal Diseases. *Annu Rev Immunol* (2022) 40:121–41. doi: 10.1146/annurev-immunol-101220-034306
16. Vu K, Garcia JA, Gelli A. Cryptococcal Meningitis and Anti-Virulence Therapeutic Strategies. *Front Microbiol* (2019) 10:1–7. doi: 10.3389/fmicb.2019.00353
17. Cogliati M. Global Warming Impact on the Expansion of Fundamental Niche of Cryptococcus Gattii VGI in Europe. *Environ Microbiol Rep* (2021) 13 (3):375–83. doi: 10.1111/1758-2229.12945
18. Raffa RB, Eltoukhy NS, Raffa KF. Implications of Climate Change (Global Warming) for the Healthcare System. *J Clin Pharm Ther* (2012) 37(5):502–4. doi: 10.1111/j.1365-2710.2012.01355.x
19. van Rhijn N, Bromley M. The Consequences of Our Changing Environment on Life Threatening and Debilitating Fungal Diseases in Humans. *J Fungi (Basel)* (2021) 7:1–18. doi: 10.3390/jof7050367
20. Traver EC, Malave Sanchez M. Pulmonary Aspergillosis and Cryptococcosis as a Complication of COVID-19. *Med Mycol Case Rep* (2022) 35:22–5. doi: 10.1016/j.mmcr.2022.01.003

21. Bhatt K, Agolli A, Patel MH, Garimella R, Devi M, Garcia E, et al. High Mortality Co-Infections of COVID-19 Patients: Mucormycosis and Other Fungal Infections. *Discoveries (Craiova)* (2021) 9(1):e126. doi: 10.15190/d.2021.5
22. Abdoli A, Falahi S, Kenarkoohi A. COVID-19-Associated Opportunistic Infections: A Snapshot on the Current Reports. *Clin Exp Med* (2021) 7:1–20. doi: 10.1007/s10238-021-00751-7
23. Roudbary M, Kumar S, Kumar A, Cernakova L, Nikoomanesh F, Rodrigues CF, et al. Overview on the Prevalence of Fungal Infections, Immune Response, and Microbiome Role in COVID-19 Patients. *J Fungi (Basel)* (2021) 7(9):1–28. doi: 10.3390/jof7090720
24. Cafardi J, Haas D, Lamarre T, Feinberg J. Opportunistic Fungal Infection Associated With COVID-19. *Open Forum Infect Dis* (2021) 8(7):ofab016. doi: 10.1093/ofid/ofab016
25. Amin A, Vartanian A, Poladian N, Voloshko A, Yegiazaryan A, Al-Kassir AL, et al. Root Causes of Fungal Coinfections in COVID-19 Infected Patients. *Infect Dis Rep* (2021) 13(4):1018–35. doi: 10.3390/idr13040093
26. Araujo G, Souza W, Frases S. The Hidden Pathogenic Potential of Environmental Fungi. *Future Microbiol* (2017) 12:1533–40. doi: 10.2217/fmb-2017-0124
27. de Sousa HR, de Frazao S, de OliveiraJunior GP, Albuquerque P, Nicola AM, et al. Cryptococcal Virulence in Humans: Learning From Translational Studies With Clinical Isolates. *Front Cell Infect Microbiol* (2021) 11:1–8. doi: 10.3389/fcimb.2021.657502
28. Gushiken AC, Saharia KK, Baddley JW. Cryptococcosis. *Infect Dis Clin North Am* (2021) 35(2):493–514. doi: 10.1016/j.idc.2021.03.012
29. Denham ST, Brown JCS. Mechanisms of Pulmonary Escape and Dissemination by Cryptococcus Neoformans. *J Fungi (Basel)* (2018) 4(1):1–17. doi: 10.3390/jof4010025
30. Shibuya K, Hirata A, Omuta J, Sugamata M, Katori S, Saito N, et al. Granuloma and Cryptococcosis. *J Infect Chemother* (2005) 11(3):115–22. doi: 10.1007/s10156-005-0387-X
31. Ristow LC, Davis JM. The Granuloma in Cryptococcal Disease. *PloS Pathog* (2021) 17(3):e1009342. doi: 10.1371/journal.ppat.1009342
32. Pagan AJ, Ramakrishnan L. The Formation and Function of Granulomas. *Annu Rev Immunol* (2018) 36:639–65. doi: 10.1146/annurev-immunol-032712-100022
33. Brunet K, Alanio A, Lortholary O, Rammaert B. Reactivation of Dormant/Latent Fungal Infection. *J Infect* (2018) 77(6):463–8. doi: 10.1016/j.jinf.2018.06.016
34. Mayer FL, Kronstad JW. Cryptococcus Neoformans. *Trends Microbiol* (2020) 28(2):163–4. doi: 10.1016/j.tim.2019.10.003
35. Rajasingham R, Smith RM, Park BJ, Jarvis JN, Govender NP, Chiller TM, et al. Global Burden of Disease of HIV-Associated Cryptococcal Meningitis: An Updated Analysis. *Lancet Infect Dis* (2017) 17(8):873–81. doi: 10.1016/S1473-3099(17)30243-8
36. Levitz SM, Golenbock DT. Beyond Empiricism: Informing Vaccine Development Through Innate Immunity Research. *Cell* (2012) 148(6):1284–92. doi: 10.1016/j.cell.2012.02.012
37. Bicanic T, Bottomley C, Loyse A, Brouwer AE, Muzoora C, Taseera K, et al. Toxicity of Amphotericin B Deoxycholate-Based Induction Therapy in Patients With HIV-Associated Cryptococcal Meningitis. *Antimicrob Agents Chemother* (2015) 59(12):7224–31. doi: 10.1128/AAC.01698-15
38. McEvoy K, Normile TG, Poeta MD. Antifungal Drug Development: Targeting the Fungal Sphingolipid Pathway. *J Fungi (Basel)* (2020) 6(3):jof6030142. doi: 10.3390/jof6030142
39. Mourad A, Perfect JR. Present and Future Therapy of Cryptococcus Infections. *J Fungi (Basel)* (2018) 4(3):75–85. doi: 10.3390/jof4030079
40. Oliveira LVN, Wang R, Specht CA, Levitz SM. Vaccines for Human Fungal Diseases: Close But Still a Long Way to Go. *NPJ Vaccines* (2021) 6(1):33. doi: 10.1038/s41541-021-00294-8
41. Ueno K, Yanagihara N, Shimizu K, Miyazaki Y. Vaccines and Protective Immune Memory Against Cryptococcosis. *Biol Pharm Bull* (2020) 43(2):230–9. doi: 10.1248/bpb.b19-00841
42. Caballero Van Dyke MC, Wormley FLJr. A Call to Arms: Quest for a Cryptococcal Vaccine. *Trends Microbiol* (2018) 26(5):436–46. doi: 10.1016/j.tim.2017.10.002
43. Nami S, Mohammadi R, Vakili M, Khezripour K, Mirzaei H, Morovati H. Fungal Vaccines, Mechanism of Actions and Immunology: A Comprehensive Review. *BioMed Pharmacother* (2019) 109:333–44. doi: 10.1016/j.biopha.2018.10.075
44. Normile TG, Bryan AM, Del Poeta M. Animal Models of Cryptococcus Neoformans in Identifying Immune Parameters Associated With Primary Infection and Reactivation of Latent Infection. *Front Immunol* (2020) 11(581750):1–21. doi: 10.3389/fimmu.2020.581750
45. Rella A, Mor V, Farnoud AM, Singh A, Shamseddine AA, Ivanova E, et al. Role of Sterylglucosidase 1 (Sgl1) on the Pathogenicity of Cryptococcus Neoformans: Potential Applications for Vaccine Development. *Front Microbiol* (2015) 6:836. doi: 10.3389/fmicb.2015.00836
46. Normile TG, McEvoy K, Del Poeta M. Steryl Glycosides in Fungal Pathogenesis: An Understudied Immunomodulatory Adjuvant. *J Fungi (Basel)* (2020) 6(25):1–16. doi: 10.3390/jof6010025
47. Bouic P, Etsebeth S, Liebenberg R, Albrecht CF, Pegel K, Van Jaarsveld P, et al. Beta-Sitosterol and Beta-Sitosterolglucoside Stimulate Human Peripheral Blood Lymphocyte Proliferation: Implications for Their Use as an Immunomodulatory Vitamin Combination. *Int J Immunopharmac* (1996) 18(12):693–700. doi: 10.1016/S0192-0561(97)85551-8
48. Donald P, Lamprecht J, Freestone M, Albrecht C, Bouic P, Kotze D, et al. A Randomised Placebo-Controlled Trial of the Efficacy of Beta-Sitosterol and Its Glucoside as Adjuvants in the Treatment of Pulmonary Tuberculosis. *Int J Tuberculosis Lung Dis* (1997) 1(6):518–22.
49. Lee JH, Han Y. Ginsenoside Rg1 Helps Mice Resist to Disseminated Candidiasis by Th1 Type Differentiation of CD4+ T Cell. *Int Immunopharmacol* (2006) 6(9):1424–30. doi: 10.1016/j.intimp.2006.04.009
50. Lee JH, Lee JY, Park JH, Jung HS, Kim JS, Kang SS, et al. Immunoregulatory Activity by Daucosterol, a Beta-Sitosterol Glycoside, Induces Protective Th1 Immune Response Against Disseminated Candidiasis in Mice. *Vaccine* (2007) 25(19):3834–40. doi: 10.1016/j.vaccine.2007.01.108
51. Pereira de Sa N, Taouil A, Kim J, Clement T, Hoffmann RM, Burke JE, et al. Structure and Inhibition of Cryptococcus Neoformans Sterylglucosidase to Develop Antifungal Agents. *Nat Commun* (2021) 12(1):5885.
52. Normile TG, Rella A, Del Poeta M. Cryptococcus Neoformans Delta-Sgl1 Vaccination Requires Either CD4+ or CD8+ T Cells for Complete Host Protection. *Front Cell Infect Microbiol* (2021) 11(739027):1–11.
53. Colombo AC, Rella A., Normile T, Joffe LS, Tavares PM, de S Araújo GR, et al. Cryptococcus Neoformans Glucuronoxylomannan and Sterylglucoside Are Required for Host Protection in an Animal Vaccination Model. *mBio* (2019) 10(2):e02909–18. doi: 10.1128/mBio.02909-18
54. Rittershaus PC, Kechichian TB, Allegood JC, Merrill AH Jr, Hennig M, Luberto C, et al. Glucosylceramide Synthase is an Essential Regulator of Pathogenicity of Cryptococcus Neoformans. *J Clin Invest* (2006) 116(6):1651–9. doi: 10.1172/JCI27890
55. Lefrancois L. Development, Trafficking, and Function of Memory T-Cell Subsets. *Immunol Rev* (2006) 211:93–103. doi: 10.1111/j.0105-2896.2006.00393.x
56. Wang Y, Wang K., Masso-Silva JA, Rivera A, Xue C, et al. A Heat-Killed Cryptococcus Mutant Strain Induces Host Protection Against Multiple Invasive Mycoses in a Murine Vaccine Model. *mBio* (2019) 10(6):02145–19. doi: 10.1128/mBio.02145-19
57. Zhai B, Wozniak KL, Masso-Silva J, Upadhyay S, Hole C, Rivera A, et al. Development of Protective Inflammation and Cell-Mediated Immunity Against Cryptococcus Neoformans After Exposure to Hyphal Mutants. *mBio* (2015) 6(5):e01433–15. doi: 10.1128/mBio.01433-15
58. Schwartz RH. T Cell Anergy. *Annu Rev Immunol* (2003) 21(1):305–34. doi: 10.1146/annurev.immunol.21.120601.141110
59. Upadhya R, Lam WC, Hole CR, Parchment D, Lee CK, Specht CA, et al. Cryptococcus Neoformans Cda1 and Cda2 Coordinate Deacetylation of Chitin During Infection to Control Fungal Virulence. *Cell Surf* (2021) 7:100066. doi: 10.1016/j.tcsw.2021.100066
60. Upadhya R, Lam WC, Maybruck B, Specht CA, Levitz SM, Lodge JK, et al. Induction of Protective Immunity to Cryptococcal Infection in Mice by a Heat-Killed, Chitosan-Deficient Strain of Cryptococcus Neoformans. *mBio* (2016) 7(3):e00547-16. doi: 10.1128/mBio.00547-16
61. Chaturvedi AK, Wormley FL. Cryptococcus Antigens and Immune Responses: Implications for a Vaccine. *Expert Rev* (2013) 12(11):1261–72. doi: 10.1586/14760584.2013.840094

62. Gibson JF, Johnston SA. Immunity to Cryptococcus Neoformans and C. Gattii During Cryptococcosis. *Fungal Genet Biol* (2015) 78:76–86. doi: 10.1016/j.fgb.2014.11.006
63. Gratz IK, Campbell DJ. Resident Memory T Cells Show That it is Never Too Late to Change Your Ways. *Nat Immunol* (2020) 21(4):359–60. doi: 10.1038/s41590-020-0637-1
64. Schietinger A, Greenberg PD. Tolerance and Exhaustion: Defining Mechanisms of T Cell Dysfunction. *Trends Immunol* (2014) 35(2):51–60. doi: 10.1016/j.it.2013.10.001
65. Chaturvedi AK, Hameed RS, Wozniak KL, Hole CR, Leopold Wager CM, Weintraub ST, et al. Vaccine-Mediated Immune Responses to Experimental Pulmonary Cryptococcus Gattii Infection in Mice. *PloS One* (2014) 9(8):e104316. doi: 10.1371/journal.pone.0104316
66. Specht CA, Lee CK, Huang H, Tipper DJ, Shen ZT, Lodge JK, et al. Protection Against Experimental Cryptococcosis Following Vaccination With Glucan Particles Containing Cryptococcus Alkaline Extracts. *mBio* (2015) 6(6):e01905–15. doi: 10.1128/mBio.01905-15
67. Fleuridor R, Lees A, Pirofski L. A Cryptococcal Capsular Polysaccharide Mimotope Prolongs the Survival of Mice With Cryptococcus Neoformans Infection. *J Immunol* (2001) 166(2):1087–96. doi: 10.4049/jimmunol.166.2.1087
68. Datta K, Lees A, Pirofski LA. Therapeutic Efficacy of a Conjugate Vaccine Containing a Peptide Mimotope of Cryptococcal Capsular Polysaccharide Glucuronoxylomannan. *Clin Vaccine Immunol* (2008) 15(8):1176–87. doi: 10.1128/CVI.00130-08
69. Milam JE, Herring-Palmer AC, Pandrangi R, Mcdonald RA, Huffnagle GB, Toews GB, et al. Modulation of the Pulmonary Type 2 T-Cell Response to Cryptococcus Neoformans by Intratracheal Delivery of a Tumor Necrosis Factor Alpha-Expressing Adenoviral Vector. *Infect Immun* (2007) 75(10):4951–8. doi: 10.1128/IAI.00176-07
70. Maziarz EK, Perfect JR. Cryptococcosis. *Infect Dis Clin North Am* (2016) 30(1):179–206. doi: 10.1016/j.idc.2015.10.006
71. Kalleda N, Amich J, Arslan B, Poreddy S, Mattenheimer K, Mokhtari Z, et al. Dynamic Immune Cell Recruitment After Murine Pulmonary Aspergillus Fumigatus Infection Under Different Immunosuppressive Regimens. *Front Microbiol* (2016) 7:1107. doi: 10.3389/fmicb.2016.01107
72. Clemons KV, Schwartz JA, Stevens DA. Therapeutic and Toxicologic Studies in a Murine Model of Invasive Pulmonary Aspergillosis. *Med Mycol* (2011) 49(8):834–47. doi: 10.3109/13693786.2011.577822

Conflict of Interest: Author MD is a Co-Founder and the Chief Scientific Officer (CSO) of MicroRid Technologies Inc.

The remaining author declare that the research was conducted in the absence of any commercial or financial relationships that could be construed as a potential conflict of interest.

Publisher's Note: All claims expressed in this article are solely those of the authors and do not necessarily represent those of their affiliated organizations, or those of the publisher, the editors and the reviewers. Any product that may be evaluated in this article, or claim that may be made by its manufacturer, is not guaranteed or endorsed by the publisher.

frontiers | Frontiers in Cellular and Infection Microbiology

ORIGINAL RESEARCH
published: 12 May 2022
doi: 10.3389/fcimb.2022.894297

Environmental Isolation of *Sporothrix brasiliensis* in an Area With Recurrent Feline Sporotrichosis Cases

*Vanessa Brito Souza Rabello[1], Fernando Almeida-Silva[1], Bruno de Souza Scramignon-Costa[1], Beatriz da Silva Motta[1], Priscila Marques de Macedo[2], Marcus de Melo Teixeira[3], Rodrigo Almeida-Paes[1], Laszlo Irinyi[4], Wieland Meyer[4,5] and Rosely Maria Zancopé-Oliveira[1]**

[1] Laboratório de Micologia, Instituto Nacional de Infectologia Evandro Chagas, Fundação Oswaldo Cruz, Rio de Janeiro, Brazil, [2] Laboratório de Pesquisa Clínica em Dermatologia Infecciosa, Instituto Nacional de Infectologia Evandro Chagas, Fundação Oswaldo Cruz, Rio de Janeiro, Brazil, [3] Núcleo de Medicina Tropical, Faculdade de Medicina, Universidade de Brasília (UnB), Brasília, Brazil, [4] Molecular Mycology Research Laboratory, Centre for Infectious Diseases and Microbiology, Faculty of Medicine and Health, Sydney Medical School, Westmead Clinical School, Marie Bashir Institute for Infectious Diseases and Biosecurity, University of Sydney, Westmead Hospital-Research and Education Network, Westmead Institute for Medical Research, Sydney, NSW, Australia, [5] Curtin Medical School, Curtin University, Perth, WA, Australia

OPEN ACCESS

Edited by:
Carlos Pelleschi Taborda, University of São Paulo, Brazil

Reviewed by:
Hector M. Mora-Montes, Universidad de Guanajuato, Mexico
Luana P. Borba-Santos, Federal University of Rio de Janeiro, Brazil

***Correspondence:**
Rosely Maria Zancopé-Oliveira
rosely.zancope@ini.fiocruz.br

Specialty section:
This article was submitted to Fungal Pathogenesis, a section of the journal Frontiers in Cellular and Infection Microbiology

Received: *11 March 2022*
Accepted: *12 April 2022*
Published: *12 May 2022*

Citation:
Rabello VBS, Almeida-Silva F, Scramignon-Costa BdS, Motta BdS, de Macedo PM, Teixeira MdM, Almeida-Paes R, Irinyi L, Meyer W and Zancopé-Oliveira RM (2022) Environmental Isolation of Sporothrix brasiliensis in an Area With Recurrent Feline Sporotrichosis Cases. Front. Cell. Infect. Microbiol. 12:894297. doi: 10.3389/fcimb.2022.894297

Sporotrichosis has been expanding throughout the Brazilian territory in recent years. New outbreaks have emerged, and consequently, the sporotrichosis agents, mainly *Sporothrix brasiliensis*, should remain in the environment somehow. Therefore, the aim of this study was to investigate the presence of *Sporothrix* spp. in the environment from an area of the Rio de Janeiro state, Brazil, with recurrent cases of human and animal sporotrichosis. Abandoned demolition timber wood samples were collected in the garden of a house where the cases of human and feline sporotrichosis have occurred in the last 10 years. The environmental survey revealed a *Sporothrix* spp. colony from the serial dilution cultures of one abandoned demolition wood sample. In addition, a fungal strain isolated from a cat with skin lesions that lived in the house was also included in the study. The species-specific PCR, and calmodulin partial sequencing identified the environmental and cat isolates as *S. brasiliensis*. Furthermore, the phylogenetic analysis performed with the partial sequences of internal transcribed spacer region and constitutive genes (calmodulin, β-tubulin, and chitin synthase) showed high similarity between environmental and cat isolates from the same geographic region. Moreover, the antifungal susceptibility test revealed that the minimal inhibitory concentration of itraconazole from the environment isolate was lower than the cat isolate, while amphotericin B and terbinafine were similar. Our results show that *S. brasiliensis* is able to maintain itself in the environmental material for years. With this, we corroborate that the eco-epidemiology of sporotrichosis is not well

understood, and despite the major occurrence of *S. brasiliensis* in Brazil, it is rarely isolated from the environment.

Keywords: *Sporothrix brasiliensis*, environment, sporotrichosis, timber wood, phylogenetic analysis, Brazil

INTRODUCTION

Sporotrichosis is a subcutaneous mycosis caused by the thermodimorphic fungi of the genus *Sporothrix*. The genus contains at least 51 species that live as saprobes on soil, decaying wood, and plant debris in environments with high humidity (~90%) (Ramírez-Soto et al., 2018). Most *Sporothrix* species are non-pathogenic, but seven species may cause human infection; those include *Sporothrix schenckii*, *S. brasiliensis*, *S. globosa*, *S. luriei*, *S. mexicana, S. pallida, and S. chilensis. These species are able to* infect warm-blooded hosts *since* they are able to develop the process called dimorphism, changing from their saprophytic filamentous stage at ambient temperature to the parasitic yeast form at 35°C–37°C. Among the pathogenic species, *S. schenckii*, *S. brasiliensis*, *S. globosa*, and *S. luriei* are often isolated from humans and animals; the remaining species rarely cause disease, being commonly isolated from environmental sources (Marimon et al., 2007; Rodrigues et al., 2016; Rodrigues et al., 2020; Valeriano et al., 2020). Sporotrichosis occurs after traumatic inoculation *with organic matter harboring these fungi. The main clinical manifestation in humans is the lymphocutaneous form, followed by the fixed cutaneous form, restricted to the local trauma area. Systemic infections are mainly developed in immunocompromised patients (*Zancope-Oliveira et al., 2011*;* Orofino-Costa et al., 2017*).*

The largest outbreak associated to an environmental source occurred at a gold mine in South Africa, between 1938 and 1949, with the description of more than 3,000 cases. The woods used to support the mines were identified as the source of the infection (Helm and Bermam, 1947; Quintal, 2000). Another sporotrichosis outbreak involved 84 sapronotic transmission cases reported in 1988, affecting the people who were exposed to *Sphagnum* moss used to protect and moisten the roots of the tree seedlings in 15 states of the United States (Dixon et al., 1991). In 2011, another outbreak in a gold mine in South Africa was reported, where patients were infected by *S. schenckii*, while environmental isolates were identified as *S. mexicana*. Despite the difference between the species, the probable source of infection was contaminated soil and untreated woods at the gold mine (Govender et al., 2015).

Although the environmental outbreaks related to human sporotrichosis were well described in different geographic regions, there is little knowledge about the ecology of the clinically relevant species related to them. *S. schenckii* is often found from environmental sources from different countries, including Brazil, Argentina, the United States, Germany, Italy, China, and India (Ramírez-Soto et al., 2018). However, other clinical species are rarely isolated from the environment, such as *S. luriei* and *S. brasiliensis*. The latter is the main species described in Brazil, causing important zoonotic outbreaks in different regions of the country (Gremião et al., 2020; Rodrigues et al., 2020). Therefore, the knowledge of *Sporothrix* spp. ecology will provide useful information to support public health management. To address this issue, the current study carried out an environmental survey in an area within a city of Rio de Janeiro state, Brazil, where recurrent cases of the sporotrichosis were reported.

MATERIALS AND METHODS

In 2020, the samples of abandoned demolition woods, from a tree from the Class Magnoliopsida, which include some species of the genera *Paubrasilia*, *Jacaranda*, *Manilkara*, and others that are extensively used in Brazilian building constructions, were collected from a house in Petrópolis, Rio de Janeiro State, Brazil (22°31'51.3"S 43°10'38.2"W), which had a pet cat with sporotrichosis confirmed by the fungal culture in 2017, and other probable human and feline sporotrichosis cases, which occurred in the last 10 years. A pool of environmental samples was collected by friction on the wood surfaces with a sterile transport swab with Amies medium, added with charcoal (ABSORVE, São Paulo, Brazil), and transported at room temperature to the Mycology Laboratory of the Evandro Chagas National Institute of Infectious Diseases (INI/FIOCRUZ). Two swab samples from abandoned woods deposited in distinct locations of the house and wood fragments were collected, with a sterile scalpel, and stored in 15 ml Falcon tubes.

Serial dilutions in sterile distilled water were performed with the swab samples. First, the swabs were vigorously mixed in 300 µl sterile distilled water and ten-fold dilutions were made up to the 10^{-5}. Each dilution was cultured in duplicate on potato dextrose agar (PDA; Becton Dickinson and Company Sparks, MD, USA) and incubated at 25°C for at least 30 days. Colonies that presented macro- and micromorphology suggestive of *Sporothrix* spp. were subcultured on PDA and thermodimorphism was evaluated on brain heart infusion agar (BHI; Becton Dickinson and Company Sparks, MD, USA) at 37°C for 7 days.

The fungal strain isolated from a cat with skin lesions compatible with sporotrichosis that lives in the house where the wood samples was collected was also included in the study. The owner allowed to include the cat in the study, so the fragments of the skin lesions were obtained by biopsy and cultured on Sabouraud dextrose, Mycosel, and BHI agars (Becton Dickinson GmbH). After isolation, the fungal strain was stored at -80°C.

DNA extraction directly from wood fragments was conducted as described by Macedo et al. (2020), using the DNeasy®

PowerSoil® Kit (Qiagen, Hilden, Germany). DNA extraction from *Sporothrix* isolates was performed from the filamentous form of the fungus according to Muniz et al. (2010), with the following modifications: the lysis buffer contained 1M Tris pH 8, 50 mM EDTA, and 20% sucrose, and the DNA was precipitated in 100% ethanol with 3 M sodium acetate.

The DNA extracted directly from the wood samples, from putative *Sporothrix* spp. colonies and from the cat isolate, were used as templates in a species-specific PCR according to Rodrigues et al. (2015). The primers for the three major pathogenic *Sporothrix* species (*S. brasiliensis*, *S. globosa*, and *S. schenckii*) were used in the reactions. The environmental DNA was tested in triplicate, to improve fungal detection odds.

A partial sequencing of the constitutive genes calmodulin, chitin synthase, and β-tubulin (Marimon et al., 2007), and the internal transcribed spacer region (ITS1/2) (Zhou et al., 2014) from clinical and environmental *Sporothrix* isolates were performed in order to conduct a phylogenetic analysis. Automated sequencing was done using the FIOCRUZ Technological Platforms. The sequences from both DNA strands were edited with the software Sequencher version 4.9 and aligned by MEGA version 7. Additional sequences of *Sporothrix* spp. deposited in the GenBank (**Table 1**) were included in the phylogenetic analysis generating a maximum likelihood (ML) tree with 1,000 bootstrap replications to estimate the branch confidence values showed on each branch.

The antifungal agents assessed were itraconazole (ITR), terbinafine (TRB), and amphotericin B (AMB). The serial dilutions of antifungal agents were prepared in dimethyl sulfoxide, and the different working concentrations of antifungal drugs, ranging from 0.015 to 8 mg/L, were distributed in 96-well microplates. The conidial suspension (1–5 × 10^4/ml) from 7-day-old *Sporothrix* spp. cultures on PDA at 35°C was prepared in 3 ml of 0.9% sterile saline solution. The susceptibility test was performed using a broth microdilution assay according to the M38-A2 CLSI reference guidelines (CLSI - Clinical and Laboratory Standards Institute, 2008). The *Sporothrix* suspension was diluted 1:50 in the RPMI 1640 medium buffered with 0.165 mol/L morpholinepropanesulfonic acid (pH 7.0), and 100 µl of each isolate were added to the wells of 96-well microplates. The fungal inoculum without any antifungal agent was used as growth controls, and the sterility controls consisted of only the RPMI medium without fungus or antifungal drugs. The reference strains *Aspergillus fumigatus* ATCC 204305 and *Aspergillus flavus* ATCC 204304 were used as the quality controls of each assay. All tests were performed at least in duplicate; MICs were determined by visual inspection after 48–72 h of incubation at 35°C, as described (CLSI - Clinical and Laboratory Standards Institute, 2008). The MIC of itraconazole and amphotericin B was determined as the lowest concentrations that completely inhibited fungal growth, and for TRB, it was the lowest concentration that resulted in at least 80% reduction in growth.

RESULTS

The skin lesion fragments from the cat (**Figure 1B**) yielded colonies with macro- and micromorphology compatible with *Sporothrix* spp. This cat was treated with itraconazole (100 mg/day) for 3 months, with apparent healing of the lesion. However, after this period, his injuries and general condition progressively worsened. The cat was admitted to a veterinary clinic and died some weeks later. At this point, the fungal isolate from this animal was stored at -80°C.

Three years later, an environmental survey was conducted in the cat´s house (**Figure 1A**) and just one putative *Sporothrix* spp. colony from the 10^{-4} serial dilution of one abandoned demolition wood grew on PDA at 25°C around 28 days after inoculation (**Figure 1C**); in the others, serial dilution was observed in the growth of saprobic fungi or other microorganisms. The *Sporothrix* spp. strain from the cat (**Figure 1E**) was re-grown and evaluated together with the environmental isolate. Both presented conversion to the yeast phase on BHI agar at 37°C, which confirmed their dimorphism (**Figures 1D, F**).

Sporothrix DNA was not detected using species-specific PCR primers for *S. brasiliensis*, *S. schenckii*, or *S. globosa* in the total DNA extracted direct from the wood scrapings. The environmental and cat isolates were identified as *S. brasiliensis* by species-specific PCR and partial calmodulin sequencing. Moreover, the phylogenetic analysis performed with partial calmodulin, chitin synthase, the

TABLE 1 | Isolates and GenBank Identification.

Isolate	Species	CAL	CHS	Bt2	ITS
CBS 120339 (IPEC 16490)	*S. brasiliensis*	AM116899	AM117417	AM116946	KP017087
CFP 01022 (IPEC 19536)*	*S. brasiliensis*	ON014839	ON014840	ON014841	OM949881
CFP 01043*	*S. brasiliensis*	MZ670750	MZ670752	MZ670754	MZ576443
CFP 01042*	*S. brasiliensis*	MZ670751	MZ670753	MZ670755	MZ576444
CBS 359.36	*S. schenckii*	AM117437	AM114872	AM116911	KP017100
FMR 8597	*S. globosa*	AM116907	AM117426	AM116964	FN549904
CBS 937.72	*S. luriei*	AM747302	AM748698	AM747289	AB128012
CBS 302.73	*S. pallida*	AM398396	AM748692	AM498343	KP017078
CBS 120341	*S. mexicana*	AM398393	AM748696	AM498344	FN549906

*Sequences generated in this study, CFP 01043 wood isolate and CFP 01043 cat isolate.

CFP, Collection of Pathogenic Fungi, Instituto Nacional de Infectologia Evandro Chagas, Fundação Oswaldo Cruz, Rio de Janeiro, Brazil; IPEC, Instituto de Pesquisa Clínica Evandro Chagas, FIOCRUZ, Rio de Janeiro, Brazil; CBS, Centraalbureau voor Schimmelcultures, Utrecht, The Netherlands; FMR, Facultat de Medicina i Cien`cies de la Salut, Reus, Spain; CAL, calmodulin gene; CHS, chitin synthase gene; Bt2, β-tubulin gene; ITS, internal transcribed spacer region.

FIGURE 1 | **(A)** Wood disposal in the garden of the studied house. **(B)** Cat with sporotrichosis. **(C, D)** *S. brasiliensis* isolated from wood. **(E, F)** *S. brasiliensis* isolated from cat. **(C, E)** Filamentous form (13 days at 25°C). **(D, F)** Yeast form (7 days at 37°C).

β-tubulin gene, and ITS region sequence showed 100% similarity between the environmental and the cat isolates from the same region (**Figure 2**).

The MIC values from the environmental and cat isolates are described in **Table 2**. In summary, the MIC of TRB was lower than those observed for the other drugs from both isolates. Moreover, the susceptibilities in strains from these two sources were similar for TRB and AMB. The MIC of ITR from the environmental isolate was at two-fold dilutions lower than that observed for the cat isolate.

DISCUSSION

During the major sporotrichosis outbreak in South Africa, *S. schenckii* was found in the timber supporting the mines,

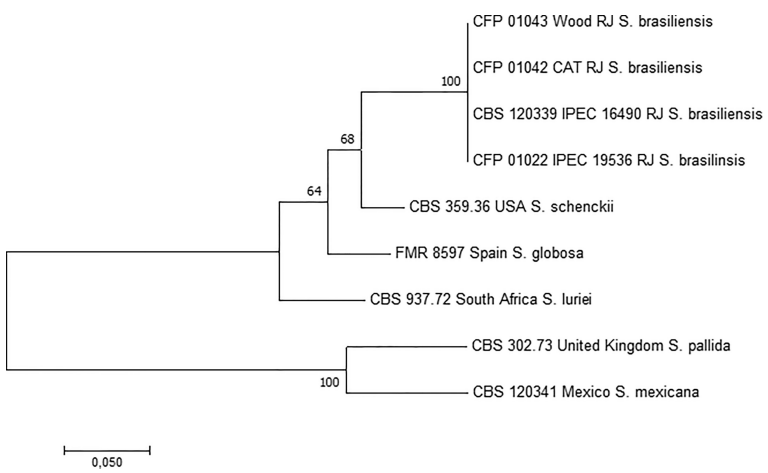

FIGURE 2 | Phylogenetic tree of *Sporothrix* spp., including the studied *S. brasiliensis* isolates studied herein, obtained by ML analysis based on partial sequences of the calmodulin, chitin synthase, β-tubulin genes, and internal transcribed spacer (ITS1, 5.8s, ITS2). The 1,000 bootstrap values are represented on the branches. RJ, Rio de Janeiro state, Brazil.

TABLE 2 | MICs (mg/L) of the *S. brasiliensis* strains evaluated in this study.

Isolates	ITR	TER	AMB
Wood	0.25	0.06	1.0
Cat	1.0	0.06	2.0

ITR, itraconazole; TRB, terbinafine; AMB, amphotericin B.

confirming it as the common environmental source of the infections of more than 3,000 miners (Quintal, 2000). The present work shows that *S. brasiliensis* may also be encountered in timber samples, which can act as environmental sources of infection for humans and animals.

The eco-epidemiology of the sporotrichosis agents is not well known. Moreover, despite the major occurrence of *S. brasiliensis* in Brazil, it is rarely isolated from the environment. Some authors attribute this factor to the low concentration of clinically relevant *Sporothrix* species in the environment (Ramírez-Soto et al., 2018; Rodrigues et al., 2020). However, the high sporotrichosis incidence in Brazil raises the possibility that the environmental *Sporothrix* burden is higher as hypothesized. A study revealed, by whole genome sequencing, that strains from Southeast Brazil, where *S. brasiliensis* first emerged, and Mid-Western Brazil, where *S. brasiliensis* emerged more recently, appear to have separated around two million years ago, supporting different environmental niches for these genotypes (Eudes Filho et al., 2020).

If the environmental *Sporothrix* burden is very high, the uncommon isolation of *Sporothrix* spp. from nature may be related to the limitations of the available detection methods or the paucity of environmental studies on the sporotrichosis agents. Poester et al. (2018) evaluated the presence of *Sporothrix* spp. in soil samples from places in Southern Brazil where zoonotic sporotrichosis also occurs. Despite the 101 samples collected from the residence of cats with sporotrichosis, none of the cultures were positive for *Sporothrix* spp., which could be related to the moderate growth of *Sporothrix* spp, making their detection in soil samples difficult due to the abundant growth of numerous other saprobic microorganisms (Poester et al., 2018). Rodrigues et al. (2014), who did not recover any culture morphologically resampling *Sporothrix* spp. after a direct plating of soil samples, also observed this. In fact, several filamentous fungi, such as *Acremonium*, *Aspergillus*, *Fusarium*, and *Penicillium*, grow faster than *Sporothrix* in culture, so they can dominate the culture media before *Sporothrix* species appear (Ramírez-Soto et al., 2018). Thus, the success of the *Sporothrix* isolation herein reported may be associated to the method of processing the swab culture with an important step of serial dilutions of the sample, reducing the number of other fungi. Moreover, the growth of the environmental sample on PDA could stimulate fungal sporulation, facilitating its isolation. On the other hand, the PDA medium may not inhibit the undesirable fungi, but it also does not hinder the growth of *Sporothrix* spp.

Human and animal cases of sporotrichosis occurred over the last 10 years in the studied house. It is interesting to note that these cases started to occur after a garden area was transformed in a rubbish disposal site. It has been described that sporotrichosis is associated in Brazil with areas of poor sanitary conditions (Silva et al., 2012; Alzuguir et al., 2020). Two hypotheses may explain the occurrence of *S. brasiliensis* in the studied house: the demolition woods already had *S. brasiliensis* that encountered mammal hosts after disposal or the woods became contaminated with the fungus after a case of sporotrichosis in a cat, which present a high fungal burden, that could have been in contact with woods. Either way, our results show that *S. brasiliensis* is able to maintain itself in this environmental material for years. This is reinforced by the isolation of genetically related strains 3 years apart and by the reports of neighbours that some cats with access to this area presented with skin lesions suggestive of sporotrichosis.

Our results also suggest that *S. brasiliensis* infections may occur by sapronotic transmission, and it does not occur exclusively *via* zoonotic transmission as has been previously reported (Rodrigues et al., 2020; Rossow et al., 2020). This is supported by the fact that the *S. brasiliensis* genotype from the environment was identical to that of the cat isolate. Our data are similar to the studies described in Argentina, where many cats with sporotrichosis by *S. brasiliensis* were rescued from abandoned old houses, which contained dirty pine wood floors as a probable source of infection (Etchecopaz et al., 2021). Furthermore, a woodworker also from Argentina acquired the fungus *via* the traumatic inoculation of a pine wood splinter with *S. brasiliensis* being identified from his lesion. However, in these cases, *S. brasiliensis* was not isolated from the pine wood (Etchecopaz et al., 2021), in contrast to that found in our study. Moreover, *S. brasiliensis* was identified in Brazil from cat's feces collected in a sand heap (Montenegro et al., 2014) and from armadillo cave soil samples in Argentina (Etchecopaz et al., 2021).

The isolation of *S. schenckii* from the environment was successfully achieved after mice inoculation with a soil sample (Rodrigues et al., 2014). Nevertheless, this method has major issues for routine use since it requires specific laboratory structure for animal housing, it is costly and time consuming, and, more importantly, it has major ethical aspects related to the use of experimental vertebrate animals. Therefore, other methods need to be used. Molecular methods are emerging as powerful tools for the detection of pathogenic fungi in environmental samples. Species-specific PCR was developed for the identification of *Sporothrix* species in pure cultures or in infected tissues, as observed in an experimental murine model of infection (Rodrigues et al., 2015). In the present study, this method was inefficient to detect *S. brasiliensis* DNA in the environmental material. Poester et al. (2018) also observed negative DNA by species-specific PCR and nested PCR for the five *Sporothrix* species (*S. brasiliensis*, *S. schenckii*, *S. globosa*, *S. mexicana*, and *S. pallida*) from soil samples. It is expected that hundreds of microorganisms co-exist with the pathogenic *Sporothrix* species in the environment, so probably the use of more sensitive methods, capable to detect small amounts of *Sporothrix* DNA among high amounts of DNA from other microorganisms, is necessary for environmental molecular studies for the agents of sporotrichosis. Another problem that

would explain the undetected DNA is that PCR inhibitors are present in environment samples, requiring a massive improvement of this method.

The cat was treated with itraconazole, and the *in vitro* susceptibility of the isolate showed good result for this drug. Therefore, the death of the cat may be related to its immune system or other unknown diseases. Furthermore, the earlier the treatment is started, the higher the chance of cure. In addition, the sporotrichosis treatment is too long mainly for cats, so it is very important to follow it strictly (Gremião et al., 2017). The indiscriminate use of antifungals may lead to the emergence of resistance mechanism drugs. Antifungal resistance is a worldwide challenge mainly for treating invasive fungal infections (Wiederhold, 2017; Fisher et al., 2022). The environmental MIC for ITR was lower than the clinical isolate; however, the number of isolates available in this study is small to make comparisons, but this should be appraised in future studies not only with *Sporothrix* isolates but with other pathogenic fungi as well.

Furthermore, it is important to highlight the issues related to the inadequate disposal of waste observed in the house studied. The demolition wood exposed to rain, humidity, and heat becomes a source for *S. brasiliensis* maintenance in the environment as a potential contamination source for humans and animals. Therefore, education activities are necessary in endemic areas to explain to people how to properly dispose demolition material and to avoid the accumulation of waste and organic matter in inappropriate places. Moreover, it is necessary to know how to treat timber wood to avoid contamination. In the 2011 outbreak of a gold mine in South Africa, it was recommended that all new timber should be treated with tar, making the use of personal protective equipment obligatory, after which, no new cases occurred anymore (Govender et al., 2015). However, some substances to prevent microorganism growth may be toxic for human, animals, and the environment. Therefore, the solution to eliminate the source in the gardens described in this study is not simple but should be discussed since this scenario is common in the hyperendemic area of zoonotic sporotrichosis in Rio de Janeiro State, Brazil (Silva et al., 2012; Alzuguir et al., 2020).

In conclusion, the main agent of sporotrichosis in Brazil, *S. brasiliensis*, may be found living in organic matter as saprobes, thus these materials can be a source of infection by this species for human and animals.

DATA AVAILABILITY STATEMENT

The original contributions presented in the study are included in the article. Further inquiries can be directed to the corresponding author.

ETHICS STATEMENT

Ethical review and approval was not required for the animal study because the study was performed with the clinical data of an animal attended in a routine dignosis for sporotrichosis. The owner of the animal has given permission to use this data after the death of the animal. Written informed consent was obtained from the owners for the participation of their animals in this study.

AUTHOR CONTRIBUTIONS

The first draft of the manuscript was written by VR, RA-P, and PM. VR designed and developed the experiments and FA-S, BS-C and BM did part of wood DNA identification. MT, LI, WM, and RZ-O analyzed the data and corrected the manuscript. All authors read and approved the final version of the manuscript.

FUNDING

This work was supported in part by Conselho Nacional de Desenvolvimento Científico e Tecnológico [CNPq 302796/2017-7] and Fundação Carlos Chagas Filho de Amparo à Pesquisa do Estado do Rio de Janeiro [FAPERJ E-26/202.527/2019]. Moreover, this study was partially supported by the Coordenação de Aperfeiçoamento de Pessoal de Nível Superior – CAPES - Finance Code 001.

ACKNOWLEDGMENTS

The authors thank the staff of the Mycology Laboratory who preserved and recovered the cat clinical strain used in this study. Automated sequencing was done using the Genomic Platform-DNA Sequencing Platform at Fundação Oswaldo Cruz—PDTIS/FIOCRUZ (RPT01A), Brazil. We also thank the support given by INI/Fiocruz (Programa Jovens Pesquisadores).

REFERENCES

Alzuguir, C. L. C., Pereira, S. A., Magalhães, M. A. F. M., Almeida-Paes, R., Freitas, D. F. S., Oliveira, L. F. A., et al. (2020). Geo-Epidemiology and Socioeconomic Aspects of Human Sporotrichosis in the Municipality of Duque De Caxias, Rio De Janeiro, Brazil, Between 2007 and 2016. *Trans. R Soc. Trop. Med. Hyg.* 114, 99–106. doi: 10.1093/trstmh/trz081

CLSI - Clinical and Laboratory Standards Institute (2008). *Reference Method for Broth Dilution Antifungal Susceptibility Testing of Filamentous Fungi. 2nd ed* (Wayne: Clinical and Laboratory Standards Institute), 52.

Dixon, D. M., Salkin, I. F., Duncan, R. A., Hurd, N. J., Haines, J. H., Kemna, M. E., et al. (1991). Isolation and Characterization of *Sporothrix Schenckii* From Clinical and Environmental Sources Associated With the Largest U.S. Epidemic of Sporotrichosis. *J. Clin. Microbiol.* 29, 1106–1113. doi: 10.1128/jcm.29.6.1106-1113.1991

Etchecopaz, A., Toscanini, M. A., Gisbert, A., Mas, J., Scarpa, M., Iovannitti, C. A., et al. (2021). *Sporothrix Brasiliensis*: A Review of an Emerging South American Fungal Pathogen, Its Related Disease, Presentation and Spread in Argentina. *J. Fungi* 7, 170. doi: 10.3390/jof7030170

Eudes Filho, J., Santos, I. B., Reis, C. M. S., Patané, J. S. L., Paredes, V., João Bernardese, J. P. R. A., et al. (2020). A Novel *Sporothrix Brasiliensis* Genomic Variant in Midwestern Brazil: Evidence for an Older and Wider Sporotrichosis Epidemic. *Emerging Microbes Infect.* 9 (1), 2515–2525. doi: 10.1080/22221751.2020.1847001

Fisher, M. C., Alastruey-Izquierdo, A., Berman, J., Bicanic, T., Bignell, E. M., Bowyer, P., et al. (2022). Tackling the Emerging Threat of Antifungal

Resistance to Human Health. *Nat. Rev. Microbiol*. doi: 10.1038/s41579-022-00720-1

Govender, N. P., Maphanga, T. G., Zulu, T. G., Patel, J., Walaza, S., Jacobs, C., et al. (2015). An Outbreak of Lymphocutaneous Sporotrichosis Among Mine-Workers in South Africa. *PloS Negl. Trop. Dis.* 9 (9), e0004096. doi: 10.1371/journal.pntd.0004096

Gremião, I. D. F., Monteiro-Miranda, L. H., Reis, E. G., Rodrigues, A. M., and Pereira, S. A. (2017). Zoonotic Epidemic of Sporotrichosis: Cat to Human Transmission. *PloS Pathog.* 13 (1), e1006077. doi: 10.1371/journal.ppat.1006077

Gremião, I. D. F., Oliveira, M. M. E., Monteiro-Miranda, L. H., Freitas, D. F. S., and Pereira, S. A. (2020). Geographic Expansion of Sporotrichosis, Brazil. *Emerg. Infect. Dis.* 26, 621–624. doi: 10.3201/eid2603.190803

Helm, M. A. F., and Bermam, C. (1947). "The Clinical, Therapeutic and Epidemiological Features of the Sporotrichosis Infection on the Mines," in *Sporotrichosis Infection on Mines of the Witwatersrand. Proceedings of the Transvaal Mine Medical Officers' Association*. Sporotrichosis Infection on Mines of the Witwatersrand. (Johannesburg: The Transvaal Chamber of Mines), 59–47.

Macedo, P. M., Scramignon-Costa, B. S., Almeida-Paes, R., Trilles, L., Oliveira, L. S. C., Zancopé-Oliveira, R. M., et al. (2020). *Paracoccidioides Brasiliensis* Habitat: Far Beyond Armadillo Burrows? *Mem. Inst. Oswaldo Cruz* 115, e200208. doi: 10.1590/0074-02760200208

Marimon, R., Cano, J., Gene, J., Sutton, D. A., Kawasaki, M., and Guarro, J. (2007). *Sporothrix Brasiliensis*, S. Globosa, and *S. Mexicana*, Three New *Sporothrix* Species of Clinical Interest. *J. Clin. Microbiol.* 45, 3198–3206. doi: 10.1128/JCM.00808-07

Montenegro, H., Rodrigues, A. M., Dias, M. A. G., Silva, E. A., Bernardi, F., and Camargo, Z. P. (2014). Feline Sporotrichosis Due to *Sporothrix Brasiliensis*: An Emerging Animal Infection in São Paulo, Brazil. *BMC Vet. Res.* 10, 269. doi: 10.1186/s12917-014-0269-5

Muniz, M. M., Morais, S. T. P., Meyer, W., Nosanchuk, J. D., and Zancope-Oliveira, R. M. (2010). Comparison of Different DNA-Based Methods for Molecular Typing of *Histoplasma Capsulatum*. *Appl. Environ. Microbiol.* 76 (13), 4438–4447. doi: 10.1128/AEM.02004-09

Orofino-Costa, R., Macedo, P. M., Rodrigues, A. M., and Bernardes-Engemann, A. R. (2017). Sporotrichosis: An Update on Epidemiology, Etiopathogenesis, Laboratory and Clinical Therapeutics. *Bras. Dermatol.* 92, 606–620. doi: 10.1590/abd1806-4841.2017279

Poester, V. R., Mendes, J. F., Groll, A. V., Klafke, G. B., Brandolt, T. M., and Xavier, M. O. (2018). *Sporothrix* Spp. Evaluation in Soil of a Hyperendenic Area for Sporotrichosis in Southern Brazil. *Med. Vet.* 19, 1–8, e-52571. doi: 10.1590/1809-6891v19e-52571

Quintal, D. (2000). Sporotrichosis Infection on Mines of the Witwatersrand. *J. Cutan Med. Surg.* 4, 51–54. doi: 10.1177/120347540000400113

Ramírez-Soto, M. C., Aguilar-Ancori, E. G., Tirado-Sánchez, A., and Bonifaz, A. (2018). Ecological Determinants of Sporotrichosis Etiological Agents. *J. Fungi (Basel)* 4 (3), 95 1-11. doi: 10.3390/jof4030095

Rodrigues, A. M., Bagagli, E., Camargo, Z. P., and Bosco, S. M. G. (2014). *Sporothrix Schenckii Sensu Stricto* Isolated From Soil in an Armadillo's Burrow. *Mycopathologia* 177 (3-4), 199–206. doi: 10.1007/s11046-014-9734-8

Rodrigues, A. M., Cruz Choappa, R., Fernandes, G. F., Hoog, G. S., and Camargo, Z. P. (2016). *Sporothrix Chilensis* Sp. Nov. (Ascomycota: Ophiostomatales), A Soil-Borne Agent of Human Sporotrichosis With Mild-Pathogenic Potential to Mammals. *Fungal Biol.* 120, 246–264. doi: 10.1016/j.funbio.2015.05.006

Rodrigues, A. M., Hoog, G. S., and Camargo, Z. P. (2015). Molecular Diagnosis of Pathogenic *Sporothrix* Species. *PloS Negl. Trop. Dis.* 9 (12), e0004190. doi: 10.1371/journal.pntd.0004190

Rodrigues, A. M., Terra-Della, P. P., Gremião, I. D., Pereira, S. A., Orofino-Costa, R., and Camargo, Z. P. (2020). The Threat of Emerging and Re-Emerging Pathogenic *Sporothrix* Species. *Mycopathologia* 185, 813–842. doi: 10.1007/s11046-020-00425-0

Rossow, J. A., Queiroz-Telles, F., Caceres, D. H., Beer, K. D., Jackson, B. R., Pereira, J. G., et al. (2020). A One Health Approach to Combatting. A One Health Approach to Combatting *Sporothrix Brasiliensis*: Narrative Review of an Emerging Zoonotic Fungal Pathogen in South America. *J. Fungi* 6, 247. doi: 10.3390/jof6040247

Silva, M. B. T., Costa, M. M., Torres, C. C. S., Galhardo, M. C. G., Valle, A. C. F., Magalhães, M. A. F. M., et al. (2012). Esporotricose Urbana: Epidemia Negligenciada No Rio De Janeiro, Brasil. *Cad. Saúde Pública* 28, 1867–1880. doi: 10.1590/S0102-311X2012001000006

Valeriano, C. A. T., Lima-Neto, R. G., Inácio, C. P., Rabello, V. B. S., Oliveira, E. P., Zancopé-Oliveira, R. M., et al. (2020). Is *Sporothrix Chilensis* Circulating Outside Chile? *PloS Negl. Trop. Dis.* 14 (3), e0008151. doi: 10.1371/journal.pntd.0008151

Wiederhold, N. P. (2017). Antifungal Resistance: Current Trends and Future Strategies to Combat. *Infect. Drug Resist.* 10, 249–259. doi: 10.2147/IDR.S124918

Zancope-Oliveira, R. M., Almeida-Paes, R., Oliveira, M. M. E., Freitas, D. F. S., and Gutierrez Galhardo, M. C. (2011). New Diagnostic Applications in Sporotrichosis. Skin Biopsy - Perspectives. *InTech*., 336. doi: 10.5772/23590

Zhou, X., Rodriguez, A. M., Peiying Feng, P., Hoog, G. S., et al. (2014). Global ITS Diversity in the *Sporothrix Schenckii* Complex. *Fungal Divers.* 66, 153–165. doi: 10.1007/s13225-013-0220-2

Conflict of Interest: The authors declare that the research was conducted in the absence of any commercial or financial relationships that could be construed as a potential conflict of interest.

frontiers | Frontiers in Cellular and Infection Microbiology

REVIEW
published: 13 June 2022
doi: 10.3389/fcimb.2022.895329

Phaeohyphomycosis in China

Yun He[1,2,3], *Hai-lin Zheng*[1,2], *Huan Mei*[1,2], *Gui-xia Lv*[1,2], *Wei-da Liu*[1,2*] *and Xiao-fang Li*[1,2*]

[1] Institute of Dermatology, Chinese Academy of Medical Science and Peking Union Medical College, Nanjing, China, [2] Institute of Dermatology, Chinese Academy of Medical Science, Jiangsu Key Laboratory of Molecular Biology for Skin Diseases and STIs, Nanjing, China, [3] Skin Disease Prevention and Treatment Institute of Yixing, Yixing, China

Background: Due to more attentions paid to melanized fungi over the past few decades and under the background of the global coronavirus disease 2019 pandemic (COVID-19) the fact that the virus itself and the immunosuppressive agents such as glucocorticoids can further increase the risk of infections of deep mycoses, the number of patients with phaeohyphomycosis (PHM) has a substantial increase. Their spectrum is broad and the early diagnosis and treatments are extremely sticky. This study aims to more comprehensively understand the clinical features of phaeohyphomycosis in China over 35 years and to establish a more applicable systematical classification and severity grades of lesions to guide treatments and prognosis.

Methods: We reviewed 174 cases of proven phaeohyphomycosis reported in Chinese and English language literature from 1987 to 2021 and we also made the accurate classification definitions and detailed information about the epidemiology, species of clinical dematiaceous fungi, minimum inhibitory concentration values, clinical features, treatments, and prognosis.

Results: The mortality of cerebral, disseminated and pulmonary phaeohyphomycosis are 55%, 36%, and 25%. Nearly 19% of patients had poor quality of life caused by the complications such as disability, disfigurements, and blindness. The overall misdiagnosis rate of phaeohyphomycosis was 74%. Moderate to severe rashes are accounting for 82% of subcutaneous phaeohyphomycosis. The areas of the head and face are mostly affected accounting for 16% of severe rashes. Nearly 30% of invasive infections of phaeohyphomycosis are triggered by recurrent lesions. Voriconazole, itraconazole, amphotericin B deoxycholate (AmB-DOC), and terbinafine were most commonly used but diagnosis and treatments of phaeohyphomycosis remain challenging in reality.

Conclusions: Our classifications are likely to be more practical and easier to popularize, and there are still also plenty of characteristics in these non-specific lesions. There're no significant variations in cure rates, or death rates between three grades of lesions. But patients with severe rashes have longer courses and lower effective rates.

Keywords: phaeohyphomycosis, melanized fungi, epidemiology, risk factors, clinical features, diagnosis, treatment strategy, drug sensitive

OPEN ACCESS

Edited by:
Carlos Pelleschi Taborda, University of São Paulo, Brazil

Reviewed by:
Shivaprakash M. Rudramurthy, Post Graduate Institute of Medical Education and Research (PGIMER), India
Luana P. Borba-Santos, Federal University of Rio de Janeiro, Brazil

***Correspondence:**
Wei-da Liu
liumycology@163.com
Xiao-fang Li
lxf3568@163.com

Specialty section:
This article was submitted to Fungal Pathogenesis, a section of the journal Frontiers in Cellular and Infection Microbiology

Received: *13 March 2022*
Accepted: *28 April 2022*
Published: *13 June 2022*

Citation:
He Y, Zheng H-l, Mei H, Lv G-x, Liu W-d and Li X-f (2022) Phaeohyphomycosis in China. Front. Cell. Infect. Microbiol. 12:895329. doi: 10.3389/fcimb.2022.895329

INTRODUCTION

Phaeohyphomycosis is a group of mycoses caused by pigmented fungi characterized by yeast-like cells, hyphae, or a combination of these in tissues. When it comes to PHM, firstly it should be distinguished from the primary implantation mycoses caused by melanized fungi including eumycetoma and chromoblastomycosis (CBM). Eumycetoma, involves deep musculoskeletal tissue, characterized by the presence of granules and sclerotia in sinus secretions (McGinnis, 1983; Revankar and Sutton, 2010). CBM, involves cutaneous tissue, characterized by the muriform cells on histopathology (McGinnis, 1983; Revankar and Sutton, 2010; Queiroz-Telles et al., 2017). Some melanized fungi may cause allergic diseases, but they were extremely rarely reported and would not be further discussed.

PHM is an opportunistic infection that has been reported in patients scattered around the world, which is prevalent in tropical and subtropical areas of the planet (Revankar et al., 2002; Revankar et al., 2004; Revankar and Sutton, 2010). More than 150 species and 70 genera of clinical pathogenic fungi of PHM have been found (Revankar and Sutton, 2010). These melanized fungi affect different hosts and cause diverse syndromes in organisms with different propensities ranging from the superficial to deep tissues which include central nervous system (CNS) infections, disseminated infections, pulmonary infections, deep-local infections, subcutaneous infections, and superficial infections. PHM has been recently found related closely to some immune deficiencies which may be natural, especially the deficiency of the caspase recruitment domain-containing protein 9 (CARD9) gene or acquired (Revankar and Sutton, 2010). Increasingly more attention has been paid to these fungi ever since the past few decades especially under the background of the COVID-19 pandemic when the immunosuppressive agents such as glucocorticoids were widely used. The number of reported patients with PHM has a substantial increase recently (Latawa et al., 2022; Borman et al., 2022). More critically, PHM is often misdiagnosed at an early stage and the treatment remains intractable. At present, there is lack of detailed information about almost all types of PHM from China during 35 years covering the scopes of clinical features, treatments, and prognosis based on a large sample, which also provides more applicable systematic classifications and the severity grads of lesions. To provide more practical information about Chinese experiences in PHM for extensive clinical workers to achieve early diagnosis and better management of this sophisticated mycosis, and therefore, we collected and analyzed the whole attainable case reports of PHM in China from 1987 to 2021.

METHODS

Literature Search

We searched for English resources from PubMed, Google Scholar, and Embase. At the same time, we also searched for Chinese resources from China National Knowledge Internet (CNKI), WanFang and WeiPu. We used the strategy "(China OR Taiwan OR Hong Kong OR Macao) and (phaeohyphomycosis OR black OR dematiaceous OR melanized OR phaeoid)" and the genus names of known clinical major dematiaceous fungi. Cases reported from 1987 to 2021were enrolled.

Inclusion and Exclusion Criteria

Criteria for study inclusion:

1. direct microscopy or histopathology showing dark septate hyphae and/or yeast-like elements from invaded tissue or
2. culture or polymerase chain reaction confirming a melanized fungus from clinical specimen and
3. compatible clinical syndrome

Criteria for study exclusion:

1. repeated reports and patients out of the territory of China and
2. patients diagnosed with chromoblastomycosis or mycetoma and
3. patients diagnosed with allergic disease caused by dematiaceous fungi.

Classification

Refer to the most authoritative reviews published by Sanjay G. Revankar and Flavio Queiroz Telles in 2002, 2004, 2010, and 2017, cases were classified as (Revankar et al., 2002; Revankar et al., 2004; Revankar and Sutton, 2010; Queiroz-Telles et al., 2017):

1. CNS phaeohyphomycosis was defined as cases of primary cerebral infections including brain abscess, meningitis, encephalitis, myelitis, and meningoencephalitis; clinical specimens mainly consist of brain lesions tissues or cerebrospinal fluid (CSF).
2. disseminated PHM were defined as cases with the recovery of the isolate from blood samples or evidence of infections at 2 noncontiguous sites;
3. pulmonary PHM were defined as cases of primary pulmonary infections including pneumonia, asymptomatic solitary pulmonary nodule, and endobronchial lesion; clinical specimens mainly consist of lung or bronchial lesion tissues, sputum, and bronchoalveolar lavage fluid (BALF);
4. deep local PHM were defined as cases of primary local-deep infections including endophthalmitis, invasive rhinosinusitis, and miscellaneous infections; clinical specimens mainly consist of deep local lesion tissues and drainage fluids;
5. subcutaneous PHM were defined as cases of primary subcutaneous infections mainly including nodular cyst, solid papules, and verrucous plaques; clinical specimens mainly consist of either skin lesion tissues or purulent aspirates;
6. keratitis PHM were defined as cases of primary corneal infections; clinical specimens mainly consist of corneal scrapings;
7. superficial PHM were defined as cases of primary superficial infections including onychomycosis, tinea nigra, cutaneous

and mucosal infections; clinical specimens mainly consist of skin or nail scrapings, and mucosal swabs.

Statistical Analysis

We calculated descriptive statistics (frequencies, means, medians) for demographic, clinical, and, laboratory variables. We applied chi-square analysis with Fisher's exact test to compare groups if needed. Excel and SPSS were used in data collection and analysis. P-value ≤ 0.05 is statistically significant.

RESULTS

163 relevant literature were collected, among which 174 patients from 142 articles met the inclusion criteria.

Epidemiology

Since 2000, there had been a rapid growth in the number of reported phaeohyphomycosis in China. The number of cases in the last 20 years was about 6.6 times that of 20 years ago (**Figure 1**). There were 118 (68%) patients from the mainland, 39 (22%) patients from Taiwan, and 17 (10%) patients from Hong Kong. Most cases were sporadic in tropical and subtropical regions, although some cases were in temperate regions, mainly between latitudes of 3°N and 53°N. Most patients came from southern China, including Taiwan, Zhejiang, Jiangsu, and Guangdong provinces (**Figure 2**).

Demographics and Risk Factors

A total of 174 patients were enrolled in this study, including 107 males and 67 females. The ratio of male to female patients was 1·6:1. The mean age at diagnosis was 48 years (range, 2–89 years; median age, 53years). The most common risk factors for phaeohyphomycosis infections were traumas (37%), diabetes (11%), and corticosteroid use (11%). Inherited CARD9 deficiency (7%) was found in either severe refractory or mild PHM infections. Malnutrition (6%), tumors (5%), kidney transplantations (3%), and chemotherapy (2%) were frequent risk factors in patients with disseminated, CNS, deep local, and pulmonary infections. Another 22% of the patients did not find any obvious risk factors (**Table 1**).

Clinical Classification and Features

In 2017, Flavio Queiroz Telles et al. proposed the spectrum of fungal diseases caused by melanized fungi in order from superficial to deep (Queiroz-Telles et al., 2017). Based on their spectrum of diseases, we reclassified the types of phaeohyphomycosis. The mortality rate was prioritized. Cerebral infections were ranked first. Disseminated infections were ranked second and pulmonary infections were ranked third. Given the highest incidence of subcutaneous and corneal infections, they were separated from the deep-local infection types, and therefore seven applicable subclasses were divided. The spectrum of clinical syndromes was summarized as follows (**Table 2**):

A. CNS Infections
B. Disseminated Infections
C. Pulmonary Infections
D. Other Deep Local Infections

▲ Eumycetoma (not included)

E. Subcutaneous Infections

▲ Chromoblastomycosis (not included)

F. Keratitis
G. Superficial Infections

A. CNS Infections

A total of 10 patients were included. Brain abscess was the most common presentation, seen in 6 cases, 3 cases of only brain abscess, and 3 cases combined with meningitis. In addition, there

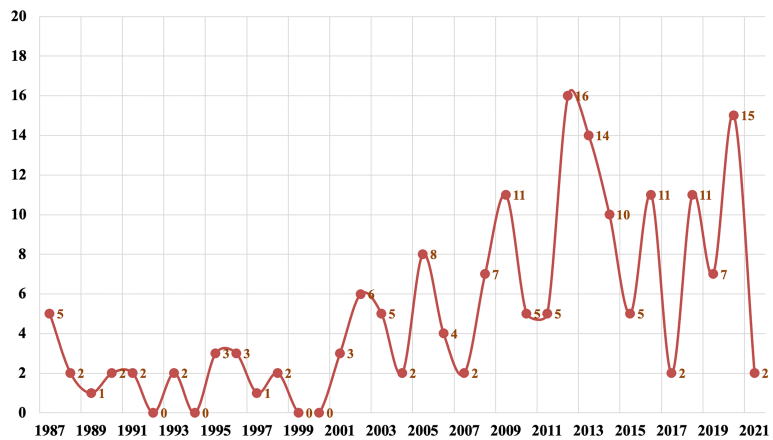

FIGURE 1 | The number of reported cases of PHM in China.

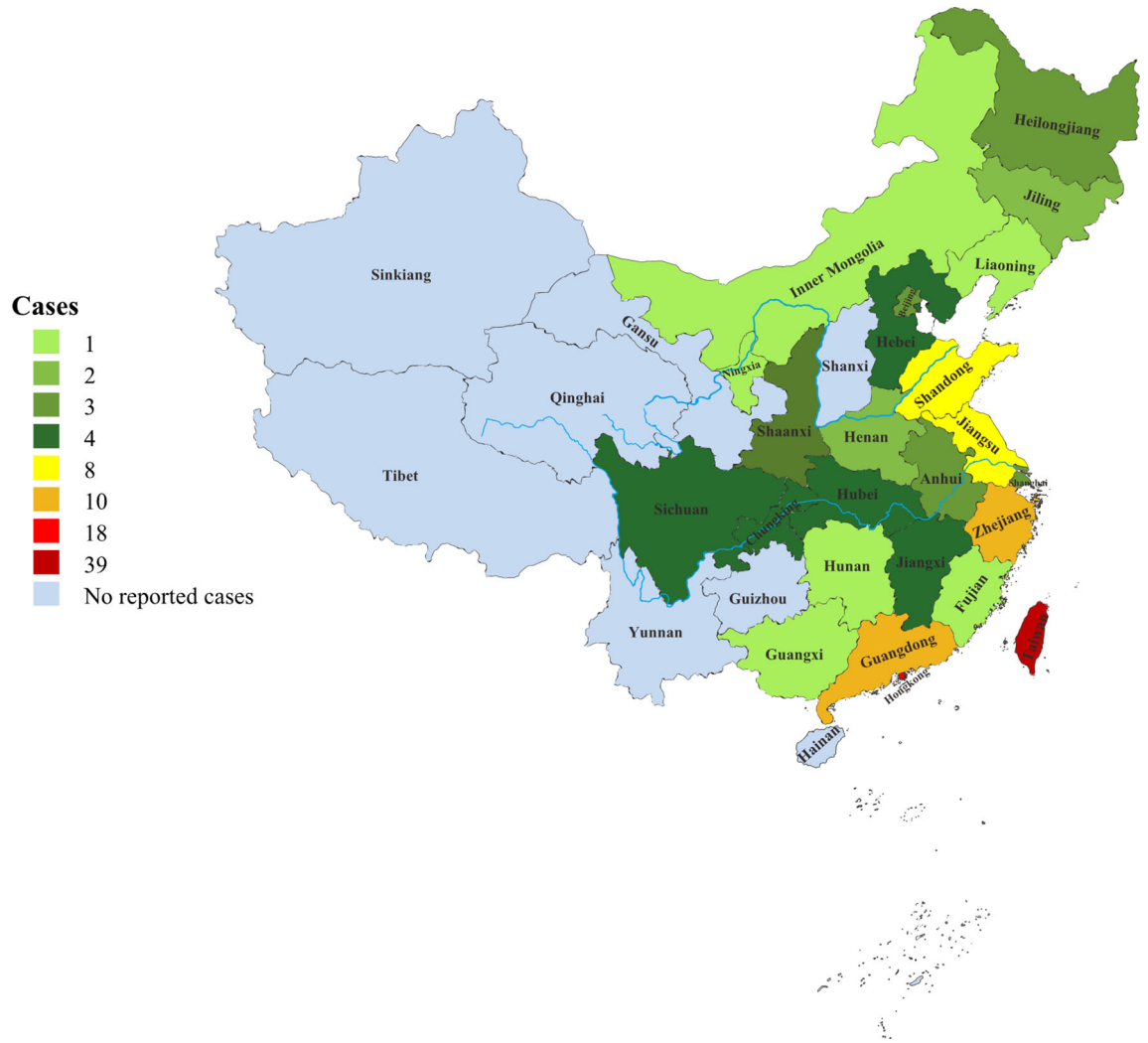

FIGURE 2 | The distribution patterns of PHM in China.

TABLE 1 | Demographics and risk factors of phaeohyphomycosis in China.

Infection type	Total	CNS	Disseminated	Pulmonary	Deep-local	Subcutaneous	Keratitis	Superficial
Demographics (Ratio %)	n=174	n=11	n=11	n=8	n=10	n=85	n=26	n=23
Male	107 (61%)	11 (100%)	5 (45%)	7 (88%)	6 (60%)	49 (58%)	16 (62%)	13 (57%)
Female	67 (39%)	0 (100%)	6 (55%)	1 (13%)	4 (40%)	36 (42%)	10 (38%)	10 (43%)
Age, mean (year)	48	29	26	54	61	51	57	37
Range (year)	2-89	4-73	9-56	10-89	45-75	2-89	22-79	2-87
Risk factor **(Ratio %)**								
Stem cell transplantation	0 (0%)	0 (0%)	0 (0%)	0 (0%)	0 (0%)	0 (0%)	0 (0%)	0 (0%)
Heart transplantation	1 (1%)	0 (0%)	0 (0%)	0 (0%)	0 (0%)	1 (1%)	0 (0%)	0 (0%)
Lung transplantation	0 (0%)	0 (0%)	0 (0%)	0 (0%)	0 (0%)	0 (0%)	0 (0%)	0 (0%)
Liver transplantation	2 (1%)	0 (0%)	0 (0%)	1 (13%)	1 (10%)	0 (0%)	0 (0%)	0 (0%)
Kidney transplantation	5 (3%)	0 (0%)	1 (9%)	1 (13%)	0 (0%)	3 (4%)	0 (0%)	0 (0%)
Graft vs host disease	1 (1%)	0 (0%)	1 (9%)	0 (0%)	0 (0%)	0 (0%)	0 (0%)	0 (0%)
Corticosteroid use	20 (11%)	0 (0%)	1 (9%)	1 (13%)	1 (10%)	14 (16%)	0 (0%)	3 (13%)

(Continued)

TABLE 1 | Continued

Infection type	Total	CNS	Disseminated	Pulmonary	Deep-local	Subcutaneous	Keratitis	Superficial
Other immunosuppressants	9 (5%)	0 (0%)	0 (0%)	1 (13%)	1 (10%)	5 (6%)	0 (0%)	2 (9%)
Malignancy	9 (5%)	1 (9%)	1 (9%)	0 (0%)	2 (20%)	4 (5%)	1 (4%)	0 (0%)
Chemotherapy	3 (2%)	0 (0%)	1 (9%)	0 (0%)	1 (10%)	0 (0%)	1 (4%)	0 (0%)
Neutropenia	2 (1%)	0 (0%)	0 (0%)	1 (13%)	1 (10%)	0 (0%)	0 (0%)	0 (0%)
HIV/AIDS	0 (0%)	0 (0%)	0 (0%)	0 (0%)	0 (0%)	0 (0%)	0 (0%)	0 (0%)
Primary T-cell immunodeficiency	1 (1%)	0 (0%)	0 (0%)	0 (0%)	0 (0%)	1 (1%)	0 (0%)	0 (0%)
CARD9 mutation	12 (7%)	1 (9%)	2 (18%)	0 (0%)	0 (0%)	9 (11%)	0 (0%)	0 (0%)
Malnutrition	10 (6%)	0 (0%)	2 (18%)	1 (13%)	1 (10%)	6 (7%)	0 (0%)	0 (0%)
Pregnancy	3 (2%)	0 (0%)	1 (9%)	0 (0%)	0 (0%)	2 (2%)	0 (0%)	0 (0%)
Trauma	65 (37%)	2 (18%)	5 (45%)	0 (0%)	4 (40%)	25 (29%)	22 (85%)	7 (30%)
Smoke	2 (1%)	0 (0%)	1 (9%)	1 (13%)	0 (0%)	0 (0%)	0 (0%)	0 (0%)
Diabetes mellitus	20 (11%)	2 (18%)	1 (9%)	0 (0%)	4 (40%)	12 (14%)	0 (0%)	1 (4%)
Chronic liver disease	2 (1%)	0 (0%)	0 (0%)	0 (0%)	0 (0%)	1 (1%)	1 (4%)	0 (0%)
Chronic pulmonary disease	11 (69%)	0 (0%)	1 (9%)	2 (25%)	0 (0%)	8 (9%)	0 (0%)	0 (0%)
Chronic renal disease	4 (2%)	0 (0%)	0 (0%)	0 (0%)	1 (10%)	3 (3%)	0 (0%)	0 (0%)
Chronic heart disease	3 (2%)	0 (0%)	0 (0%)	0 (0%)	0 (0%)	3 (3%)	0 (0%)	0 (0%)
No risk factor	38 (22%)	3 (27%)	0 (0%)	2 (25%)	1 (10%)	19 (22%)	2 (8%)	11 (48%)

were 2 cases of encephalitis, 2 cases of myelitis, and 2 cases of meningoencephalitis. The early clinical manifestations were fever, headache, intracranial hypertension, change in consciousness and behavior, hemiplegia, and defect in the visual field. Changes in consciousness and behavior included anxiety, retardation, coma, convulsions, *etc.* Hemiplegia was usually manifested as unilateral limb weakness. The late stage of CNS infections presented with extensive ventricular obstruction, cerebral infarction hydrocephalus, and cerebral hernia, leading to central respiratory failure eventually.

B. Disseminated Infections

A total of 11 patients were included. The most common manifestations were fever and swelling of superficial lymph nodes. Fevers were seen in 6 cases and swollen lymph nodes were seen in 5 cases. The most common original sites of disseminated infections included skins (4), lungs (2), brain (1), lymph node (1), pharynx (1), eye (1), and blood (1). The initial skin manifestations included generalized black warty patches (2) and dark facial erythemas (2). Respiratory and CNS complaints were commonly seen in 3 cases with clinical signs of cough with

TABLE 2 | Infection types of the phaeohyphomycosis in China.

Infection types	Subtypes	Total (Ratio %)	Reference
central nervous system infection	–	11 (6%)	(Wang et al., 1991; Lirng et al., 1995; Lv et al., 2001; Chang et al., 2009; Huang et al., 2011; He, 2012; Chen et al., 2013; Hu et al., 2014; Tong et al., 2020; Bai et al., 2020; Lai et al., 2021)
disseminated infection	–	11 (6%)	(Dai et al., 1987; Wan et al., 1987; Li, 1988; Jiang and Zhang, 1991; Wang et al., 2003; Tseng et al., 2005; Dong et al., 2009; Zhang et al., 2017; Yao, 2018; Wang et al., 2019; Zhang et al., 2019)
pulmonary infection	–	8 (5%)	(Zhao et al., 2002; Woo et al., 2008; Xu et al., 2010; To et al., 2012; Woo et al., 2013; Ye et al., 2014; Wang et al., 2016; Liu et al., 2018)
deep local infection	endophthalmitis	3 (2%)	(Jin et al., 1996; Sun et al., 2010; Liu et al., 2015)
	acute invasive rhinosinusitis	1 (1%)	(Fang et al., 2011)
	hepatic infection	1 (1%)	(Tsang et al., 2021)
	bone and joint infection	2 (1%)	(To et al., 2012; Wang et al., 2014)
	peritonitis	1 (1%)	(Lau et al., 2003)
	pleuritis	1 (1%)	(Liu et al., 1997)
	lymphnoditis	1 (1%)	(Liou et al., 2002)
subcutaneous infection		85 (49%)	(Zheng et al., 1988; Wang et al., 1989; Lv, 1990; Zhao et al., 1990; Zhang et al., 1990; Hsu and Lee, 1993; Lin et al., 1995; Chuan and Wu, 1995; Li et al., 1996; Zhao et al., 2001; Liou et al., 2002; Chen et al., 2003; Matsushita et al., 2003; Yang

(Continued)

TABLE 2 | Continued

Infection types	Subtypes	Total (Ratio %)	Reference
			et al., 2004; Lv et al., 2005; Xia et al., 2005; You et al., 2005; Li et al., 2005; Yu et al., 2006; Hang et al., 2006; Chen et al., 2006; Chen et al., 2008; Liu and Wu, 2008; Huang et al., 2008; Fan et al., 2009; Zhou et al., 2009; Lin et al., 2009; Jin et al., 2009; Zeng et al., 2010; Lin et al., 2010; Zhang et al., 2010; Lv et al., 2011; Sang et al., 2011; Sang et al., 2012; Dong et al., 2012; Zhou et al., 2012; Lin et al., 2012; Li et al., 2012; Ge et al., 2012; Woo et al., 2013; Hsiao et al., 2013; Cai et al., 2013; Liu et al., 2013; Chen et al., 2014; Wang et al., 2014; Tsang et al., 2014; Tsang et al., 2014; Hsu et al., 2015; Hu et al., 2015; Zhang and Lian, 2015; Wang et al., 2015; Chen et al., 2016; Zhou et al., 2016; Chen et al., 2016; Hu et al., 2016; Ng et al., 2017; Ge et al., 2017; Zhou et al., 2018; Wang et al., 2018; Xie et al., 2018; Feng et al., 2018; Yang et al., 2018; Yang et al., 2019; Liu et al., 2019; Wang et al., 2019; Huang et al., 2019; Guo et al., 2019; Gong et al., 2020; Linqiang et al., 2020; Chen et al., 2021; Yu et al., 2021; Pan et al., 2021)
keratitis		26 (15%)	(Huang et al., 1998; Liu et al., 2002; Zhu and Xu, 2003; Tsai et al., 2006; Zhang et al., 2006; Cao and Wu, 2008; Li et al., 2009; Yang et al., 2009; Liu et al., 2011; Lu et al., 2012; Qiu and Yao, 2013; Wang et al., 2016; Zhong et al., 2007; Hung et al., 2020)
superficial infection	tinea nigra	10 (6%)	(Gu et al., 1996; Liu et al., 2001; Dai and Zhang, 2004; Wu et al., 2005; Pi et al., 2005; Qu et al., 2007; Wang et al., 2008; Tan et al., 2014; Lu et al., 2016; Guo et al., 2016)
	cutaneous	4 (2%)	(Hsu and Lee, 1993; Li et al., 2008; Woo et al., 2013; Chen et al., 2016)
	onychomycosis	9 (5%)	(Yu et al., 2009; Huang et al., 2009; Sun and Ju, 2011; Woo et al., 2013; Wen et al., 2016; Shi et al., 2016)

sputum, dyspnea, and hemiplegia left. Four patients' original infections came from the eyes, pharynx, and face finally spreading to the center in the advanced disease stages. One patient's pulmonary infection eventually progressed to fatal sepsis. All five patients died. The positive blood cultures were seen in 3 patients and blood was the only site of infection in one patient. All infected sites by dematiaceous fungi were ranged in order from the commonest to the least common, including skin (6), brain (5), lymph node (4), bone (4), blood (3), lung (3), sinus (2), pharynx (2), oral (1), eye (1), muscle (1), liver (1), gall (1) and spleen (1). The mean number of organs involved was 3 per patient (range, 1–7 organs).

C. Pulmonary Infections

A total of 8 patients were included. The clinical manifestations included pneumonia (5), asymptomatic pulmonary nodules (2), and endobronchial lesions (2). The commonest early symptoms were fever, cough with sputum, and exacerbation to empiric antibiotic therapies. The number of melanized fungi pneumonia added up to 5 progressing rapidly to respiratory failure, hypoxemia, and sepsis in short term. Three of these patients died of multiple organ failures due to uncontrolled fungal pneumonia.

D. Other Deep Local Infections

a. Endophthalmitis

Three patients were included. Palpebral tuberosity was presented in one patient. A progressive corneal ulcer to endophthalmitis was seen in the other two cases. The initial symptoms had foreign body sensations and impaired visions. Later there would be increased intraocular pressures and intense pains.

b. Acute Invasive Rhinosinusitis

One patient was included. Left nasal obstruction with yellow discharge and burning pain from the face to the head were the initial symptoms. Left eyelid ptosis, impaired vision, and exophthalmos occurred for half a month. Progressive peripheral facial paralysis combined with vision and hearing loss was seen in the late stage of the infection, which resulted in severe Rhino-Orbito-Brain Infection Syndrome.

c. Miscellaneous Infections

Two patients with bone and joint infections mainly presented suppurative arthritis of the right knees, progressive painful swellings, and joint fluids. One patient with hepatic infection had liver abscesses and progressive abdominal pain. Lymphnoditis was seen in one patient with two palpable lymph nodes in the left axilla (2 x 2 cm and 1.5 x 1 cm). Peritonitis in a single case in which the clinical features included diarrhea, progressive aggravated periumbilical pain, tenderness, and rebound pain. Pleuritis in one patient had the manifestation of progressive aggravated right thoracalgia with massive pleural effusion.

E. Subcutaneous Infections

A total of 85 patients were included. Referred to the authoritative review of Flavio Queiroz Telles, subcutaneous lesions were classified into three grades (**Table 3**, **Table 4**, **Figure 3**, **Figure 4**) (Revankar and Sutton, 2010). Moderate to severe rashes are the most common accounting for 82% (70 of 85). Infiltrating plaque (72%, 28 of 39) and solid or cystic nodules (44%, 17 of 39) were the most common in moderate rashes. Verrucous plaques in severe rashes (45%, 14 of 31) were more common. Mild lesions were dominated by single plaque and nodules (67%, 10 of 15). Secondary lesions mostly included crusts, purulence, and ulcers. Vesicular, purpura, and sinus were less common. Mild and moderate lesions were mostly seen on the arms and legs, while severe lesions mostly occurred on the areas of the head, face, and upper limbs. In the late stages of infections, the invasions of the nasal mucosa, eyes, pharynx, muscles, bones, and lymphatics were not rare (26%, 8 of 31). About 36% of disseminated types of

TABLE 3 | Clinical severity gradation and criteria classification in patients with subcutaneous PHM.

Severity Grade	Classification Criteria
Mild	a single plaque, nodule, or eschar with a diameter<5 cm
Moderate	single or multiple lesions such as nodules, plaques, or verrucous occurring alone or in combination, covering one or two adjacent skin areas, with a diameter between 5–15 cm
Severe	any type of skin lesion alone or in combination covering extensive body areas or invasion of subcutaneous fat, muscle, bone, or other adjacent tissue and not identified as the disseminated infection

phaeohyphomycosis in China developed from chronic and recurrent rashes. The chief complaints of these patients were pain (12%, 10 of 85) and itching (25%, 21 of 85). There're no significant differences in either curative rates (P=2.06) or death rates (P=2.57) among mild, moderate, and severe rashes. They are approaching a level of significant differences in effective rates and the average treatment courses among the three kinds of rashes. The data showed that the more severe the rash is, the lower the effective rates (P=0.08) and the longer average treatment course (125,134 and 239 days respectively, P=0.098)

TABLE 4 | Severity gradation and clinical manifestation in patients with subcutaneous PHM.

Severity of disease	Mild n=15	Moderate n=39	Severe n=31	Total n=85
Diameter				
≤5cm	15 (100%)	0 (0%)	0 (0%)	15 (18%)
>5cm and ≤15cm	0 (0%)	39 (100%)	2 (6%)	41 (48%)
>15cm	0 (0%)	0 (0%)	29 (94%)	29 (34%)
Adjacent Tissue Invasion				
Fat	0 (0%)	0 (0%)	2 (6%)	2 (2%)
Muscle	0 (0%)	0 (0%)	2 (6%)	2 (2%)
Nasal Mucosa	0 (0%)	0 (0%)	1 (3%)	1 (1%)
Maxilla	0 (0%)	0 (0%)	1 (3%)	1 (1%)
Type of Lesion				
Papule	1 (7%)	5 (13%)	9 (29%)	15 (18%)
Nodule	5 (33%)	17 (44%)	16 (52%)	38 (45%)
Plaque	5 (33%)	28 (72%)	21 (68%)	54 (64%)
Verruca	2 (13%)	10 (26%)	14 (45%)	26 (31%)
Tumor	3 (20%)	1 (3%)	3 (10%)	7 (8%)
Swelling	0 (0%)	7 (18%)	4 (13%)	11 (13%)
Vesicle	0 (0%)	0 (0%)	1 (3%)	1 (1%)
Purpura	0 (0%)	2 (5%)	2 (6%)	4 (5%)
Purulence	2 (13%)	23 (59%)	12 (39%)	37 (44%)
Black Dot	0 (0%)	3 (8%)	2 (6%)	5 (6%)
Errhysis	0 (0%)	0 (0%)	5 (16%)	5 (6%)
Ulceration	1 (7%)	17 (44%)	11 (35%)	29 (34%)
Necosis	0 (0%)	2 (5%)	2 (6%)	4 (5%)
Crust	4 (27%)	21 (54%)	17 (55%)	42 (49%)
Cicatricial	0 (0%)	3 (8%)	7 (23%)	10 (12%)
Sinus	0 (0%)	0 (0%)	1 (3%)	1 (1%)
Infected Body Part				
One Body Part				
Head and neck	3 (20%)	10 (26%)	5 (16%)	18 (21%)
Upper limb	8 (53%)	14 (36%)	4 (13%)	26 (31%)
Lower limb	4 (27%)	12 (31%)	3 (10%)	19 (22%)
Trunk	0 (0%)	0 (0%)	1 (3%)	1 (1%)
Bottock	0 (0%)	0 (0%)	2 (6%)	2 (2%)
Two Body Parts				
Head and neck+Upper limb	0 (0%)	1 (3%)	2 (6%)	3 (4%)
Head and neck+Trunk	0 (0%)	0 (0%)	2 (6%)	2 (2%)
Head and neck+Buttock	0 (0%)	0 (0%)	1 (3%)	1 (1%)
Upper limb+Lower limb	0 (0%)	0 (0%)	3 (10%)	3 (4%)
Upper limb+Trunk	0 (0%)	0 (0%)	1 (3%)	1 (1%)
Three Body Parts or More	0 (0%)	0 (0%)	7 (23%)	7 (8%)
Symptom				
Pain	2 (13%)	5 (13%)	3 (10%)	10 (12%)
Itchy	3 (20%)	9 (23%)	9 (29%)	21 (25%)

FIGURE 3 | Clinical types of lesions observed in patients with PHM. **(A)** Glossy papules lesions on the right hand. (Reproduced from reference Linqiang et al. (2020) [original **Figure 1B**]) **(B)** Yellowish verrucous plaques on the left hand. (Reproduced from reference Chen et al. (2008) [original **Figure 1A**]) **(C)** Sporotrichoid nodules lesions on the left forearm. (Reproduced from reference Yu et al. (2021) [original **Figure 1D**]) **(D)** Swelling erythematous erosions and necrosis on the left little finger. (Reproduced from reference Lin et al. (2009) [original **Figure 1**]) **(E)** Infiltrative erythematous plaques surrounded by little papules on the left forearm. (Reproduced from reference Wang et al. (2004) [original **Figure 2**]) **(F)** Infiltrating red plaques on both sides of the face and the upper lip; disfiguring verrucous plaques and ulcers on either side of the nasal ala. (Reproduced from reference Wang et al., (2004) [original **Figure 1**]) **(G) (H)** Nodules, papules, hemorrhagic vesicles, and pustules lesions on the bilateral forearm and trunk. (Reproduced from reference Pan et al. (2021) [original **Figure 1A, B**]) **(I)** Infiltrative swelling erythematous plaques on the face with purulent, smelly discharge. (Reproduced from reference Yan et al. (2016) [original **Figure 1A**]).

will be. We concluded that the severity of lesions is directly related to the prognosis of the disease and the immune state, which may predict the patient's clinical outcome.

F. Keratitis

A total of 26 patients were involved. The main manifestations were inflammatory infiltrations of the corneal epithelium. They began as well-defined grayish-white or brown patches and then progressed to deep ulcers, which could be accompanied by anterior chamber inflammatory exudations, empyemas, and pupil deformations. The clinical manifestations mainly included foreign body sensations, blurred visions, photophobia tears, and swelling pains. Moreover, empirical antibiotic therapy often failed. In the known data there were 14 cases of right eyes and 7 cases of left eyes. There were two cases of central types, one case of paracentral type, and one case of peripheral type. In addition, seven ulcers were spanning from the peripheral to the paracentral corneas. The available data on sizes of the corneal ulcers were large (>6mm) in 2 cases, medium (2-6mm) in 6 cases, and small (<2mm) in 2 cases.

FIGURE 4 | Lesions of PHM with different severity grades. **(A–C)** Mild forms (**(A)**: Reproduced from reference Linqiang et al. (2020) [original **Figure 1A**]); **(B)**: Reproduced from reference Huang et al. (2008) [original **Figure 1**]; **(C)**: Reproduced from reference Lin et al. (2010) [original **Figure 1A**]); **(D–F)** Moderate forms (**(D)**: Reproduced from reference Liu et al. (2013) [original **Figure 1**]; **(E)**: Reproduced from reference Yu et al. (2021) [original **Figure 1G**]; **(F)**: Reproduced from reference Lv et al. (2005) [original **Figure 1**]); **(G–I)** Severe forms (Reproduced from reference Huang et al. (2019) [original Figure **A–C**]).

G. Superficial Infections

a. Onychomycosis

Nine patients were included. The first toenail was the preferred site in the disease. The nails majorly developed turbid and thickened with debris. And then the infected nails cracked, exfoliated, and destroyed. The colors of nails were potentially from white-yellow to black-brown.

b. Tinea Nigra

Ten patients were included. Lesions were characterized by the round, banded, or irregular black patches with scaling occurring on the palms and anterior thorax.

c. Cutaneous Lesion

Four patients were included. Dark-brown macules and papules were found on the lower jaw, crus, and pedis. One patient was accompanied by interphalangeal macerations, erosions, and rhagades on the left foot.

Diagnosis

Fast diagnosis is often critical for the survival of fatal invasive fungal infections, especially crucial for the drugs of systemic phaeohyphomycosis as the usually poor outcome of treatment. The European Society of Clinical Microbiology and Infectious Diseases (ESCMID) and European Confederation of Medical

Mycology (ECMM) joint clinical guidelines recommended the diagnosis of systemic PHM in 2014 including histopathology, culture, and sequencing for definitive species identification (Chowdhary et al., 2014).

Traditionally, the diagnosis of PHM requires a combination of the patient's clinical manifestations and mycological confirmations (**Figure 5**). The most specific and persuasive diagnostic elements are yellowish-brown hyphae with or without budding cells in skin scrapings, stained tissue slices, aspirated pus, or surgical drainage (Chowdhary et al., 2014). The evidence can be obtained directly by KOH microscopic examination, pathology, fungal culture, or animal models. When the infections are superficial or on the corneal, diagnosis can be made by direct microscopy, and biopsy is not needed. However, pathological biopsy remains the gold standard when diagnosing cerebral, pulmonary, and deep-local infections, as it is not uncommon that the early-stage CSF, BALF and drainage fluid examinations generally show negative fungal cultures or smears. In our study, pieces of evidence of fungal elements were found in 88% (153 of 174) cases that underwent pathological examinations. In subcutaneous infections, pathological diagnosis is based on the clinical manifestations of PHM lesions (Queiroz-Telles et al., 2017). Microscopically, the nodular cyst mainly has palisading epithelioid macrophages at the inner edge of the abscess. The lumen of the abscess often contains necrotic debris mixed with polymorphonuclear leukocytes and the mycelium is prominently seen in the wall of the abscess. The solid papules revealed a thickening epidermis near the hair follicles. Dermal edema, capillary dilation with inflammatory cell infiltration, and acanthosis with granuloma formation are common. Dark fungal elements can be seen within giant cells in the tissue. The old verrucous plaques show hyperkeratosis, parakeratosis, and acanthosis. Lymphocytes, histiocytes, plasma cells, and giant cells are always surrounded by a thick zone of fibroblasts and collagen. The fungal cells are present as yeastlike cells in short chains or toruloid hyphae. The detection rate of fungal elements can be improved in pathologic examination by special staining. Hematoxylin and eosin stain (H&E) stain are the most used, Fontana-Masson stain and Gomori methenamine silver (GMS) stain are sensitive for the detection of fungal cells when fungal elements are scarce (Yan et al., 2019).

However, different species of dark molds cannot be distinguished by pathological sections alone. That's why we emphasize the necessity of simultaneous culture. Isolation on common sabouraud dextrose agar (SDA) is feasible. It is recommended to turn to plant-based media such as potato dextrose agar (PDA), corn, and oat dextrose agar due to the poor sporulation in part of dark fungi. Most pathogens can

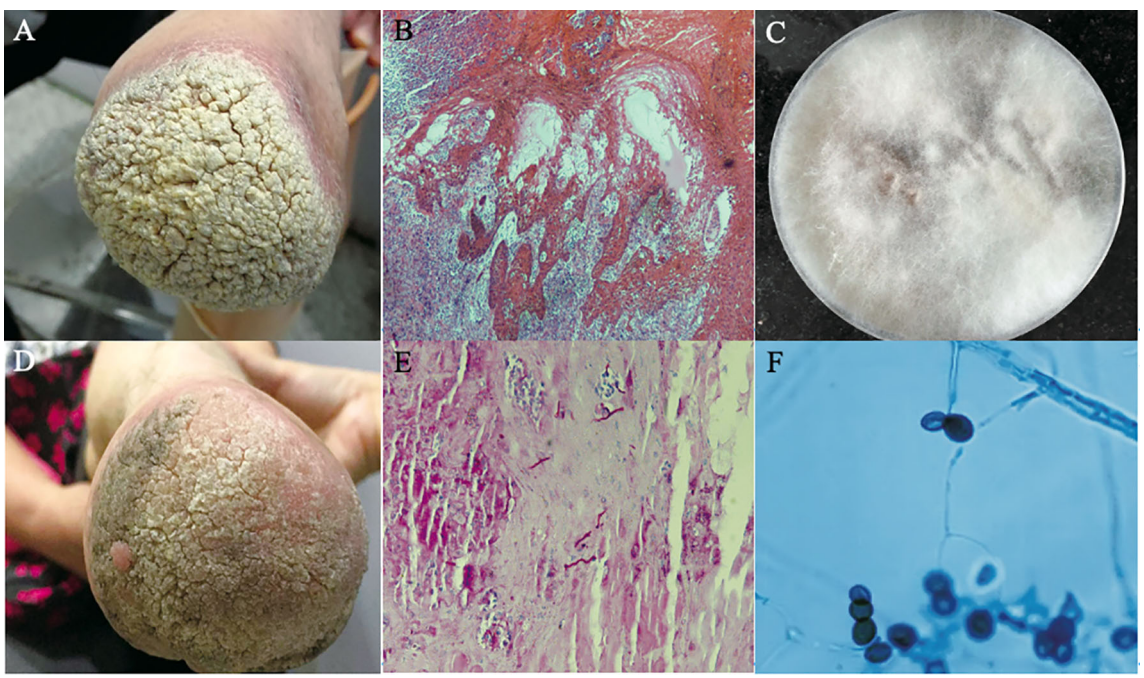

FIGURE 5 | Diagnosis of a case of PHM caused by *Arthrinium phaeospermum*. **(A)** Hypertrophic verrucous plaques with basal infiltrating erythema at the distal left lower extremity in a 59-year-old female with a history of double limb amputations for 20 years; **(B)** Resolved lesions upon follow up after one month; **(C)** Hematoxylin-eosin **(HE)** stained tissue sections showed papillomatous hyperplasia of the spinous layer, mild interspinous cell edema, vascular hyperplasia of the dermal papillary layer, scattered dotted cell infiltration and collagen fiber hyperplasia (HE × 40); **(D)** Periodic acid-Schiff (PAS) stained tissue sections showed scattered hyphae on the epidermis (PAS × 100); **(E)** Colonies on sabouraud dextrose agar (SDA) at 26°C for 2 weeks were hairy, velvety and greyish-white on the front and orange on the back; **(F)** Structures under microculture on potato dextrose agar (PDA) showed that transparent conidia grew from calabash type mother cells and produced lateral conidia. The lens of the conidia eye was black and brown, with a linear bud splitting in middle latitude (lactophenol-cotton blue stain × 400); (Reproduced from reference Zhou et al. (2016) [original **Figure 1**–6]).

develop visible colonies during 1–2 weeks from the initial pale white to the dark colony. The specimens ought to be incubated at 25° to 30°C for 4 weeks before being discarded as negative. Nearly 99% (173 of 174) cases in China obtained dark fungi strains through cultures. Morphological identifications were done in 167 cases. However, confirmation of phenotypic characteristics highly depends on experienced specialists and needs a long cycle. And its limitation of identification to the genus level makes it impossible to provide an early definitive specific diagnosis.

Conservative culture methods have demerits and cannot offer reliable and rapid information to achieve optimal disease management. Sequence analysis of the internal transcribed spacer (ITS) and D1/D2 regions of rDNA are recommended for effective and accurate molecular identification of dark fungi, among which the ITS region has been widely regarded as the universal barcode for the classification of dark fungi. Nearly 54% (94 of 174) cases in China obtained definitive species based on sequence analysis combined with morphological characteristics except for one patient directly through ITS sequencing without fungal culture. It confirms the theory that molecular identification directly from clinical samples is another alternative approach for species identification. The molecular approach especially nuclear ITS sequencing was the most used, accounting for 85% (80 of 94). In addition, 5.8s rDNA, 18s rDNA, 26s rDNA, 28s rDNA, β-tubulin, β-actin, Chitin synthase, Plasma membrane ATPase, (glyceraldehyde-3-phosphate dehydrogenase) *gpd*, (translation elongation factor 1-alpha) *TEF*, (RNA polymerase II largest subunit) *RPB1*, and (the second largest subunit of RNA polymerase II) *RPB2* were used in combination with ITS sequences to verify inter/intra specific variations and to identify new species.

Although the molecular methods are faster than controversial techniques, they have higher cost and are susceptible to contamination due to multi-step processes. Sometimes DNA fragments encoding melanin may inhibit PCR amplification and the limited existing GenBank database may bring difficulty in identifying dark fungi strains (Paul et al., 2017). Around 2010, a technology named MALDI-TOF MS was introduced into the clinical microbiology territory as a more effective and faster diagnostic technique than DNA sequencing (Lau, 2021). It would take 5-9 days for sequence identification of melanized fungi whereas it would take shorter times about 3-7 days for MALDI-TOF MS (Paul et al., 2019). There was also one strain identified as *Phialemonium* species by the use of matrix-assisted laser desorption ionization time–of–flight mass spectrometry (MALDI-TOF MS). With the continuous improvement of the database in the future, this technology will become mature and more widely used for dark mold identification.

In our study, there were a total of 55 dark fungi strains that caused PHM in China (**Supplementary file Table 2**). The most common species of strains were *Exophiala* spp. (33%, 58 of 174) Twelve strains were first reported to cause PHM in the world (**Table 5**). The species identification in China mainly depends on a combination of phenotypic and morphologic features. And also, we found plenty of points of differences in clinical pathogenic strains between China and foreign countries (**Table 6**).

Differential Diagnosis

Clinically, clinical presentations of phaeohyphomycosis are particularly non-specific in the early stages. They can mimic a variety of infectious and other diseases (**Table 7**). It is super important to distinguish PHM from a big variety of other confusable diseases as early as possible.

Treatment and Outcome

In this study, we have made a detailed framework to link the treatment with the prognosis of the phaeohyphomycosis patients in China (**Table 8**, **Supplementary Table 3**). The main antifungal agents used in cerebral PHM were triazoles plus amphotericin B deoxycholate (AmB-DOC)/liposomal amphotericin B (L-AmB), among triazoles voriconazole was the most used. Cerebral cysts were usually combined with surgeries. The disseminated infections mainly used triazoles plus AmB-DOC/L-AmB, terbinafine, or 5–fluorocytosine (5-FC). Voriconazole, itraconazole, fluconazole, and ketoconazole all had been tried. Most pulmonary infections were initially treated with combination therapy, including caspofungin plus AmB-DOC or voriconazole, and maintained with oral itraconazole or voriconazole in the stable phases. Deep-local

TABLE 5 | Twelve strains first reported to cause phaeohyphomycosis in the world.

First Auther (Reference)	Year	Region	Sex/age	Subtype	Genus
Chen Qiuxia (Hang et al., 2006)	2008	Guangdong	M/43 y	subcutaneous	*Cladosporium sphaerospermum*
Dong Mingli (Lu et al., 2016)	2008	NA	M/77 y	subcutaneous	*Knufia epidermidis*
Dong Mingli (Wang et al., 2003)	2009	Jiangsu	F/20 y	CNS	*Exophiala asiatica*
Lv Guixia (Lin et al., 2010)	2011	NA	M/57 y	subcutaneous	*Corynespora cassiicola*
Ge Yiping (Li et al., 2012)	2012	Zhejiang	M/7 y	subcutaneous	*Ochroconis tshawytschae*
Patrick C Y Woo (Xu et al., 2010)	2013	Hong Kong	F/68 y	onychomycosis	*Exophiala hongkongensis*
Chi-Ching Tsang (Liu et al., 2013)	2014	Hong Kong	M/55 y	subcutaneous	*Phialemoniopsis hongkongensis*
Chi-Ching Tsang (Wang et al., 2014)	2014	Hong Kong	M/74 y	subcutaneous	*Hongkongmyces pedis*
Wang Luxia (Lu et al., 2012)	2015	Guangdong	M/54 y	corneal	*Bipolaris oryzae*
Guo Yanyang (Gong et al., 2020)	2019	Shaanxi	F/19 y	subcutaneous	*Pallidocercospora crystallina*
Deng Linqiang (Chen et al., 2021)	2020	Jiangxi	F/45 y	subcutaneous	*Hongkongmyces snookiorum*
Chi-Ching Tsang (Liu et al., 2015)	2021	Hong Kong	M/65 y	Liver	*Pleurostoma hongkongense*

F, female; M, male; NA, not available

TABLE 6 | The differences in strains in PHM between China and foreign countries.

Infection Types	Domestic (No., ratio%)	Foreign (Revankar and Sutton, 2010)
CNS	*Exophiala dermatitidis* (4, 36%); *Cladophialophora bantiana* (2, 18%).	*Cladophialophora bantiana; Rhinocladiella mackenziei; Ochroconis gallopava*
Disseminated	*Exophiala dermatitidis* (3, 27%); *Exophiala spinifera* (2, 18%)	*Scedosporium apiospermum; Exophiala dermatitidis; Exophiala oligosperma*
Pulmonary	*Chaetomium* spp (2, 25%); *Exophiala* spp (2, 25%).	*Scedosporium prolificans; Cladophialophora bantiana*
Subcutaneous	*Exophiala* spp (25, 29%); *Cladosporium* spp (6, 7%); *Phialophora* spp (5, 6%); *Veronaea* spp (5, 6%); *Alternaria* spp (4, 5%); *Arthrinium* spp (4, 5%); *Corynespora* spp (4, 5%).	*Stenella araguata;Phoma eupyrena; Chaetomium globosum*
Keratitis	*Colletotrichum* spp (8, 31%); *Chaetomium* spp (5, 19%); *Curvularia* spp (5, 19%); *Exserohilum* spp (3, 12%).	*Curvularia* spp.;*Bipolaris* spp.;*Exserohilum spp*
Tinea nigra	*Hortaea werneckii* (10, 100%)	*Stenella araguata; Phoma eupyrena; Chaetomium globosum*

TABLE 7 | Main differential diagnoses of phaeohyphomycosis in China.

	Associated Disease(s)
Infectious, Agent	
Fungi	***Cryptococcus*** (cerebral cryptococcosis and cryptococcosis cutis); **Melanized fungi** (chromoblastomycosis and eumycetoma); ***Sporothrix*** (sporotrichosis cutis); ***Zygomycota*** (rhinofacial zygomycosis)
Bacteria	**Bacterium** (cerebral abscess, liver abscess, pneumonia, pleurisy, chronic purulent nasosinusitis, impetigo, and cellulitis); **Tuberculosis** (pulmonary tuberculosis, osseous tuberculosis, orbital tuberculosis, proliferative lymph tuberculosis, and lupus vulgaris); **Cutibacterium acnes** (facial acne)
Viruses	**HPV** (verruca vulgaris and plane warts); **HSV** (herpes simplex); **EV70** (acute hemorrhagic conjunctivitis)
Noninfectious	
Tumors	**Malignancy** (cerebral malignant tumors, lung squamous cell carcinoma, orbital malignant reticulohistiocytoma, thoracolumbar metastasis, skin squamous cell carcinoma); **Benign tumor** (sebaceous gland hyperplasia)
Others	discoid lupus erythematosus, pyogenic granuloma, sarcoidosis, tophus, allergic cutaneous vasculitis, lichen planus, fixed drug eruption, pigmentary purpuric, and eczema

HPV, human papilloma virus; HSV, herpes simplex virus; EV70, enterovirus type 70.

infections were mainly used AmB-DOC plus voriconazole or itraconazole. Most mild subcutaneous infections and keratitis were initially treated with triazoles, including itraconazole, voriconazole, and posaconazole. Severe subcutaneous mainly chose triazoles combined with AmB-DOC and terbinafine. Terbinafine is lipophilic and widely distributed in organizations, especially in the stratum corneum, which has been mostly used for subcutaneous and superficial infections. But as we counted, triazoles are still the dominant antifungal agents in skin infections. Itraconazole was given in doses of 200mg to 400mg daily, voriconazole in doses of 100mg to 800mg daily, and terbinafine in doses of 250mg to 500mg daily. All corneal infections had resorted to keratoplasty when drug therapies were not effective. Among echinocandins, only caspofungin was used in pulmonary infections, mainly in combination with voriconazole and AmB-DOC. Posaconazole, a new triazole, was infrequently used and was tried as a single agent in one patient with cerebral PHM and another patient with severe subcutaneous PHM. The median treatment duration of all PHM in China was 60 days (range, 1–4745days).

Other treatments included surgeries and physical therapies. The operative rates were 60% (6 of 10), 36% (4 of 11), 35% (9 of 26), and 12% (15 of 84) respectively in the deep-local, CNS, corneal, and subcutaneous infections. The physical therapies contained thermotherapy, cryotherapy, laser, and 5-aminolevulinic acid-photodynamic therapy (ALA-PDT). Hyperthermia was used marginally in subcutaneous PHM (8%, 7 of 84) and disseminated PHM (9%, 1 of 11).

AmB-DOC/L-AmB and voriconazole were used most frequently in CNS, disseminated and pulmonary infections that improved or cured at the end of follow-up. The efficacy of L-AmB was better than AmB-DOC in some individual cases, whereas AmB-DOC was mainly used in China as we counted. The overall mortality rates of these three infections were 82% (9 of 11), 55% (6 of 11), and 75% (6 of 8) and their authentic mortality rates due to fungal infections were 55% (6 of 11), 36% (4 of 11) and 25% (2 of 8) respectively. The effective rates in the late stages were extremely low. Four patients with severe pulmonary infections all died despite attempts to use a variety of antifungal drugs including caspofungin. The cure rate of early surgical excision of localized brain cysts was 75% (3 of 4) and the effective rate was 100% (4 of 4). The subcutaneous PHM had an overall effective rate of 66% (56 of 85), and a cure rate of 45% (38 of 85). The subcutaneous nodules were resected in only 10 patients of whom the cure rate was 70% (7 of 10). In addition, among the 48 PHM patients who used a single antifungal agent–itraconazole at a certain stage, 11 cases had little effect and 24 cases were cured, so the effective rate was 73% (35 of 48) and the

TABLE 8 | Therapy for phaeohyphomycosis in 174 patients in China.

No. (Ratio%) Therapy*	Total n=174	CNS n=11	Disseminated n=11	Pulmonary n=8	Deep-local n=10	Subcutaneous n=84	Keratitis n=26	Superficial n=23
Monotherapy								
Triazoles								
FLC	9 (5%)	2 (18%)	1 (9%)	1 (13%)	1 (10%)	1 (1%)	3 (12%)	0 (0%)
ISA	0 (0%)	0 (0%)	0 (0%)	0 (0%)	0 (0%)	0 (0%)	0 (0%)	0 (0%)
ITC	68 (39%)	0 (0%)	3 (27%)	4 (50%)	3 (30%)	48 (57%)	7 (27%)	3 (13%)
KCZ	6 (3%)	0 (0%)	0 (0%)	0 (0%)	2 (20%)	3 (4%)	1 (4%)	0 (0%)
POS	2 (1%)	1 (9%)	0 (0%)	0 (0%)	0 (0%)	1 (1%)	0 (0%)	0 (0%)
VRC	16 (9%)	4 (36%)	3 (27%)	1 (13%)	1 (10%)	7 (8%)	0 (0%)	0 (0%)
Echinocandins								
CAS	1 (1%)	0 (0%)	0 (0%)	1 (13%)	0 (0%)	0 (0%)	0 (0%)	0 (0%)
MFG	0 (0%)	0 (0%)	0 (0%)	0 (0%)	0 (0%)	0 (0%)	0 (0%)	0 (0%)
Others								
AmB-DOC	12 (7%)	1 (9%)	2 (18%)	0 (0%)	2 (20%)	7 (8%)	0 (0%)	0 (0%)
L-AmB	2 (%)	1 (9%)	0 (0%)	1 (13%)	0 (0%)	0 (0%)	0 (0%)	0 (0%)
TBF	10 (6%)	0 (0%)	0 (0%)	1 (13%)	0 (0%)	9 (11%)	0 (0%)	0 (0%)
5-FC	1 (1%)	0 (0%)	1 (9%)	0 (0%)	0 (0%)	0 (0%)	0 (0%)	0 (0%)
KI	2 (1%)	0 (0%)	0 (0%)	0 (0%)	0 (0%)	2 (2%)	0 (0%)	0 (0%)
Combination therapy								
Azole + AmB-DOC	10 (6%)	3 (27%)	3 (27%)	0 (0%)	3 (30%)	1 (1%)	0 (0%)	0 (0%)
Azole + L-AmB	4 (2%)	3 (27%)	1 (9%)	0 (0%)	0 (%)	0 (0%)	0 (0%)	0 (%)
Azole + Echinocandin	2 (1%)	0 (0%)	0 (0%)	2 (25%)	0 (0%)	0 (0%)	0 (0%)	0 (0%)
Azole + KI	1 (1%)	0 (0%)	0 (0%)	0 (0%)	0 (0%)	1 (1%)	0 (0%)	0 (0%)
Azole + TBF	14 (8%)	0 (0%)	1 (9%)	0 (0%)	1 (10%)	12 (14%)	0 (0%)	0 (0%)
Azole+5-FC	3 (2%)	1 (9%)	1 (9%)	0 (0%)	0 (0%)	1 (1%)	0 (0%)	0 (0%)
Two Triazoles	3 (2%)	0 (0%)	0 (0%)	0 (0%)	1 (10%)	0 (0%)	2 (8%)	0 (0%)
AmB-DOC + Echinocandin	1 (1%)	0 (0%)	0 (0%)	1 (13%)	0 (0%)	0 (0%)	0 (0%)	0 (0%)
AmB-DOC + TBF	1 (1%)	0 (0%)	0 (0%)	0 (0%)	0 (0%)	1 (1%)	0 (0%)	0 (0%)
L-AmB + TBF	1 (1%)	0 (0%)	0 (0%)	1 (13%)	0 (0%)	0 (0%)	0 (0%)	0 (0%)
AmB-DOC + 5-FC	2 (2%)	1 (9%)	0 (0%)	0 (0%)	0 (0%)	1 (1%)	0 (0%)	0 (0%)
L-AmB + 5-FC	1 (%)	1 (9%)	0 (0%)	0 (0%)	0 (0%)	0 (0%)	0 (0%)	0 (0%)
NS + KI	2 (1%)	0 (0%)	1 (9%)	0 (0%)	0 (0%)	1 (1%)	0 (0%)	0 (0%)
Triple-Drug Combination	3 (2%)	1 (9%)	1 (9%)	0 (0%)	0 (0%)	1 (1%)	0 (0%)	0 (0%)
Four-Drug Combination	0 (0%)	0 (0%)	0 (0%)	0 (0%)	0 (0%)	0 (0%)	0 (0%)	0 (0%)
Non-Systematic Therapy								
Cryotherapy	2 (1%)	0 (0%)	0 (0%)	0 (0%)	0 (0%)	2 (2%)	0 (0%)	0 (0%)
Laser	2 (1%)	0 (0%)	0 (0%)	0 (0%)	0 (0%)	2 (2%)	0 (0%)	0 (0%)
Local Drug Infiltration	58 (33%)	1 (9%)	1 (9%)	0 (0%)	4 (40%)	16 (19%)	20 (77%)	16 (70%)
ALA-PDT	2 (1%)	0 (0%)	0 (0%)	0 (0%)	0 (0%)	2 (2%)	0 (0%)	0 (0%)
Surgery	37 (21%)	4 (36%)	2 (18%)	0 (0%)	6 (60%)	15 (18%)	9 (35%)	1 (4%)
Thermotherapy	8 (5%)	0 (0%)	1 (9%)	0 (0%)	0 (0%)	7 (8%)	0 (0%)	0 (0%)
Unknow	19 (11%)	2 (18%)	1 (9%)	1 (13%)	0 (0%)	6 (7%)	2 (8%)	6 (26%)

FLC, fluconazole; ISA, isavuconazole; ITC, itraconazole; KCZ, ketoconazole; POS, posaconazole; VRC, voriconazole; CAS, caspofungin; MFG, micafungin; 5-FC, 5-fluorocytosine; AmB-DOC, amphotericin B deoxycholate; L-AmB, liposomal amphotericin B; TBF, terbinafine; ALA-PDT, 5-aminolevulinic acid-photodynamic therapy.
**Some patients were treated with more than one antifungal or combination of antifungal drugs in different periods.*

cure rate was 50% (24 of 48). The effective rates of keratitis and superficial PHM were 77% (20 of 26) and 70% (16 of 23). Their prognosis was favorable except for the permanent vision loss in a portion of keratitis.

In Vitro Antifungal Susceptibility

In this study, 38 clinical fungal isolates from clinical specimens provided the minimum inhibitory concentration (MIC)/minimal effective concentration (MEC) values (**Supplementary Table 4**). We further linked the 16 dematiaceous fungal isolates' MIC values to their clinical efficacy when a single triazole agent–itraconazole was used (**Supplementary Table 5**). At present, there is no clinical or epidemiological cut-off point for drug susceptibility of melanized fungi, so we reported the results based on the previous literature (Revankar and Sutton, 2010), MIC/MEC of ≤1 μg/ml was used as the index of potential sensitivity to most antifungal drugs to treat melanized molds, flucytosine (5-FC) (<50 μg/ml) excluded.

As a result, the drug resistance rate to fluconazole among the clinical dematiaceous fungi was the highest, accounting for 93% (25

of 27). The average MICs of echinocandins were higher than triazole drugs and had high variability *in vitro* activity. Most clinical strains were susceptible to terbinafine (89%, 16 of 18), voriconazole (86%, 18 of 21), and itraconazole (77%, 27 of 35). The average MICs of terbinafine were the lowest among all antifungal agents. AmB (56%, 18 of 32) was relatively less susceptible *in vitro*. Furthermore, the coincidence rate of itraconazole between MICs and clinical efficacy was 81% (13 of 16).

DISCUSSION

In the last 35 years, the quantity of phaeohyphomycosis was growing year by year, especially in southern China (Huang et al., 2019). The overall development of detection techniques of melanized fungi and more attention paid to this disease particularly contributed to the explosive growth. The widespread use of immunosuppressive agents, and improved microbiologic and gene testing techniques also made the incidence of PHM fast increase.

Melanized fungi are widely distributed in China. According to the sample research made in southwest China, there were at least 100 species of dark molds in the provinces of Guangxi, Guizhou, Hainan, Yunnan, and Chungking (Ma, 2018). There is probably underestimating of the disease in southwest China. The actual incidence of PHM may be higher in the less developed southern regions of China, such as Yunnan, Guizhou, and Hainan. No case has beenN reported till now which may be due to the lack of adequate awareness and the lack of advanced molecular methods which aid in identifying the agents of PHM, which might be the cause of underreporting of cases in these less developed areas. It may be the truth not just in China, but all around the world, especially the disadvantaged tropical countries.

The growing body of melanotic fungi pathogenesis is being gradually discovered and refined nowadays (Eisenman et al., 2020). One of the major virulence factors is the cell-wall melanin, which was once thought to prevent the fungi from an oxidative explosion inside phagocytes. However, other mechanisms of melanin have been elucidated such as impacting host cell signaling (Shi et al., 2019), blocking the autophagy pathway LC3-associated phagocytosis (LAP) (Andrianaki et al., 2018), and interfering with recognition of the fungal cells through an identified receptor called MelLec that is diffusely expressed in epithelial tissues (Stappers et al., 2018). Furthermore, a recent founding has verified that some fungi can get resistant to antifungals by increasing melanin production (Heidrich et al., 2021). On the other hand, transcriptomics research on melanotic fungal genomes is recognized as cutting-edge and promising. Several studies made efforts to find genetic profiles by comparing rare human neurotropic pathogens with other known black fungi and made transcriptomic analysis of an albino mutant comparing its melanized strains, which showed that not only some highly expressed melanin genes but also some differentially expressed genes (DEGs) which associated with survival pathway, cell growth, and metabolic pathways (Chen et al., 2014; Li et al., 2016; Bombassaro et al., 2020).

In our research, we find that the most common risk factors are trauma. Traumatic implantation mainly comes from the departments of agriculture, fishery, forestry, mining, construction, and sanitation. The above occupations are difficult to avoid the daily invisible contamination injuries so more occupational protections are needed. The other major factors that reduced immune functions include malnutrition, tumors, and kidney transplantations. Under the background of the global COVID-19 pandemic, Simin Laiq was the first to report a case of *Fonsecaea*-associated cerebral PHM in a 73 years old Omani diabetic lady who presented headache and visual disturbance 6 weeks after recovery from COVID-19 pneumonia (Laiq et al., 2022). Actually, treatment with steroids and exacerbation of diabetes during COVID-19 infection may lead patients to be immunocompromised and more susceptible to fungal infections. Notably, with the popularization of genetic testing technology, inherited CARD9 deficiency was found in 12 patients from China in recent 5 years. This group of patients usually were tricky to cure and had a long course of the disease, indicating that anti-fungal immunodeficiency caused by the CARD9 gene mutation was one of the pathogenic factors. A large portion of PHM patients without known immunodeficiencies may have the potential mutations of the CARD9 gene if the gene test could be done in the past (Huang et al., 2019).

There is no uniform approach for the treatment of PHM. We advocate early diagnosis and treatment of PHM. Surgery is the most important for cerebral cysts, but may also be critical for other forms of local lesions such as subcutaneous nodules, keratitis, bone and joint infection, and catheter removal. There is also no standard approach when it comes to antifungal drugs. Global guidelines for rare mold infections proposed by the European Confederation of Medical Mycology (ECMM) union with the International Society for Human and Animal Mycology and the American Society for Microbiology (ISHAM) in 2021 strongly recommend itraconazole or voriconazole as the first-line treatment for superficial PHM and subcutaneous PHM (Hoenigl et al., 2021). When referring to disseminated PHM involved CNS and local-deep organs, posaconazole and voriconazole plus L-AmB are moderately recommended as first-line drug treatments. Echinocandins and terbinafine may be combined with them but are not recommended to be applied solely. In 2014, the guidelines for PHM made by the experts of ESCMID and ECMM showed the recommendations that topical 5% natamycin and amphotericin B (0.15–0.3%) were strongly regarded as the first-line therapy for most keratitis. Oral triazoles with surgery or even an intracorneal injection of voriconazole (1%) as moderately recommended salvage therapy for severe and refractory corneal infections. When it comes to cerebral infections, first and foremost is complete excision of brain abscesses (grade AII) rather than only partial excision or aspiration. When surgery is not possible, a triazole combined with an echinocandin plus flucytosine is moderately recommended to be the first-line therapy (grade BIII). Voriconazole and posaconazole (grade CII) are marginally recommended while AmB-DOC therapy alone is in the lowest recommended grade which is against use (Chowdhary et al., 2014).

Isavuconazole and ravuconazole are two new triazoles antifungal agents. In 2019 a study using these two agents to test

their *in vitro* susceptibility of a broad spectrum of dematiaceous fungi showed better antifungal activity than itraconazole, voriconazole, and posaconazole, especially against *Bipolaris spicifera* and *Veronaea botryosa* (Zheng et al., 2020). And also, in 2022 a research project verified that ravuconazole could be recognized as a promising drug candidate for the treatment of eumycetoma and is at present being examined in a randomized, double-blinded clinical trial for mycetoma. In the clinical trial, the efficacy of weekly treatment of fosravuconazole at 200 or 300 mg is compared to the daily of itraconazole at 400 mg in mycetoma patients (Lim et al., 2022). However, the clinical safety and efficacy of these two antifungal agents in the treatment of PHM have not been reported. Detailed case reports of success and failure experiences still need to be explored and accumulated in the later stage. Thus, it can be seen, that antifungal susceptibility test *in vitro* plays a critical role in the management of fungal infections and the selection of optimal drug therapy.

When it comes to morbidity, subcutaneous PHM has the highest incidence. We found that the severity grades of lesion have a close correlation with the pathogens' virulence and the patient's immune status, which may predict the patient's clinical outcome. In our statistics, severe rashes are much more pleomorphic, covering almost all types of rashes, including scars and sinus. Areas rich in capillaries such as the head and face are mostly affected accounting for 16% in severe cases. It's easy to cause disfigurement, disability, and hematogenous spread. The data suggested that the grade of the lesion has a level of significant correlation with the course of the disease (P=0.098) and the effective rate (P=0.08). But there's no significant variation in cure rate (P=2.06), or death rate (P=2.57) between mild, moderate, and severe rashes. We hypothesized that the more severe rash was related to the stronger pathogen's virulence and the lower patient's immune status. The worse rashes have higher dark fungal loads, and these strains may become resistant to antifungal agents for long-term treatment. Notwithstanding, the follow-up periods can be recorded from the whole literature in this study ranging from 4 weeks to 4 years. Many patients are lost to follow-up because there are no standard cure criteria for the PHM. Lots of people who responded to therapy did not have a prolonged follow-up, and therefore the final cure rates of severe PHM may be much lower and the death rates may be much higher in reality.

Overall, with the increasing attention paid to this kind of infection, the continuous improvement of diagnostic methods, the iterative updating of new drugs with better efficacy, and the deepening of clinical research, it is expected to realize the early diagnosis of dark fungal infections with high sensitivity and specificity and more targeted individual treatment.

CONCLUSION

A total of 174 phaeohyphomycosis patients have been reported in China in the past 35 years. Among these CNS, disseminated and pulmonary types have the highest mortality. The subcutaneous type is the most common, and the corneal type ranks second. Most cases are concentrated in southeast China. The early clinical manifestations of PHM are nonspecific and its misdiagnosis rate is as high as 74%. Nearly 30% of invasive infections of PHM start from persistent and recurrent lesions. Subcutaneous lesions can be divided into three grades: mild (15, 18%), moderate (39, 46%), and severe (31, 36%). We discover that there're no significant variations in cure rate, or death rate between three grades of lesions. But patients with severe rashes have much lower effective rates and the immune status of this population is relatively weaker. Treatment of PHM remains tricky. Our researchers need to conduct more studies: 1, To fully understand the melanin and other virulence factors in dark fungi. 2, To find more additional susceptible gene mutations in patients. 3, And to explore the possibility of discovering more effective and promising agents.

AUTHOR CONTRIBUTIONS

All authors listed have made a substantial, direct, and intellectual contribution to the work, and approved it for publication.

FUNDING

This study was funded by the National Science and Technology Infrastructure of China (Project No. National Pathogen Resource Center–NPRC–32) and the National Science and Technology Major Project (2018ZX10734404).

SUPPLEMENTARY MATERIAL

The Supplementary Material for this article can be found online at: https://www.frontiersin.org/articles/10.3389/fcimb.2022.895329/full#supplementary-material

REFERENCES

Andrianaki, A. M., Kyrmizi, I., Thanopoulou, K., Baldin, C., Drakos, E., Soliman, S., et al. (2018). Author Correction: Iron Restriction Inside Macrophages Regulates Pulmonary Host Defense Against *Rhizopus* Species. *Nat. Commun.* 9 (1), 5015. doi: 10.1038/s41467-018-07301-y

Bai, J., Liu, Y., Zhang, N. N., Wen, Y., Peng, Y., and Cheng, H. (2020). Central Nervous System Phaeohyphomycosis Caused by *Exophiala Dermatitidis*: Report of Two Cases. *J. Chin. Clin. Med. Imaging* 31 (6), 76–77. doi: 10.12117/jccmi.2020.06.018

Bombassaro, A., Schneider, G. X., Costa, F. F., Leão, A., Soley, B. S., Medeiros, F., et al. (2020). Genomics and Virulence of *Fonsecaea Pugnacius*, Agent of Disseminated Chromoblastomycosis. *Front. Genet.* 11. doi: 10.3389/fgene.2020.00822

Borman, A. M., Fraser, M., Patterson, Z., Linton, C. J., Palmer, M., and Johnson, E. M. (2022). Fungal Infections of Implantation: More Than Five Years of Cases of Subcutaneous Fungal Infections Seen at the UK Mycology Reference Laboratory. *J. Fungi (Basel)* 8 (4), 343. doi: 10.3390/jof8040343

Cai, Q., Lv, G. X., Jiang, Y. Q., Mei, H., Hu, S. Q., Xu, H. B., et al. (2013). The First Case of Phaeohyphomycosis Caused by Rhinocladiella Basitona in an Immunocompetent Child in China. *Mycopathologia* 176 (1-2), 101–105. doi: 10.1007/s11046-013-9645-0

Cao, X. Y., and Wu, K. (2008). Keratohelcosis Due to *Colletotrichum Dematium*: A Case Report. *Chin. J. Mycol* 3 (4), 217–218. doi: 10.3969/j.issn.1673-3827.2008.04.008

Chang, X., Li, R., Yu, J., Bao, X., and Qin, J. (2009). Phaeohyphomycosis of the Central Nervous System Caused by *Exophiala Dermatitidis* in a 3-Year-Old Immunocompetent Host. *J. Child Neurol.* 24 (3), 342–345. doi: 10.1177/0883073808323524

Chen, Z., Jiang, Y., Wang, D., Zheng, M., Liu, X., et al. (2021). Enhancement in Serum (1-3)-β-D-Glucan Level by Cutaneous Alternariosis: A Case Report and Literature Review. *Microb. Pathog.* 150, 104703. doi: 10.1016/j.micpath.2020.104703

Chen, Q. X., Li, C. X., Huang, W. M., Shi, J. Q., Li, W., and Li, S. F. (2008). Subcutaneous Phaeohyphomycosis Caused by *Cladosporium Sphaerospermum*. *Mycoses* 51 (1), 79–80. doi: 10.1111/j.1439-0507.2007.01417.x

Chen, Y. T., Lin, H. C., Huang, C. C., and Lo, Y. H. (2006). Cutaneous Phaeohyphomycosis Caused by an Itraconazole and Amphoterecin B Resistant Strain of *Veronaeae Botryosa*. *Int. J. Dermatol.* 45 (4), 429–432. doi: 10.1111/j.1365-4632.2006.02619.x

Chen, C. Y., Lu, P. L., Lee, K. M., Chang, T. C., Lai, C. C., Chang, K., et al. (2013). Acute Meningitis Caused by. *Cladosporium Sphaerospermum Am. J. Med. Sci.* 346 (6), 523–325. doi: 10.1097/MAJ.0b013e3182a59b5f

Chen, Z., Martinez, D. A., Gujja, S., Sykes, S. M., Zeng, Q., Szaniszlo, P. J., et al. (2014). Comparative Genomic and Transcriptomic Analysis of *Wangiella Dermatitidis*, a Major Cause of Phaeohyphomycosis and a Model Black Yeast Human Pathogen. *G3 (Bethesda)* 4 (4), 561–578. doi: 10.1534/g3.113.009241

Chen, Y. C., Su, Y. C., Tsai, C. C., Lai, N. S., Fan, K. S., and Liu, K. C. (2014). Subcutaneous Phaeohyphomycosis Caused by *Exophiala Jeanselmei*. *J. Microbiol. Immunol. Infect.* 47 (6), 546–549. doi: 10.1016/j.jmii.2012.06.006

Chen, C. C., Tsai, Y. J., and Hu, S. L. (2003). Lymphocutaneous Phaeohyphomycosis Caused by. *Veronaea Botryosa Dermatol. Sin.* 2 (1), 375–383. doi: 10.1007/s11046-016-9989-3

Chen, W. T., Tu, M. E., and Sun, P. L. (2016). Superficial Phaeohyphomycosis Caused by Aureobasidium Melanogenum Mimicking Tinea Nigra in an Immunocompetent Patient and Review of Published Reports. *Mycopathologia* 181 (7–8), 555–560. doi: 10.3969/j.issn.1673-3827.2016.06.008

Chen, M., Zhang, J., Dong, Z., and Wang, F. (2016). Cutaneous Phaeohyphomycosis Caused by *Exophiala Dermatitidis*: A Case Report and Literature Review. *Indian J. Dermatol. Venereol Leprol* 82 (2), 173–177. doi: 10.4103/0378-6323.171013

Chen, X. W., Zhu, H. M., and Wen, H. (2016). A Case of Cutaneous Mycosis Caused by *Arthrinium Phaeospermum*. *Chin. J. Mycol* 11 (6), 357–360.

Chowdhary, A., Meis, J. F., Guarro, J., de Hoog, G. S., Kathuria, S., Arendrup, M. C., et al. (2014). ESCMID and ECMM Joint Clinical Guidelines for the Diagnosis and Management of Systemic Phaeohyphomycosis: Diseases Caused by Black Fungi. *Clin. Microbiol. Infect.* 20 Suppl 3, 47–75. doi: 10.1111/1469-0691.12515

Chuan, M. T., and Wu, M. C. (1995). Subcutaneous Phaeohyphomycosis Caused by *Exophiala Jeanselmei*: Successful Treatment With Itraconazole. *Int. J. Dermatol.* 34 (8), 563–566. doi: 10.1111/j.1365-4362.1995.tb02955.x

Dai, W. L., Ren, Z. F., Wan, J. Z., Liu, H. Y., Chen, R. E., Wang, D. L., et al. (1987). Systemic Phaeohyphomycosis Due to *Exophiala Spinifera*: The First Case Report in China. *Chin. J. Dermatol.* 20 (1), 13–15. URL: https://d.wanfangdata.com.cn/periodical/zhpf198701009

Dai, X. Y., and Zhang, H. P. (2004). A Case of Tinea Manuum Nigra. *J. Clin. Dermatol.* 33 (5), 290–291. doi: 10.3969/j.issn.1000-4963.2004.05.012

Dong, B. L., Li, D. S., Chen, L. Q., Huang, M., and Zhou, L. P. (2012). Cutaneous Phaeohyphomycosis Caused by *Exophiala Jeanselmei*: A Case Report. *Chin. J. Derm Venereol* 26 (11), 1018–1020. URL:http://qikan.cqvip.com/Qikan/Article/Detail?id=43648813

Dong, M. L., Li, R. Y., De Hoog, G. S., Wang, Y. X., and Wang, D. L. (2009). *Exophiala Asiatica*, a New Species From a Fatal Case in China. *Med. Mycol* 47 (1), 101–109. doi: 10.1080/13693780802538019

Eisenman, H. C., Greer, E. M., and McGrail, C. W. (2020). The Role of Melanins in Melanotic Fungi for Pathogenesis and Environmental Survival. *Appl. Microbiol. Biotechnol.* 104 (10), 4247–4257. doi: 10.1007/s00253-020-10532-z

Fang, G. L., Zhang, Q. H., Zhu, L., and Li, D. M. (2011). Clinical Study of Chronic Invisive Sinusitis Caused by Dematiaceous Fungi. *Chin. J. Otorhinolaryngol Head Neck Surg.* 25 (20), 916–919. doi: 10.3969/j.issn.1001-1781.2011.20.002

Fan, Y. M., Huang, W. M., Li, S. F., Wu, G. F., Li, W., and Chen, R. Y. (2009). Cutaneous Phaeohyphomycosis of Foot Caused by *Curvularia Clavata*. *Mycoses* 52 (6), 544–546. doi: 10.1111/j.1439-0507.2008.01646.x

Feng, Y. M., Wu, L. J., Wang, M. M., Sun, L., Zeng, X. S., Shen, Y. N., et al. (2018). Facial Cutaneous Phaeohyphomycosis Caused by *Microsphaeropsis Arundinis*: A Case Report. *Chin. J. Dermatol.* 51 (5), 382–384. doi: 10.3760/cma.j.issn.0412-4030.2018.05.015

Ge, Y. P., Lv, G. X., Shen, Y. N., Li, M., Deng, S. W., De Hoog, S., et al. (2012). First Report of Subcutaneous Phaeohyphomycosis Caused by *Ochroconis Tshawytschae* in an Immunocompetent Patient. *Med. Mycol* 50 (6), 637–640. doi: 10.3109/13693786.2011.653834

Ge, H., Pan, M., Chen, G., Liu, X., Shi, T., and Zhang, F. (2017). The First Case of Cutaneous Phaeohyphomycosis Caused by *Bipolaris Spicifera* in Northern China: A Case Report. *Exp. Ther. Med.* 14 (3), 1875–1878. doi: 10.3892/etm.2017.4765

Gong, Y., Chen, Z., Ma, Y., Jiang, W., Hu, Y., and Shi, Y. (2020). Cutaneous Phaeohyphomycosis Caused by *Pyrenochaeta Unguis-Hominis* in a Diabetic Patient: A Case Report. *Australas. J. Dermatol.* 61 (2), e221–e222. doi: 10.1111/ajd.13177

Guo, Y. Y., Liu, Y., Yan, D., Wu, Z. Y., Zhao, M., Zhao, X. D., et al. (2016). A Case Report of Tinea Nigra Palmaris Caused by. *Hortaea Werneckii J. Clin. Dermatol.* 45 (10), 736–739. doi: 10.16761/j.cnki.1000-4963.2016.10.021

Guo, Y., Zhu, Z., Gao, J., Zhang, C., Zhang, X., Dang, E., et al. (2019). The Phytopathogenic Fungus *Pallidocercospora Crystallina*-Caused Localized Subcutaneous Phaeohyphomycosis in a Patient With a Homozygous Missense CARD9 Mutation. *J. Clin. Immunol.* 39 (7), 713–725. doi: 10.1007/s10875-019-00679-4

Gu, H. Y., Shen, W. M., Wang, D. L., and Xue, J. B. (1996). A Case of Tinea Nigra Palmaris Caused by *Hortaea Werneckii*. *Chin. J. Dermatol.* 29 (5), 354–355. URL: http://qikan.cqvip.com/Qikan/Article/Detail?id=2267378

Hang, X. F., Gu, J. L., Xu, H., and Wen, H. (2006). Combined Incubation in Treatment of Phaeohyphomycosis: A Case Report. *Chin. J. Mycol* 1 (3), 168–169. doi: 10.3969/j.issn.1673-3827.2006.03.014

He, J. W. (2012). "Therapy and Diagnosis of Phaeohyphomycosis of the Central Nervous System. [Master's Thesis]," (Fuzhou, China: Fujian Medical University).

Heidrich, D., Pagani, D. M., Koehler, A., Alves, K. O., and Scroferneker, M. L. (2021). Effect of Melanin Biosynthesis Inhibition on the Antifungal Susceptibility of Chromoblastomycosis Agents. *Antimicrob. Agents Chemother.* 65 (8), e0054621. doi: 10.1128/AAC.00546-21

Hoenigl, M., Salmanton-García, J., Walsh, T. J., Nucci, M., Neoh, C. F., Jenks, J. D., et al. (2021). Global Guideline for the Diagnosis and Management of Rare Mould Infections: An Initiative of the European Confederation of Medical Mycology in Cooperation With the International Society for Human and Animal Mycology and the American Society for Microbiology. *Lancet Infect. Dis.* 21 (8), e246–e257. doi: 10.1016/S1473-3099(20)30784-2

Hsiao, Y. W., Chia, J. H., Lu, C. F., and Chung, W. H. (2013). Molecular Diagnosis and Therapeutic Experience of Subcutaneous *Pyrenochaeta Romeroi* Infection: A Case Report and Review of the Literature. *Int. J. Dermatol.* 52 (10), 1237–1240. doi: 10.1111/j.1365-4632.2011.05173.x

Hsu, C. C., Chang, S. S., Lee, P. C., and Chao, S. C. (2015). Cutaneous Alternariosis in a Renal Transplant Recipient: A Case Report and Literature Review. *Asian J. Surg.* 38 (1), 47–57. doi: 10.1016/j.asjsur.2012.08.010

Hsu, M. M., and Lee, J. Y. (1993). Cutaneous and Subcutaneous Phaeohyphomycosis Caused by *Exserohilum Rostratum*. *J. Am. Acad. Dermatol.* 28, 340–344. doi: 10.1016/0190-9622(93)70050-4

Huang, W. M., Fan, Y. M., Li, W., and Yang, W. W. (2011). Brain Abscess Caused by Cladophialophora Bantiana in China. *J. Med. Microbiol.* 60 (Pt12), 1872–1874. doi: 10.1099/jmm.0.032532-0

Huang, W. M., Fan, Y. M., Li, W., and Zhang, G. X. (2009). Superficial White Onychomycosis Caused by *Nigrospora Sphaerica*: A Case Report. *Chin. J. Dermatol.* 42, 522–524. doi: 10.3760/cma.j.issn.0412-4030.2009.08.002

Huang, F. C., Huang, S. T., and Tseng, S. H. (1998). Mycotic Keratitis Caused by *Bipolaris* Species–Report of Two Cases. *Tzu Chi Med. J.* 10 (4), 345–349. http://www.scopus.com/inward/record.url?scp=0032406575&partnerID=8YFLogxK

Huang, W. M., Li, W., Guo, H. W., Luo, Y. C., and Chen, Q. X. (2008). Subcutaneous Phaeohyphomycosis Caused by *Cladosporium Cladosporieides*. *Chin. J. Mycol* 3 (3), 157–160. doi: 10.3969/j.issn.1673-3827.2008.03.008

Huang, C., Zhang, Y., Song, Y., Wan, Z., Wang, X., and Li, R. (2019). Phaeohyphomycosis Caused by *Phialophora Americana* With CARD9 Mutation and 20-Year Literature Review in China. *Mycoses* 62 (10), 908–919. doi: 10.1111/myc.12962

Hu, B., Li, S. Y., Hu, H. L., Chen, T. M., Guo, X., Zhang, Z. X., et al. (2014). Central Nervous System Infection Caused by *Exophiala Dermatitidis* in a Case and Literature Review. *Chin. J. Pediatr.* 52 (8), 620. doi: 10.3760/cma.j.issn.0578-1310.2014.08.015

Hu, W., Ran, Y., Zhuang, K., Lama, J., and Zhang, C. (2015). *Alternaria Arborescens* Infection in a Healthy Individual and Literature Review of Cutaneous Alternariosis. *Mycopathologia* 179 (1-2), 147. doi: 10.1007/s11046-014-9822-9

Hu, S. Q., Zhan, P., Lv, G. X., Mei, H., Zeng, X. S., and Liu, W. D. (2016). A Case of Cutaneous *Arthrinium Phaeospermum* Infection After Lower Limb Amputation. *Chin. J. Dermatol.* 49 (10), 726–728. doi: 10.3760/cma.j.issn.0412-4030.2016.10.012

Hung, N., Hsiao, C. H., Yang, C. S., Lin, H. C., Yeh, L. K., Fan, Y. C., et al. (2020). Colletotrichum Keratitis: A Rare Yet Important Fungal Infection of Human Eyes. *Mycoses* 63 (4), 407–415. doi: 10.1111/myc.13058

Jiang, Y. L., and Zhang, F. T. (1991). Systemic Phaeohyphomycosis Caused by *Wangiella Dermatitidis*: A Case Report. *J. Clin. Dermatol.* 3, 137–139. URL: http://qikan.cqvip.com/Qikan/Article/Detail?id=561157

Jin, X. Z., Li, F. Q., Xia, J. X., and Wang, P. F. (1996). A Case of Phaeohyphomycosis Caused by *Exophiala Jeanselmei* in Jilin Province. *Chin. J. Dermatol.* 29 (5), 356. http://qikan.cqvip.com/Qikan/Article/Detail?id=2267379

Jin, H., Xu, A., Liu, J., Xia, X., and Lou, X. (2009). A Case of Phaeohyphomycosis Caused by *Exophiala Jeanselmei*. *Chin. J. Dermatol.* 42 (6), 437. doi: 10.3760/cma.j.issn.0412-4030.2009.06.029

Lai, S., Duque, J., Chung, B. H., Chung, T. W., Leung, D., Ho, R. S., et al. (2021). Invasive Cerebral Phaeohyphomycosis in a Chinese Boy With CARD9 Deficiency and Showing Unique Radiological Features, Managed With Surgical Excision and Antifungal Treatment. *Int. J. Infect. Dis.* 107, 59–61. doi: 10.1016/j.ijid.2021.04.052

Laiq, S., Al Yaqoobi, M., Al Saadi, M., Rizvi, S., Al Hajri, Z., Al Azri, S., et al. (2022). *Fonsecaea* Associated Cerebral Phaeohyphomycosis in a Post-COVID-19 Patient: A First Case Report. *Clin. Infect. Pract.* 13, 100126. doi: 10.1016/j.clinpr.2021.100126

Latawa, A., Panda, I., Kaur, H., Aggarwal, A., Radotra, B. D., Gupta, K., et al. (2022). Cerebral Phaeohyphomycosis: The 'Dark Side' of Fungal Infections. *Clin. Neurol. Neurosurg.* 214, 107173. doi: 10.1016/j.clineuro.2022.107173

Lau, A. F. (2021). Matrix-Assisted Laser Desorption Ionization Time-Of-Flight for Fungal Identification. *Clin. Lab. Med.* 41 (2), 267–283. doi: 10.1016/j.cll.2021.03.006

Lau, S. K., Woo, P. C., Chiu, S. K., Leung, K. W., Yung, R. W., and Yuen, K. Y. (2003). Early Diagnosis of *Exophiala* CAPD Peritonitis by 18S Ribosomal RNA Gene Sequencing and its Clinical Significance. *Diagn. Microbiol. Infect. Dis.* 46 (2), 95–102. doi: 10.1016/s0732-8893(03)00014-2

Li, L. W. (1988). Deep Infection in the Orbit and Eyeball Caused by. *Exophiala Jeanselmei Chin. J. Pract. Ophthalmol.* 6 (12), 745–746. https://kns.cnki.net/kcms/detail/detail.aspx?FileName=ZZZY198812021&DbName=CJFQ1988

Li, D. M., de Hoog, G. S., Saunte, D. M., van den Ende, A. H., and Chen, X. R. (2008). *Coniosporium Epidermidis* Sp. *Nov. A* New Species From Human Skin. *Stud. Mycol* 61, 131–136. doi: 10.3114/sim.2008.61.13

Li, D. S., Duan, Y. Q., Chen, L. Q., and Dong, B. L. (2012). "Phaeohyphomycosis Caused by Cladosporium Cladosporioides: A Case Report". in *Paper Presented at the 19th Annual Meeting of Chinese Society of Dermatology*(Chengdu, China).

Li, X. Q., Guo, B. L., Cai, W. Y., Zhang, J. M., Huang, H. Q., Zhan, P., et al. (2016). The Role of Melanin Pathways in Extremotolerance and Virulence of *Fonsecaea* Revealed by *De Novo* Assembly Transcriptomics Using Illumina Paired-End Sequencing. *Stud. Mycol* 83, 1–18. doi: 10.1016/j.simyco.2016.02.001

Lim, W., Nyuykonge, B., Eadie, K., Konings, M., Smeets, J., Fahal, A., et al. (2022). Screening the Pandemic Response Box Identified Benzimidazole Carbamates, Olorofim and Ravuconazole as Promising Drug Candidates for the Treatment of Eumycetoma. *PloS Negl. Trop. Dis.* 16 (2), e0010159. doi: 10.1371/journal.pntd.0010159

Lin, Y. Z., Li, X. Y., Nishimura, Z., Gao, S. Q., Gao, J. G., Li, X. Y., et al. (1995). First Case of Phaeohyphomycosis Caused by *Chaetomium Murorum* in China. *Chin. J. Dermatol.* 28 (6), 367–369. http://qikan.cqvip.com/Qikan/Article/Detail?id=1622834

Lin, Y. P., Li, W., Yang, Y. P., Huang, W. M., and Fan, Y. M. (2012). Cutaneous Phaeohyphomycosis Caused by *Exophiala Spinifera* in a Patient With Systemic Lupus Erythematosus. *Lupus* 21 (5), 548–551. doi: 10.1177/0961203311428460

Linqiang, D., Yiguo, C., Heping, X., Dongke, C., Longhua, H., Xiaomei, G., et al. (2020). Subcutaneous Phaeohyphomycosis Caused by *Hongkongmyces Snookiorum* in a Kidney Transplant Patient: A Case Report. *BMC Infect. Dis.* 20 (1), 562. doi: 10.1186/s12879-020-05295-x

Lin, S. C., Sun, P. L., Ju, Y. M., and Chan, Y. J. (2009). Cutaneous Phaeohyphomycosis Caused by *Exserohilum Rostratum* in a Patient With Cutaneous T-Cell Lymphoma. *Int. J. Dermatol.* 48 (3), 295–298. doi: 10.1111/j.1365-4632.2009.03803

Lin, N. X., Zheng, Y. C., Zeng, J. S., Huang, C. Z., Lian, X., Mao, Y. H., et al. (2010). A Case of Phaeohyphomycosis Caused by *Exophiala Spinifera* Superimposed on Basal Cell Carcinoma. *Chin. J. Dermatol.* 43 (4), 226–229. doi: 10.3760/cma.j.issn.0412-4030.2010.04.002

Liou, J. M., Wang, J. T., Wang, M. H., Wang, S. S., and Hsueh, P. R. (2002). Phaeohyphomycosis Caused by *Exophiala* Species in Immunocompromised Hosts. *J. Formos Med. Assoc.* 101 (7), 523–526. doi: 10.1016/S0885-3924(02)00413-X

Lirng, J. F., Tien, R. D., Osumi, A. K., Madden, J. F., McLendon, R. P., and Sexton, D. (1995). Cerebral Phaeohyphomycosis Complicated With Brain Abscess: A Case Report. *Zhonghua Yi Xue Za Zhi (Taipei)* 55 (6), 491–495.

Li, J. Z., Sun, S. T., Li, J., Hu, Z. M., Yue, J., Han, L., et al. (2009). Fungal Keratitis Caused by *Alternaria Alternata*: A Case Report. *Chin. J. Exp. Ophthalmol.* 27 (8), 648. doi: 10.3760/cma.j.issn.2095-0160.2009.08.027

Liu, J. M., Li, B. L., Wang, S. M., and Zheng, H. J. (1997). Pleural Effusion Caused by *Alternaria Alternata*: A Case Report. *Clin. Focus* 12 (16), 766. https://kns.cnki.net/kcms/detail/detail.aspx?FileName=LCFC199716037&DbName=CJFQ1997

Liu, S. J., Li, Y. C., and Wei, X. C. (2018). Invasive Pulmonary Infection Due to *Cladosporium Cladosporioides*: A Rare Case Report. *Chin. J. Mycol* 13 (2), 91–92. doi: 10.3969/j.issn.1673-3827.2018.02.008

Liu, W. D., Shen, Y. N., Lv, G. X., Chen, W., and Chen, W. (2002). Two Cases of Fungal Keratitis Caused by *Alternaria Alternata* and Successfully Treated With Itraconazole. *J. Clin. Dermatol.* 31 (8), 504–505. doi: 10.3969/j.issn.1000-4963.2002.08.014

Liu, L. F., and Wu, R. R. (2008). "Facial Phaeohyphomycosis: A Case Report.", in *Paper Presented at Zhejiang Dermatology Academic Conference*(Shaoxing, China).

Liu, Z. H., Xia, X. J., Zhong, Y., Sang, B., Lv, W. W., Wang, M., et al. (2013). Phaeohyphomycosis Caused by *Microsphaeropsis Arundinis*: A Case Report. *Chin. J. Dermatol.* 46 (8), 554. doi: 10.3760/cma.j.issn.0412-4030.2013.08.006

Liu, M., Xin, X., Li, J., and Chen, S. (2015). The First Case of Endophthalmitis Due to *Rhinocladiella Basitona* in an Immunocompetent Patient. *Diagn. Microbiol. Infect. Dis.* 83 (1), 49–52. doi: 10.1016/j.diagmicrobio.2015.05.014

Liu, C. L., Xu, H. Y., Li, H., Yuan, W. L., and Yang, Z. K. (2011). Fungal Keratitis Caused by *Alternaria Alternata*: A Case Report. *Lab. Med. Clin.* 8 (3), 374. doi: 10.3969/j.issn.1672-9455.2011.03.072

Liu, H., Zhang, J., Chen, Y., Xue, R., Zeng, W., Xi, L., et al. (2019). Phaeohyphomycosis Due to *Exophiala Spinifera* Greatly Improved by ALA-PDT: A Case Report. *Photodiagnosis Photodyn Ther.* 28, 297–299. doi: 10.1016/j.pdpdt.2019.10.002

Liu, Z. X., Zhang, J., Zhang, X. J., and Tai, X. X. (2001). A Case of Chest Tinea Nigra. *Chin. J. Lepr Skin Dis.* 17 (3), 201. doi: 10.3969/j.issn.1009-1157.2001.03.033

Li, H. Y., Xu, B., Zhou, Y. C., and Su, H. H. (1996). Chronic Mucocutaneous Candidiasis Caused by *Trichophyton Mentagrophytes* and *Alternaria* Sp.: A Case Report. *Chin. J. Dermatol.* 29 (5), 381. https://kns.cnki.net/kcms/detail/detail.aspx?FileName=ZHPF199605053&DbName=CJFQ1996

Li, L., Zhang, Q. Q., Wang, J. J., and Zhu, M. (2005). "Cutaneous Phaeohyphomycosis Due to Cladophialophora Bantiana: A Case Report.", in *Paper Presented at the 1st National Conference on Deep Fungal Infection* (Xiamen, China).

Lu, S., Cai, W. Y., and Mao, Y. P. (2016). A Case Report and Brief Survey of Tinea Nigra Cases Reported in Mainland China. *Chin. J. Mycol* 11 (5), 279–281. doi: 10.3969/j.issn.1673-3827.2016.05.007

Lu, X. H., Gao, Y., Li, S. X., Wang, M., Wang, T., and Gao, H. (2012). Clinical and Etiological Study of Five Keratitis Cases Due to *Curvularia Lunata*. *Chin. J. Lab. Med.* 35 (5), 469–471. doi: 10.3760/cma.j.issn.1009-9158.2012.05.018

Lv, Y. C. (1990). Rare Mycoses From Taiwan. *Jpn J. Med. Mycol* 31 (3), 179–185. doi: 10.3314/jjmm.31.179

Lv, G. X., Ge, Y. P., Shen, Y. N., Li, M., Zhang, X., Chen, H., et al. (2011). Phaeohyphomycosis Caused by a Plant Pathogen, *Corynespora Cassiicola*. *Med. Mycol* 49 (6), 657–661. doi: 10.3109/13693786.2011.553635

Lv, G. X., Shen, Y. N., Chen, W., Hu, S. Q., Li, H. Z., and Liu, W. D. (2005). Cutaneous Mycosis Caused by *Arthrinium Phaeospermum*. *Chin. J. Dermatol.* 38 (4), 232–234. doi: 10.3760/j.issn:0412-4030.2005.04.012

Lv, G. X., Shen, Y. N., Chen, W., Qin, C. L., Liu, W. D., and Wu, S. X. (2001). Phaeohyphomycosis Caused by *Bipolaris Spicifera*: First Case Report in China. *Chin. J. Dermatol.* 34 (5), 358–360. doi: 10.3760/j.issn:0412-4030.2001.05.010

Ma, Y. R. (2018). *Morphological and Molecular Phylogenic Studies of Dematiaceous Hyphomycet on Dead Branches From Five Provisions in Southern China. [Master's Thesis]* (Tai'an, China: Shandong Agricultural University).

Matsushita, A., Jilong, L., Hiruma, M., Kobayashi, M., Matsumoto, T., Ogawa, H., et al. (2003). Subcutaneous Phaeohyphomycosis Caused by *Veronaea Botryosa* in the People's Republic of China. *J. Clin. Microbiol.* 41 (5), 2219–2222. doi: 10.1128/JCM.41.5.2219-2222.2003

McGinnis, M. R. (1983). Chromoblastomycosis and Phaeohyphomycosis: New Concepts, Diagnosis, and Mycology. *J. Am. Acad. Dermatol.* 8 (1), 1–16. doi: 10.1016/s0190-9622(83)70001-0

Ng, C. Y., de Hoog, S., Li, H. E., Lee, Y. Y., Chen, C. B., and Sun, P. L. (2017). Cutaneous Exophiala Oligosperma Infection in a Patient With Bullous Pemphigoid With a Review of the Literature. *Mycopathologia* 182 (5-6), 539–547. doi: 10.1007/s11046-016-0104-6

Pan, Y., Dai, W., and Fang, S. (2021). Cutaneous Phaeohyphomycosis Caused by *Exserohilum Rostratum*: A Case With Unusual Presentation. *Clin. Exp. Dermatol.* 46 (3), 569–571. doi: 10.1111/ced.14477

Paul, S., Singh, P., Rudramurthy, S. M., Chakrabarti, A., and Ghosh, A. K. (2017). Matrix-Assisted Laser Desorption/Ionization-Time of Flight Mass Spectrometry: Protocol Standardization and Database Expansion for Rapid Identification of Clinically Important Molds. *Future Microbiol.* 12, 1457–1466. doi: 10.2217/fmb-2017-0105

Paul, S., Singh, P., Sharma, S., Prasad, G. S., Rudramurthy, S. M., Chakrabarti, A., et al. (2019). MALDI-TOF MS-Based Identification of Melanized Fungi is Faster and Reliable After the Expansion of In-House Database. *Proteomics Clin. Appl.* 13 (3), e1800070. doi: 10.1002/prca.201800070

Pi, X. B., Wu, Q. K., and Li, J. H. (2005). A Case of Tinea Manuum Nigra. *Chin. J. Dermatol.* 38 (8), 527. doi: 10.3760/j.issn:0412-4030.2005.08.029

Qiu, W. Y., and Yao, Y. F. (2013). Mycotic Keratitis Caused by Concurrent Infections of *Exserohilum Mcginnisii* and *Candida Parapsilosis*. *BMC Ophthalmol.* 13 (1), 37. doi: 10.1186/1471-2415-13-37

Queiroz-Telles, F., de Hoog, S., Santos, D. W., Salgado, C. G., Vicente, V. A., Bonifaz, A., et al. (2017). Chromoblastomycosis. *Clin. Microbiol. Rev.* 30 (1), 233–276. doi: 10.1128/CMR.00032-16

Qu, B., Xia, X. J., Huang, F. L., Li, L. L., and Xu, A. E. (2007). A Case of Pediatric Tinea Nigra. *Chin. J. Dermatol.* 40 (8), 510. doi: 10.3760/j.issn:0412-4030.2007.08.026

Revankar, S. G., Patterson, J. E., Sutton, D. A., Pullen, R., and Rinaldi, M. G. (2002). Disseminated Phaeohyphomycosis: Review of an Emerging Mycosis. *Clin. Infect. Dis.* 34 (4), 467–476. doi: 10.1086/338636

Revankar, S. G., and Sutton, D. A. (2010). Melanized Fungi in Human Disease. *Clin. Microbiol. Rev.* 23, 884–928. doi: 10.1128/CMR.00019-10

Revankar, S. G., Sutton, D. A., and Rinaldi, M. G. (2004). Primary Central Nervous System Phaeohyphomycosis: A Review of 101 Cases. *Clin. Infect. Dis.* 38 (2), 206–216. doi: 10.1086/380635

Sang, H., Zheng, X. E., Kong, Q. T., Zhou, W. Q., He, W., Lv, G. X., et al. (2011). A Rare Complication of Ear Piercing: A Case of Subcutaneous Phaeohyphomycosis Caused by *Veronaea Botryosa* in China. *Med. Mycol* 49 (3), 296–302. doi: 10.3109/13693786.2010.513340

Sang, H., Zheng, X. E., Zhou, W. Q., He, W., Lv, G. X., Shen, Y. N., et al. (2012). A Case of Subcutaneous Phaeohyphomycosis Caused by *Cladosporium Cladosporioides* and its Treatment. *Mycoses* 55 (2), 195–197. doi: 10.1111/j.1439-0507.2011.02057.x

Shi, D., Lu, G., Mei, H., de Hoog, G. S., Zheng, H., Liang, G., et al. (2016). Onychomycosis Due to *Chaetomium Globosum* With Yellowish Black Discoloration and Periungual Inflammation. *Med. Mycol Case Rep.* 13, 12–16. doi: 10.1016/j.mmcr.2016.09.001

Shi, M., Sun, J., Lu, S., Qin, J., Xi, L., and Zhang, J. (2019). Transcriptional Profiling of Macrophages Infected With. *Fonsecaea Monophora Mycoses* 62 (4), 374–383. doi: 10.1111/myc.12894

Stappers, M., Clark, A. E., Aimanianda, V., Bidula, S., Reid, D. M., Asamaphan, P., et al. (2018). Recognition of DHN-Melanin by a C-Type Lectin Receptor is Required for Immunity to. *Aspergillus Nat.* 555 (7696), 382–386. doi: 10.1038/nature25974

Sun, P. L., and Ju, Y. M. (2011). Onychomycosis Caused by *Phaeoacremonium Parasiticum*: First Case Report. *Mycoses* 54, 172–174. doi: 10.1111/j.1439-0507.2009.01789.x

Sun, S., Yuan, G., Zhao, G., Chen, H., and Yu, B. (2010). Endophthalmitis Caused by *Phialophora Verrucosa* and *Streptococcus Intermedius*: A Case Report. *Med. Mycol* 48 (8), 1108–1111. doi: 10.3109/13693786.2010.511283

Tan, H., Xu, Y., Yang, X. C., Zhong, B. Y., Lan, X. M., and Zhou, C. J. (2014). Tinea Nigra Palmaris: A Case Report. *J. Chin. Dermatol.* 43 (6), 354–355. doi: 10.16761/j.cnki.1000-4963.2014.06.003

To, K. K., Lau, S. K., Wu, A. K., Lee, R. A., Ngan, A. H., Tsang, C. C., et al. (2012). *Phaeoacremonium Parasiticum* Invasive Infections and Airway Colonization Characterized by Agar Block Smear and ITS and β-Tubulin Gene Sequencing. *Diagn. Microbiol. Infect. Dis.* 74 (2), 190–197. doi: 10.1016/j.diagmicrobio.2012.06.014

Tong, X. C., Qiu, Y. L., Wang, H. W., Tan, F. R., Ben, S. Q., and Xu, T. M. (2020). Cerebral Phaeohyphomycosis in an Immunocompetent Patient. *Med. Mal Infect.* 50 (8), 756–758. doi: 10.1016/j.medmal.2020.09.002

Tsai, T. H., Chen, W. L., Peng, Y., Wang, I. J., and Hu, F. R. (2006). Dematiaceous Fungal Keratitis Presented as a Foreign Body–Like Isolated Pigmented Corneal Plaque: A Case Report. *Eye (Lond)* 20 (6), 740–741. doi: 10.1038/sj.eye.6701995

Tsang, C. C., Chan, K. F., Chan, W., Chan, J., Au-Yeung, R., Ngan, A., et al. (2021). Hepatic Phaeohyphomycosis Due to a Novel Dematiaceous Fungus, *Pleurostoma Hongkongense* Sp. *Nov.*, and Importance of Antifungal Susceptibility Testing. *Emerg. Microbes Infect.* 10 (1), 81–96. doi: 10.1080/22221751.2020.1866955

Tsang, C. C., Chan, J. F., Ip, P. P., Ngan, A. H., Chen, J. H., Lau, S. K., et al. (2014). Subcutaneous Phaeohyphomycotic Nodule Due to *Phialemoniopsis Hongkongensis* Sp. *J. Clin. Microbiol.* 52 (9), 3280–3289. doi: 10.1128/JCM.01592-14

Tsang, C. C., Chan, J. F., Trendell-Smith, N. J., Ngan, A. H., Ling, I. W., Lau, S. K., et al. (2014). Subcutaneous Phaeohyphomycosis in a Patient With IgG4-Related Sclerosing Disease Caused by a Novel Ascomycete, Hongkongmyces Pedis Gen. Et Sp. *Nov.*: First Report of Human Infection Associated With the Family Lindgomycetaceae. *Med. Mycol* 52 (7), 736–747. doi: 10.1093/mmy/myu043

Tseng, P. H., Lee, P., Tsai, T. H., and Hsueh, P. R. (2005). Central Venous Catheter-Associated Fungemia Due to. *Wangiella Dermatitidis J. Formos Med. Assoc.* 104 (2), 123–126. doi: 10.1016/j.jpainsymman.2004.05.010

Wan, J. Z., Dai, W. L., Ren, Z. F., and Chen, R. E. (1987). Phaeohyphomycosis Due to *Exophiala Spinifera* in China, Scanning Electron Microscope Observation at Tached. *J. Clin. Dermatol.* 16 (1), 4–5.

Wang, L., Al-Hatmi, A. M., Lai, X., Peng, L., Yang, C., Lai, H., et al. (2016). *Bipolaris Oryzae*, a Novel Fungal Opportunist Causing Keratitis. *Diagn. Microbiol. Infect. Dis.* 85 (1), 61–65. doi: 10.1016/j.diagmicrobio.2015.11.020

Wang, C. H., Chen, W. T., Ting, S. W., and Sun, P. L. (2019). Subcutaneous Fungal Infection Caused by a Non-Sporulating Strain of *Corynespora Cassiicola* Successfully Treated With Terbinafine. *Mycopathologia* 184 (5), 691–697. doi: 10.1007/s11046-019-00393-0

Wang, T. K., Chiu, W., Chim, S., Chan, T. M., Wong, S. S., and Ho, P. L. (2003). Disseminated *Ochroconis Gallopavum* Infection in a Renal Transplant

Recipient: The First Reported Case and a Review of the Literature. *Clin. Nephrol.* 60 (6), 415–423. doi: 10.5414/cnp60415

Wang, Q., Li, H., Chen, H. B., Lin, J. H., and Wang, H. (2014). Infected by *Phaeoacremonium Parasiticum* After Joint Replacement: A Case Report. *Chin. J. Lab. Med.* 37 (5), 391–193. doi: 10.3760/cma.j.issn.1009-9158.2014.05.018

Wang, H., Liu, Y., Chen, S. C., Long, Y., Kong, F., and Xu, Y. C. (2016). *Chaetomium Atrobrunneum* and *Aspergillus Fumigatus* in Multiple Tracheal Aspirates: Copathogens or Symbiosis. *J. Microbiol. Immunol. Infect.* 49 (2), 281–285. doi: 10.1016/j.jmii.2015.12.011

Wang, D. L., Li, R. Y., and Wang, X. H. (1989). A Case Report of Phaeohypomycosis Caused by *Exophiala Spinifera*. *J. Chin. Dermatol.* 22 (4), 262–263. URL: http://qikan.cqvip.com/Qikan/Article/Detail?id=197579

Wang, J. J., Li, L., Xiao, J. R., Zhu, M., and Zhang, Q. Q. (2004). Subcutaneous Phaeohyphomycosis Caused by *Curvularia Clavata*. The First Case Report in China. *Chin. J. Dermatol.* 37 (8), 443–445. doi: doi:10.3760/j.issn:0412-4030.2004.08.001

Wang, X. B., Li, Z. H., Ye, F. S., and Li, Y. (2008). Tinea Nigra Palmaris in a Child: A Case Report. *J. Clin. Dermatol.* 37 (11), 721–722. doi: 10.3969/j.issn.1000-4963.2008.11.011

Wang, D. L., Nishimura, Z., Gong, Z. C., Wang, X. H., and Li, Y. N. (1991). Classification and Identification of *Exophiala Dermatitidis*. *Chin. J. Dermatol.* 1, 21–23. http://qikan.cqvip.com/Qikan/Article/Detail?id=678918

Wang, X., Wang, W., Lin, Z., Wang, X., Li, T., Yu, J., et al. (2014). CARD9 Mutations Linked to Subcutaneous Phaeohyphomycosis and TH17 Cell Deficiencies. *J. Allergy Clin. Immunol.* 133 (3), 905–908. doi: 10.1016/j.jaci.2013.09.033

Wang, L., Wang, C., Shen, Y., Lv, G., She, X., Zeng, R., et al. (2015). Phaeohyphomycosis Caused by *Exophiala Spinifera*: An Increasing Disease in Young Females in Mainland China? Two Case Reports and Review of Five Cases Reported From Mainland China. *Mycoses* 58 (3), 193–196. doi: 10.1111/myc.12295

Wang, C., Xing, H., Jiang, X., Zeng, J., Liu, Z., Chen, J., et al. (2019). Cerebral Phaeohyphomycosis Caused by *Exophiala Dermatitidis* in a Chinese CARD9-Deficient Patient: A Case Report and Literature Review. *Front. Neurol.* 10. doi: 10.3389/fneur.2019.00938

Wang, X., Zhang, R., Wu, W., Song, Y., Wan, Z., Han, W., et al. (2018). Impaired Specific Antifungal Immunity in CARD9-Deficient Patients With Phaeohyphomycosis. *J. Invest. Dermatol.* 138 (3), 607–617. doi: 10.1016/j.jid.2017.10.009

Wen, Y. M., Rajendran, R. K., Lin, Y. F., Kirschner, R., and Hu, S. (2016). Onychomycosis Associated With *Exophiala Oligosperma* in Taiwan. *Mycopathologia* 181, 83–88. doi: 10.1007/s11046-015-9945-7

Woo, P. C., Lau, S. K., Ngan, A. H., Tse, H., Tung, E. T., and Yuen, K. Y. (2008). *Lasiodiplodia Theobromae* Pneumonia in a Liver Transplant Recipient. *J. Clin. Microbiol.* 46 (1), 380–384. doi: 10.1128/JCM.01137-07

Woo, P. C., Ngan, A. H., Tsang, C. C., Ling, I. W., Chan, J. F., Leung, S. Y., et al. (2013). Clinical Spectrum of *Exophiala* Infections and a Novel *Exophiala* Species, *Exophiala Hongkongensis*. *J. Clin. Microbiol.* 51, 260–267. doi: 10.1128/JCM.02336-12

Wu, Q. K., Li, Q. X., Luo, X. Q., and He, Y. C. (2005). A Case of Pediatric Tinea Nigra Caused by *Exophiala Werneckii*. *Chin. J. Lab. Med.* 28 (4), 448. doi: 10.3760/j:issn:1009-9158.2005.04.037

Xia, X. J., Zhou, S. M., and Xu, A. E. (2005). Phaeohypomycosis Caused by *Exophiala Jeanselmei*: A Case Report. *Chin. J. Lepr Skin Dis.* 21 (3), 217–218. doi: 10.3969/j.issn.1009-1157.2005.03.022

Xie, Z., Wu, W., Meng, D., Zhang, Q., Ma, Y., Liu, W., et al. (2018). A Case of Phaeohyphomycosis Caused by *Corynespora Cassiicola* Infection. *BMC Infect. Dis.* 18 (1), 444. doi: 10.1186/s12879-018-3342-z

Xu, X. L., Yang, P. H., Zhang, G. C., Sun, Y. Q., Fan, X., Liu, J. Y., et al. (2010). A Case of Pulmonary Infection Caused by *Alternaria* Sp. combined with *Candida krusei*. *Chin. J. Mycol* 5 (4), 234–235. doi: 10.3969/j.issn.1673-3827.2010.04.012

Yang, H., Cai, Q., Gao, Z., Lv, G., Shen, Y., Liu, W., et al. (2018). Subcutaneous Phaeohyphomycosis Caused by *Exophiala Oligosperma* in an Immunocompetent Host: Case Report and Literature Review. *Mycopathologia* 183 (5), 815–820. doi: 10.1007/s11046-018-0279-0

Yang, H. H., Chen, H. C., Wu, Y. H., Lin, Y. C., and Sun, P. L. (2004). Cutaneous Phaeohyphomycosis Caused by *Exophiala Jeanselmei*-Successful Treatment With the Combination of Itraconazole, Topical Heat Followed by Additional Cryotherapy. *Dermatol. Sin.* 22 (4), 327–332.

Yang, S. J., Ng, C. Y., Wu, T. S., Huang, P. Y., Wu, Y. M., and Sun, P. L. (2019). Deep Cutaneous *Neoscytalidium Dimidiatum* Infection: Successful Outcome With Amphotericin B Therapy. *Mycopathologia* 184 (1), 169–176. doi: 10.1007/s11046-018-0308-z

Yang, Z. H., Zhou, W. T., and Yu, Y. F. (2009). Fungal Keratitis Caused by *Alternaria* Sp.: A Case Report. *Chin. J. Ophthalmol.* 45 (9), 836–837. doi: 10.3760/cma.j.issn.0412-4081.2009.09.016

Yan, X. X., Yu, C. P., Fu, X. A., Bao, F. F., Du, D. H., Wang, C., et al. (2016). CARD9 Mutation Linked to *Corynespora Cassiicola* Infection in a Chinese Patient. *Br. J. Dermatol.* 174 (1), 176–179. doi: 10.1111/bjd.14082

Yao, L. (2018). *A Case Report of Disseminated Phaeohyphomycosis Due to M.arundinis and Literatures Analysis. [Master's Thesis]* (Nanning, China: Guangxi Medical University).

Ye, F., Wu, L. L., Su, D. H., Zeng, Q. S., and Chen, R. C. (2014). Pulmonary Phaeohyphomycosis Due to *Exophiala Jeanelmei*: A Case Report and Review of Literature. *Chin. J. Infect. Chemother.* 14 (3), 229–234. doi: 10.3969/j.issn.1009-7708.2014.03.015

You, H. Y., You, G., Li, X. J., Liu, B. M., Zhang, M. L., and Wang, J. (2005). A case of cutaneous alternariosis. *J. Clin. Dermatol.* 34 (2), 82–84. doi: 10.3969/j.issn.1000-4963.2005.02.007

Yu, Y. H., Sun, P. L., Lee, C. H., Su, C. J., and Tseng, H. C. (2021). Deep Cutaneous Fungal Infection by *Pleosporales*: An Exceptional Pathogen in Tropical Taiwan. *J. Dermatol.* 48 (3), 413–417. doi: 10.1111/1346-8138.15698

Yu, J., Wan, Z., Lu, Q. Y., Chen, W., and Wang, X. H. (2009). Onychomycosis Caused by *Trichophyton Rubrum* and *Cladosporium Cladosporioides* in Psoriasis Patient: One Case Report. *Chin. J. Mycol* 4, 298–300. doi: 10.3969/j.issn.1673-3827.2009.05.013

Yu, J., Yang, S., Zhao, Y., and Li, R. (2006). A Case of Subcutaneous Phaeohyphomycosis Caused by *Chaetomium Globosum* and the Sequences Analysis of *C. Globosum*. *Med. Mycol* 44 (6), 541–545. doi: 10.1080/13693780500525235

Zeng, Y. B., Li, L., Mei, L. H., Gan, H. H., Wang, H. F., Quan, Z., et al. (2010). A Case of Pemphigoid Accompany With Cutaneous Alternariosis. *Chin. J. Derm Venereol* 24 (5), 456–457. URL: http://qikan.cqvip.com/Qikan/Article/Detail?id=33889422

Zhang, Z. Y., and Lian, C. H. (2015). "Deep Fungal Infection Caused by Aureobasidium Pullulans: A Case Report". in *National Annual Conference of Integrated Traditional Chinese and Western Medicine for Dermatology and Venereal Diseases*(Changsha, China).

Zhang, H. P., Lv, G. X., Yang, L. J., Wu, Z. F., and Liu, W. D. (2006). Fungal Keratitis Caused by *Exerohilum Rostratum*: A Case Report. *Chin. J. Ophthalmol.* 42 (6), 560. doi: doi:10.3760/j:issn:0412-4081.2006.06.021

Zhang, H., Ran, Y., Li, D., Liu, Y., Xiang, Y., Zhang, R., et al. (2010). *Clavispora Lusitaniae* and *Chaetomium Atrobrunneum* as Rare Agents of Cutaneous Infection. *Mycopathologia* 169 (5), 373–380. doi: 10.1007/s11046-009-9266-9

Zhang, R. J., Wang, X. W., Wan, Z., and Li, R. Y. (2017). CARD9 Mutations and Related Immunological Research of One Case With Disseminated Phaeohyphomycosis. *J. Microbes Infect.* 12 (1), 14–23. 10.3969/j.issn.1673-6184.2017.01.004

Zhang, H. E., Wang, D. L., and Zhao, B. A. (1990). Subcutaneous Phaeohypomycosis Caused by *Veronaea Botryosa*: A Case Report. *Chin. J. Dermatol.* 23 (2), 96–98. http://qikan.cqvip.com/Qikan/Article/Detail?id=425909

Zhang, X. L., Ye, H., Lu, J. J., and Lv, X. J. (2019). Infection Caused by *Aureobasidium Pullulans*: One Case Report and Literature Review. *Chin. J. Infect. Chemother.* 19 (6), 621–626. doi: 10.16718/i.1009-7708.2019.06.008

Zhao, Y. M., Deng, C. R., Chen, X., Liu, M. L., Chen, S. P., Wang, Z., et al. (1990). *Arthriniuim Phaeospermum* Causing Dermatomycosis, a New Record of China. *Acta Mycol Sin.* 9 (3), 232–235. http://qikan.cqvip.com/Qikan/Article/Detail?id=406849

Zhao, W., Kuang, X. Z., Li, H. G., Li, R. Y., Wang, X. H., and Wang, D. L. (2001). Phaeohyphomycosis Caused by *Cladosporium Herbarum*: The First Case Report in China. *Chin. J. Lepr Skin Dis.* 17 (2), 89–90. doi: 10.3969/j.issn.1009-1157.2001.02.006

Zhao, J. Y., Wang, Z. F., Li, R. Y., Wang, D. L., and Bai, Y. P. (2002). Pemphigus Patient With Pulmonary Fungal Infection Caused by *Ochroconis Gallopava*: The First Case Report in China. *Nalt Med. J. China* 82 (19), 1310–1313. doi: doi:10.3760/j:issn:0376-2491.2002.19.005

Zheng, H., Song, N., Mei, H., Dong, J., Li, D., Li, X., et al. (2020). *In Vitro* Activities of Ravuconazole and Isavuconazole Against Dematiaceous Fungi. *Antimicrob. Agents Chemother.* 64 (9), e00643–e00620. doi: 10.1128/AAC.00643-20

Zheng, Q., Yang, F. Z., Feng, G. Z., and Yu, S. (1988). Facial Phaeohypomycosis of the Face Caused by *Exophiala Jeanselmei*. *J. Harbin Med. Univ* 22 (3), 206–208. https://kns.cnki.net/kcms/detail/detail.aspx?FileName=HYDX198803023&DbName=CJFQ1988

Zhong, B. Y., Yang, X. C., Hao, J., Zhai, Z. F., Wang, L., and Hao, F. (2007). Keratohelcosis Due to *Exserohilum Rostratum*: A Case Report. *J. Clin. Dermatol.* 36 (11), 712–714. doi: 10.3969/j.issn.1000-4963.2007.11.017

Zhou, Y. B., Chen, P., Sun, T. T., Wang, X. J., and Li, D. M. (2016). Acne-Like Subcutaneous Phaeohyphomycosis Caused by *Cladosporium Cladosporioides*: A Rare Case Report and Review of Published Literatures. *Mycopathologia* 181 (7), 567–573. doi: 10.1007/s11046-016-9995-5

Zhou, C. J., Deng, J., Wang, L., Zhong, B. Y., Li, Q. J., and Hao, F. (2009). Phaeohyphomycosis Caused by *Exophiala Jeanselmei*: A Case Report. *J. Clin. Dermatol.* 38 (3), 161–163. doi: 10.3969/j.issn.1000-4963.2009.03.010

Zhou, X. Y., Hu, Y. X., Hu, Y. Q., Liu, K. X., Wang, L. X., Wei, Q. Z., et al. (2012). Cutaneous and Subcutaneous Phaeohyphomycosis Caused by *Exophiala Jeanselmei* After Renal Transplantation: A Case Report. *J. South Med. Univ* 32 (8), 1206–1210. doi: 10.3969/j.issn.1673-4254.2012.08.31

Zhou, T., Tu, Y., Li, Q., and He, L. (2018). A Case of Cutaneous Alternariosis. *J. Clin. Dermatol.* 47 (4), 229–231. doi: 10.16761/j.cnki.1000-4963.2018.04.011

Zhu, L., and Xu, H. (2003). Mycotic Keratohelcosis Caused by *Alternaria Alternata*: A Case Report. *Zhejiang Clin. Med. J.* 5 (2), 148. doi: 10.3969/j.issn.1008-7664.2003.02.054

Conflict of Interest: The authors declare that the research was conducted in the absence of any commercial or financial relationships that could be construed as a potential conflict of interest.

Publisher's Note: All claims expressed in this article are solely those of the authors and do not necessarily represent those of their affiliated organizations, or those of the publisher, the editors and the reviewers. Any product that may be evaluated in this article, or claim that may be made by its manufacturer, is not guaranteed or endorsed by the publisher.

frontiers | Frontiers in Cellular and Infection Microbiology

ORIGINAL RESEARCH
published: 16 June 2022
doi: 10.3389/fcimb.2022.847950

Hemophagocytic Lymphohistiocytosis Secondary to Disseminated Histoplasmosis in HIV Seronegative Patients: A Case Report and Review of the Literature

Hongchao Chen[1†], Qing Yuan[2†], Hangbin Hu[2†], Jie Wang[2], Meihong Yu[2], Qing Yang[1] and Tingting Qu[2]*

[1] Deparment of Laboratory Medicine, The First Affiliated Hospital, Zhejiang University School of Medicine, Hangzhou, China, [2] State Key Laboratory for Diagnosis and Treatment of Infectious Diseases, Collaborative Innovation Center for Diagnosis and Treatment of Infectious Diseases, National Clinical Research Center for Infectious Diseases, Zhejiang University School of Medicine First Affiliated Hospital, Hangzhou, China

OPEN ACCESS

Edited by:
Fupin Hu,
Fudan University, China

Reviewed by:
Binghuai Lu,
China-Japan Friendship Hospital, China
Mei Kang,
Sichuan University, China

***Correspondence:**
Tingting Qu
qutingting@zju.edu.cn

[†]These authors have contributed equally to this work

Specialty section:
This article was submitted to Fungal Pathogenesis, a section of the journal Frontiers in Cellular and Infection Microbiology

Received: 03 January 2022
Accepted: 06 May 2022
Published: 16 June 2022

Citation:
Chen H, Yuan Q, Hu H, Wang J, Yu M, Yang Q and Qu T (2022) Hemophagocytic Lymphohistiocytosis Secondary to Disseminated Histoplasmosis in HIV Seronegative Patients: A Case Report and Review of the Literature. Front. Cell. Infect. Microbiol. 12:847950. doi: 10.3389/fcimb.2022.847950

Hemophagocytic lymphohistiocytosis (HLH) secondary to *Histoplasma capsulatum* infection is a rare disorder with poor outcome. Although cases of patients with human immunodeficiency virus (HIV) infection have been well documented, little study has reported in the setting of HIV seronegative. In this study, we report a case of HLH secondary to histoplasmosis in an immunocompetent patient in China and review all cases on this situation. The objective was to summary their epidemiology, clinical characteristics, diagnostic approaches, and therapeutic response. A 46-year-old male cooker presented fever, fatigue, anorexia, and weight loss. Bone marrow examination suggest fungus organism and hemophagocytosis, and further, bone marrow culture confirmed *Histoplasma capsulatum*, as the etiology of HLH. The patient was successfully treated. We reviewed a total of the 13 cases (including our patient) of HLH with histoplasmosis in intact immunology patients. Twelve of the 13 patients are from endemic areas, and nine of the 12 cases are from emerging endemic areas, India and China. Three patients had sojourn history may related to the disease onset. Twelve of the 13 cases fulfilled HLH-2004 criteria. The diagnosis of *Histoplasma capsulatum* infection was established by histological examination (13 of 13), culture (4 of 13), molecular method (2 of 13), and antigen or serological assays (2 of 13). Amphotericin B, posaconazole, and itraconazole show favorable activity against the fungus, seven patients used specific treatment for HLH. For analysis of outcomes, two of the 13 patients died. Our present case report and literature review show that disseminated *Histoplasma capsulatum* infection with HLH in the immunocompetent population becomes increasingly common in emerging endemic areas and have high mortality. It is necessary for clinicians to improve the awareness of disease diagnosis due to the atypical population and disease presentation. Timely diagnosis and early use of antifungal agents will lead to favorable prognosis.

Keywords: *Histoplasma capsulatum*, histoplasmosis, hemophagocytic lymphohistiocytosis, HIV seronegativity, immunocompetence, liposomal amphotericin B

INTRODUCTION

Histoplasma capsulatum is an environmental dimorphic fungus that causes histoplasmosis (Scheel et al., 2014). With a worldwide incidence, epidemic distribution mainly in North America and Latin American countries (Matos Baltazar et al., 2016). Many areas of Asia, including India, Southeast Asia, and China along Yangtze River, are also endemic (Wheat et al., 2016; Azar et al., 2020). Infection occurs when inhalation of fungal spores or hyphae from the environment soil, and the lung is the primary organ of infection. *H. capsulatum* can disseminate throughout the body in immunocompromised persons (Crossley et al., 2016; Matos Baltazar et al., 2016), who are at least 10 times more likely to develop progressive disseminated histoplasmosis (PDH) than the general individuals (Azar et al., 2020), without timely diagnosis and treatment can lead to fatal illness. In immunocompetent and non-respiratory patients, they are usually clinically silent or mild manifestations, and diagnosis is often so challenging that the rate of underdiagnosis is high.

Hemophagocytic lymphohistiocytosis (HLH) is a rare clinical disorder, charactered by unbridled and persistent immune activation of natural killer (NK), cytotoxic T cell. Failure to control the immune response leads to injury of multiple organs (Solomon et al., 2018). It can be divided into familial and acquired. Familial hemophagocytic lymphohistiocytosis (FHL) has a fundamental property of autosomal recessive inheritance, which is typically onset in infancy period (Bryceson et al., 2007). Acquired HLH is association with systemic infections, malignant diseases, or autoimmune disorders, cases onset mainly in adults (Al-Samkari and Berliner, 2018). Most cases of HLH secondary to *Histoplasma capsulatum* infection present in immunocompromised patients (Gil-Brusola1 et al., 2007; Nguyen et al., 2020; Castejón-Hernández et al., 2021), and clinicians are vigilant in diagnosing the disease in endemic areas.

Here, we present a rare case of an immunocompetent cooker with *Histoplasma* infection and secondary HLH, which was successfully treated by immunoglobulin and high-dose prednisone immunosuppression combined with antifungal therapy. A review of literature on this situation is also performed.

CASE PRESENTATION

In late August 2020, a 46-year-old male was admitted to our emergency department, with complaints of intermittent fever associated with fatigue and anorexia lasting for a month. He also complained of 30-kg weight loss within 5 months. The patient first visited a local hospital 2 weeks ago. Because of fever and lymphadenopathy, a bone marrow aspiration was performed. The bone marrow smear revealed hemophagocytosis and yeast-like bacteria; fungal infection was considered. However, no fungus was cultured in the bone marrow culture. Therefore, empirical antifungal treatment of Voriconazole was prescribed. After taking the drug, the patient developed insomnia and was replaced by itraconazole, without symptom improvement. He works as a cooker and gets up at 1 a.m. every day. He contacted with a soil-based environment for building and construction around his house. He lived in a rural area in Southeast China for more than 40 years and never traveled to foreign countries.

At physical examination, the patient has temperature of 39.7°C, pulse rate of 129/min, respiratory rate of 18/min, and blood pressure of 119/63mm of hg and has normal oxygen saturation. He had pallor and hepatosplenomegaly. Heart and lung auscultation were unremarkable.

The laboratory examination indicated pancytopenia at admission: hemoglobin, 63 g/L; platelet, 44×10^9/L; leucocytes, 1.6×10^9/L; neutrophils, 1.3×10^9/L. The C-reactive protein (CRP) level was 44.4 (normal, < 8) mg/L, and procalcitonin (PCT) level was 1.65 (normal, <0.15) ng/ml. Fibrinogen levels was decreased (1.0g/L). Serum ferritin was markedly elevated (2,775.0 ng/ml). The CD4 cell count was 120 cells/μl. He had mild abnormal serum levels of aspartate aminotransferase (AST) with 81U/L, alanine aminotransferase (ALT) with 53 U/L, and glutamyl transpeptidase (GGT) with 118 U/L, respectively. There was a decline in albumin levels, 32.0 g/L. The kidney function markers were within normal ranges. The patient had a detectable level of (1 → 3)-β-d-glucan, 212.56 (normal, < 60) pg/ml, and the GM (galactomannan) level was not elevated. Serological results for human immunodeficiency virus (HIV), Epstein–Barr virus, cytomegalovirus, hepatitis virus B and C, COVID-19, and the T-cell spot test for tuberculosis infection (T-SPOT) were negative. His blood culture did not grow any pathogenic organism. **Table 1** shows the results of relevant blood investigations.

Computed tomography (CT) of the chest was normal but the abdominal CT showed hepatosplenomegaly and posterior peritoneum lymphadenopathy (**Figure 1**). PET/CT revealed hepatosplenomegaly and posterior peritoneum lymphadenopathy and bone marrow with high FDG uptake, suggesting lymphoma probably. A bone marrow puncture was done at admission which displayed hemophagocytosis and negative result for bacterial culture. Hematoxylin and eosin (HE)–stained bone marrow demonstrated oval or round organisms with amaranth nuclei and capsule-like unstained halos around these organisms observed in the cytoplasm of phagocytes (**Figure 2**). The fungus culture of bone marrow was also sent to laboratory for further identification. After 8 weeks of initial plating on potato dextrose agar (PDA) medium at 25°C and subsequently sub-cultured at intervals of 2 weeks in Columbia blood agar medium at 25°C. These are shown in **Figure 3**, which finally confirmed as *Histoplasma capsulatum*.

The patient received empirical treatment with oral itraconazole from the day of admission (200 mg three times daily for 7 days). At day 2 after admission, the body temperature was back to normal. The laboratory examination were repeated at day 4 after admission: hemoglobin, 69 g/L; platelet, 67×10^9/L; leucocytes, 4.7×10^9/L, neutrophils: 4.2×10^9/L. Serum ferritin declined to 1,264.3 ng/ml. After the results of the bone marrow puncture come out, liposomal amphotericin B was prescribed (1.0 mg/kg daily for 10 days), followed by oral itraconazole (200 mg twice daily for a total of at least 12 months). For HLH, the patient received treatment with prednisone 40 mg daily and intravenous immunoglobulin 20 g daily for 5 days. The blood cell

TABLE 1 | Results of relevant blood investigations.

Test	Result
Autoimmunological antibodies	Negative
Leucocytes	1.6 × 10E9/L (normal, 4–10)
Hemoglobin	63 g/L (normal, 131–172)
Platelet	44 × 10E9/L (normal, 83–303)
C-reactive protein	44.4 mg/L (normal, <8)
Procalcitonin	1.65 ng/ml (normal, <0.15)
Fibrinogen	1.0 g/L (normal, 2-4)
Hepatic function test results	Mild abnormal
Prothrombin time(PT)	13.7 s (normal, 10-13.5)
D-dimer	2,451 μg/L (normal, <700)
Serum ferritin	2,775.0 ng/ml (normal, <323)
Renal function test results	Within normal range
Immunoglobulin A	77.0 mg/dl (normal, 100–420)
Immunoglobulin M	14.0 mg/dl (normal, 30–220)
Immunoglobulin G and complement proteins C3 and C4	Within normal range
Blood culture	Negative

count, CRP, PCT, and serum ferritin improved substantially after a week. The CD4 cell count also recovered normal after a week.

In this case, the patient presented with HLH with fever, splenomegaly, elevated ferritin, hypofibrinogenemia, blood cell abnormalities, and hemophagocytosis. Although he had no immunocompromised disease and never went to epidemic area, but he had been short of sleeping time for long time, and there was a lot of dust around his house because of building a road. It is unclear whether this may have been a risk factor for disease.

LITERATURE REVIEW

Case report and case series for HLH and histoplasmosis were identified in the five databases (Pubmed, Embase, Web of science, China National Knowledge Infrastructure, and Wanfang Data) by using search criteria ("lymphohistiocytosis, hemophagocytic" [MeSH Terms] AND "Histoplasmosis" [MeSH Terms]). The case being reported here is also included in the analysis and review of literature. The following criteria were used for the inclusion: 1) fulfilled HLH 2004 criteria or have a definition of HLH; 2) the infection of *Histoplasma capsulatum* is confirmed by standard methods; 3) immunity is normal, excluding diseases with compromised immunity, immunosuppressive medications therapy, and autoimmune diseases. In the past, clinicians' understanding of HLH was relatively insufficient, so it cannot be ruled out that we have missed some literature on HLH secondary to *H. capsulatum* infections.

A total of 90 articles were retrieved from the databases without time limit, including 77 papers in English, 8 in Spanish, and 2 in Chinese. After discarding three articles for

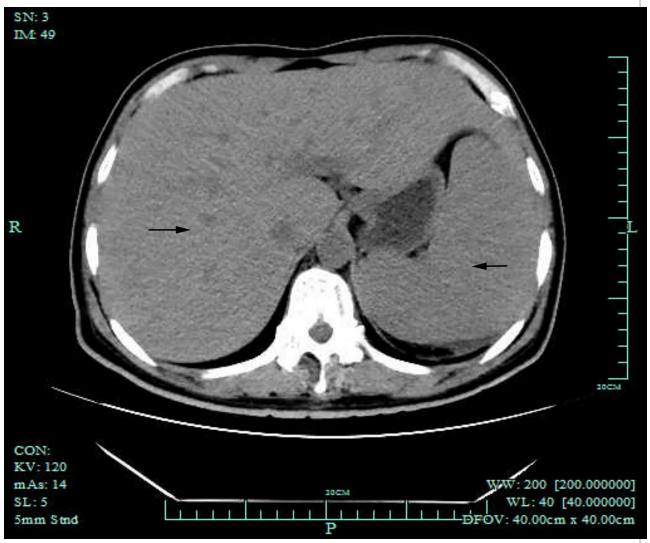

FIGURE 1 | Abdominal CT scan showed splenomegaly and hepatomegaly (black arrows).

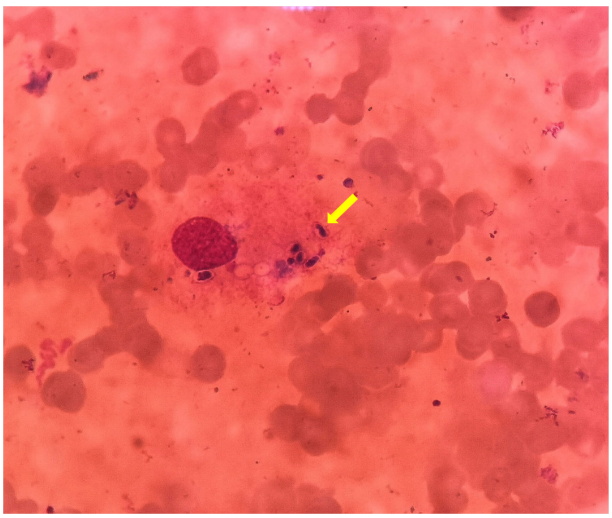

FIGURE 2 | HE stain of bone marrow puncture images (×1,000). These oval or round organisms with amaranth nuclei and capsule-like unstained halos around observed in the cytoplasm of phagocytes (yellow arrow).

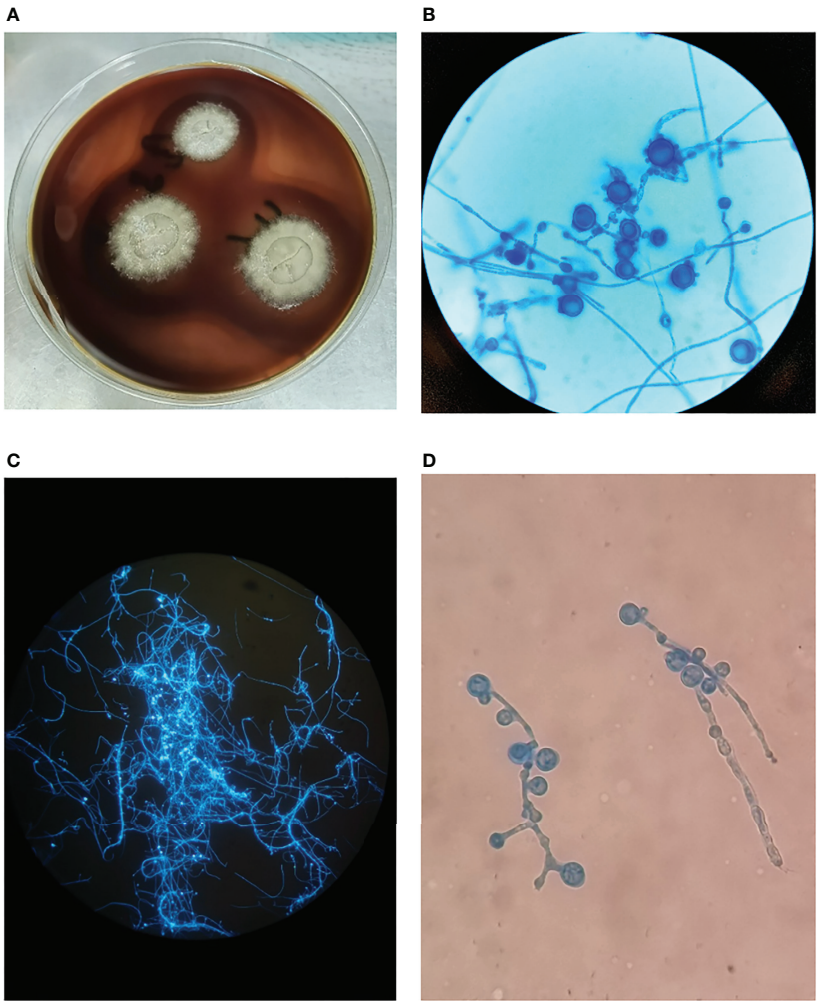

FIGURE 3 | **(A)** The colonies of *Histoplasma capsulatum* on Columbia blood agar medium after subculture, the fungus is milky white with villous hyphae in the outer ring. **(B)** Cogwheel-like macroconidia of *Histoplasma capsulatum* stained with Lactophenol cotton blue after subculture, ×400 magnification. **(C)** Hyphae and spores are bright blue fluorescent in Fluorescence staining, 100× magnification. **(D)** Lactophenol cotton blue staining in primary culture with cogwheel-like macroconidia, ×400 magnification.

incomplete information, the remaining 87 literature contain a total of 128 patients. This review of literature identified 12 articles with 12 cases (9.4%), presenting a confirmed HLH with histoplasmosis of intact immunology. For the excluded articles, 65 of 128 (50.8%) patients were infected with HIV; 20 of 128 (15.6%) had rheumatic disease; 15 of 128 (11.7%) had organ transplant history (14 cases with renal transplant, and one case with heart transplant); and 3 of 128 (2.3%) had hematologic malignancy. Immunosuppressive medications therapy containing tumor necrosis factor inhibitors, steroid hormone, and chemotherapy were used in 43 of 128 (33.6%) patients. Details are displayed in the **Supplementary Materials**.

The features of the 12 patients and our case with competent immunology are summarized in the **Table 2**. Two of them were infants, and the others were all older than 16 years. Among the 13 cases whose sex was mentioned, 10 were male patients, including our patient. Five patients were China born (including our patient), two of them had a sojourn history in Africa, four patients were India born, three patients were America born, and one patient was Germany born but had a visiting of a bat cave when she had traveling in Thailand 8 months before onset. Three patients had job as cooker, blood bank worker, and homemaker; occupations of other seven patients were unknown.

The nonspecific clinical syndrome consists of fever (13 of 13), weight loss (8 of 13), anorexia (5 of 13), fatigue (4 of 13), and cough (4 of 13). Among 13 patients whose laboratory tests were mentioned, significant cytopenias involving at least two cell lines, elevated ferritin, hypertriglyceridemia, elevated LDH, elevated hepatobiliary enzymes, and organomegaly (hepatomegaly, splenomegaly, and lymphadenopathy) are common symptoms. NK cell activity was detected in three study, but only one patient

TABLE 2 | Case reports on HLH due to histoplasmosis in HIV seronegative patients.

Reference	(Kashif et al., 2015)	(Mukherjee and Basu, 2015)	(Sonavane et al., 2016)	(Ferguson-Paul et al., 2016)	(Schulze et al., 2017)	(Bommanan et al., 2017)	
Published year	2015	2015	2016	2016	2017	2017	
Number of cases	1	1	1	1	1	1	
Home country	USA	India	India	USA	Germany	India	
Age/Gender	34y/M	52y/M	43y/F	6m/F	59y/F	32y/M	
Occupation	/	/	homemaker	NA	/	/	
History of sojourn	Nigeria	/	/	–	Thailand/ Costa Rica	–	
Clinical manifestation							
Fever	+	+	+	+	+	+	
Fatigue	–	–	+	–	–	–	
Rash	–	+	–	–	–	–	
Weight loss	+	–	+	–	+	+	
Anorexia	+	–	+	–	–	–	
Cough	–	–	+	–	–	–	
Foot edema	–	+	+	–	–	–	
Co-infections	–	–	M.TB	–	EBV/Hafnia alvei	–	
Underlying disease	Sickle cell disease	COPD/DM/EN	TB	–	breast cancer	–	
Leucocytes (k/μl)	10	4.2	2.6	/	12.37	1.4	
Neutrophils (k/μl)	/	/	/	1.5	/	1.2	
Hemoglobin (g/dl)	4.9	6	7	5.9	5.8	7.9	
Platelet (k/μl)	48	/	91	11	128	40	
Triglycerides (mg/dl)	135	/	NR	378	270	/	
fibrinogen (g/L)	0.69	/	0.53	0.78	/	/	
NK cell activity	/	/	/	NR	/	/	
Serum ferritin (μg/L)	7,493	3.06	891.7	1,218	99,919	3,339	
Soluble CD25 (U/ml)	/	/	/	21,530	4,445	/	
ALT (U/L)	5,058	/	23	/	44	62	
AST (U/L)	16,637	/	28	/	39	52	
LDH	1,466	/	296	/	306	/	
Hepatomegaly	+	+	+	+	–	+	
Splenomegaly	+	+	+	+	–	+	
Lymphadenopathy	+	+	–	–	+	–	
Pulmonary disorders	+	/	+	+	+	–	
Number of HLH-2004 criteria	6	3	6	7	5	5	
Hemophagocytosis	BM Bx	BM Bx	BM Path	BM Path	BM Path	BM Path	
Diagnosis of histoplasmosis							
Path	LN Bx	liver/spleen Bx	BM Path	BM Path	colon/liver/LN/ lung Bx	BM Path	
Culture	/	/	/	/	/	/	
Antigen assays	–	/	/	Serum/urine/CSF	/	/	
Antibody assays	/	/	/	+	/	/	
Molecular method	/	/	/	/	+	/	
Antifungal treatment	AmB/Itra	AmB	AmB/Itra	AmB/Itra	AmB/Posa	AmB	
HLH-specific treatment	DE	–	–	DE	–	–	
Outcomes	Died	Died	Recovery	Recovery	Recovery	Recovery	
Reference	(Xiong et al., 2017)	(Pancoast et al., 2019)	(Gupta et al., 2019)	(L Xiaolin et al., 2021)	(Song et al., 2021)	(Sijie et al., 2022)	PS
Published year	2017	2019	2019	2020	2021	2022	–
Number of cases	1	1	1	1	1	1	1
Home country	China	USA	India	China	China	China	China
Age/Gender	37y/M	3m/M	29y/M	27y/M	16y/M	44y/M	46y/M
Occupation	blood bank worker	NA	/	/	NA	/	Cooker
History of sojourn	–	/	/	/	/	Kenya	–
Clinical manifestation							
Fever	+	+	+	+	+	+	+
Fatigue	–	–	–	+	–	+	+
Rash	–	–	–	–	–	–	–

(Continued)

TABLE 2 | Continued

Reference	(Kashif et al., 2015)	(Mukherjee and Basu, 2015)	(Sonavane et al., 2016)	(Ferguson-Paul et al., 2016)	(Schulze et al., 2017)	(Bommanan et al., 2017)	
Weight loss	+	–	+	–	–	+	+
Anorexia	–	–	+	–	–	+	+
Cough	+	–	+	–	–	+	–
Foot edema	–	–	–	–	–	+	–
Co-infections	CMV HSV	–	–	HBV	–	–	–
Underlying disease	–	–	–	Hepatitis	–	–	–
Leucocytes (k/μl)	1.86	/	3.9	3.45	2.35	2.2	1.6
Neutrophils (k/μl)	1.23	/	/	/	0.84	1.63	1.3
Hemoglobin (g/dl)	8.6	/	8.4	8.7	11.8	6.3	6.3
Platelet (k/μl)	2	/	79	32	62	4	44
Triglycerides (mg/dl)	/	213	304	/	1.44	/	NR
Fibrinogen (g/L)	/	1.32	<1.5	3.6	1.6	/	1
NK cell activity	/	/	/	/	NR	Below NR	/
Serum ferritin (μg/L)	543.3	830	>2,000	1,900	403.8	2,545	2775
Soluble CD25 (U/ml)	/	9,560	/	>7,500	>44,000	35,854	/
ALT (U/L)	82	/	/	98.6	32	40	53
AST (U/L)	70	/	/	32.3	45	49	81
LDH	352	/	579	468	/	/	122
Hepatomegaly	+	+	+	+	+	+	+
Splenomegaly	+	+	+	+	+	–	+
Lymphadenopathy	+	–	–	+	+	–	+
Pulmonary disorders	+	–	–	+	–	+	–
Number of HLH-2004 criteria	5	6	5	6	5	6	6
Hemophagocytosis	BM Path	BM Path	–	BM Path	BM Path	BM Path	BM Path
Diagnosis of histoplasmosis							
Path	BM Path	BM Path	BM Path	BM Path	BM Path	BM Path	BM Path
Culture	blood	/	/	/	BM	BM	BM
Antigen assays	/	serum/urine	/	/	/	/	/
Antibody assays	/	/	–	/	/	/	/
Molecular method	/	/	/	/	/	+	/
Antifungal treatment	AmB	AmB/Itra	AmB/Itra	AmB	AmB	AmB/Itra	AmB/Itra
HLH-specific treatment	IVIG	–	–	DEP	DEP	IVIG	IVIG/ Prednisone
Outcomes	Recovery	Recovery	Recovery	Recovery	Recovery	Recovery	Recovery

PS, present study; NR, normal range; NA, not applicable; DE, dexamethasone and etoposide; DEP, liposome doxorubicin, etoposide, and methylprednisolone; IVIG, intravenous immunoglobulin; Bx, biopsy; LN, lymph node; BM, bone marrow; Path, histopathology; COPD, chronic obstructive pulmonary disease; DM, diabetes-mellitus; EN, erythema nodosum; TB, tuberculosis; CSF, cerebrospinal fluid; EBV, Epstein–Barr virus; AmB, amphotericin B; Itra, itraconazole; Posa, posaconazole.

showed low activity. High-soluble interleukin-2 receptors (CD25) were confirmed in six cases. Pulmonary disorders with cough or imaging presentation were showed in seven cases. Hemophagocytosis was visualized in bone marrow histopathology or biopsy in 12 patients. For diagnosis of HLH, except one patient with insufficient information only meet three of eight HLH-2004 criteria; the other 12 patients with PDH all fulfilled at least five of eight HLH-2004 criteria.

In the cases reviewed, histological and cytological examinations in bone marrow (10 cases) and colon/liver/lymph node/lung/spleen (three cases) lead to fast diagnosis of Histoplasma capsulatum. The fungal was culture in three cases in bone marrow and one case in blood. The etiology was identified by molecular methods in two patients. Antigen and serological assays of histoplasma capsulatum were less used in clinical practice, only detected in two patients.

All patients are treated with first line systemic antifungal formulation with liposomal amphotericin B, and eight disseminated infection patients received step down to azoles as recommended by the Infectious Diseases Society of America (Wheat et al., 2007). Seven patients used itraconazole, and one severe patient took posaconazole due to increasing *in vitro* activity. For specific treatment of HLH, four cases were initiated with immunosuppressed treatment recommended by HLH-94 protocol and clinical trials, and three cases were treated with intravenous immunoglobulin. For analysis of outcomes, 2 of the 13 (15.4%) patients died, clinical status deteriorated rapidly in 1 patient, and the other had complicated underlying disease. Condition was improved in 11 patients after antifungal and HLH-specific treatment.

DISCUSSION

Environmental soil is the reservoir of *Histoplasma capsulatum* (Kauffman, 2007). Contaminated soil of bird or bat cave, especially that found beside chicken coops or under blackbird

roosts, provides a luxuriant condition for mold growth (Kauffman, 2007). In the cases reviewed, the tourism exposure risk to a bat cave of 1 patient who live in non-endemic countries is specified. Histoplasmosis is endemic worldwide; in our literature review, five cases were from China and four cases were from Africa, and two Chinese patients had a history of sojourn in Africa. This suggests that clinicians need to raise awareness of the diagnosis of *Histoplasma capsulatum* infection in both areas. From its discovery in the United States, a century ago to now its spread around the world, there are three main reasons: convenient travel and enhanced connectivity increases imported and exported cases of histoplasmosis; climate change and anthropogenic land utilization creates conditions that are more conducive to fungi (Azar et al., 2020); and the HIV pandemic and the widely use of immunosuppressive agents results in more cases of histoplasmosis (Wheat et al., 2016). Our case report and literature reviews are of great value in the context of a worldwide epidemic. Furthermore, after retrieving data of literatures from five databases, we found that the HLH with histoplasmosis in immunocompetent patient is extremely rare but had high mortality. Therefore, it is necessary to for clinicians to understand and recognize the disease.

Given what we already know, histoplasmosis endemic is highly associated with AIDS (Colombo et al., 2011; Rangwala et al., 2012; Nacher et al., 2013; Pan et al., 2013; Benedict et al., 2016). Our initial search results are consistent with this conclusion, a half of histoplasmosis infection cases were patients with HIV infection. An analysis on the United States reveals that the frequency of HIV-associated histoplasmosis hospitalizations has been decreased in the highly active antiretroviral therapy (HAART) era. In contrast, significant increases were observed for none of comorbidities and HIV seronegative immunosuppressed-associated hospitalizations (Benedict et al., 2016). Our literature search results are consistent with this trend.

A clear trigger usually was identified in most patients who recognized with acquired HLH. A retrospective multicenter study revealed that infectious trigger for the pathogenesis of HLH attribute to 33% adult patients (Schram et al., 2016). Common infectious agents incorporate EBV among viral infection as the most commonly implicated, Rickettsia and Mycobacterium among the bacteria, histoplasma among fungal pathogen, Plasmodium, Leishmania, and Babesia among parasites (Al-Samkari and Berliner, 2018).

The HLH-2004 criteria are used for diagnosis. Family history or molecular diagnosis is accord with HLH, or five of these eight criteria must be present (fever, splenomegaly, bicytopenia, hyper triglyceridemia and/or hypofibrinogenemia, hemophagocytosis, low/absent NK cell activity, hyperferritinemia, and high-soluble interleukin-2 receptor levels) (Henter et al., 2007). In our review of the literature, 12 patients with disseminated histoplasmosis meet the above five of the eight criteria, but one patient with insufficient information only fulfilled three criteria, and the definition of HLH was also given in the literature. NK cell activity were detected in only three cases, and high-soluble interleukin-2 receptor (CD25) were detected in half cases, as these tests might not be available in many medical centers (Ramos-Casals et al., 2014).

The standard diagnosis methods of histoplasmosis include growth of mold in culture and confirmation of yeast on cytopathology or histopathology of clinical specimens. Histoplasmosis mold form requires 6 weeks to grow in culture and may lead to delays in patient treatment. By contrast, histopathology and cytology have faster diagnosis process but lower sensitivity and specificity (Azar et al., 2020). Antigen detection represents a valuable diagnostic tool and a useful measure of treatment response (Swartzentruber et al., 2009; Hage et al., 2011). Serum antibodies have limited diagnosis utility for produced 4 to 8 weeks after acute histoplasmosis infection (Azar et al., 2020) and can yield false-negative and false-positive results (Gil-Brusola1 et al., 2007). Molecular diagnosis is used for the identification of suspected histoplasma capsulatum isolated from culture, and it characterized by rapid turnaround times, less susceptibility to host factors, and high sensitivity and specificity (Azar et al., 2020).

In our review, histological and cytological examination of all patients showed early indication of *H. capsulatum*; the fungus was further confirmed in bone marrow or blood culture in four studies. *H. capsulatum* was recognized by molecular diagnosis in two cases. Antigen and serum antibodies detection were used less common. As evidenced by the literature review presented here, the standard diagnosis methods also have valuable utility in immunocompetent patients.

HLH is a disorder of unchecked immune activation, and the main goal of treatment is to control the immune response that includes immunosuppressive and myelosuppressive agents. Specific treatment for HLH usually requires chemotherapy or HSCT accord to HLH-94 protocol, as is more common in familial HLH. In the cases reviewed, two patients were treated with dexamethasone and etoposide (DE); two patients were treated with Liposome doxorubicin, etoposide, and methylprednisolone (DEP). Three patients were initiated with intravenous immunoglobulin.

It is worth noting that 11 patients experienced clinical improvement and survived. Two of these patients had been deteriorating and died. Previous literature reviews suggest that the mortality rate of HIV-infected patients with HLH caused by disseminated histoplasmosis is 10%–44% (Gil-Brusola1 et al., 2007; Subedee and Van Sickels, 2015; Nguyen et al., 2020). Our result reveals similar prognosis of 15% mortality in immunocompetent patients, although our sample size is small.

Familial HLH is typically determined by genetic defect in immune function; most patients are infants under 2 years of age, but research has revealed that about 15% adult patients harbor mutations in familial HLH genes (Feldmann et al., 2002). *H. capsulatum* infections as a trigger for secondary HLH are primarily consider in our study, but exon detection of HLH mutated genes, NK cell activity, soluble interleukin-2 receptor (sIL2R), and interferon (IFN)-γ should be tested to support our speculation. Unfortunately, we did not verify it further. The presence of other hidden immunodeficiency disorders is also uncertain.

In summary, we provide a case report and literature review on hemophagocytic lymphohistiocytosis with histoplasmosis in immunocompetent patients, demonstrating the clinical features, diagnostic methods, and therapeutic outcomes. To the best of our knowledge, this is the first review in intact immunology patients. Prior analyses of HLH with histoplasmosis have been limited to a single immunocompetent case or to a specific patient population with AIDS (Subedee and Van Sickels, 2015; Nguyen et al., 2020). However, the number of cases in the literature that we were able to retrieve is limited. A significant proportion of patients may remain unreported or have been underdiagnosed. In view of the global epidemic trend and the improvement of fungal environment, it is necessary for clinicians to raise awareness of the incidence of this fungus in the general population.

DATA AVAILABILITY STATEMENT

The original contributions presented in the study are included in the article/**Supplementary Material**. Further inquiries can be directed to the corresponding author.

ETHICS STATEMENT

Written informed consent was obtained from the individual for the publication of any potentially identifiable images or data included in this article.

AUTHOR CONTRIBUTIONS

HC, HH, and JW contributed to collection and collation the clinical data. QYu, HH, and HC contributed to extract data from literature and manuscript writing. TQ, MY, and QYa contributed to manuscript revisions and approved the final manuscript. All authors contributed to the article and approved the submitted version.

SUPPLEMENTARY MATERIAL

The Supplementary Material for this article can be found online at: https://www.frontiersin.org/articles/10.3389/fcimb.2022.847950/full#supplementary-material

REFERENCES

Al-Samkari, H., and Berliner, N. (2018). Hemophagocytic Lymphohistiocytosis. *Annu. Rev. Pathol.* 13, 27–49. doi: 10.1146/annurev-pathol-020117-043625

Azar, M. M., Loyd, J. L., Relich, R. F., Wheat, L. J., and Hage, C. A. (2020). Current Concepts in the Epidemiology, Diagnosis, and Management of Histoplasmosis Syndromes. *Semin. Respir. Crit. Care Med.* 41 (1), 13–30. doi: 10.1055/s-0039-1698429

Benedict, K., Derado, G., and Mody, R. K. (2016). Histoplasmosis-Associated Hospitalizations in the United States 2001-2012. *Open Forum Infect. Dis.* 3 (1), ofv219. doi: 10.1093/ofid/ofv219

Bommanan, K. B. K., Naseem, S., and Varma, N. (2017). Hemophagocytic Lymphohistiocytosis Secondary to Histoplasmosis. *Blood Res.* 52 (2), 83–83. doi: 10.5045/br.2017.52.2.83

Bryceson, Y. T., Rudd, E., Zheng, C., Edner, J., Ma, D., Wood, S. M., et al. (2007). Defective Cytotoxic Lymphocyte Degranulation in Syntaxin-11 Deficient Familial Hemophagocytic Lymphohistiocytosis 4 (FHL4) Patients. *Blood* 110 (6), 1906–1915. doi: 10.1182/blood-2007-02-074468

Castejón-Hernández, S., Reynaga-Sosa, E. A., Navarro-Aguirre, M., and Vilamala-Bastarras, A. (2021). Hemophagocytic Lymphohistiocytosis (HLH) Caused by Disseminated Histoplasmosis by H. Capsulatum Var. Duboisii in HIV Patient: A Case Report. *Enferm Infecc Microbiol. Clin. (Engl Ed)* 39 (2), 102–103. doi: 10.1016/j.eimc.2020.04.001

Colombo, A. L., Tobón, A., Restrepo, A., Queiroz-Telles, F., and Nucci, M. (2011). Epidemiology of Endemic Systemic Fungal Infections in Latin America. *Med. Mycol* 49 (8), 785–798. doi: 10.3109/13693786.2011.577821

Crossley, D., Naraharisetty, V., and Shearer, G.Jr. (2016). The Mould-Specific M46 Gene is Not Essential for Yeast-Mould Dimorphism in the Pathogenic Fungus Histoplasma Capsulatum. *Med. Mycol* 54 (8), 876–884. doi: 10.1093/mmy/myw040

Feldmann, J., Le Deist, F., Ouachée-Chardin, M., Certain, S., Alexander, S., Quartier, P., et al. (2002). Functional Consequences of Perforin Gene Mutations in 22 Patients With Familial Haemophagocytic Lymphohistiocytosis. *Br. J. Haematol* 117 (4), 965–972.

Ferguson-Paul, K., Mangum, S., Porter, A., Leventaki, V., Campbell, P., and Wolf, J. (2016). Hemophagocytic Lymphohistiocytosis and Progressive Disseminated Histoplasmosis. *Emerg. Infect. Dis.* 22 (6), 1119–1121. doi: 10.3201/eid2206.151682

Gil-Brusola1, A., Pemán, J., Santos, M., Salavert, M., Lacruz, J., and Gobernado, M. (2007). Disseminated Histoplasmosis With Hemophagocytic Syndrome in a Patient With AIDS: Description of One Case and Review of the Spanish Literature. *Rev. Iberoam Micol* 24 (4), 312–316.

Gupta, N., Vinod, K. S., Mittal, A., Kumar, A. P. A., Kumar, A., and Wig, N. (2019). Histoplasmosis, Heart Failure, Hemolysis and Haemophagocytic Lymphohistiocytosis. *Pan Afr Med. J.* 32, 43. doi: 10.11604/pamj.2019.32.43.14954

Hage, C. A., Kirsch, E. J., Stump, T. E., Kauffman, C. A., Goldman, M., Connolly, P., et al. (2011). Histoplasma Antigen Clearance During Treatment of Histoplasmosis in Patients With AIDS Determined by a Quantitative Antigen Enzyme Immunoassay. *Clin. Vaccine Immunol.* 18 (4), 661–666. doi: 10.1128/cvi.00389-10

Henter, J. I., Horne, A., Aricó, M., Egeler, R. M., Filipovich, A. H., Imashuku, S., et al. (2007). HLH-2004: Diagnostic and Therapeutic Guidelines for Hemophagocytic Lymphohistiocytosis. *Pediatr. Blood Cancer* 48 (2), 124–131. doi: 10.1002/pbc.21039

Kashif, M., Tariq, H., Ijaz, M., and Gomez-Marquez, J. (2015). Disseminated Histoplasmosis and Secondary Hemophagocytic Syndrome in a Non-HIV Patient. *Case Rep. Crit. Care* 2015, 295735–295735. doi: 10.1155/2015/295735

Kauffman, C. A. (2007). Histoplasmosis: A Clinical and Laboratory Update. *Clin. Microbiol. Rev.* 20 (1), 115–132. doi: 10.1128/cmr.00027-06

Matos Baltazar, L., Nakayasu, E. S., Sobreira, T. J., Choi, H., Casadevall, A., Nimrichter, L., et al. (2016). Antibody Binding Alters the Characteristics and Contents of Extracellular Vesicles Released by Histoplasma Capsulatum. *mSphere* 1 (2), e00085-15. doi: 10.1128/mSphere.00085-15

Mukherjee, T., and Basu, A. (2015). Disseminated Histoplasmosis Presenting as a Case of Erythema Nodosum and Hemophagocytic Lymphohistiocytosis. *Med. J. Armed Forces India* 71, S598–S600. doi: 10.1016/j.mjafi.2015.01.001

Nacher, M., Adenis, A., Mc Donald, S., Do Socorro Mendonca Gomes, M., Singh, S., Lopes Lima, I., et al. (2013). Disseminated Histoplasmosis in HIV-Infected Patients in South America: A Neglected Killer Continues on its Rampage. *PLoS Negl. Trop. Dis.* 7 (11), e2319. doi: 10.1371/journal.pntd.0002319

Nguyen, D., Nacher, M., Epelboin, L., Melzani, A., Demar, M., Blanchet, D., et al. (2020). Hemophagocytic Lymphohistiocytosis During HIV Infection in Cayenne Hospital 2012-2015: First Think Histoplasmosis. *Front. Cell Infect. Microbiol.* 10. doi: 10.3389/fcimb.2020.574584

Pan, B., Chen, M., Pan, W., and Liao, W. (2013). Histoplasmosis: A New Endemic Fungal Infection in China? Review and Analysis of Cases. *Mycoses* 56 (3), 212–221. doi: 10.1111/myc.12029

Pancoast, M., Finstad, K., Lemley, T., Pele, N., Fasipe, F., and Elsaid, M. (2019). Secondary Hemophagocytic Lymphohistiocytosis in an Infant With Disseminated Histoplasmosis. *Pediatr. Blood Cancer* 66, S82–S83. doi: 10.1002/pbc.27713

Ramos-Casals, M., Brito-Zerón, P., López-Guillermo, A., Khamashta, M. A., and Bosch, X. (2014). Adult Haemophagocytic Syndrome. *Lancet* 383 (9927), 1503–1516. doi: 10.1016/s0140-6736(13)61048-x

Rangwala, F., Putcharoen, O., Bowonwatanuwong, C., Edwards-Jackson, N., Kramomthong, S., Kim, J. H., et al. (2012). Histoplasmosis and Penicilliosis Among HIV-Infected Thai Patients: A Retrospective Review. *Southeast Asian J. Trop. Med. Public Health* 43 (2), 436–441.

Scheel, C. M., Zhou, Y., Theodoro, R. C., Abrams, B., Balajee, S. A., and Litvintseva, A. P. (2014). Development of a Loop-Mediated Isothermal Amplification Method for Detection of Histoplasma Capsulatum DNA in Clinical Samples. *J. Clin. Microbiol.* 52 (2), 483–488. doi: 10.1128/jcm.02739-13

Schram, A. M., Comstock, P., Campo, M., Gorovets, D., Mullally, A., Bodio, K., et al. (2016). Haemophagocytic Lymphohistiocytosis in Adults: A Multicentre Case Series Over 7 Years. *Br. J. Haematol* 172 (3), 412–419. doi: 10.1111/bjh.13837

Schulze, A. B., Heptner, B., Kessler, T., Baumgarten, B., Stoica, V., Mohr, M., et al. (2017). Progressive Histoplasmosis With Hemophagocytic Lymphohistiocytosis and Epithelioid Cell Granulomatosis: A Case Report and Review of the Literature. *Eur. J. Haematol* 99 (1), 91–100. doi: 10.1111/ejh.12886

Sijie, C., Li, C., Pan, Z., Zhengguo, L., and Hao, Z. (2022). A Case of Disseminated Histoplasmosis. *Chin. J. Infect. Dis.* 40 (03), 178–180. doi: 10.3760/cma.j.cn311365-20210615-00214

Solomon, I. H., Li, H., Benson, L. A., Henderson, L. A., Degar, B. A., Gorman, M. P., et al. (2018). Histopathologic Correlates of Familial Hemophagocytic Lymphohistiocytosis Isolated to the Central Nervous System. *J. Neuropathol. Exp. Neurol.* 77 (12), 1079–1084. doi: 10.1093/jnen/nly094

Sonavane, A. D., Sonawane, P. B., Chandak, S. V., and Rathi, P. M. (2016). Disseminated Histoplasmosis With Haemophagocytic Lymphohistiocytosis in an Immunocompetent Host. *J. Clin. Diagn. Res.* 10 (3), OD03–OD05. doi: 10.7860/JCDR/2016/15839.7337

Song, D., Wang, J., and Wang, Z. (2021). Hemophagocytic Lymphohistiocytosis Secondary to Disseminated Histoplasmosis in an Immunocompetent Patient. *Infect. Dis. Now* 51 (3), 308–309. doi: 10.1016/j.medmal.2020.09.019

Subedee, A., and Van Sickels, N. (2015). Hemophagocytic Syndrome in the Setting of AIDS and Disseminated Histoplasmosis: Case Report and a Review of Literature. *J. Int. Assoc. Provid AIDS Care* 14 (5), 391–397. doi: 10.1177/2325957415570740

Swartzentruber, S., Rhodes, L., Kurkjian, K., Zahn, M., Brandt, M. E., Connolly, P., et al. (2009). Diagnosis of Acute Pulmonary Histoplasmosis by Antigen Detection. *Clin. Infect. Dis.* 49 (12), 1878–1882. doi: 10.1086/648421

Wheat, L. J., Azar, M. M., Bahr, N. C., Spec, A., Relich, R. F., and Hage, C. (2016). Histoplasmosis. *Infect. Dis. Clin. North Am.* 30 (1), 207–227. doi: 10.1016/j.idc.2015.10.009

Wheat, L. J., Freifeld, A. G., Kleiman, M. B., Baddley, J. W., McKinsey, D. S., Loyd, J. E., et al. (2007). Clinical Practice Guidelines for the Management of Patients With Histoplasmosis: 2007 Update by the Infectious Diseases Society of America. *Clin. Infect. Dis.* 45 (7), 807–825. doi: 10.1086/521259

Xiaolin, L., Dingzhi, W. A. N. G., Yang, G. U. O., and Guo'an, C. (2021). One Case Report of Hemophagocytic Syndrome Secondary to Disseminated Histoplasma Capsulatum Infection. *Chin. J. Infect. Chemother.* 21 (04), 473–475. doi: 10.16718/j.1009-7708.2021.04.018

Xiong, X.-F., Fan, L.-L., Kang, M., Wei, J., and Cheng, D.-Y. (2017). Disseminated Histoplasmosis: A Rare Clinical Phenotype With Difficult Diagnosis. *Respirol Case Rep.* 5 (3), e00220. doi: 10.1002/rcr2.220

Conflict of Interest: The authors declare that the research was conducted in the absence of any commercial or financial relationships that could be construed as a potential conflict of interest.

Publisher's Note: All claims expressed in this article are solely those of the authors and do not necessarily represent those of their affiliated organizations, or those of the publisher, the editors and the reviewers. Any product that may be evaluated in this article, or claim that may be made by its manufacturer, is not guaranteed or endorsed by the publisher.

Frontiers in
Cellular and Infection Microbiology

Investigates how microorganisms interact with their hosts Explores bacteria, fungi, parasites, viruses, endosymbionts, prions and all microbial pathogens as well as the microbiota and its effect on health and disease in various hosts.

Discover the latest Research Topics

See more →

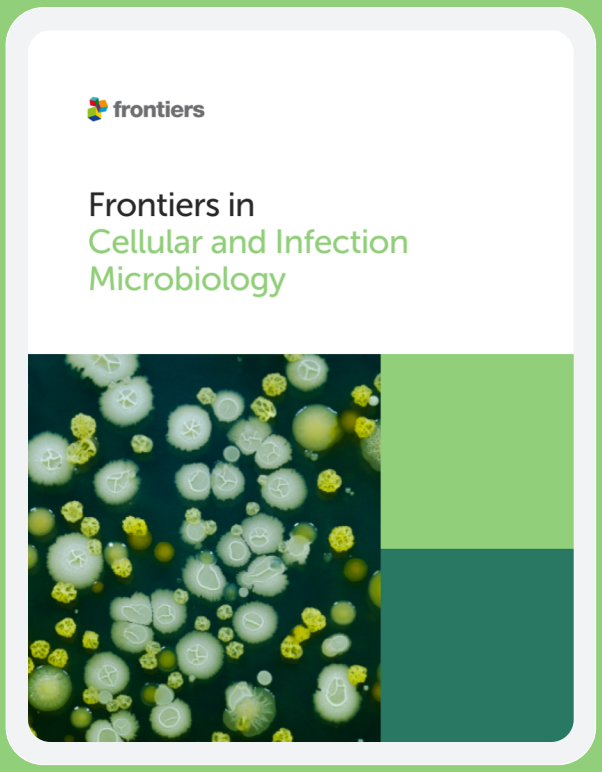

Frontiers

Avenue du Tribunal-Fédéral 34
1005 Lausanne, Switzerland
frontiersin.org

Contact us

+41 (0)21 510 17 00
frontiersin.org/about/contact